

Powerline Communications: Significant Technologies to become Ready for Integration

Von der Fakultät für Ingenieurwissenschaften
der Universität Duisburg-Essen
zur Erlangung des akademischen Grades eines
Doktors der Ingenieurwissenschaften
genehmigte Dissertation

von
Andreas Schwager
aus Backnang

Referent: Prof. Dr.-Ing. Holger Hirsch

Korreferent: Prof. Dr.-Ing. habil. Klaus Dostert

Tag der mündlichen Prüfung: 12.5.2010

Abstract

In-house PLT (Powerline Telecommunication) enables new and highly convenient networking functions without the need for additional cables on mains-powered devices. Since wireless networks are not able to reach sufficient throughput between different rooms or even floors, PLC is considered to be the ideal backbone home network medium, providing complementary and seamless interaction with wireless networks.

The need to communicate information is not new. The historical overview of this thesis compares the development of PLT to radio broadcast technologies. The consumer expects technologies to operate without interferences. Today, there are coexistence problems between these two technologies. Why does this happens, and how the problems can be resolved are the main issues of this thesis.

Initial calculations of the channel capacity provide encouraging results for using the mains cabling as a communication medium. Chapter 3 forecasts how PLT modems could develop in the future. The usage of frequencies above 30 MHz will increase the throughput rate. Next, the utilization of the 3rd wire (the protective earth) for communication enhances the coverage and the reliability of powerline transmissions. The reception of common mode signals and the usage of MIMO technologies enable 8 transmission paths between one pair of outlets, which improves the performance of the bad, strongly attenuated channels.

Today, the main challenge for the mass deployment of PLT is the lack of harmonized international standards on interoperability and electromagnetic interference. The absence of a standard results in the undesirable situation of PLT modems interfering with technologies from different vendors and also with radio applications. Solutions for solving these problems are given in chapter 4 and chapter 5.

The approach of ‘Smart Notching’ - monitoring the existence of receivable radio broadcast stations at the time and location where a PLT modem is operating, received wide resonance in the PLT and radio broadcast communities. ‘Smart Notching’, also called ‘Dynamic Notching’ or ‘Adaptive Notching’ is considered to be the key factor in solving the endless discussions about the interferences to HF radio broadcast. Details on the creation of ETSI TS 102 578 and the implementation of a demonstrator system is documented in chapter 5. Field tests conducted together with the EBU verified the efficiency of the concept. The jointly executed tests by representatives from the radio broadcast and the PLT communities became a historical event which brought the two technologies, radio receivers and PLT modems, back into one house. Finally, a vision of the future coordination of EMC and conclusions are presented.

Zusammenfassung

Heutige Modems zur Powerline Telekommunikation (PLT) können im Betrieb den Empfang von Kurzwellen-Rundfunk beeinträchtigen, wenn Modem und Rundfunk-Empfänger in unmittelbarer Nachbarschaft betrieben werden. Eine neue Generation von PLT Modems, in denen das Konzept von 'Smart Notching' - dem intelligenten Einfügen von Lücken in das Kommunikationsspektrum - implementiert ist, zeigt keine Interferenzen mit dem Empfang von Rundfunkdiensten.

Das Rauschen auf der Niederspannungsinstallation enthält neben sonstigen Signalen - durch andere Geräte hervorgerufen - aufgrund der Antennenwirkung Information über Rundfunksender. Beim 'Smart Notching' erkennen PLT Modems am Betriebsort die Existenz von Rundfunksignalen, indem sie das Signalspektrum auf der Netzleitung messen. Die Echtzeit-Bewertung der aktuellen Situation am Betriebsort ermöglicht eine Adaption des PLT Systems. Damit wird die Elektromagnetische Verträglichkeit nicht a priori (zum Herstellungs-Zeitpunkt) durch Schirmung oder eine globale Reduktion des Sendepiegels, sondern durch Design des Verfahrens (welches während des Betriebs angewendet wird) hergestellt.

Diese Doktorarbeit beschreibt nach einem kurzen Überblick zur Historie des Rundfunks und der Datenübertragung über das Energieverteilnetz Messungen zur Ermittlung der theoretischen Kanalkapazität. Anschließend wird ein Ausblick gegeben, wohin sich zukünftige PLT Modems entwickeln werden. Dies sind vor allem der Frequenzbereich oberhalb von 30 MHz sowie die Nutzung der dritten Kupferader in den Netzleitungen: der Schutz Erde. Die Verwendung von MIMO-Algorithmen (aus der kabellosen Funkübertragung (z.B. WiFi) bereits bekannt) verbessert vor allem die Wahrscheinlichkeit, eine hohe Datenrate im Gebäude sicher zu verteilen.

Sorge bereitet bei PLT ebenfalls die Koexistenz mit weiteren PLT-Systemen, sowie zu xDSL. Hierfür wird ein Vorschlag gemacht, um die Interferenzen zu nicht kompatiblen PLT- oder DSL-Systemen zu vermeiden, ohne dass die Systeme sich gegenseitig gezielt Informationen zusenden.

Das bereits oben erwähnte Konzept des 'Smart Notching' wird detailliert erläutert und die Implementierung eines Demonstrators auf FPGA-Basis dokumentiert. Abschließend wird noch beschrieben, wie 'Smart Notching' gemeinsam mit der EBU getestet wurde und wie es seinen Weg in die Welt der Standardisierung gefunden hat. Der Veröffentlichung des Standards ETSI TS 102 578 wurde im Juli 2008 einstimmig von ETSI PLT zugestimmt.

Acknowledgment

First of all my gratitude to Prof. Dr. Holger Hirsch and Prof. Dr. Klaus Dostert for supervising this thesis.

This thesis was created in the Sony EuTEC labs at the Stuttgart Technology Center [Sony_STC], Germany, where research studies and realization of demonstrator systems on powerline communications were performed. Without the support of Sony, this thesis could not have been written. I like to express much appreciation to everybody giving assistance, especially to Yukio Osaka-san and to Hajime Inoue-san for supporting this activity.

Special acknowledgement goes to all of the delegates attending the ETSI PLT meetings for the fruitful discussions, and the trust that ETSI TS 102 578 [Schw_07b] will end the long lasting debates about interferences between PLT and HF radio reception.

Thanks as well to the EBU for their participation to the plugtests [Schw_08c] and releasing their statement with regard to ETSI specification of PLT ‘Smart Notching’ system [EBU_08].

Kudos must be extended to all EuTEC colleagues at Stuttgart Technology Center of Sony Deutschland GmbH, especially Gralf Gädeken, Lothar Stadelmeier and Stephen Tiedemann for their contributions to the development of the SISO PLT system. Special thanks as well to Carsten Merkle for his support in the field of DRM radio broadcast and everybody creatively contributing to this paper.

Much gratitude goes to Dr. Dietmar Schill and the EuTEC management of Sony’s Technology Center in Stuttgart for supporting the creation of this document.

Thanks to Bernd Wörl for access to isolation chambers, discussions and support on EMI measurements.

I would like to express my warmest gratitude to Dr. Mike Hate (EBU) and Prof Dr. Holger Hirsch (University Duisburg-Essen) for their contributions to ETSI STF 332 [Schw_07a] and the subsequent e-mail exchange. Especially pleasant was their neutrality and discussions without prejudice. Thanks as well to Serafin Arroyo and Pedro Gomez (both from DS2) for the participation at the ETSI PLT plugtests to verify the ‘Smart Notching’ concept.

Acknowledgments to Dietmar, Ben, Lothar, Daniel, Altfried, Niko, Weiyun, Werner and Gavin for reviewing this thesis and their fruitful comments.

My heartfelt appreciation goes to Werner Bäschlin for his excellent support on regulatory matters, analog components for PLT and all the untiring discussions. The knowledgebase of analog components is very large and valuable and unfortunately often gets lost due to the focus on the digital matters by the younger engineers.

I'm also deeply thankful to Weiyun Lu for her great support and motivation during implementation of the smart notching concept into a demonstrator system during her internship and diploma thesis.

I will forever be indebted to my loving wife, Andrea, for reviewing this thesis, improving my poor English and all the mental support and tolerance she gave me during the studies at university Duisburg-Essen and during the development of this thesis.

Stuttgart, May 2010

Andreas Schwager

Contents

Abstract	II
Acknowledgment.....	IV
Contents.....	VI
List of Figures	VIII
List of Tables.....	XII
Glossary	XIII
<i>Acronyms.....</i>	<i>XIII</i>
<i>Symbols.....</i>	<i>XIX</i>
1 Historical Overview and Motivation	1
1.1 History of PLT and Radio Broadcast.....	1
1.2 Motivation.....	6
1.2.1 Application, User View.....	6
2 Potential of Powerline Telecommunications	9
2.1 HF Properties of the Mains Network.....	9
2.1.1 Measurements in Buildings.....	9
2.1.2 Impedance Modulating Devices.....	14
2.2 Theoretical Channel Capacity.....	18
3 Outlook for Next Generation PLT Modems	23
3.1 Frequency Range $f > 30\text{MHz}$	23
3.2 MIMO PLT	25
3.2.1 Use of Protective Earth	26
3.2.2 CM provides another Reception Path	27
3.2.3 MIMO PLT Couplers.....	30
3.2.4 Measurements in Buildings.....	31
4 Coexistence between PLT Systems	38
4.1 Overview.....	38
4.2 Frequency.....	39
4.3 Time	39
4.4 Power.....	41
4.4.1 Adaptation of the Transmit Power to the Channel Attenuation	41
4.4.2 Adaption of the PSD to the actual Data Throughput Requirement	44
4.4.3 Total Average PSD Reduction.....	46
4.5 Dynamic Coexistence without Interoperability Channel	46
5 Coexistence between PLT and HF Radio broadcast	55
5.1 Overview.....	55
5.2 Concept of ‘Smart Notching’	59
5.2.1 Radio Signal Spectrum on Powerlines.....	60
5.2.2 Sensitivity of SW-Radio Receivers.....	66
5.2.3 Threshold to detect Radio Services.....	77
5.2.4 Requirements of a Notch.....	82

5.2.5	Adaptive OFDM, Channel and Noise Estimation	92
5.2.6	Impact on PLT Throughput.....	97
5.3	<i>Implementation in a Demonstrator System</i>	99
5.3.1	PLT Modem System	99
5.3.2	Notch Filter Environment	106
5.3.3	Detection of the Presence of Radio Services	109
5.3.4	Notching.....	114
5.4	<i>Verification of ‘Smart Notching’ in Buildings</i>	131
5.5	<i>Standardization of ‘Smart Notching’</i>	134
5.5.1	EBU Statement.....	135
5.5.2	ETSI PLT, CISPR I PT PLT, ECANB, CENELEC, IEEE, ITU and others	135
6	Outlook to Future EMC Coordination.....	137
7	Conclusions	140
	Appendix A: EBU Statement	141
	Appendix B: Units.....	142
	Curriculum Vitae.....	143
	Bibliography	144

List of Figures

Figure 1: House with PLT applications

Figure 2: Rear side of A/V receiver with 7.1 Surround Sound

Figure 3: Overview of noise characteristics

Figure 4: Differential Mode Impedance at a single location into a power plug

Figure 5: Schematic of power supply

Figure 6: Measurement setup to verify effects of impedance modulating devices

Figure 7: Outcome of an impedance modulating device in frequency domain on a PLT channel

Figure 8: Behavior of an impedance modulating device in time domain

Figure 9: Attenuation and noise of a PLT channel

Figure 10: Cumulative channel capacity by different feeding power levels

Figure 11: *SNR* of PLT in 3 frequency ranges and feeding power levels

Figure 12: SISO PLT modems connected to the mains

Figure 13: MIMO PLT modems connected to the mains

Figure 14: Generation of common mode signals

Figure 15: CM and DM attenuation

Figure 16: MIMO PLT channel matrix

Figure 17: Star style MIMO PLT probe

Figure 18: Triangle style MIMO PLT probe

Figure 19: Receiving with a star style probe at an outlet

Figure 20: Calibration of 2 probes for throughput measurement

Figure 21: Comparison of straight MIMO channels: P-N, N-PE and P-PE

Figure 22: MIMO measurement results, all paths

Figure 23: Proposal of frequency split

Figure 24: Allocation of time slots for inter PLT coexistence

Figure 25: Signaling the usage of time slots

Figure 26: Classical architecture with receiver AGC

Figure 27: Transmitter AGC for adaptive transmit power management

Figure 28: Attenuation of a channel with AGC setup information

Figure 29: Statistical analysis of the minimum channel attenuation

Figure 30: Transmit PSD vs. channel attenuation motivated by throughput rate

Figure 31: Two flats with a PLT communication in each

Figure 32: SNR and noise at each receiving power outlet

Figure 33: Interference from neighbor's PLT communication

Figure 34: Unusable frequencies are released by one system

Figure 35: 2nd PLT system frees frequencies with high interference

Figure 36: Radiation from PLT (at e.g. an impedance mismatch)

Figure 37: Radio signals ingressing a house's mains wiring

Figure 38: Fading of HF radio broadcast

Figure 39: Detection of radio services. Setup for measurements in buildings

Figure 40: In-door electrical field of the 49m band, any location any time

Figure 41: Signal ingress in the 49m band, measured connected at a power outlet

Figure 42: Radiation from PLT

Figure 43: Selection of AM-Radio receivers and radio dummy

Figure 44: A.F. signal and noise behavior of AM receivers depending on RF input level

Figure 45: Setup to measure the sensitivity of AM receivers

Figure 46: Snapshots from field measurement in an anechoic chamber

Figure 47: Sensitivities of AM receivers with power supply

Figure 48: Sensitivities of AM receivers, battery powered

Figure 49: Sensitivities of AM receivers with CM and DM noise on powerlines

Figure 50: Setup to measure the sensitivity of AM receiver where auto scan stops

Figure 51: Noise figure F_a according to [ITUR_07]

Figure 52: Threshold to detect HF radio broadcast ingress

Figure 53: Definition of reception factor, measurement setup in a flat

Figure 54: Cumulative probability of reception factor

Figure 55: Notch providing protection to an AM service

Figure 56: Notch causing interference to an AM service

Figure 57: Relative value of the radio frequency protection as a function of the carrier-frequency separation

Figure 58: Relative RF protection ratios A_{rel} (dB) for a narrow-band system

Figure 59: Adaptive channel modulation. Simulation of a frequency scan using the channel data of a measured in-house PLT channel

Figure 60: Channel and noise measurement of the PLT demonstrator performed during communication

Figure 61: Gaps in between training symbols enhance noise measurement quality

Figure 62: Screenshot of the PLT system monitor application

Figure 63: HD video streaming application via PLC demonstrator system

Figure 64: Block schematic of ‘Smart Notching’ demonstrator system

Figure 65: Implementation of ‘Smart Notching’ demonstrator in FPGAs

Figure 66: Block schematic of FPGA hosting the notch filters

Figure 67: Screenshot of ‘Smart Notching’ demonstrator system

Figure 68: Noise measurement with HF radio bands

Figure 69: Enlargement of noise measurement in 49 m and 41 m HF radio bands (red) and notched carriers

Figure 70: Enhancement of FFT resolution bandwidth

Figure 71: Tune notch to HF radio broadcast raster

Figure 72: OFDM side lobes. Comparison of various window functions

Figure 73: OFDM symbol with GI and window

Figure 74: Consecutive OFDM symbols, Guard Interval, windowing, roll-off,

Figure 75: Sideband attenuation comparisons with different roll-off factors

Figure 76: OFDM spectra with different notch widths and depths achieved with different roll-off factors

Figure 77: 2nd order IIR filter direct form I

Figure 78: Notch filter stages and frequency response of a filter having 3 notches

Figure 79: Illustration of pole-zero locations on the unity circle

Figure 80: Algorithm to calculate IIR filter coefficients

Figure 81: Magnitude and pole-zero plot of a notch

Figure 82: Magnification of the pole-zero plot for proving filter stability

Figure 83: Frequency response of simulated notch filters

Figure 84: Measured notch filters, 45 carriers in 11 notches: 1 sub-stage

Figure 85: Measured notch filters, 45 carriers in 11 notches: 3 sub-stages

Figure 86: Group delay of single notch filter

Figure 87: Impulse response of notch filter 1 sub-stage

Figure 88: Impulse response of notch filter 3 sub-stages

Figure 89: Implementation of the notchfilter in VisualElite

Figure 90: Measured notch with thresholds from ETSI TS 102 578 [Schw_08d]

Figure 91: Block schematic to boost carriers influenced by the side slopes of a notch

Figure 92: Frequency hopping of a notch recorded at verification of the demonstrator

Figure 93: Result of subjective assessment of sound quality

Figure 94: EMC coordination, ideal and real conditions

List of Tables

Table 1: Median results of measurements on powerlines

Table 2: Measurement results in the higher frequency range

Table 3: Data throughput utilization of typical in-house PLT applications

Table 4: Sensitivities of AM receiver where automatic stations scan stops

Table 5: Adjacent channel selectivity from minimum receiver requirements for DRM

Table 6: Relative RF protection ratios (dB) AM interfered by digital (e.g. DRM)

Table 7: Digital (64-QAM, protection level No. 1) interfered by AM

Table 8: Digital (64-QAM, protection level No. 1) interfered by digital

Table 9: Relative RF protection for AM interfered with by AM

Table 10: Definition of a notch: avoid adjacent carrier interference

Table 11: PLT system basic parameters

Glossary

Acronyms

AC	Alternating Current
ACS	Adjacent Channel Selectivity
ADC	Analog to Digital Converter
ADSL	Asymmetric Digital Subscriber Line
AE	Auxiliary Equipment
AEG	http://www.aeg.de
A.F.	Audio Frequency
AFC	Automatic Frequency Control
AFE	Analog Front End
AGC	Automatic Gain Control
AM	Amplitude Modulation
AMR	Automatic Meter Reading
ASK	Amplitude Shift Keying
A/V	Audio / Video
AV	Average Detector (at R&S screen shot)
Avg	Average
BBC	British Broadcasting Corporation http://www.bbc.co.uk/
BER	Bit Error Rate
BPL	Broadband over Powerline
C	general-purpose computer programming language
CAZAC	Constant Amplitude Zero Autocorrelation
CB	Citizens' band radio
CD	Committee draft
CD	Compact Disc
CDCF	Commonly Distributed Coordination Function
CDF	Cumulative Distribution Function
CDV	Committee draft for voting
CE	Consumer Electronic
CE marking	is a mandatory conformity mark on many products placed on the market in the European Economic Area (EEA)
CENELEC	European Committee for Electrotechnical Standardization
CISPR	Comité International Spécial des Perturbations Radioélectriques

CLK	Clock
CLRWR	Clear write (at R&S screen shot)
CM	Common Mode
CTRL	Control
DAC	Digital to Analog Converter
DC	Direct Current
DC	Document for Comments
DCR	Device Control Register Bus
DDR SDRAM	Double Data Rate Synchronous Dynamic Random Access Memory
Det	Detector
DM	Differential Mode
DMA	Direct Memory Access
DQAM	QAM demodulator
DRM	Digital Radio Mondial [ETSI_05] http://www.drm.org/
DS2	http://www.ds2.es
DSL	Digital Subscriber Line
DSM	Dynamic Spectrum Management
DUT	Device under Test
DVB	Digital Video Broadcasting
DVB-C2	2 nd generation of DVB standard for cable television
DVB-NGH	DVB standard for next generation handheld devices
DVB-S	DVB standard for satellite television
DVB-T2	2 nd generation of DVB standard for terrestrial television
DVD	Digital Versatile Disc or Digital Video Disc
DVI	Digital Visual Interface
DX	long distance, telegraphic shorthand for "distance"
EBU	European Broadcasting Union http://www.ebu.ch/
ECANB	Group of Notified Bodies under the EMC Directive http://circa.europa.eu/Public/irc/enterprise/emccbnb/home
EFS	electric field probe
EMC	Electromagnetic Compatibility
EMI	Electromagnetic Interference
EN	European Norm
ETH	Ethernet
ETSI	European Telecommunication Standardization Institute http://www.etsi.org
ETSI PLT	Technical Committee on PLT at ETSI http://www.etsi.org/PLT

EUT	Equipment under Test
EuTEC	European Technology Center http://www.stuttgart.sony.de/
FAC	DRM Fast Access Channel
FCC	Federal Communications Commission
FEC	Forward Error Correction
FFT	Fast Fourier Transform
FIR	Finite Impulse Response
FM	Frequency Modulation
FPGA	Field-programmable Gate Array
Frequ	Frequency
FS	Frame Start
FSK	Frequency Shift Keying
GI	Guard Interval
GUI	Graphical User Interface
HAM	Nickname for amateur radio operator
HD	High Definition
HDD	Hard Disk Drive
HD-PLC	High Definition Powerline Communication http://www.hd-plc.org/
HDTV	High-Definition Television
HF	High Frequency range: from 3 MHz to 30 MHz
HiFi	High fidelity
HTTP	Hypertext Transfer Protocol
i.LINK	IEEE 1394
ICI	Inter Carrier Interference
IEEE	Institute of Electrical and Electronics Engineers http://www.ieee.org
IEV	International Electrotechnical Vocabulary
IFBW	Intermediate Frequency Bandwidth
IFFT	Inverse Fast Fourier Transform
IIR	Infinite Impulse Response
IP	Internet Protocol
IP core	semiconductor Intellectual Property core
ISI	Inter Symbol Interference
ISN	Impedance Stabilization Network
Lb2plb	Local Bus to PLB
LCPTV	Line Cycle Periodic Time Variant

LDPC	Low-density Parity-check Code
LiIF	Line Interface Filter
Lin Mag	Linear Magnitude
LTE	Long Term Evolution
MAC	Medium Access Control
max	maximum
MAXH	max-hold, Maximum Hold
MIMO	Multiple Input - Multiple Output
min	minimum
MINH	min-hold, Minimum Hold
MPEG	Moving Picture Experts Group
MPEG_TS	MPEG Transport Stream
MSC	DRM Main Service Channel
N	Neutral wire of the electric power
OFDM	Orthogonal Frequency Division Multiplexing
OPB	On-Chip Peripheral Bus
P	Phase or live wire of the electric power
PAR	Peak to Average Ratio
PC	Personal Computer
PCI	Peripheral Component Interconnect
PDA	Personal Digital Assistant
PE	Protective earth wire of the electric power
PGA	Programmable Gain Amplifier
Phy	Physical Layer
PK	Peak Detector (at R&S screen shot)
PLB	Processor Local Bus
PLC	Powerline Communication
PLT	Powerline Telecommunication
PLNoise.mxxx dBm/Hz	Noise on powerlines with PSD of $-xxx$ dB(m/Hz)
PLSC	Powerline Signal Coupler
PPC	PowerPC (short for Power Performance Computing), a RISC processor
PSD	Power Spectral Density in dB(m/Hz)
PSK	Phase Shift Keying
Pxx	Plug number xx or Power outlet number xx
QAM	Quadrature Amplitude Modulation
QoS	Quality of Service

QPK	Quasi-Peak
QPSK	Quadrature Phase-Shift Keying
RAM	Random-Access Memory
RCD	Residual Current Device
RCS	Ripple Carrier Signalling
Ref	Reference
RF	Radio Frequency
RISC	Reduced Instruction Set Computer
RMS	Root Mean Square, (RM at R&S screen shot)
Rod.PS	with Rod Antenna and mains power supply
Rod.Bat	with Rod Antenna and battery supply
RS	Reed Solomon
RS-232	Recommended Standard 232, similar to ITU-T V.24
R&D	Research and Development
R&S	Rohde & Schwarz http://www.rohde-schwarz.de
R&S xxx	a device from Rohde & Schwarz
Rx	Receiver
RxLi	Receiver Line Interface Filter
S1, ... S4	Signal 1 to Signal 4
S11, S21	S-Parameter or Scattering parameter
SA	Sample Detector (at R&S screen shot)
SCART	Syndicat des Constructeurs d'Appareils Radiorécepteurs et Téléviseurs
SD	Standard Definition
SDC	DRM Service Description Channel
SGL	Single Sweep (at R&S screen shot)
SHF	Super High Frequency range: from 3 GHz to 30 GHz
SINPO	Signal Strength, Interference, Noise, Propagation and Overall
SISO	Single Input Single Output
STF	Special Task Force from ETSI
SW	Short Wave
SWT	Sweep Time (at R&S screen shot)
t1, ... t3	Timing 1, ... Timing 3
TCP	Transmission Control Protocol
TDM	Time Domain Units
TF	Transfer Function
TG	Tracking Generator (at R&S screen shot)

TGN	Technical Guideline Notes (document from the ECANB)
TR	Technical Report from ETSI
TrS	Training Symbol
TS	Technical Standard from ETSI
TV	Television
Tx	Transmitter
TxLi	Transmitter Line Interface Filter
UDP	User Datagram Protocol
UK	United Kingdom
UPA	Universal Powerline Association http://www.upaplc.org
US	United States
USB	Universal Serial Bus
USSR	Union of Soviet Socialist Republics
UWB	Ultra-Wideband
V2	Xilinx Virtex-II FPGA
V2P	Xilinx Virtex-II Pro FPGA
VBW	Video Bandwidth (at R&S screen shot)
VCXO	Voltage Controlled crystal Oscillator
VDSL	Very high bit rate DSL
VGA	Video Graphics Array
VHDL	Very (High Speed Integrated Circuits) Hardware Description Language
VHF	Very High Frequency range: from 30 MHz to 300 MHz
VLS	VideoLAN Server
VoIP	Voice over Internet Protocol
WiFi	WiFi Alliance http://wi-fi.org/
xDSL	family of Digital subscriber line technologies
Zr	converted to Impedance

Symbols

$'a', 'b'$	Filter coefficients
a, b, c, d, e	Steps to define the slopes of a notch
$A(x)$	Distance from bottom level of the notch
Att	Attenuation in dB
BW	Bandwidth in Hz
c	Carrier index
C	Capacitance in F
CC	Channel Capacity in Mbps
$D_u S_h$	Upper decile deviation of the wanted signal in dB
E	Electrical Field in dB(μ V/m)
f	Frequency in Hz
F_w, F_{am}	(Median) Noise figure in dB
F_s	Sampling Frequency
H	Transfer function
I	Current in A (I_P , I_N and I_{PE} are currents along the P, N and PE wires)
Im	Imaginary part
k_{sym}	Coupling factor in dB(μ V/m)-dBm: radiated E-Field measured in the outside of a building minus the differentially fed signal to an outlet in the building. Defined in [ETSI_03a]
K	Index aligned to HF radio broadcast raster
LCL	Longitudinal Conversion Loss in dB
M	Margin in dB
n	Any number
Noi	Noise signal voltage in dB μ V
NP	Noise Power in dBm
$NPSD$	Noise Power Spectral Density in dB(m/Hz)
NSD	Voltage of Noise Spectral Density in dB(μ V/Hz)
$p_{1,2}$	Pole in the Pole-zero plot
P	Power in W or dBm
PSD	Power Spectral Density in dB(m/Hz)
R	Resistor in Ω
RBW	Resolution Bandwidth
Re	Real part
$ReFa$	Reception factor in dB(μ V/m)-dBm: E-Field of a radio station measured indoor minus the ingress signal measured differentially at an outlet. Defined in [Schw_08c]

SNR	Signal to Noise Ratio in dB
SNR_{lin}	Signal to Noise Ratio as linear factor
T, t	Time in s
U	Voltage in V or dB μ V
$z_{1,2}$	Zero in the Pole-zero plot
Z	Impedance in Ω
Δf	Frequency interval
ΔT	Change in time
α	Attenuation factor
β	Roll off factor
β_0	Angle to set the notch frequency
ω	Angular frequency

1 Historical Overview and Motivation

The historical overview compares the development of powerline communication and radio transmissions. The coexistence between these two technologies forms the main part of this thesis.

Later, the motivation for PLC is described from the view of the consumer electronic industry.

1.1 History of PLT and Radio Broadcast

Since the Town Crier no longer exists, inventors have been looking for new ways to transport information from the source to the customer. Installing new wires between them is cumbersome, expensive and sometimes not practical. Both radio broadcast and powerline transmissions have been used to solve this problem. A historical overview highlights some milestones of how the two technologies have developed.

The early days of the powerline communications and radio broadcast can be found in many sources. In [Brow_99a] and [Brow_99b] Prof. Brown from University of Lancaster wrote that the idea of using powerlines for signalling is not new. Prof. Dostert from Karlsruhe University in [Dost_01] and Dr. Ahola in [Ahol_03] gave an overview on the history of the usage of power transmission wires for data communication. [Barn_66] and [Barn_68] give an historical overview of radio broadcasting. The history of broadcasting began before radio was invented. The term "broadcasting" had been used in farming to define the tossing of scattering in all directions.

Edward Davy proposed remote electricity supply metering for the purpose of checking the voltage levels of batteries at unmanned sites in the London-Liverpool telegraph system in 1838. In those early days Michael Faraday discovered electromagnetic induction during his studies. He found the line or the field of forces of a magnet. Later, James C. Maxwell was able to formulate the thoughts of Faraday mathematically. He developed his theory of electromagnetism where he predicted the existence of electromagnetic waves. The first action and reaction over distance - caused by electricity - was documented by the dentist M. Loomis in the US in 1864. His transmissions passed a few km. In the 1880's Heinrich Hertz validated Maxwell's theory through experimentation. He demonstrated the transmission and reception of the electromagnetic waves, predicted by Maxwell, and thus was the first person to intentionally transmit and receive radio. From a historical point of view, the data transmission via powerline pre-

ceded radio transmissions! 10 years later Guglielmo Marconi began to conduct experiments, building much of his own equipment in his home in Italy. His goal was to use radio waves to create a practical system of "wireless telegraphy"—i.e. the transmission of telegraph messages without connecting wires as used by the electrical telegraph. This wasn't a new idea. Numerous investigators had been exploring wireless telegraph technologies for over 50 years, but none had proven commercially successful. Marconi did not discover any new and revolutionary principle in his wireless-telegraph system. Instead, he assembled and improved an array of facts, unifying and adapting them to his system.

On 15th of March, 1901 the patent office in Berlin granted the patent No. 118717 to the French inventor C. Loubery [Loub_01]. It was the first notable description of a remotely controlled load management system. This is why the IEEE standardization group P1901 [IEEE_09] selected this number for their name. Loubery used a multiple carrier signal, with one frequency carrier to control one target device. The client implemented a dedicated fixed filter to detect 'his' frequency. The bit rate was not very high, but it was clearly a powerline communication. In those days, customers were charged different prices, depending on the application that used the electricity. For example electricity for light was charged at a lower rate than the power of a heating device. Rapidly, toasters appeared on the market equipped with an Edison screw fitting instead of a plug. This probably caused the business model to change.

The first audio radio broadcasts of entertainment and music for a general audience were performed by Reginald Fessenden, on the evening of December 24, 1906 (Christmas Eve). Fessenden used the alternator-transmitter to send out a short program from Brant Rock, which included him playing the song 'O Holy Night' on the violin and reading a passage from the Bible. On December 31, New Year's Eve, a second short program was broadcast. The main audience for both these transmissions was an unknown number of shipboard radio operators along the Atlantic Coast.

Around the turn of the century, Marconi began to investigate the possibility of sending a radio signal over the Atlantic, in order to compete with the transatlantic telegraph cables. According to his announcement on the 12th of December 1901 a wireless message was transmitted from Ireland to Newfoundland. The distance between the two points was around 3,500 kilometers. At this moment, radio transmissions show unique properties which make it difficult for PLT to compete with them.

The first known coexistence problem came about when the Cable Telegraphy Society sued Marconi. An interim injunction forced Marconi to stop his experiments. It is not known if this

coexistence problem was motivated by technical or economical reasons. However, this initiative didn't achieve the intended result, as it was an excellent advertisement for Marconi. Later, they found the wireless transmission to be a useful extension to communication over cable.

Two radio operators aboard the Titanic - Jack Phillips and Harold Bride - were not employed by the White Star Line but by the Marconi International Marine Communication Company. Following the sinking of the ocean liner, survivors were rescued by the Carpathia of the Cunard Line that had received their wireless distress signal. When it docked in New York, Marconi went aboard with a reporter from the New York Times to talk to Bride, the surviving operator. On 18 June 1912, Marconi gave evidence to the Court of Inquiry into the loss of the Titanic regarding the marine telegraphy's functions and the procedures for emergencies at sea. Britain's postmaster-general summed up, referring to the Titanic disaster, "Those who have been saved, have been saved through one man, Mr. Marconi ... and his marvelous invention." Radio transmissions had justified their existence in rather dramatic fashion.

One of the first long distance radio broadcasts was transmitted at the beginning of World War I from Nauen transmitter station near Berlin. All German ocean liners were informed about the new situation over distances of more than 8000 km. Most ships of the merchant fleet could reach neutral harbors. Nauen was a research station of Telefunken. It was built on wetlands to enable the antennae to be better earthed. The wetlands almost caused the foundations of the building to sink.

The Carrier Frequency Transmission of voice over high voltage transmission networks began in the 1920's. The network provided a bidirectional communication channel which was important for management and monitoring purposes, because at the beginning of electrification, just a telephone network could not cover the communication between transformer stations and power plants. Due to favorable transmission characteristics, low noise and relatively high carrier frequencies (15-500 kHz), distances of up to 900 km were reached with a transmission power of 10 W. Initially, only voice was transmitted and amplitude modulation was used. Later, telemetering and controlling functions were also implemented.

In the 1930's, RCS (ripple carrier signalling) was introduced on the medium (10-20 kV) and in low voltage (240/415V) distribution systems. According to Prof. Dostert, the first practical applications of RCS systems, constructed in Germany, were the Telenerg project by Siemens in Potsdam and the Transkommando implemented by AEG in Magdeburg and Stuttgart. From the very beginning, RCS was used to transmit digital information. The ASK (Amplitude Shift Keying) and FSK (Frequency Shift Keying) modulation methods were mainly used because of

their simplicity of implementation. Due to the low carrier frequency used and simple narrow-band modulation methods, the data rates of RCS systems were low.

In 1933, FM (frequency modulation) radio was patented by inventor Edwin H. Armstrong. In an audio broadcast program, FM minimizes interference from electrical equipment and the atmosphere.

Sometimes PLT was even used for transmitting radio programs over powerlines. When operated in the AM radio band, it is known as a carrier current system. Such devices were in use in Germany, where it was called Drahtfunk, and in Switzerland, where it was called Telefonrundspruch, and used telephone lines. In the USSR PLT was very common for broadcasting since the 1930s because of its low cost and easy accessibility. In Norway, the radiation of PLT systems from powerlines was sometimes used for radio transmissions. These facilities were called Linjesender, and the radio program was fed into the lines by special transformers. Filters for the carrier frequencies of the PLT systems were installed in substations and at line branches, in order to prevent uncontrolled propagation. Technologies operated in these early days bring us very close to the main topic of this thesis.

Consumer PLT products such as baby alarms have been available since at least 1940 [Broa_84]. Later, meter reading and load balancing systems were developed for utilities. In the 1970's individual meters could be addressed to manage water heater and air conditioning consumption in order to prevent peaks in usage during the high consumption times of the day. Ripple control techniques injected pulsed sine waves using frequencies up to 2 kHz to remote control power consumers.

In 1954 Regency introduced a pocket transistor radio, powered by a "standard 22.5V Battery". In 1960 Sony introduced their first transistor radio, small enough to fit in a vest pocket, and able to be powered by a small battery. It was durable, because there were no tubes to burn out. Over the next twenty years, transistors displaced tubes almost completely except for very high power, or very high frequency, uses.

Building automation systems allow monitoring and controlling the mechanical and lighting systems in a building. They keep the building climate within a specified range, provide lighting based on an occupancy schedule, monitor system performance and device failures and provide email and/or text notifications to building engineering staff. Digital modulation techniques on powerlines were enhanced to phase shift keying where several kilobits per second could be transmitted.

Next generation powerline devices were based on more effective modulation methods providing higher data transfer rates. The transmit power was decreased by means of increasing the frequency of the carrier signals and using more sophisticated communication electronics. The invention of integrated circuits launched the development of low-cost components for powerline communications. Due to the advances in modulation schemes, processing capacity and error control, the data transfer capacity for powerline communications improved significantly.

The idea of using electricity distribution networks and domestic networks for broadband communications arose in the 1990's, alongside the development of the Internet. Investments into research of powerline channel characteristics, modulation techniques and communication protocols increased dramatically. The first large-scale trial was carried out by Norweb in Great Britain, in 1997. The results of this test were negative and led them to withdraw from further trials. However, the reasons for the withdrawal were believed to be due to the resistance of radio amateurs [Floo_05] and strong regulations regarding radiation of cables, which made the business economically unviable. Incidentally, Norweb used a much higher feeding PSD (Power Spectral Density) than PLT modems do today. Later, several distribution companies in Europe have carried out powerline communications field trials on public low voltage distribution networks.

Data rates over a powerline communication system vary widely. Low-frequency (about 100-200 kHz) carriers injected into mains lines may carry one or two analog voice circuits, or telemetry and control circuits with an equivalent data rate of a few hundred bits per second. However, these circuits could be many kilometers long. Higher data rates generally imply shorter ranges. A local area network operating at millions of bits per second may only cover one floor of an office building, but eliminates installation of dedicated network cabling.

Spread Spectrum systems from MainNet or Yitran and GPSK system from Ascom transmitted several Mbps via the powerlines. Finally, PLT modems using hundreds of communication carriers adapt more flexibly to the PLT channel and succeeded on the market.

Modern powerline modems offer a throughput rate of up to 200 Mbps on the physical layer. This number should be considered with caution as it doesn't guarantee the maximum throughput to the final application on any platform. From the physical throughput rate, the guard interval (to make the OFDM transmission immune against multipath transmissions), the preamble (for synchronization of transmitter and receiver, as well for channel estimation), error correction and the overhead caused by MAC (Medium Access Control) layer must be subtracted in order to estimate the throughput on the IP (Internet Protocol) layer. TCP (Transmission Con-

trol Protocol) or UDP (User Datagram Protocol) causes further reduction to this number. Finally, the maximum throughput rate can only be achieved in buildings between 2 outlets with a very low attenuation. The throughput rate is individual for every link due to the adaptive constellation. After considering an average link and the overheads described above, around 45 Mbps can be expected for an application using TCP.

Today, Internet radio consists of sending radio-style audio programming over streaming Internet connections. Radio multicast or broadcast and data transmission over powerline have once again merged onto one wire.

The sources of media consumption in modern private households are: newspaper, radio & TV broadcast and the Internet. Internet applications gain more relevance in a private home. [EIAA_04] found that the time of internet usage burdens mainly the shares of watching TV. The share of the newspaper is slightly decreasing. Listening to radio broadcast is almost not affected. Unfortunately some parts of the media shares which gain or stay at least stable may cause interference with the others. The main interference exists between the HF Radio broadcast reception, which is very valuable, because this broadcast goes half-way around the globe and the powerline communication, which is very valuable as well, because it makes internet access ubiquitous, you can enjoy it everywhere in the house. Unfortunately these two technologies interfere with each other. They use the same frequency range. In the past radio broadcast was done several times via powerlines. So why shouldn't these technologies coexist?

1.2 Motivation

1.2.1 Application, User View

The target of Home Networking is to connect all digital electronic consumer devices within the home. The consumer should be able to access all services and data at any time and any place in his home, regardless of where the electronic devices which host these services are located.

Apart from the different wired networks such as Ethernet, i.LINK or USB, several wireless systems are already available on the market and work well for local clusters within a single room. As soon as 'room to room' connectivity is needed, the limitations of these solutions become clear: On the one hand, data throughput of wireless connections, which typically make use of ISM frequencies, e.g. 2.4 GHz, decreases dramatically if the signal has to pass through walls or ceilings made of concrete. Such materials cause signals reflections resulting in a high attenuation. On the other hand, wired media is inconvenient to install especially to provide inter-room connections.

To enable real broadband throughput for ‘room to room’ connectivity, an in-home backbone that connects individual devices or clusters in the house with minimum installation effort is desirable. PLT, PLC or BPL (Broadband over Powerline) fulfills these requirements: Modern modulation techniques enable the power network to transport high data rate services. Figure 1 shows applications which could be realized with a PLT in-home backbone.

In such a scenario, all consumer electronic devices that are connected to the mains are equipped with a PLT modem. Wireless devices such as PDAs communicate with the PLT network via an access point. Storage devices and the Internet gateway can be located anywhere in the house. Video services coming from cameras or baby monitors are available on all displays. Speakers would no longer need dedicated audio cables. TV might be received through a Satellite dish on top of the roof or a cable network access point in the basement. The average modern European private home contains up to two phone jacks or coax plugs and around 40 power outlets. Today in the US, a new single family building has an average 256 m² floor area [AHS_07] and 82 power outlets. The powerline network is the most ubiquitous network in buildings.

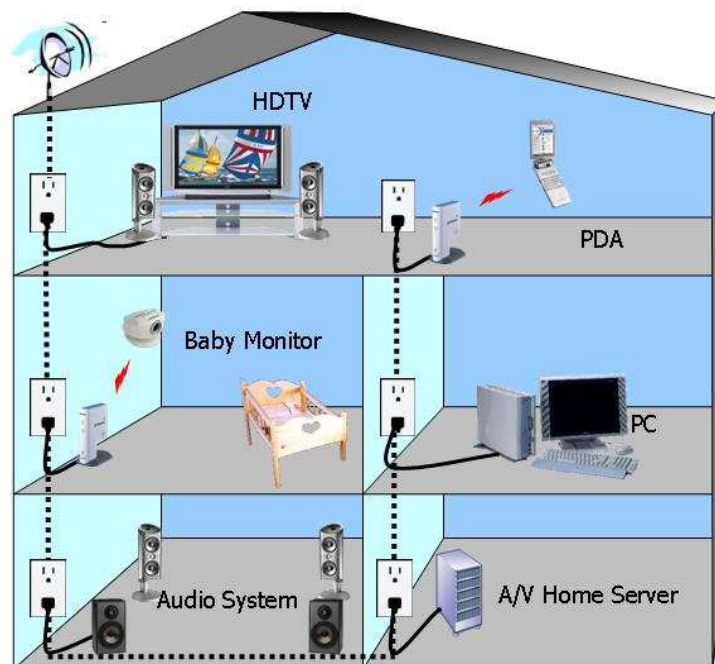


Figure 1: House with PLT applications

Powerline networking provides a huge gain of comfort for the customer. A 7.1 Surround Sound receiver¹ (figure 2) is a good example where only experienced users are able to connect all cables correctly. The variation between different cable types such as SCART, Chinch,

¹ E.g. Sony STR-DA5000ES

Twisted Pair, Optical, VGA, DVI, etc. is enormous. Most support calls which come through Sony Service are generated by the ‘no problem found’ syndrome. A customer describes the problem: “My new TV does not work”. Commonly, the solution cannot be resolved over the phone. A service technician goes out to fix the problem. Often, the reason is no batteries in the remote controller or the antenna cable is not plugged in. However, the power cord is always connected. This is a natural thing which all consumers understand. If application data were also to be streamed via this power cord, it will enhance customer satisfaction.

Another application for PLT is Internet access delivery [Dost_01]. Today, most industrial nations are covered quite well by xDSL access via phone lines. The benefit of phone lines is that the number of customers sharing a line is less than that of a powerline. In Germany around 200 houses are connected to each transformer station, which share the communication resources of a single line. Internet access delivery via PLT could be expected to be successful mainly in those rural areas where xDSL is not deployed, or in Third World countries where currently no telecommunication network exists.

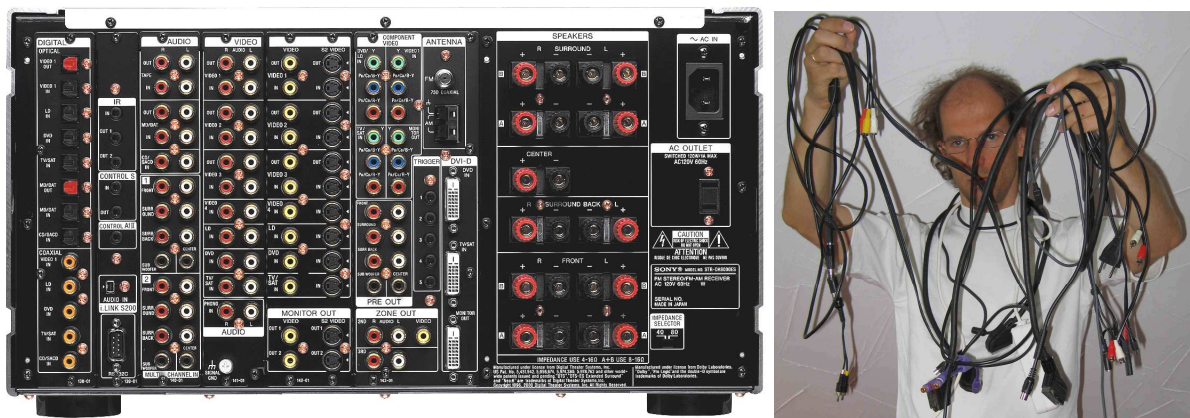


Figure 2: Rear side of A/V receiver with 7.1 Surround Sound¹

Additionally, there is a huge potential for Smart Grid and AMR (Automatic Meter Reading) applications. AMR allows new, flexible power billing scenarios. The price of the electricity depends on the availability of renewable sources such as solar or wind energy. Up to the minute price information could be used to control the usage of heating or air conditioning systems. Performing load balancing by the remotely controlling high energy consuming devices could reduce the need for expensive peak power production. This could help utility companies to reduce the costs of standby power generation, which could be passed down to the consumer. A lot of research funding is currently invested in this area due to the potential reduction in greenhouse gas emissions.

2 Potential of Powerline Telecommunications

The physical characteristics of the communication media should be analyzed before commencing with any new telecommunication application. This allows us to estimate the potential of the technology in terms of data throughput and coverage. If the potential exceeds the requirements [Schw_05d] it is worth considering PLT as a useful candidate for communication. For a reliable in-house communication medium, the coverage is far more important than the throughput rate. E.g. if an HD video transmission (MPEG 2) requires a throughput rate of up to 20 Mbps over the UDP layer, a coverage of such a stream of only 97% is not sufficient. This would result in 3 out of 100 customers returning their new TV sets. The coverage needs to be greater than 99.xxxx % in order to be commercially successful. Finally it should be considered that more than one PLT application can share the communication resources on the wires. Here, the probability of achieving the required throughput rate is analyzed.

2.1 HF Properties of the Mains Network

In order to derive the theoretical communication properties of the powerline wires, the starting point is typically the Telegraph Equations. This approach is frequently found in literature (e.g. [Vick_00], [Schz_03] and [Zimm_00]). Reproducing the complex wiring structure of a building with all connected devices in a calculation and respecting Maxwell's equations in material the approach becomes highly complex.

In this investigation, the properties of the powerline wires are found by using empirical measurements in buildings and statistical analysis.

2.1.1 Measurements in Buildings

In order to determine transmission characteristics and properties of the PLT channel, extensive measurements were carried out in various buildings in Spain, the Netherlands and Germany. Some of these measurements were performed by the ETSI STF 222 [Schw_02]. STF222 generated the TR (technical reports): [ETSI_03a], [ETSI_03b], [ETSI_03c], [Schw_03a], [Schw_03b] and [Schw_04b]. A detailed description of how the measurements were performed and statistical analysis of the results are described in the ETSI TRs.

Important measurement parameters are:

- Attenuation:
 - between 2 outlets within a flat or house,
 - to an outlet in the flat or house of a neighbor and
 - across phases
- Noise
- Radiation (coupling factor k_{sym} : radiated E-Field measured in the outside related to the differentially fed signal to an outlet in the building. This quantity is defined in [ETSI_03a])
- Impedance
 - Differential Mode: Z_{DM}
 - Common Mode: Z_{CM}
- Return Loss
- Differential Mode to Common Mode conversion e.g. Longitudinal Conversion Loss (LCL, defined in [ITUT_96] and [ETSI_03a])

The results of the measurements can be summarized as median values for the important parameters:

	50% (median) value for the frequency range of 1-30 MHz
Attenuation within flat (Att)	42 dB
Crosstalk between phases additional to single-phase installation	12 dB
Additional Isolation from / to neighbor (located in the same building)	>19 dB
Noise Floor (Noi)	11 dB(μV) ($RBW = 9$ kHz, Avg. Det.)
Return Loss	7 dB (20% power loss at coupler due to impedance mismatch)
Impedance Z_{DM}	102 Ω
Impedance Z_{CM}	230 Ω
Longitudinal Conversion Loss LCL	33 dB
coupling factor k_{sym}	63 dB($\mu V/m$)-dBm

Table 1: Median results of measurements on powerlines

Summary of the results:

Today's PLT modems with a feeding PSD (power spectral density) of $P_{\text{feed}} = -55 \text{ dB(m/Hz)}$ have a dynamic range of up to 90 dB. The median attenuation in buildings of 42 dB is almost half of the total dynamic range of PLT modems. The additional attenuation caused by the polyphase installation in Germany of 12 dB affects the throughput of a PLT modem, but it is not a significant obstacle for such a technology when the total dynamic range is taken into consideration.

It is difficult to give any statistical numbers for the additional attenuation to a neighbor. Today's network analyzers have a dynamic range of up to 120 dB. Roughly speaking, if the neighbor lives in a separate house with a garden, the attenuation to his outlets is higher than the dynamic range of the measurement equipment. Practically, if the receiver does not detect the transmitted signals during a measurement campaign in the field, this combination of outlets is not included in the data collection. Therefore, the 19 dB value presented in table 1 is calculated from the values of pairs of outlets where signals from the feeding outlet were detected. It shows that statistically there is some additional attenuation to the neighbor, but a potential crosstalk from the neighbor's flat should be expected by a PLT system. Interference from a neighbor is only possible when the attenuation is smaller than the dynamic range of PLT modems, and when the signal received from the neighbor's PLC system is larger than the local noise floor. Such cases were only found in multiple apartment buildings. Here, the average size of an apartment affects the level of coupling. For example in Japan, where apartments are statistically smaller than in the US, the attenuation to neighbors is also expected to be smaller. However, if the flats are smaller, the lengths of the powerline wires inside the apartments are also shorter, reducing the attenuation. In such a case, a PLT modem might reduce the transmission power in order to minimize interferences. The potential of interference to a neighbor would be identical for everyone. Coexistence between PLT systems will be discussed in chapter 4 of this thesis.

The background noise levels are frequency dependent. [Schw_03a] describes a detailed analysis of measured noise level in buildings. Figure 5 in [Schw_03a] plots the cumulative probability of exceeding a noise level depending on the frequency. The needles of the ingress of short wave radio broadcast signals cause narrow band interference to PLT, however these can be easily identified in the radio transmission bands. The benefits of these phenomena are discussed in chapter 5. Additionally, the background noise becomes exponentially large in the lower frequencies. Many noise sources such as switching power supplies create a noise spectrum which drops in amplitude toward the higher frequencies. Furthermore, the lower the frequency, the lower the attenuation of the wires. The accumulation of many noise sources at low

frequencies from various mains appliances in the neighborhood generates the unwanted background signals. In order to immunize against interference from noise, PLT modems have to implement forward error correction algorithms, which typically consist of interleavers in the time and frequency domain as well as block and convolutional coders. Usually, PLT modems are designed to have their minimum sensitivity set to somewhat lower than the average background noise found in buildings.


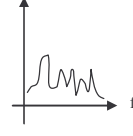
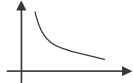
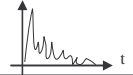
	Time of occurrence	Source	Characteristic
Narrow Band Noise	Always constant, depends on fading	Radio Broadcast, Amateur Radio Transmission	
Wideband, continuous working Noise	Remains for long time, often periodic	dimmed light or switching power-supplies	
Occasional Noise	Occasionally	injected by tram or train, temporal used devices like drill, inductive cooker	
Background Noise	Permanent, changes on day or week time	accumulation of hundreds of noise sources	
Impulsive Noise	Very Temporal, very short time	light switch	

Figure 3: Overview of noise characteristics

[Baig_03] describes many noise sources on powerlines. In this thesis a collection of many noise recordings is given, which include statistics on day and week time variations of the noise. Various appliances were monitored and classified. Such a database might be used to stress PLT modems during performance tests or to implement a PLT system which is robust and immune to such interferers.

Differential Mode Impedance Z_{DM} and Return Loss are closely related. Figure 4 shows a screenshot of a network analyzer measuring the complex differential input impedance of a typical outlet. The x-axis goes up to 100 MHz. The y-axis is converted to show the S11 Parameter in Ohms with $100\ \Omega$ per division (yellow line). The blue line shows the phase of the S11 measurement using a scale of 50° per division. It can be seen that good impedance matching at such an outlet is difficult for PLT modems. If the inhabitant of the flat toggles e.g. a light switch, the input impedance will change. Today's configurable analog components must be improved in order to realize good impedance matching. The median return loss of 7 dB related to the source impedance of $Z_{DM} = 100\ \Omega$ gives a good reason to investigate further. The me-

dian Differential Mode Impedance Z_{DM} measured during the ETSI campaign is 102Ω . As PLT modems do not individually adapt to the frequency dependent input impedance of the connected outlet, it is recommended to terminate them with a smooth 102Ω resistance. This minimizes reflection of the feed signals immediately at the outlet, in a statistical sense. [LiQi_04], [Gold_05], [Bull_03] and others investigated impedance matching for PLT modems.

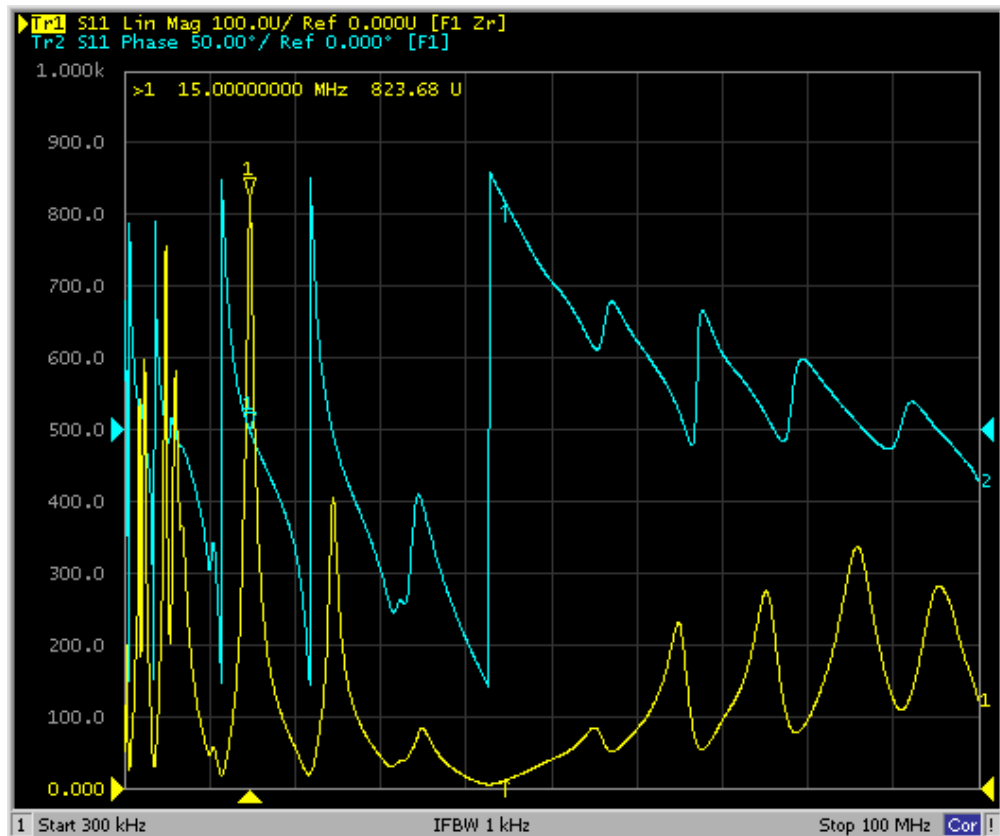


Figure 4: Differential Mode Impedance at a single location into a power plug

Yellow: absolute impedance in ohm. Blue: phase angle of the impedance.

It is important to consider the Common Mode Impedance and Longitudinal Conversion Loss parameters when generating a reproducible environment in the lab in which to test PLT modems. An ISN (Impedance Stabilization Network) has to be created for the assessment of the interference potential of PLT modems (in the frequency range smaller than 30 MHz). From a physical point of view, this ISN should have identical LCL and Z_{CM} properties to those found in real operating conditions. [CISPR_06] proposes several such ISNs. They are used for the assessment of all telecommunication applications. Even though it is quite simple for an engineer to measure the LCL and Z_{CM} parameters in buildings, these values are heavily discussed in standardization bodies such as [CISPR_05].

Instead of reproducing the physical characteristics of the wires with an ISN in the lab, the interference potential of PLT modems could also be measured directly in the field using a coupling factor k_{sym} . The scenario feeds differential mode signals into the mains grid of a building and measures the radiation using an outside antenna. The certification of PLT modems in the US was specified by the FCC using this technique [FCC_04]. Such a coupling becomes relevant in chapter 5.

Many measurement campaigns have been carried out all around the world in order to collect data on the properties of the powerlines [Amem_06], [OPERA_07]. (Unfortunately political interests may prevent many of them from being made public). The statistical results of these measurement campaigns show similar results. The variation of one of the parameters above from one outlet to another outlet is very high, but the variation of the result of a large statistical mass of measurements from one location in the world compared to another location is low. Some differences could be found when countries with installations of 230 V are compared to countries with 110 V installations [Amem_06], due to the larger diameter of the wires, the Z_{DM} is lower in 110 V installations.

2.1.2 Impedance Modulating Devices

Powerline channels are usually quasi-static. Of course, the noise is time-variant, but the channel itself only changes if a user switches on a light or plugs in or removes a device from the power supply. The changes in network topology are caused by a complex impedance added to or removed from the network. It will affect one of the multiple reflections of the channel. Usually, it is unknown if the channel improves or becomes worse when it changes. PLT modems adapt their communication settings to the changing channel conditions (see chapter 5.2.5). This quasi-static channel would be a nice situation for PLT modems. Unfortunately, the world is not that simple.

Small sized power supplies, which do not embed a heavy power transformer, contain bridge rectifier diodes and a blocking capacitor delivering the DC directly from the 230V AC. A switching element then generates the alternating current for the voltage transformation. Some devices control the frequency of the switching element by the load (power consumption) of the low voltage on secondary side. The bridge rectifier diodes and the DC blocking capacitor depicted in figure 5 are harmful to PLT.

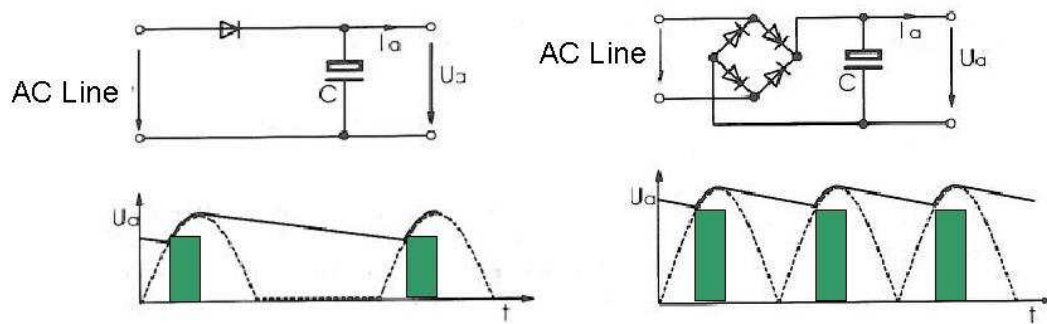


Figure 5: Schematic of power supply. U_a in time domain.

The rectifier diodes conduct during charging periods of the capacitor. Depending on the impedance of the circuit behind the bridge rectifier diodes, the high frequency signals of PLT might be shortcut. If the diodes are in blocking mode, the device has a different input impedance compared to the conducting mode. Depending on whether one or four diodes are used, the impedance of the mains changes twice every 10 ms or 20 ms in a 50 Hz installation. The power consumption of the connected load defines the duty cycle of such an impedance modulation. For PLT, this causes a Line Cycle Periodic Time Variant Channel. Today, such power supplies are commonly used in mobile phone chargers, power supplies for notebooks or energy saving light bulbs.

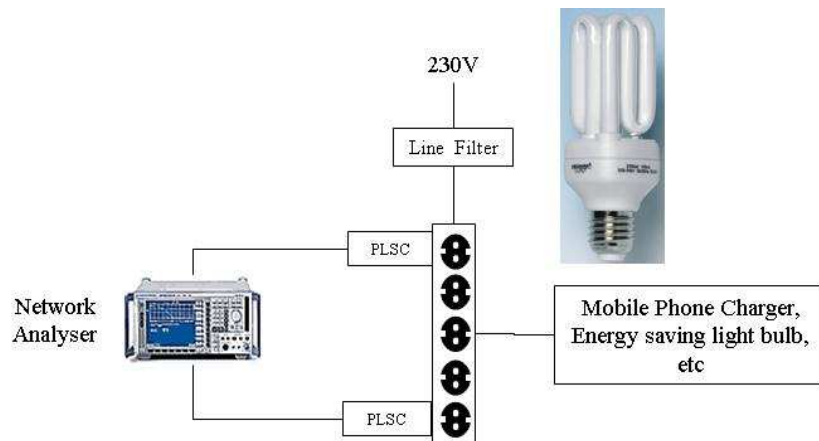
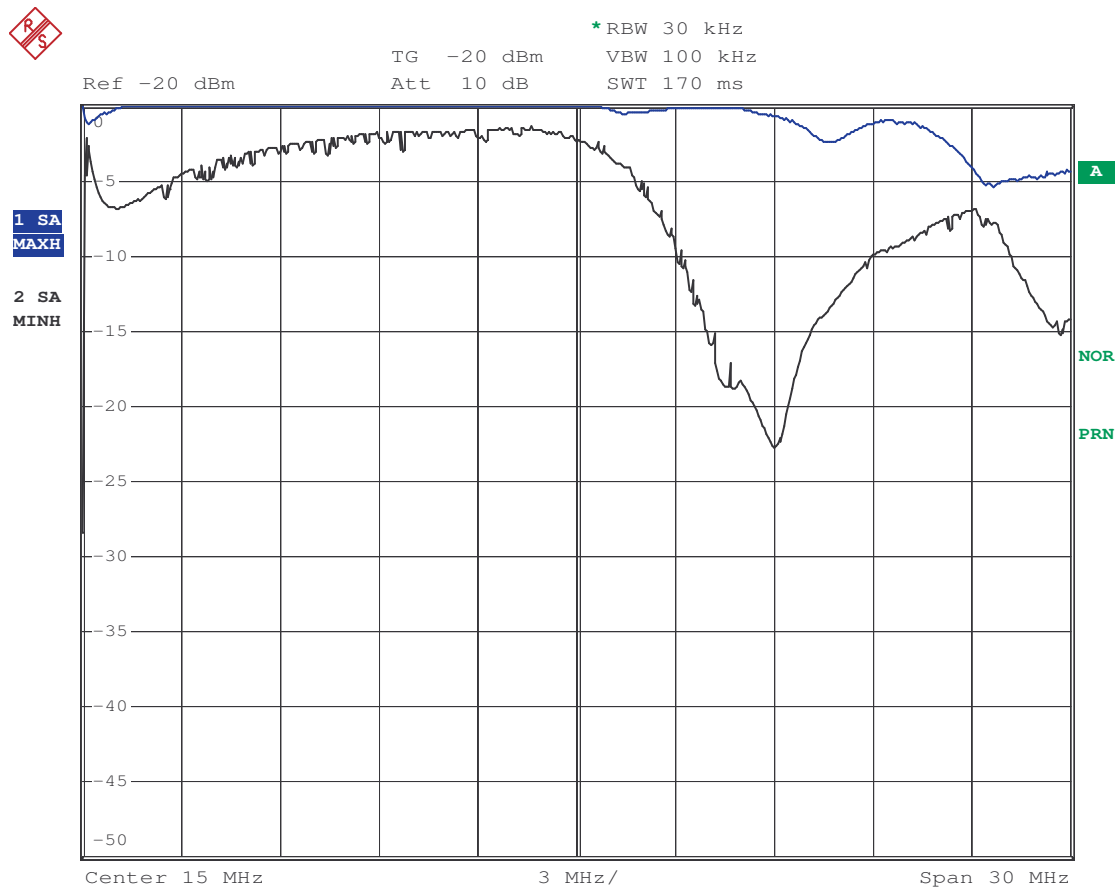


Figure 6: Measurement setup to verify effects of impedance modulating devices

The effects on PLT can be verified using the setup shown in figure 6. A network analyzer connected to the test channel using 2 PLSC (Powerline Signal Couplers) measures the changes of the channel transfer function. A line filter isolates the test channel from the outside. This filter has high impedance at the frequencies of interest. Figure 7 visualizes the S_{21} of the PLT channel on a multiple outlet extension. Frequency sweeps are performed with 2 traces: one (blue) with the max-hold function, the other (black) with the min-hold function. Here, the de-

vice toggling its input impedance causes impact on the PLT channel of more than 20 dB at 21 MHz, in this particular example.



Date: 3.JUN.2005 10:50:13

Figure 7: Outcome of an impedance modulating device in frequency domain on a PLT channel. X-axis goes from 0 Hz to 30 MHz. Y-axis represents the attenuation using a scale of 5dB per division.

A network analyzer configured to perform sweeps in the time domain with a frequency span of 0 Hz helps to show the impedance modulating effect. Figure 8 shows the result for S_{21} of the time sweep measurement at the frequency $f = 23\text{MHz}$. A mobile phone charger was used as an impedance modulating device. It is visible that the channel changes are synchronous with the 50 Hz line cycle. (The period is 20 ms.) The impedance of the device changes twice every line cycle period. The black trace is recorded with the batteries of the mobile phone fully charged, in order to reduce the load connected to secondary side. The blue trace is recorded with the batteries of the phone in charging mode, resulting in a higher load. This can be identified at the duty cycle of the two traces.

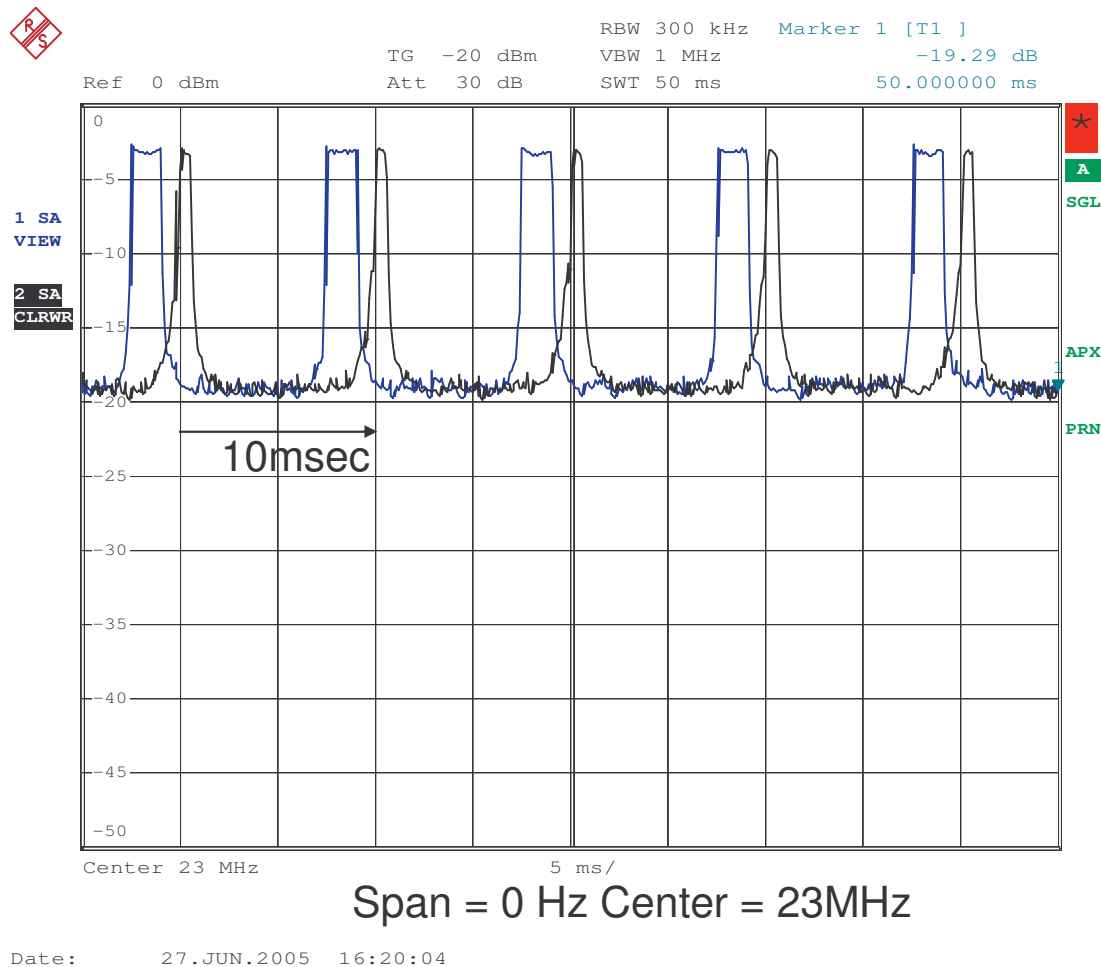


Figure 8: Behavior of an impedance modulating device in time domain. X-axis is scaled in 5 ms per division. Y-axis represents the attenuation using a scale of 5dB per division

The measurement results presented in figure 7 and figure 8 is an example which depends on the channel, the length of the used wires and the impedance modulating device.

Additionally, [Corr_06] studies the line cycle dependent behavior of the powerline. It includes consequences on the noise, the channel transfer function and the impedance of the mains.

For PLT, this causes transmission channel characteristics to change four times for every line cycle period. It is a LCPTV (Line Cycle Periodic Time Variant) channel. It is beneficial that the impedance toggles between two channel conditions. The channel changes, but returns to the previous channel conditions. A PLT modem might perform with one constant channel estimation setting and use the FEC for correcting the bits captured during the time period when the other channel is present. (For channel estimations and adaptive modulations of PLT modems see chapter 5.2.5.) Furthermore, in order to reduce the bit error rates, a modem could

measure when the channel changes and the MAC layer could shift the data transmissions into constant channel periods. Additionally, a MIMO (Multiple Input - Multiple Output) time coding scheme such as Alamouti improves the immunity of PLT modems in the presence of LCPTV channels. The Alamouti scheme for PLT was analyzed in [Schw_08a].

2.2 Theoretical Channel Capacity

The capacity of data throughput of powerline can be derived from the HF data obtained in various measurement campaigns. This is an important factor in helping to decide whether powerlines are a useful medium for in-house data communication, Figure 9 shows measurement results (attenuation and noise) of a sample PLT channel in a private building. The horizontal axis represents the frequency range from 0 Hz up to 30 MHz and the vertical axis represents the PSD (power spectral density) of the signals. The red line is the feeding PSD of a PLT modem, $P_{feed} = -55$ dB(m/Hz) in this example. After subtracting the channel attenuation from the transmitted signal, the green line marks the received level. The red area is the loss within the cables, within the attached equipment and is due to radiation. For this example, a channel with relatively high attenuation was selected. The measurement was conducted in a ~ 150 m² flat with a three-phase installation. Fading characteristics in the frequency domain (of more than 50 dB) are visible and caused by many reflections at wire stubs and connected devices. The blue line is the noise recorded at the receiving outlet. The green area between the received signal and the noise indicates the *SNR* (signal to noise ratio) which PLT could use for communication.

Care must be taken when comparing results from absolute values measured in this way. Spectrum analyzers or oscilloscopes are usually very good at relative measurements. Network analyzers are intended for making measurements in a closed environment, without additional signals from the outside. It is difficult to isolate a building from the outside. The noise generating devices inside the building might be switched off during the measurements, which could influence the frequency transfer function. In order to prevent signal ingress from the outside an isolation chamber has to be constructed around the building. In an open environment, the signals received by the network analyzer must be greater than the noise signals, otherwise the measured data are influenced by the noise.

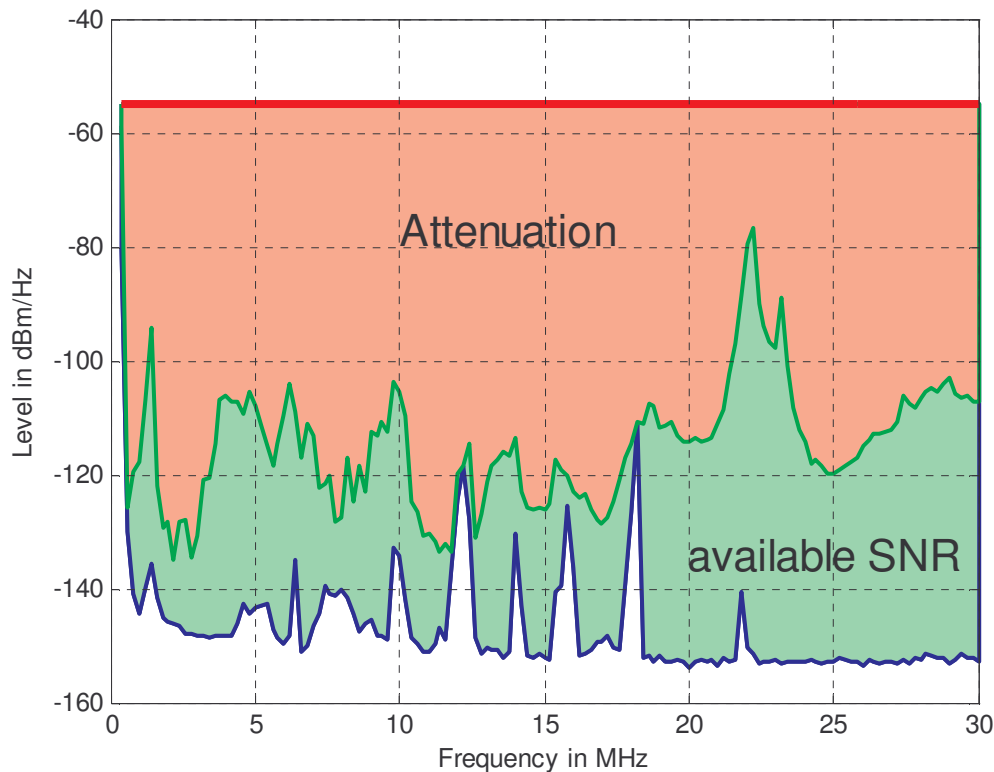


Figure 9: Attenuation and noise of a PLT channel

Furthermore, the signal transmitted by a PLT modem has different characteristics in time or in frequency domain to that of the noise signals.

- In time domain, PLT modems send burst data with an unknown duty cycle. Spectrum analyzers offer a wide selection of detectors to record time variant data: Peak, quasi-peak, RMS, average and sample. The selection of the detector influences the measured results. Using the sample detector, the result value is not reproducible because it could be any value between the min and max values which is captured. The peak detector has the maximum weighting factor as it only records the signal peak value, ignoring any quiet signals within the sample interval. The average detector weights periods with signals and without signals equally. Quasi-peak and RMS are in between peak and average with a weighting factor specified in the standards for measurement receivers and spectrum analyzer CISPR 16-1-1 [CISPR_99]. In analog receivers, the psychophysical annoyance of the interference interpreted by humans gives parameters to define a weighting factor. The quasi-peak detector was invented to cover this subjective effect for AM bands. Nevertheless, the subjective effect depends on whether the receiver is acoustic or visual. In digital receivers the interference is measured by the BER, which is minimized by error correction codecs. Both noise and signal levels are compared in order to calculate the theoretical

channel capacity. Here, a digital communication signal protected with FEC is to be compared with a noise signal recorded by a spectrum analyzer. None of the available detectors weights both levels correctly. The average detector was chosen because of its balanced weighting of periods with and without signals. Compared to quasi-peak, the average detector is also fast and useful for sweep measurements [CISPR_99].

- In the frequency domain, the spectral behavior of a notched PLT signal (see chapter 5) differs from any noise signal found in a building. Noise signals do not show deep frequency exclusions or notches. An OFDM spectrum usually has a flat shape at the top, similar to a rectangle seen on a spectrum analyzer. A resolution bandwidth of 9 kHz was chosen for the measurements described here, because it is smaller than the OFDM carrier spacing of today's PLT modems and provides acceptable sweep timings for e.g. a 30 MHz span. The video bandwidth was chosen to be larger than 30 MHz, in order to record all signals within the desired frequency span.

The noise spectral density NSD in $\text{dB}(\mu\text{V}/\text{Hz})$ is calculated from the measured noise and resolution bandwidth RBW of the measurement equipment:

$$NSD = Noi - 10 * \log_{10}(RBW) \quad (1)$$

The noise power spectral density $NPSD$ in $\text{dB}(\text{m}/\text{Hz})$ is derived using Z_{DM} and Ohm's law. The probes used for all differential mode measurements used in this thesis have an impedance Z_{DM} of 100Ω .

$$NPSD = 2 * NSD - 10 * \log_{10}(Z_{DM}) \quad (2)$$

The transmit signal level must be specified in order to calculate theoretical channel capacity. Today, the maximum transmit PSD of PLT modems is under discussion in regulatory committees. In contrast, maximum PSD levels have previously been set individually by each country. Ideally, [CISPR_05] will find a compromise which can be accepted worldwide. Here, PSD_{feed} of $-55 \text{ dB}(\text{m}/\text{Hz})$, $-67 \text{ dB}(\text{m}/\text{Hz})$ and $-93 \text{ dB}(\text{m}/\text{Hz})$ is used to provide some comparisons with feeding levels.

If noise $NPSD_{receive}$, attenuation Att and feeding PSD are known, the SNR is calculated by

$$SNR = PSD_{feed} - Att - NPSD_{receive} \quad (3)$$

In [Shan_49], Shannon presented his theorem to calculate the maximum theoretical throughput (Capacity C) for any communication channel:

$$C = \int_{f_{Start}}^{f_{Stop}} \log_2(1 + SNR_{lin}) df \quad (4)$$

Using the settings described above for the measurement equipment, many noise and attenuation sweeps were recorded in the frequency range up to 30 MHz. The attenuation sweeps are combined with noise measurements of the receiving outlet to generate figure 10. A total of 519 capacity calculations are incorporated in the plot.

The cumulative probability or CDF (cumulative distribution function) of the channel capacity is presented in figure 10. The horizontal axis shows the theoretical data throughput from 0 to 800 Mbps. The vertical axis on the left side represents the CDF. The likelihood of achieving a certain throughput is reciprocal (right side vertical axis). From figure 10, the 50% value of the feeding PSD of -55 dB(m/Hz) is read to be 360 Mbps. In other words, a PLT connection between every second combination of pairs of outlets will provide a theoretical capacity of 360 Mbps. More interesting than the 50% point is the lower left corner of figure 10, which indicates the coverage to achieve any connection with a minimum throughput. For example a MPEG 2 encoded video stream (which is transmitted, today e.g. via DVB-S and forwarded via PLT in-home network) requires a throughput rate of up to 20 Mbps on the UDP layer. The MPEG stream is encapsulated in UDP frames. Due to overhead of the IP protocol stack, the MAC layer, the encoding of the FEC, the OFDM guard interval and the phy layer preamble (channel estimation, time- and frequency sync of OFDM), such a transmission requires a raw data rate of around 50 Mbps on the physical layer. According to figure 10, the 50 Mbps are available in 97% of all PLT links in private homes. This would result in a return rate of 3% of HDTV devices offering video streaming via powerlines. If a lower PSD such as -93 dB(m/Hz) (blue curve, derived out of [BNetzA_01]) is used by PLT - which was proposed to the regulatory committees - 1 out of 5 combinations of outlets will not provide any link or connection. The blue curve still shows zero Mbps with a cumulative probability of 0.2. In this case, the two PLT modems would simply not 'see' each other. A transmission of an HDTV video stream would then be possible in 45% of outlet combinations.

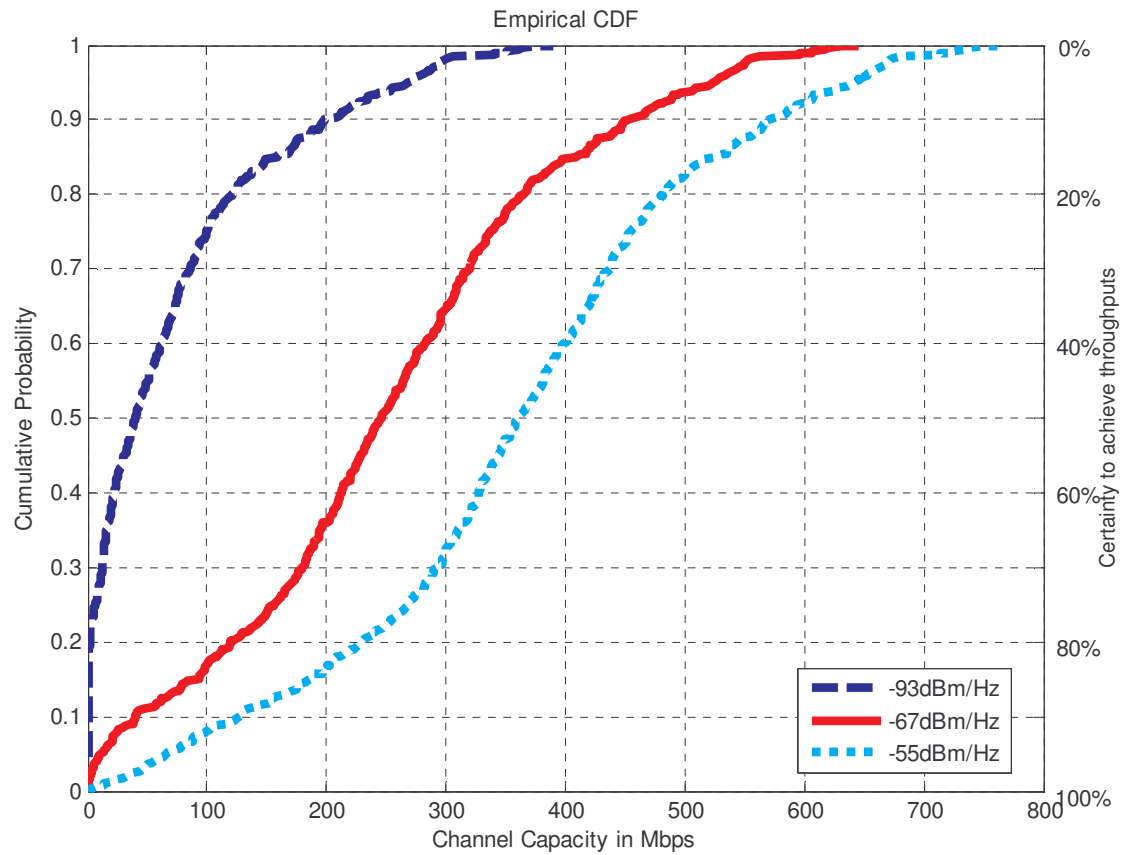


Figure 10: Cumulative channel capacity by different feeding power levels. X-axis shows the throughput rate in Mbps. Left y-axis is the cumulative probability factor to achieve this throughput. Certainty is plotted on the right-hand y-axis.

If there is more than one active powerline communication link within a building, the channel capacity must be shared which will reduce the resources available to a single PLT link.

Such coverage raises the motivation to improve today's PLT technology. In chapter 3, a forecast is given for the development of PLT modems in the future. In particular, the use of MIMO technologies (described in chapter 3.2) will significantly increase the coverage of highly attenuated (low bit rate) connections.

3 Outlook for Next Generation PLT Modems

In near future, PLT modems will improve their performance by using constellations higher than 1024 QAM, more efficient FEC codecs like Low-density parity-check code [LDPC], using the frequency range above 30 MHz and adopting MIMO technologies. The latter two are expected to provide most of the improvements and are analyzed in detail below.

3.1 Frequency Range $f > 30\text{MHz}$

Today's PLT modems use a frequency range up to 30 MHz. This is not a physical limit. In principal, analog to digital converters become more expensive at higher frequencies. However, the 30 MHz limit is due to the regulatory barrier at this frequency as specified in [CISPR_06]. Anechoic EMC chambers are not designed to measure at lower frequencies. Rules to assess the interference potential of telecommunication devices change from a conducted assessment in $f < 30\text{ MHz}$ to a radiated assessment in $f > 30\text{ MHz}$. (Today's PLT modems are assessed using an ISN. If they would operate above 30 MHz, the radiated field would be responsible for EMI assessments according to [CISPR_06].) In the meantime, several standardization bodies such as IEEE P1901 [IEEE_09] or ITU-T G.Hn [GHn_08] specify systems in the higher frequency range, but as of today, most PLT products on the market do not use this range.

Again, the first step when entering a new field is to perform measurements in this area to check if it is suited for PLT. Table 2 presents the median results of the interesting parameters of measurements in the frequency range from 3 MHz up to 100 MHz.

	50% value (median) for the frequency range of 3-100 MHz
Attenuation within flat (Att)	47 dB
Crosstalk between phases additional to single-phase installation	5 dB
Additional Isolation from / to neighbor	31 dB
Noise Floor (Noi)	4 dB μV ($RBW = 9\text{ kHz}$, Avg. Det)
Coupling factor k_{sym}	45 dB($\mu\text{V/m}$)-dBm

Table 2: Measurement results in the higher frequency range

Comparing the results from table 1 to table 2, some interesting facts are observed:

As expected, the attenuation is higher in the upper frequency range. The median value increases by 5 dB. The additional attenuation caused by crosstalk to another phase is reduced. In this range, the PLT networks in Germany have similar properties to other networks in the rest of the world. The isolation to the neighbor is much better than at the lower frequencies. An additional 12 dB significantly reduces the risk of interferences from the PLT systems installed in a neighbor's flat. It is beneficial for PLT that the noise level decreases by 7 dB. If the isolation to a neighbor becomes better, the accumulation of many noise sources is reduced. At higher frequencies the noise being present at an outlet is mainly generated in the same flat. Finally the coupling factor k_{sym} is reduced by 18 dB. Consequently, if the feeding at higher frequencies is done with the same PSD as at the lower frequencies, there is 18 dB less radiation outside of a building. Of course, care has to be taken not to interfere with emergency services or the FM broadcast frequencies. [Schw_04b] shows details of the measurement tools, settings and a statistical analysis of the measurements in the higher frequency range.

If the attenuation at higher frequencies is slightly higher (disadvantageously for PLT), but the noise is lower (PLT benefits) than at the lower frequencies, a comparison of the *SNR* values will show the motivation of PLT to use these frequency ranges. Figure 11 compares the *SNR* calculated with equation 3 on the basis of measurements in the frequency ranges 3 - 30 MHz, 33 - 60 MHz and 63 - 90MHz.

If the market situation, where current PLT modems use the frequencies below 30 MHz is monitored, it is surprising to see that the higher frequencies are physically better suited for PLT. Considering the additional advantages of having significantly lower interference from any neighbor and less radiation outside a building, the motivation to deploy PLT systems in the higher frequencies is very high. Of course there is no reason to stop at 100 MHz. Although there will also be interferences to FM service in the VHF range they could also be notched by PLT. Details of the properties of PLT channels at frequencies above 30 MHz were published in 2004 in [Schw_04b] and [Schw_05a].

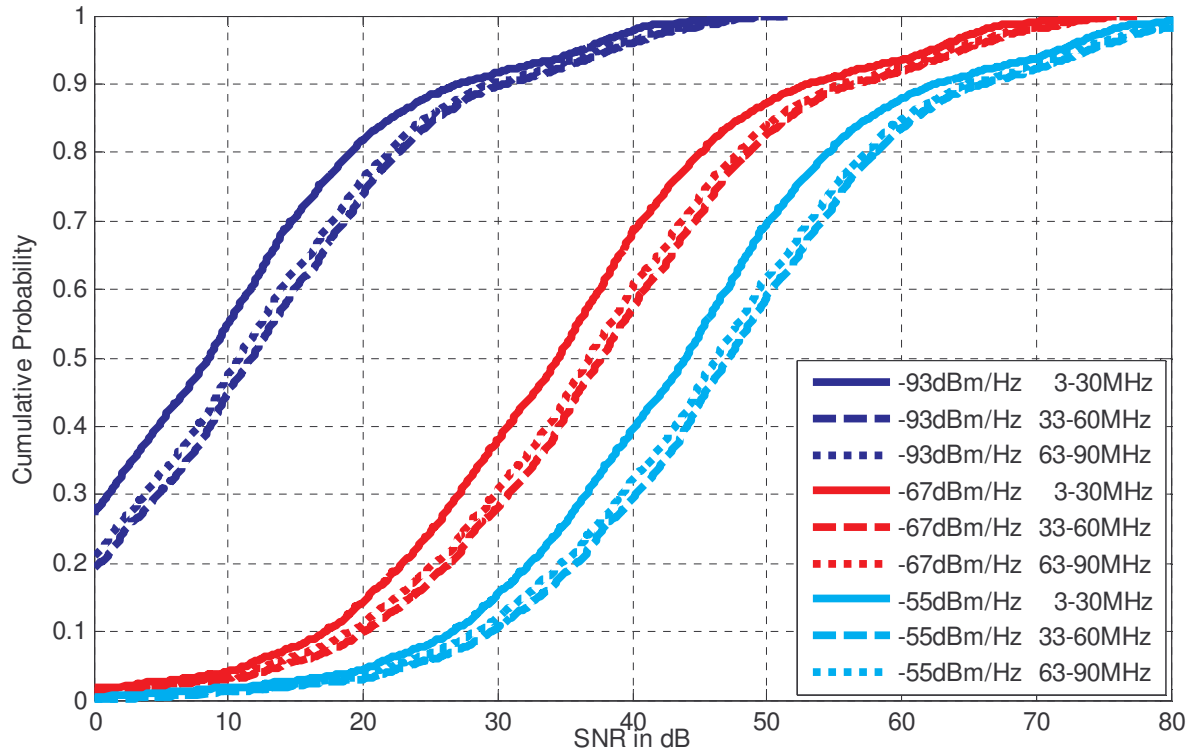


Figure 11: SNR of PLT in 3 frequency ranges and feeding power levels. X-axis shows the SNR in dB. Y-axis is the cumulative probability factor to achieve this SNR.

The new additional frequency resources should be used efficiently. The higher frequencies are more attenuated by longer distances, as shown from measurements and theoretical analysis [Zimm_00]. In order to share the rare communication resources optimally, communication over short distances such as between devices stacked in one rack (HiFi stereo systems, HDD recorders, TV) should use the highest possible frequencies. Communications via medium distances for example within a room or along a wire from one fuse should use the frequencies in the middle of the spectrum. It is expected that in countries with ring installations (UK and Commonwealth) medium distances will frequently be found between adjacent rooms. The lower frequencies shall be reserved to applications carrying data via long distances such as video streaming from a satellite dish mounted on top of the roof to a TV located some floors lower in the building. This should be respected by the PLT interoperability standards. A mechanism which automatically selects the optimum frequency range is described in chapter 4.5.

3.2 MIMO PLT

MIMO, Multiple Input – Multiple Output [Paul_03], [Spei_05] or [W_MIMO] coding is state of the art in many modern communication systems (e.g. [IEEE802.16], [3GPP]). MIMO

systems utilize multiple transceivers for sending and receiving. Draft 802.11n [IEEE80211n] devices utilizing MIMO were already available on the market, even before the standard was approved. MIMO is part of LTE for mobile phones [Dahl_06] and broadcast systems such as DVB-T2 or DVB-NGH. MIMO is also used in wired communication cabling for instance in DSL for near end crosstalk cancellations [Lind_08] or [Gini_00]. As a general rule, wherever MIMO is used, it beats the performance of the SISO (Single Input – Single Output) systems. [Sart_01] is the first known proposal of using MIMO over PLT, but this proposal uses the three-phase cabling to establish multiple channels. Another idea to feed signals to powerline via 2 ports is described in [Khad_03] which uses common mode signals fed onto the mains to cancel unwanted signals that may cause interferences to radio applications. [Khad_03] describes a MISO PLT system. However, outlets in private buildings only use one phase. Even if the building is equipped with three-phase installations like in Germany, the three-phase cable is only used for stoves or boilers.

It is an interesting question whether MIMO could also improve data rates over PLT, if only a single-phase plug is available. However, in Europe, the US and many other parts of the world (with Japan being a notable exception) new electricity installations use 3 wires for connecting a single plug. All flats protected with RCD (residual current devices) must have a separate protective earth wire installed. For example, the protective earth is mandatory for all new installations in Germany since the early 1970's.

The following measurements will demonstrate the benefits of using MIMO over PLT.

3.2.1 Use of Protective Earth

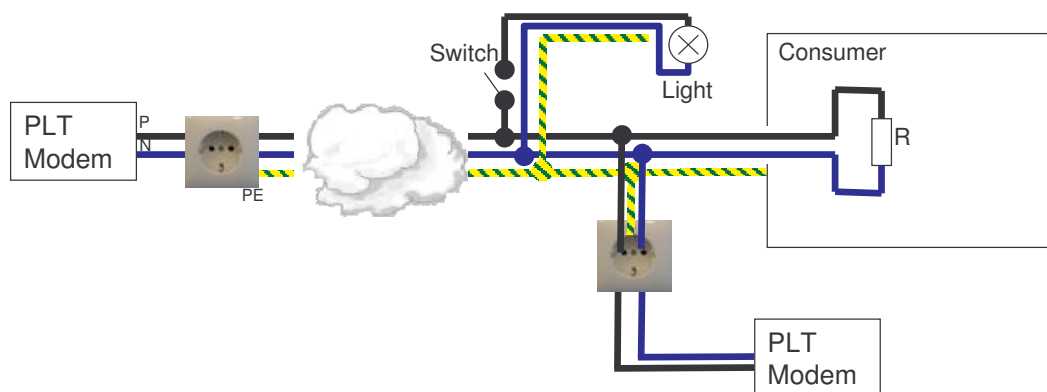


Figure 12: SISO PLT modems connected to the mains

Figure 12 shows an example of a mains installation and use of SISO PLT systems in a private building. In Germany, the phase (or live) wire is colored black, neutral has a blue isolation

and the protective earth is green-yellow. Today's PLT modems are connected to the mains via the phase and the neutral wire. This provides one communication channel when signals are fed symmetrically between these wires. The 3rd wire - the protective earth - is available in most power outlets, but PLT modems don't use it.

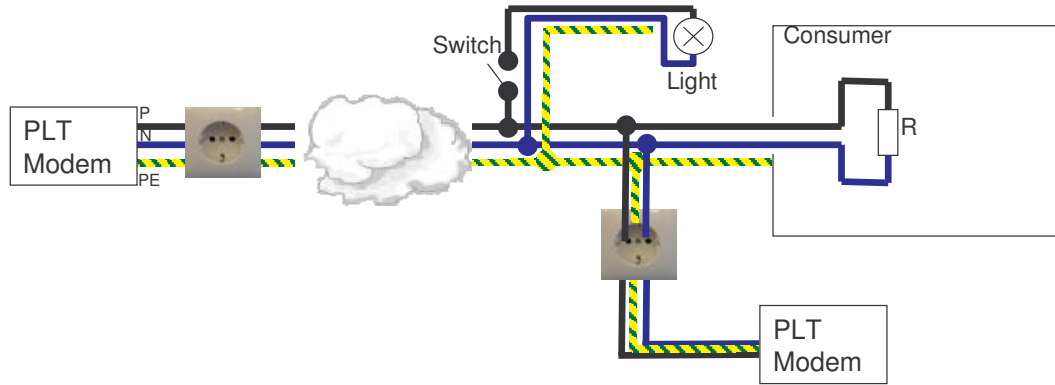


Figure 13: MIMO PLT modems connected to the mains

MIMO PLT modems also utilize the protective earth. This enables them to feed differentially between phase and neutral ($P - N$), phase and protective earth ($P - PE$) and neutral and protective earth ($N - PE$). According to Kirchhoff's law, the sum of the 3 feeding signals has to be zero. Only 2 out of the 3 feeding possibilities can be used independently. The two optimal paths out of the three possibilities can be selected for feeding. A MIMO PLT modem acting as a receiver is able to use all 3 differential channels. The 3rd channel contributes additional performance in all channel measurements performed. Parasitic components inside the coupler enable additional paths for the HF signals.

The protective earth is grounded inside (e.g. at the foundations) or outside (at the transformer station) the building. The grounding has to provide low impedance for the 50 Hz AC power. However, the high frequency signal measurements show the PE wire to be a rather excellent communication path and by no means represent a short-circuit, this is due to the inductivity of the grounding wires.

3.2.2 CM provides another Reception Path

As described above, PLT modems feed their signals U_{DM} symmetrically into the mains. Unfortunately, from a radiations point of view, these DM (differential mode) signals are converted into CM (common mode) signals U_{CM} . According to the Biot-Savart law, the common mode current I_{CM} is responsible for radiations. This is why the feeding of CM signals must be avoided. Figure 14 shows in detail how the DM signals are converted into common mode.

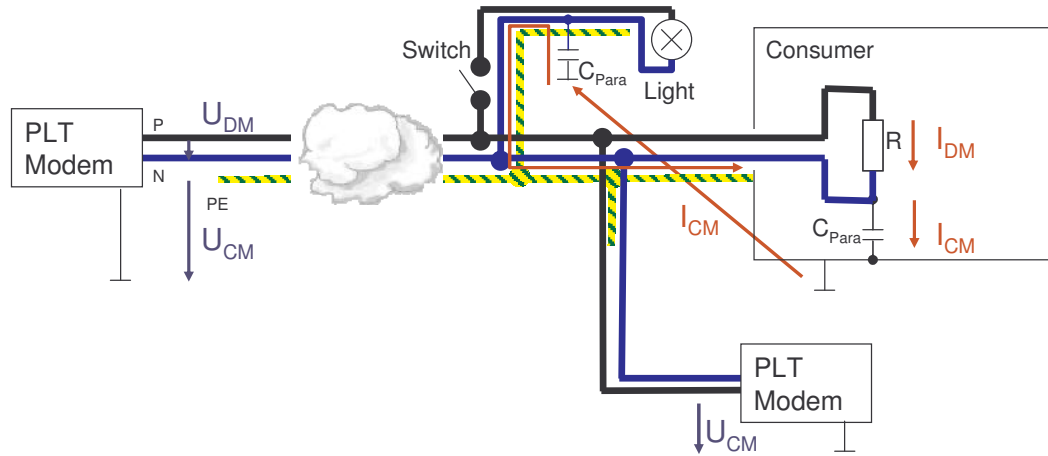


Figure 14: Generation of common mode signals

In a symmetrical network, the differential current I_{DM} flows from its feeding point via the network back to its source. In the case of an asymmetry like parasitic capacitance (C_{Para}), a small part of the RF current flows to the ground or to any other consumer device. I_{CM} may return to its source via any other asymmetry in the network. Normally, there are many asymmetries in any connected devices and also in the mains grid itself. An open light switch is an excellent example of an asymmetric circuit. A measure for the asymmetry of the network is the LCL parameter discussed in chapter 2.1.1.

If the signals are converted to common mode, they propagate over the network. Figure 15 compares the attenuation of CM and DM signals. For each pair of outlets, the DM and the CM attenuation were measured and compared. The number of measurements is quite low, but the results show a clear tendency. The median attenuation of CM signals is 16 dB less than the median DM attenuation. The CM signals clearly find a shorter or a less attenuated way from source to sink. Since [Amem_06] measured LCL values of 16 dB one can conclude that some CM signals arrive at the receiver with higher intensity than DM signals, even if DM signals were injected. This effect is evident in highly attenuated links over a long distance. The unwanted (from a radiation point of view) CM signals can be used as another reception path for MIMO PLT modems.

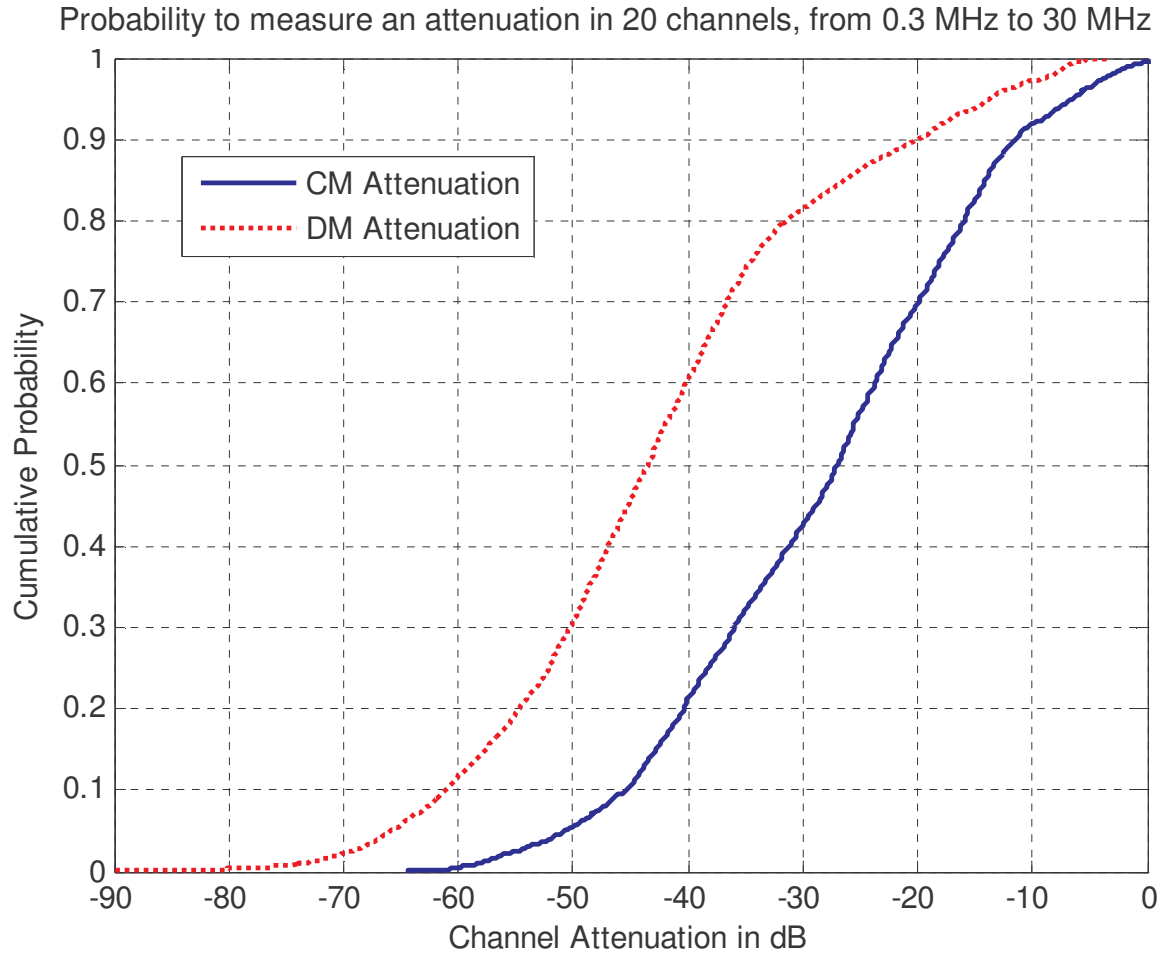


Figure 15: CM and DM attenuation

In order to measure the CM signal, it is necessary to use a large ground plane to provide a low capacitance to earth. HDTV devices consume most of the PLT data in private buildings and are equipped with a large backplane. This backplane could also be used for CM-PLT signal reception. A typical application for PLT is the extension of the access internet link from the phone jack to the TV. Usually, such applications require asymmetric payload traffic. If common mode signals are received in the downlink (from xDSL modem to the HDTV) but not in the uplink, the physical parameters of the MIMO channel support the requirements of the application.

If the MIMO PLT receiver is able to sense CM signals, the MIMO channel matrix expands to 2×4 . As shown in figure 16, the number of individual communication channels increases.

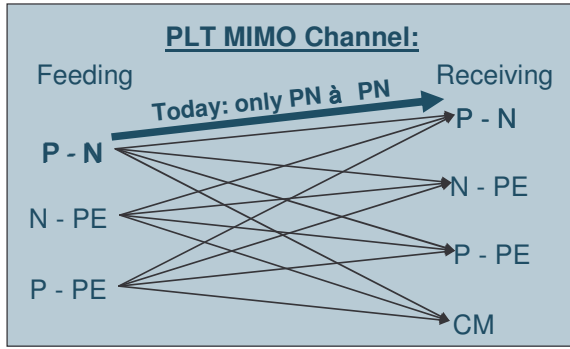


Figure 16: MIMO PLT channel matrix

3.2.3 MIMO PLT Couplers

In order to measure the properties of the MIMO channels, it is necessary to develop new probes. It is possible to arrange the probe in either a star or a triangle configuration. The star probe (or longitudinal coupler) has the additional benefit of providing a simple way to measure CM signals. The triangle style probe (or transversal coupler) has the advantage that it doesn't create any CM signal when used for feeding. In the final implementation of a MIMO PLT modem, it is likely that a combination of both probes will be embedded. The probes used for network analyzer measurements perform a $100 : 50 \Omega$ impedance matching. As measured in chapter 2.1.1 between phase and neutral it is expected to have similar impedance Z_{DM} when the protective earth is used.

3.2.3.1 Star Style Coupler for Receiving

All currents are added at the center of the star style probe. The sum of the currents I_P , I_N and I_{PE} must be zero. This center node is shown on the right side of the schematic in figure 17. The mains are connected at P, N and PE, shown on the left. The 4 receiving signal connectors are marked with S1 to S4. The differential mode signals are terminated with 50Ω .

MIMO coding provides better gain than SISO systems if the individual MIMO paths exhibit maximum diversity. The coupler itself should produce as little additional coupling between the three wires as possible. The CM choke blocks the common mode current from the star transformers. The choke simultaneously acts as a transformer which allows the reception of the CM signal. The load of S4 must be of high impedance, so that the choke function is not compromised. A termination of the CM choke using the impedance matching that of the network would remove diversity from the received signals as well as having a negative impact on the total performance of the MIMO PLT system.

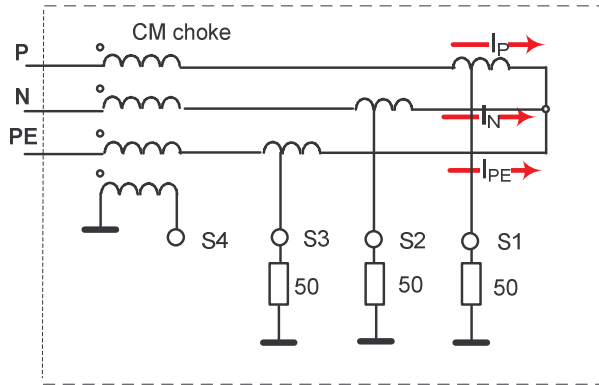


Figure 17: Star style MIMO PLT probe

Due to the possibility of receiving CM signals, the star style probe is used in the receiving modem.

3.2.3.2 Triangle Style Coupler for Transmitting

Figure 18 shows the schematic of the triangle style probe. Its center is located in the loop where the 3 voltages are added. This loop can be identified in the schematic in figure 18 on the left side across the 3 coils. The sum of the 3 voltages U_{P-N} , U_{N-PE} and U_{PE-P} is 0. There is no simple way to receive CM signals using a triangle style probe. The triangle style probe is preferred for the transmitter, because it avoids feeding CM signals into the mains. If the probe is used for signal feeding the 3rd port (S3) is not terminated.

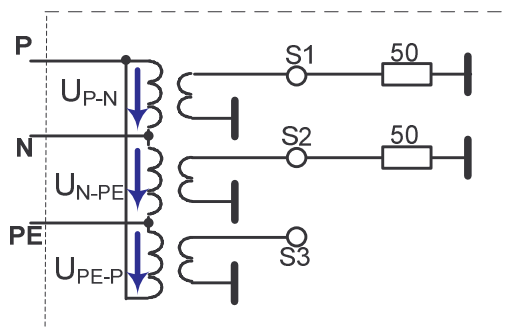


Figure 18: Triangle style MIMO PLT probe

3.2.4 Measurements in Buildings

Safety components to protect human operator and sensitive measurement equipment (as described in e.g. [Schw_03b] and [Gane_03]) are not included into the principal schematics of

figure 17 and figure 18. SHF (super high frequency) range measurement equipment is extremely sensitive, whereas devices whose spectrum ends in the VHF range are much more robust against high voltage peaks. Voltage peaks of more than 1000 V may occur in powerlines, during any switching transition, e.g. during the plugging or unplugging of a probe or if a light switch is toggled. There is a high risk that this could damage the expensive measurement equipment. To protect the devices, switches can be added into the probe's signal lines to the analyzers. These switches must be open during plugging or unplugging of the coupler. Care must be taken to avoid toggling a light switch when measurement equipment is connected. Appliances which toggle their power mode automatically, such as a refrigerator, should be disconnected during the measurement procedure. Alternatively, the complete flat could also be disconnected from the mains. Verification measurements are necessary to ensure that the disconnection does not influence the results. If the master switch is located at a distance from the living unit under test, e.g. in the basement of a multiple dwelling building, this does not usually affect attenuation measurements inside the flat. If the complete flat is disconnected from the mains, the noise generated by devices in the building as well the impedance modulating devices (described in chapter 2.1.2) can no longer be monitored. Finally, the calibration has to be verified one more time when the recordings are complete to ensure that nothing has been damaged during the measurement period.

Once the individual MIMO channels have been identified and the probes created, measurements in buildings can be performed. This would prove whether the idea could satisfy the expectations. Figure 19 shows a snapshot taken during the measurements where a star-style probe is connected to an outlet. The measurements are made with a vector network analyzer. Two star-style probes were used to enable bi-directional measurements. The connector of the CM choke (S4 in figure 17) is unterminated, in order to provide minimum coupling between the individual channels by the choke. The 3 connectors of the differential path (S1, S2 and S3 in Figure 17) were terminated with $50\ \Omega$ during CM measurements. The ground plane for providing a high capacity or low HF impedance to the earth should be as large as possible. However, the measurement procedure becomes physically uncomfortable when the ground plane is too large. Here, the size of the metal plate was almost $1\ \text{m}^2$. A good check to see whether the size of the plate is sufficient is testing to see whether the results are no longer affected by touching the equipment with bare hands. In this case, the capacity of the metal plate is sufficiently large. Adding another capacity by touching the equipment in parallel to the capacitance of the metal plate no longer provides an additional increase in capacitance.

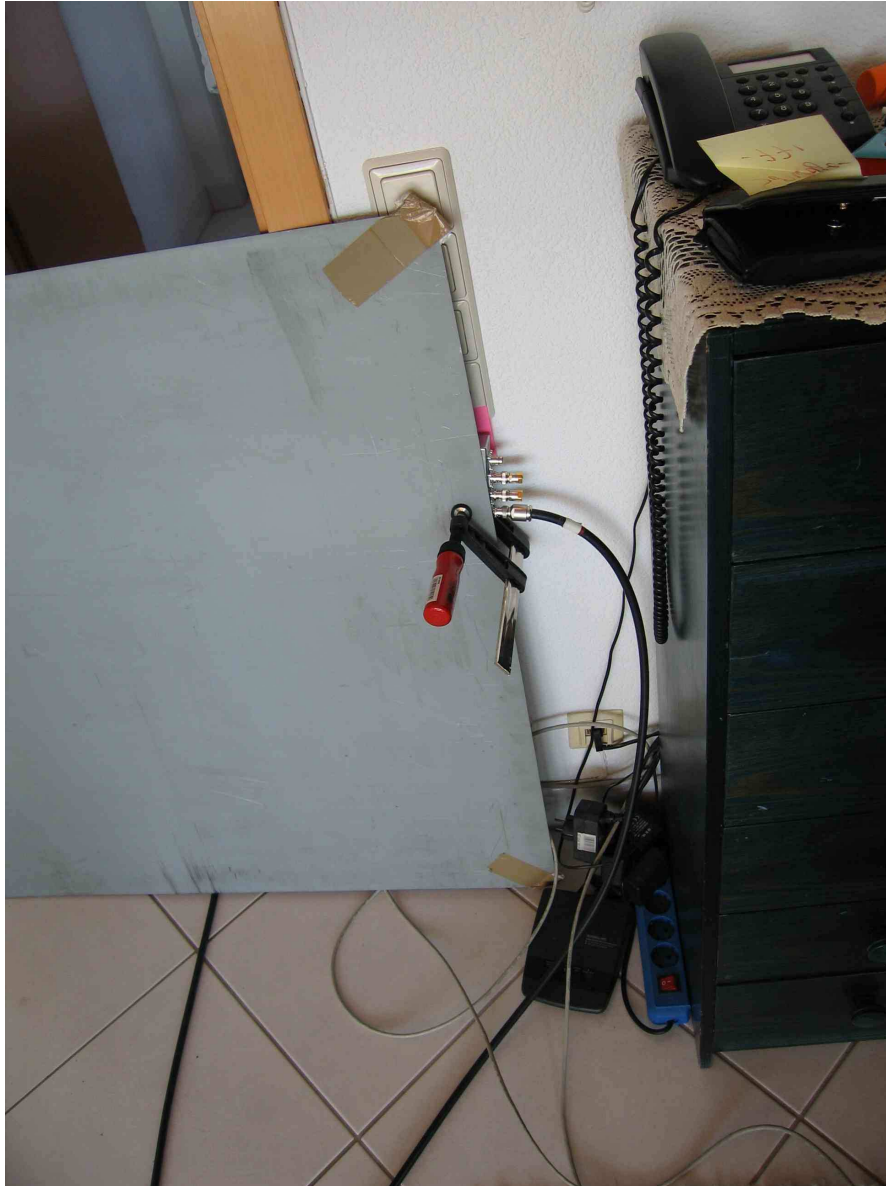


Figure 19: Receiving with a star style probe at an outlet

Measurement results are only as good as the calibration of the equipment used. Special calibration kits had to be created for the MIMO measurements. Figure 20 was taken during the calibration of the throughput measurements. Both star style probes were tightly connected to a large metal plate. In the ‘Through’ calibration kit, all lines are directly connected between the 2 female power sockets. The calibration of the differential to common mode path was performed with a calibration kit where the feeding wire (e.g. P if fed via S1 in figure 17) of the first star probe was split and connected to the 3 wires (P, N and PE) of the second star style probe. All channels were recorded bi-directionally. The differential channels show identical transfer functions on the return path. In a terminated passive n-port network without active components, all channels must be identical if the direction is toggled. If the termination on one side changes, the channel transfer function also changes. This might happen when the metal plate is moved.

The capacity of the metal plate is in parallel to the termination of the measurement receiver or the PLT modem. The capacity depends up on the orientation and location of the plate in the front of the outlet. This results in a change of the CM transmission channels. However, an HDTV is not usually moved once installed in the customers flat.



Figure 20: Calibration of 2 probes for throughput measurement

Figure 21 shows the attenuations independent of frequency of the straight differential MIMO paths ($P - N$ to $P - N$, $N - PE$ to $N - PE$ and $P - PE$ to $P - PE$) in a building in Germany. Surprisingly, the channel between phase and protective earth exhibits the lowest attenuation. An additional burden might be expected on all combinations where a phase line is used, because of the three-phase installations in Germany. In this particular flat, the combination used by SISO modems ($P - N$) doesn't give the best results. SISO PLT system designers might revise the usage of the 3 wires in the AC power plug. (Of course, this has to be verified in more buildings worldwide.) The dotted lines in figure 21 exclusively represent the attenuation to the outlet in the basement. The flat where the measurements were recorded was located on the 2nd floor. There was one additional storage room in the basement. Usually, buildings are grounded in the foundations. The neutral and protective earth lines are connected near the basement outlet (in this 30 year old building). This results in a high attenuation, especially for the low frequencies of the $N - PE$ path.

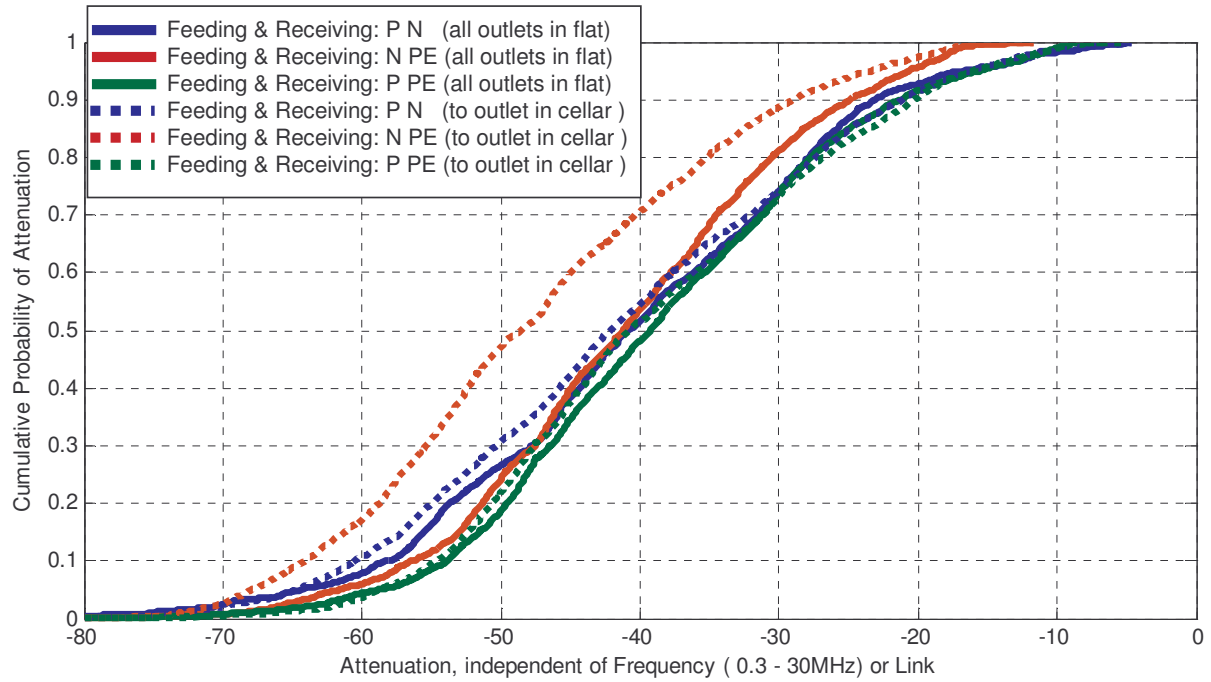


Figure 21: Comparison of straight MIMO channels: P-N, N-PE and P-PE

The frequency transfer functions of all 12 individual MIMO paths between a pair of outlets are plotted in figure 22. The traditional path used by the SISO systems is highlighted in bold magenta. As discussed above, the traditional path only performs best at certain frequencies. Some coupling between the lines is visible. E.g. at 3.5 MHz all lines show a deep fading. At this frequency, the variance of the attenuation between all paths is quite low. At other frequencies such as from 16 to 17 MHz the variance between the individual paths is more than 50 dB. Here, only a small correlation between the signals exists. MIMO performance increases if there is high diversity – no coupling – between the individual paths.

Additionally, the sum of the voltage of the differential received signals is given in figure 22 (bold blue line). The fact that only two of the three feeding possibilities can be used simultaneously is taken into account. The two feeding possibilities were chosen for the blue curve in such a way that the most signal power arrives at the receiver. Of course, a final implementation of a MIMO PLT modem has to consider regulatory circumstances. So, the individual feeding level at one port might be lower than that of today's SISO modems. This reduction could be up to a maximum of 6 dB for each path. Water filling algorithms will inject the optimal amount of power on each transmission port. The effects of water filling for power allocation at MIMO PLT are simulated in [Schw_09]. If a PLT modem is not capable of MIMO coding algorithms, but sums up the power of the analog signals collected by the differential receiving paths, the bold blue line gives an indication of the expected gain compared to the best single differential

path. The distance from the bold blue line to the best single path is significantly higher than 6 dB over wide frequency spans. Therefore, a potential reduction of the transmission PSD will not affect the total picture.

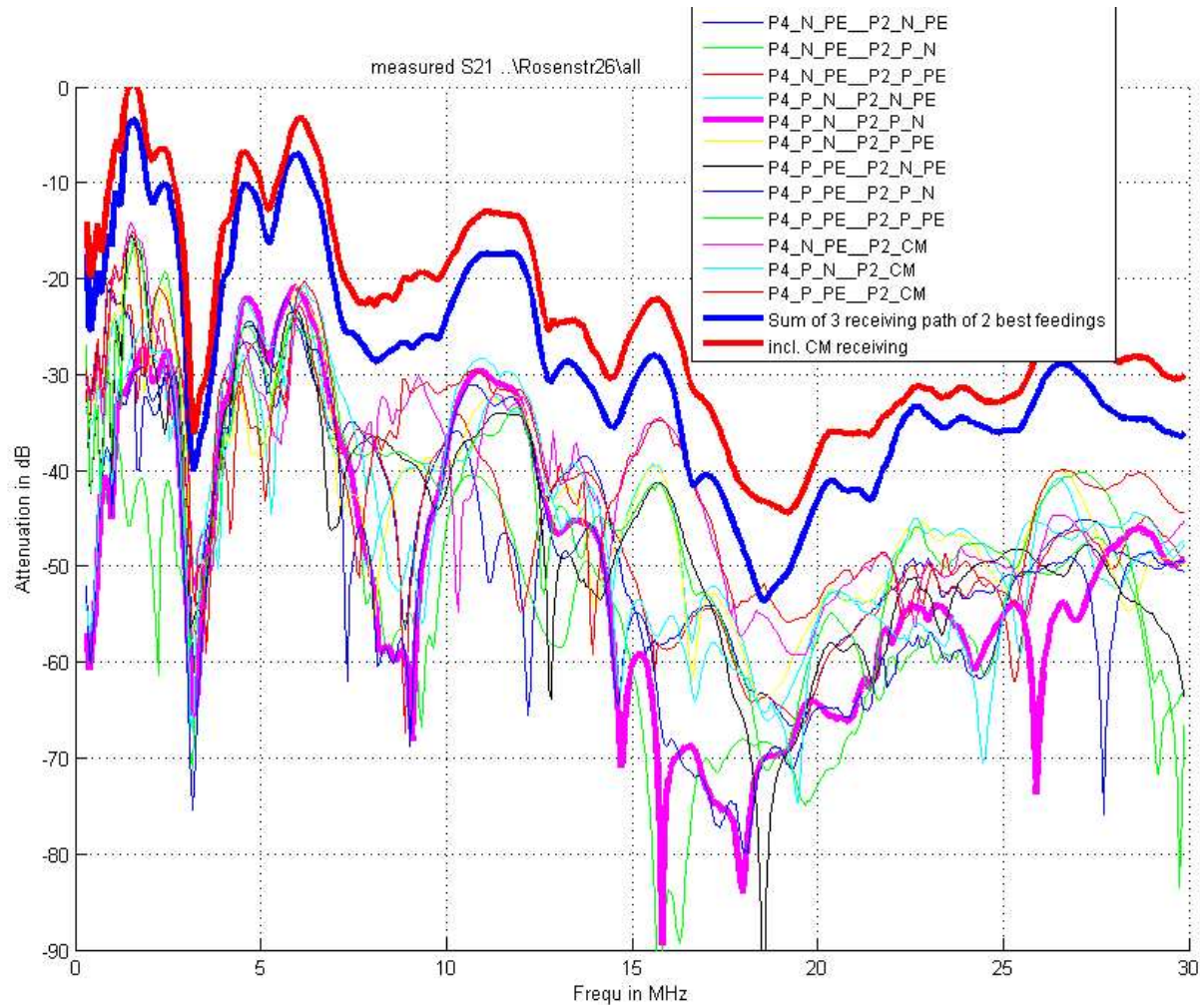


Figure 22: MIMO measurement results, all paths. X-axis is the frequency from 0 to 30 MHz. Y-axis is the frequency response in dB.

The bold red line in figure 22 shows the sum of the four received signals including the common mode signal. It is clear to see the additional gain when effort is spent to receive CM signals.

Additionally, the noise shows some diversity between the four reception paths. The noise level is statistically equivalent on all paths. Noise of electromagnetic fields ingressing into the mains is stronger on the common mode path.

In summary, it is expected that the use of MIMO PLT will result in an increase of the reliability of data transmission. The coverage of PLT in buildings will improve. Poor, highly attenuated links show the greatest potential for improvement, especially when the reception of the common mode signals is possible. A comparison of potential MIMO schemes such as ‘Spatial Multiplexing with Eigenbeamforming’ or ‘Alamouti’ including the calculation of channel capacities was presented in [Schw_08a]. It shows that the gain of MIMO over PLT and the motivation for using it becomes even more apparent.

4 Coexistence between PLT Systems

4.1 Overview

In these early pioneer days of PLT, where no globally accepted interoperability standard exists, several non-interoperable and even non-coexistent PLT systems are on the market. This is similar to wireless transmissions, where systems such as Hiperlan2, Zigbee, Bluetooth, IEEE 802.11 implementations, Radio LAN, UWB, HomeRF and others potentially competing systems have been marketed. Some of these radio systems interfere with each other. In the meantime, each of them has found its niche or application scenario. Finally, the number of different radio systems surviving on the market has reduced, benefiting coexistence.

In the PLT world, there are still new systems with new data formats entering the market. Various systems interfere with each other. In general, one system appears as an unintended noise source to another. Often, even newer revisions of technology from the same manufacturers are not backwards compatible with previous revisions.

In the consumer electronic industry, there is a high demand for standards and interoperability. Customers rightly expect that products from all manufacturers work together well. Compared to the “good old” analog world, digital technologies enable manufacturers to easily develop incompatible systems, accidentally or otherwise.

The recommendation for customers buying PLT systems is to use the same technology when they wish to purchase additional devices. It is not recommended to operate different systems inside one flat due to possible incompatibilities as the likelihood that malfunctions occur is quite high. This coexistence problem is a serious issue, especially between systems operated in neighbor flats, meaning that the selection of the devices is no longer under control of one person.

Some players in PLT industry have attempted to solve the problem by proposing solutions to standardization bodies [IEEE_09]. [Schw_05b] gives an overview of the history of proposals to ETSI PLT. In the meantime, there are many proposals for static or dynamic allocations of communication resources. A static split of resources is simple to implement, but it is often a waste of resources due to its inflexibility. Unfortunately, the dynamic concepts in today’s standardization process (e.g. in [IEEE_09]) are not concepts for pure coexistence, as they require the exchange of some bits of information to synchronize individual networks and to inform

each other which resources are allocated to which device. Such proposals tend to specify a channel of interoperability, not coexistence.

Generally speaking coexistence is realized by freeing unused resources. As required in ETSI TR 102 494 [Schw_05d], any communication demands an amount of space within the cube of time, frequency and power. Only the desired volume of the whole cube of resources should be allocated. A negative example would be if the full frequency span is used all the time with maximum PSD just to indicate that the modem is in operation, without transmitting any data.

This chapter gives a rough overview of how coexistence might be realized between PLT modems in the time or frequency domain. Adaptive power management is introduced, which in most cases solves the uncontrolled interference problems between neighbor flats. Finally, a proposal is presented which provides a dynamic split of communication resources without addressing information from one system to another. This proposal is also applicable to coexistence problems between xDSL and PLT.

4.2 Frequency

The simplest proposal for coexistence works in the frequency domain. In the year 2000, ETSI standardized a split at 10 MHz between access and in-house modems [ETSI_00]. Figure 23 shows a simple representation of the concept according to the standard. The resource split is either static or fixed and does not require any interoperability channel. If an access PLT system only transfers a very low amount of data, the in-house system loses all frequencies below 10 MHz. This results in an unnecessarily high loss of communication resources.

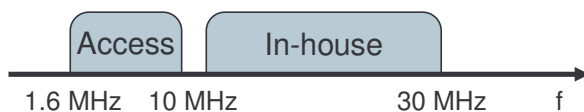


Figure 23: Proposal of frequency split

The sharing of communication resources in the frequency domain could be combined with other concepts as described below.

4.3 Time

Coexistence proposals in the time domain require synchronization. The AC line cycle could be used as a reference in the absence of a sync signal.

CEPCA [CEPCA_05] introduced a signal called CDCF (Commonly Distributed Coordination Function) which can be detected with a correlation operation at the receiver. This signal doesn't need to pass the system's individual demodulation and FEC chain. The signal must be extremely robust compared to all of the channel and noise challenges of the powerlines. The CDCF is transmitted by the master of the participating PLT devices and defines which TDM (Time Domain Units) are allocated to which PLT systems in the next synchronization period (figure 24 and figure 25). A synchronization period or the location of the CDCF and TDM is aligned to the 50 Hz (or 60 Hz) AC line cycle.

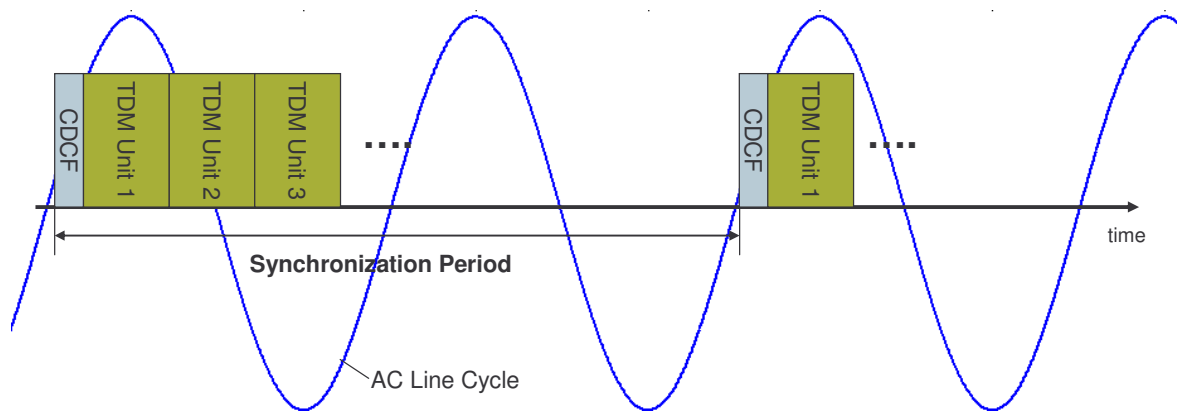


Figure 24: Allocation of time slots for inter PLT coexistence

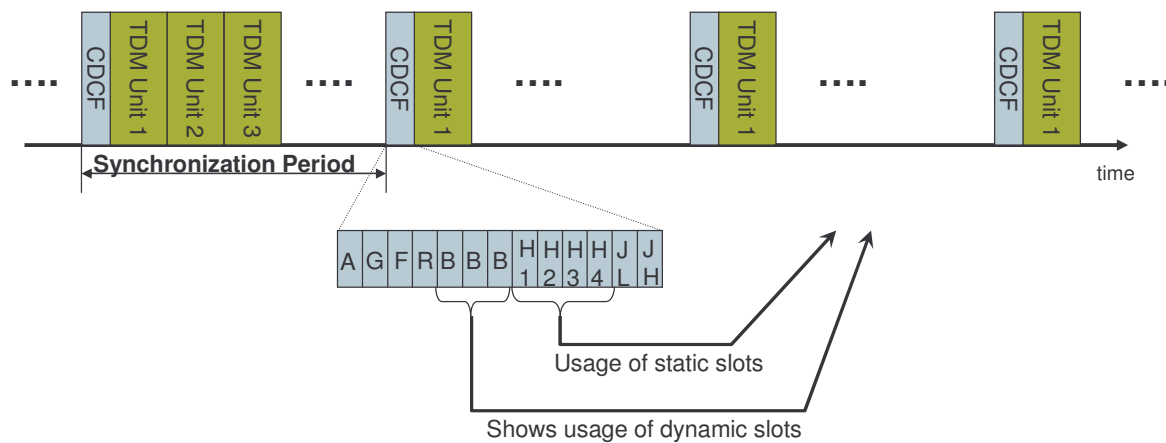


Figure 25: Signaling the usage of time slots

Figure 25 shows that quite a lot of information needs to be distributed among the non-coexisting PLT systems. A synchronization period is aligned to the AC line cycle. These fields are transmitted at specified timings relative to the zero crossings of the AC line cycle. The information is given by allocation of the fields inside the CDCF. The individual fields inside the CDCF are used to show:

- if an access PLT system is present (A)
- if a ITU-T G.Hn [GHn_08] device is present (G)
- if sharing of resources in frequency mode is also supported (F)
- if the actual allocation of resources has to be resynchronized (R) because a new system has been added
- if one of the dynamic slots inside the next TDM unit can be used (B)
- if one of the static slots reserved for in-house systems can be used (H)
- if a system would like to claim additional resources and request a static slot with high or low priority (JL / JH)

Further details can be found in [IEEE_09] for example. A technical report showing test cases of how such a coexistence scenario might be verified was approved by ETSI [Schw_08b].

4.4 Power

In the case of interference, one solution is to share the communication resources, as discussed above. Another way to solve the problem is to reduce the probability of creating interference. This could be done by the reduction of the transmit PLT signal applying adaptive Power Management. This also reduces the probability of interference to radio services. It is possible to calculate the reduction of interference risk using statistical parameters.

The transmit power could be adapted to the attenuation of the channel showing a high spread, which is often strongly frequency dependent. For every application, the communication medium has to reliably provide a certain data throughput rate. PLT modems with a fixed transmit PSD require a transmit level sufficiently high enough to deal with even very poor channels. However, channels are often quite good and the transmit PSD can be reduced in the majority of deployment cases. This would reduce the probability of interference to PLT systems in the neighboring flats as well as to radio services.

Moreover, the transmit PSD might be adapted to the actual data throughput requirement of the application, which is often considerably lower than the maximum modem performance. For this purpose, the modem and/or the system manager continuously checks the margin between the actual throughput requirement and the throughput potential. If the margin is excessive, the transmit PSD can be reduced to the level necessary for reliable transmission.

4.4.1 Adaptation of the Transmit Power to the Channel Attenuation

As discussed in chapter 2.1, the transmission loss of the mains has a very high variance. It is strongly frequency dependent and the average attenuation depends strongly up on the structure

of the mains, the influence of the various electrical apparatus connected to it and the distance between the modems. Hence, today's PLT modems have a total dynamic range of up to 90 dB. About 60 dB are handled by the ADC (analog-digital converter) of the Rx modem and about 30 dB (at least) are managed by an AGC (automatic gain control). In the classical architecture, shown in figure 26, the Tx (transmit) modem always sends with full power and the AGC in the Rx (receive) modem prevents overloading the ADC.

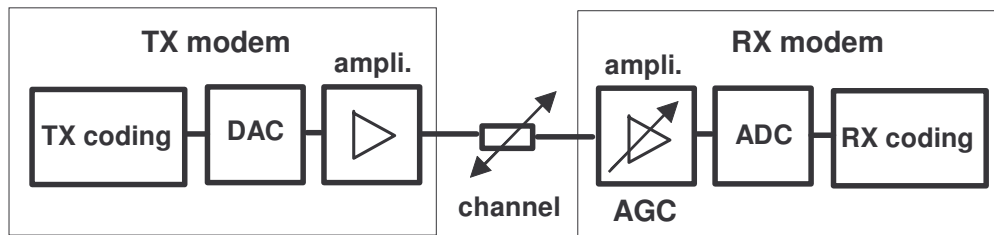


Figure 26: Classical architecture with receiver AGC

The architecture shown in figure 27 is a better solution for the reduction of the interference potential to PLT systems in neighboring flats. If the level of the received signals exceed a certain threshold, the Rx modem requests the Tx modem to reduce its transmit power accordingly. This is also the solution used in state of the art mobiles of cellular radio systems.

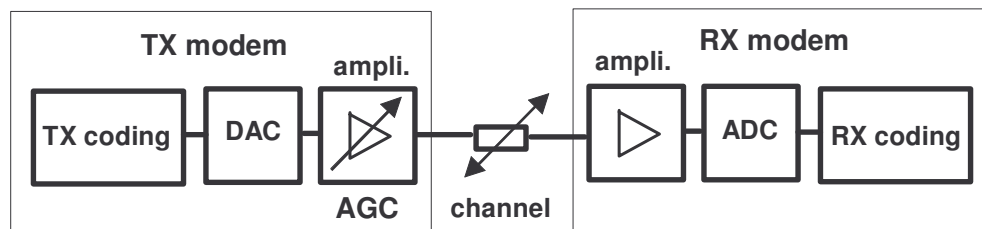


Figure 27: Transmitter AGC for adaptive transmit power management

The AGC has to prevent overloading the receiver ADC with strong signals. Thus, the peak signal response, i.e. the input signal at the frequency with the minimum channel attenuation is controlled by the AGC. The threshold is set to around 30 dB in highly attenuated channels. In case the minimum attenuation is lower, the AGC comes into action. Figure 28 shows a typical example measured in the field.

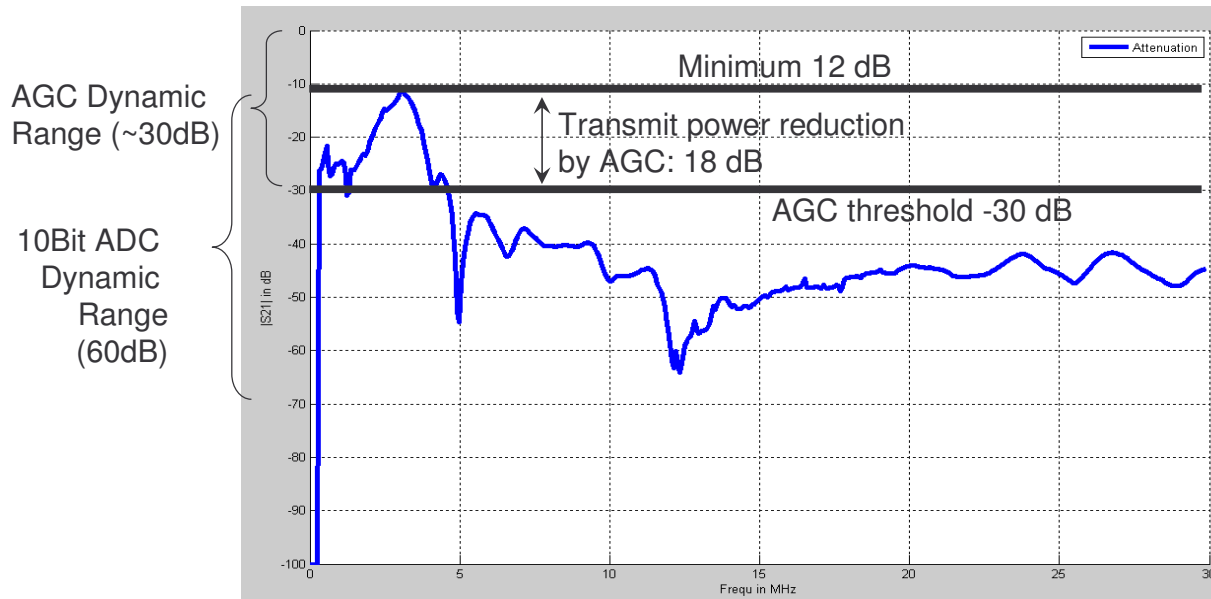


Figure 28: Attenuation of a channel with AGC setup information. X-axis shows the frequency range and the y-axis the attenuation (of the transfer function $|S_{21}|$) in dB

The insertion loss of the channel varies widely over the frequency band. In this case, there is a recorded minimum attenuation of 12 dB and a maximum attenuation of 64 dB. In order to use the dynamic range of the ADC - typically 60 dB - at best, it should cover the variations of the received signal. Therefore the top of the 60 dB is adjusted by the AGC to include the minimum level of 12 dB. (No clipping will occur at the ADC.) Compared to the maximum gain of the AGC of 30 dB it introduces an attenuation of 18 dB at either the transmitting or the receiving side. For the great majority of in-house PLT systems, both approaches are operationally equivalent, but only transmitter AGC provides the desired EMC benefit.

As previously mentioned, Transmit Power Management is a statistical means to reduce the probability of interference. The transmit power reduction could be anywhere from 0 to 30 dB. To assess the effectiveness, it is necessary to estimate the median value of the reduction and its spread. Figure 29 shows the distribution function of the minimum channel attenuation, based on measurements as discussed in [Schw_02]. The graph of figure 29 shows a median value of 19.7 dB for the minimum attenuation of a frequency transfer function. Hence, the power is reduced by an average $PSD_{reduce\ by\ att}$ of 10.3 dB. Approximately 23 % of the modems would reduce their transmit power by at least 20 dB.

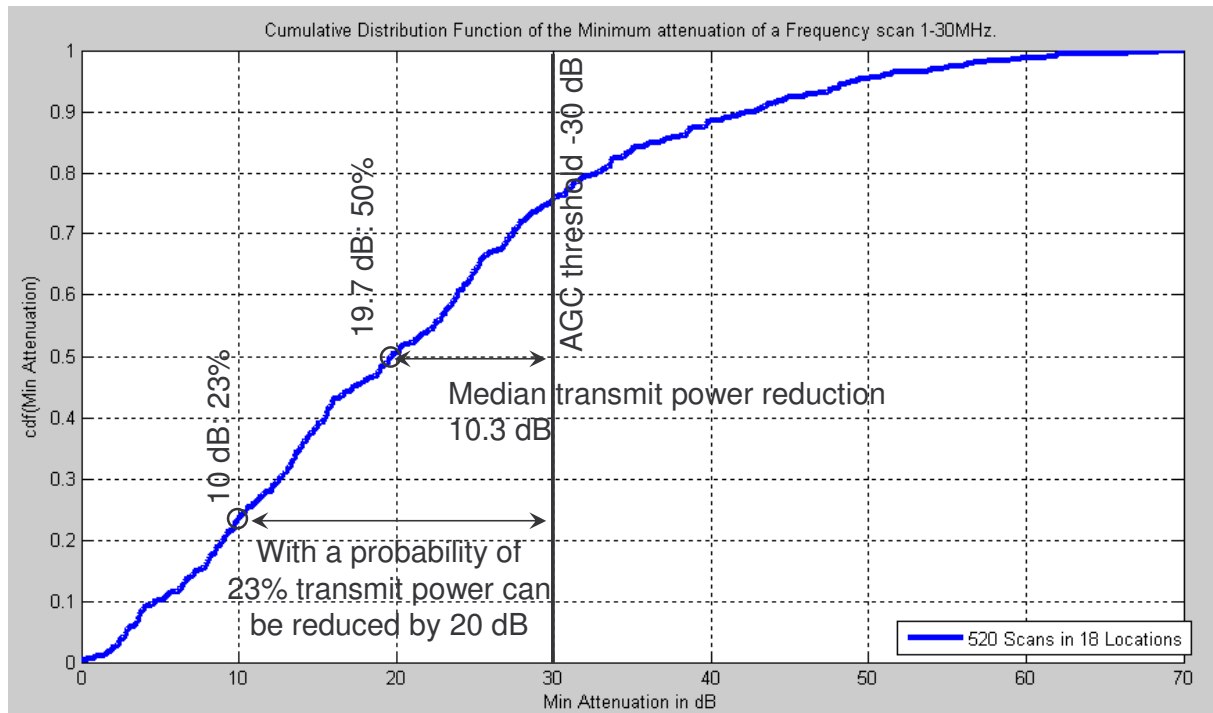


Figure 29: Statistical analysis of the minimum channel attenuation

4.4.2 Adaption of the PSD to the actual Data Throughput Requirement

For in-house PLT applications, another significant parameter to investigate is the actual data throughput requirement. For a given application, the PLT link must provide a certain minimum data throughput with high reliability. The PLT modems with fixed transmit PSD require a safety margin to manage the data throughput in all cases. If one adapts the transmit PSD not only to the minimum channel attenuation, but also to the actual data throughput requirement, the average transmit PSD is reduced even further, as well the probability of interference to neighboring PLT systems or radio services.

The following analysis gives an estimate of how much average PSD reduction can be expected by proper Transmit Power Management.

Measurements of the data throughput of PLT modems show a descending slope at high attenuations when increasing the channel attenuation. The data throughput drops by approximately 50% when the attenuation is increased by 6 dB. Figure 30 shows the transmit PSD in the function of the channel attenuation (chapter 4.4.1) between the two corresponding modems with the data throughput as parameter.

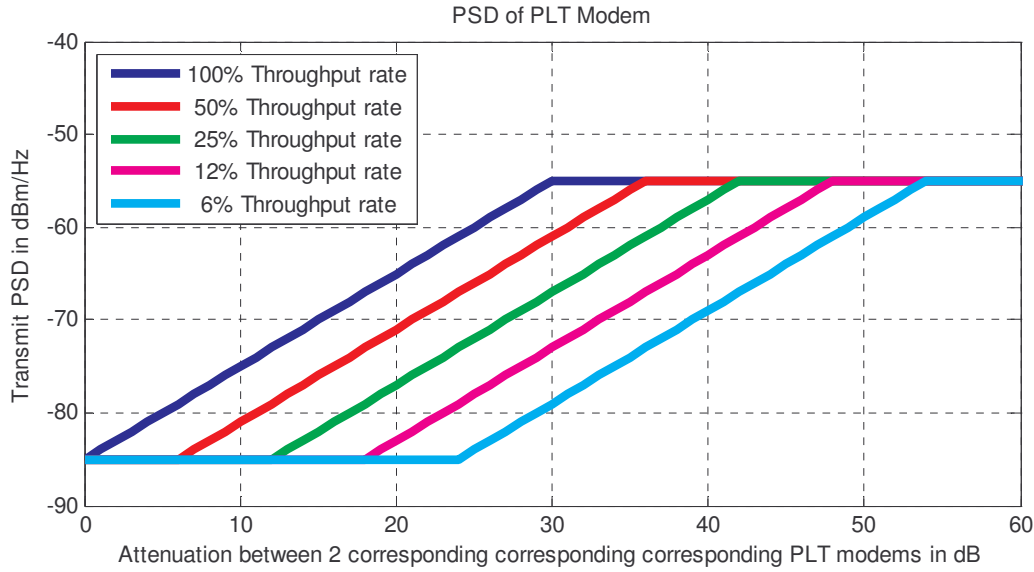


Figure 30: Transmit PSD vs. channel attenuation motivated by throughput rate

Table 3 shows a comparison between the real data throughput requirement and the throughput potential of the modems typically used for a handful of in-house PLT applications (physical layer throughputs). Both, application data rates and physical layer data rates are compared. Due to various overhead and FEC requirements of the individual application it is difficult to make a fair comparison. For instance, a UDP video stream has less overhead than a voice over IP application. Table 3 shows a rough estimation of the low utilization of today's applications.

Theoretically, if the actual data throughput of a PLT transmission does not require all available resources, the usage of resources might be reduced in the time domain, frequency domain or power domain (as described above). Some of today's state of the art PLT modems reduce the usage of resources in the time domain. The duty cycle of transmission is varied. Assuming the PLT system in a neighboring flat is synchronized with the timings of the interfering system, the reduction in the time domain works as an interference mitigation technique. However, due to existing natural decoupling to neighboring flat (as measured in chapter 2.1.1), the reduction in the power domain would be an additional benefit. Hence two properties creating coexistence add constructively. Furthermore, there is the big advantage of systems which not need to be synchronized.

In-house application	Typ. data throughput requirement for this application	Data throughput potential due to attenuation of a typical link for this application	Data throughput utilization
Video TV – SD (MPEG2)	6 Mbps	~20 Mbps (from satellite dish to TV)	30 %
Video DVD (MPEG2)	12 Mbps	200 Mbps (within living room)	6 %
ADSL extension (in avg. DSL rate today)	12 Mbps	100 Mbps (from phone jack to PC)	12 %
Audio CD	2.8 Mbps	200 Mbps (within living room)	1.4 %
VoIP (phone)	0.2 Mbps	100 Mbps (from phone jack to PC)	0.2 %

Table 3: Data throughput utilization of typical in-house PLT applications

$PSD_{\text{reduce by throughput}}$ could be taken from figure 30 and assuming an average throughput from table 3.

4.4.3 Total Average PSD Reduction

Taking into account the two motivations for reducing the transmission PSD described in chapter 4.4.1 and 4.4.2, an average transmit PSD reduction of:

$$PSD_{\text{total_reduce}} = PSD_{\text{reduce by Att}} + PSD_{\text{reduce by throughput}} \quad (5)$$

might be expected.

If the transmit power of PLT modems is reduced, it would reduce the potential of interference to the neighboring flat and the potential of coexistence problems dramatically.

4.5 Dynamic Coexistence without Interoperability Channel

A new coexistence scheme is applicable to inter PLT coexistence in the home as well as to coexistence between PLT and xDSL. It is based on the idea of modems permanently measuring the background noise and detecting interference from the other communication systems. If another system is identified, each system has to measure the level of interference in the frequency domain. Usually - due to the fading PLT channel - only some frequencies interfere. The idea is that the frequencies with a high level of interference are no longer allocated by the

modem's communication subcarriers (i.e. this works only for adaptive OFDM systems). The other interfering communication system releases the frequencies with high interference accordingly. This enables more non-interfered communication resources on both sides, which could then be reused. Both systems benefit in terms of throughput compared to the previous interfering situation. Usually, the *SNR* is quite low in the interfered frequencies. In the worst case, the *SNR* is even negative. The modem doesn't lose throughput capacity if these unusable frequencies are omitted. If both modems follow this concept accordingly, the adaptive frequency split is finalized after several iterations of snooping for noise and allocation of subcarriers.

The concept of dynamic coexistence for PLT modems without interoperability channel was proposed in [Schw_05e].

This coexistence scenario is explained step by step in the example shown in figure 31 to figure 35. Figure 31 gives an overview of the local situation. The scenario describes two neighboring flats where the PLT systems cause interference with each other. One pair of PLT modems is communicating in each flat. The curves presented in the figures below were taken from measurements in a real building. It is a two family building in Germany, in a rural area. The building consists of 3 levels: basement, ground floor allocated by flat 1 and 1st floor allocated by flat 2.

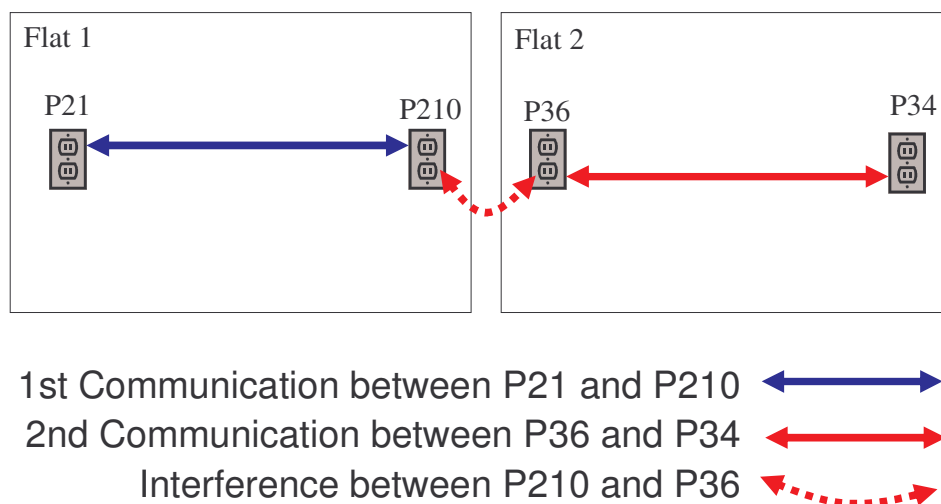


Figure 31: Two flats with a PLT communication in each one

In flat 1, PLT is assumed to communicate between outlet P21 (plug number 21) and outlet P210 (marked with a blue arrow in figure 31). Additionally, there is communication between P36 and P34 in flat 2 (red arrow). The interference occurs between P210 and P36 (dashed red arrow). There was no interference detected from P21 or P34 to the other flat.

All channel transfer functions between all power plugs and the noise at each plug were recorded while performing the measurement in the building. The figures presented below, including the calculations of the theoretical channel capacity, were generated using Matlab [MATW] and equation 4. Each figure shows the local situation at the power outlet P210 in flat 1 and at power outlet P36 in flat 2. The available *SNR* for each communication is marked with green area as introduced in figure 9. Again, the x-axis represents the frequency range from 0 Hz up to 30 MHz, the y-axis represents the PSD from -150 to -50 dB(m/Hz).

As shown in figure 32, the link between P21 and P210 provides attenuation between ~23 dB at 11 MHz and ~57 dB at 19 MHz. It is an average PLT link. The noise floor also shows an average value. The *SNR* varies between 5 dB at 7 MHz and 60 dB at 11 MHz. This provides a capacity of a maximum of 426 Mbps for a SISO PLT system.

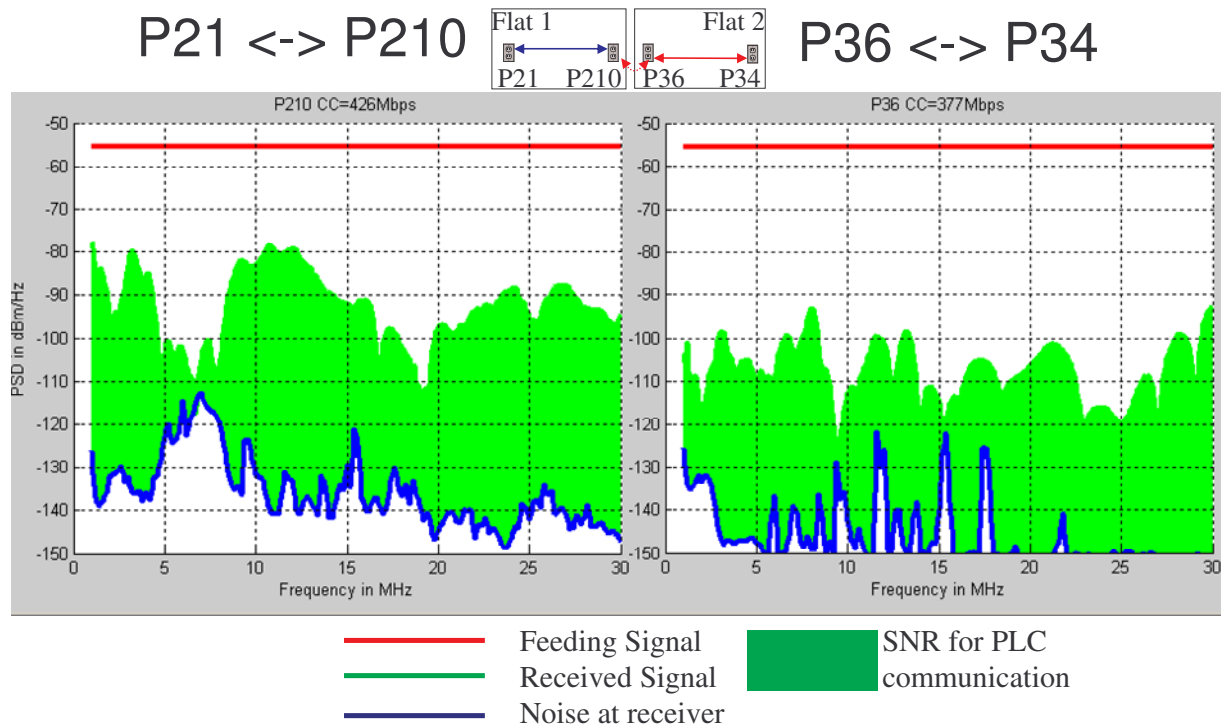


Figure 32: *SNR* and noise at each receiving power outlet. 2 plots having the frequency range from 0 to 30 MHz in x-axis and signal levels from -150 to -50 dB(m/Hz) in y-axis

In flat 2, the noise level is very low. The ingress of the HF radio broadcast signals is indicated by the blue spikes at the bottom. It is interesting to see that the ingress of HF radio broadcast is much better in the top level flat, indicating that the antenna gain of the mains grid is better in the top flat. The attenuation of the link between P36 and P34 is higher than an average PLT link. A channel capacity of 377 Mbps could be expected between power outlets P34

and P36. Figure 32 shows the ideal case, if there would be no PLT interference from one flat to the other.

In figure 33, the cyan line shows the level of PLT interference from P36 to P210. As already described in chapter 3.2.4, the channel is identical in both directions. If the feeding PSD is identical on both sides, the level of interference is also identical between the flats. With a median value of around 55 dB, the decoupling between these two flats is quite low. Here, the dominant interference case is shown. The channel capacities CC given above are reduced to 157 Mbps in flat 1 and to 63 Mbps in flat 2 due to the coupling from the PLT system in the other flat. Checking the green areas in flat 2, there is very little useful SNR left for communication. In case of interference, the sum of the capacities of both transmissions is is:

$$CC_{total\ interfering} = CC_{flat1\ interf.} + CC_{flat2\ interf.} = 157\ Mbps + 63\ Mbps = 220\ Mbps \quad (6)$$

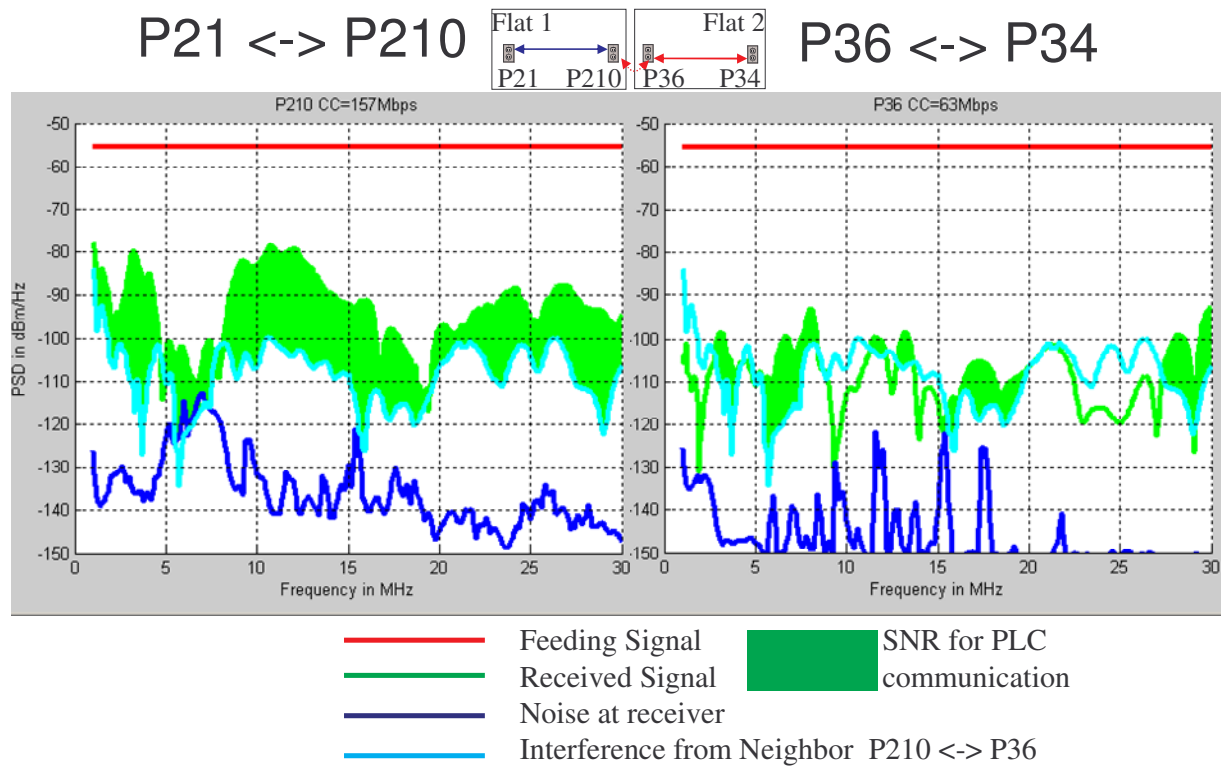


Figure 33: Interference from neighbor's PLT communication

The channel estimator in the receiving PLT modem in flat 2 identifies the frequencies with negative SNR . These frequencies (e.g. between 22 MHz and 27 MHz) no longer carry useful information, so the transmitter should no longer allocate these unusable frequencies. This is

shown in figure 34. In some cases this frequencies have to be negotiated with the communication partner device.

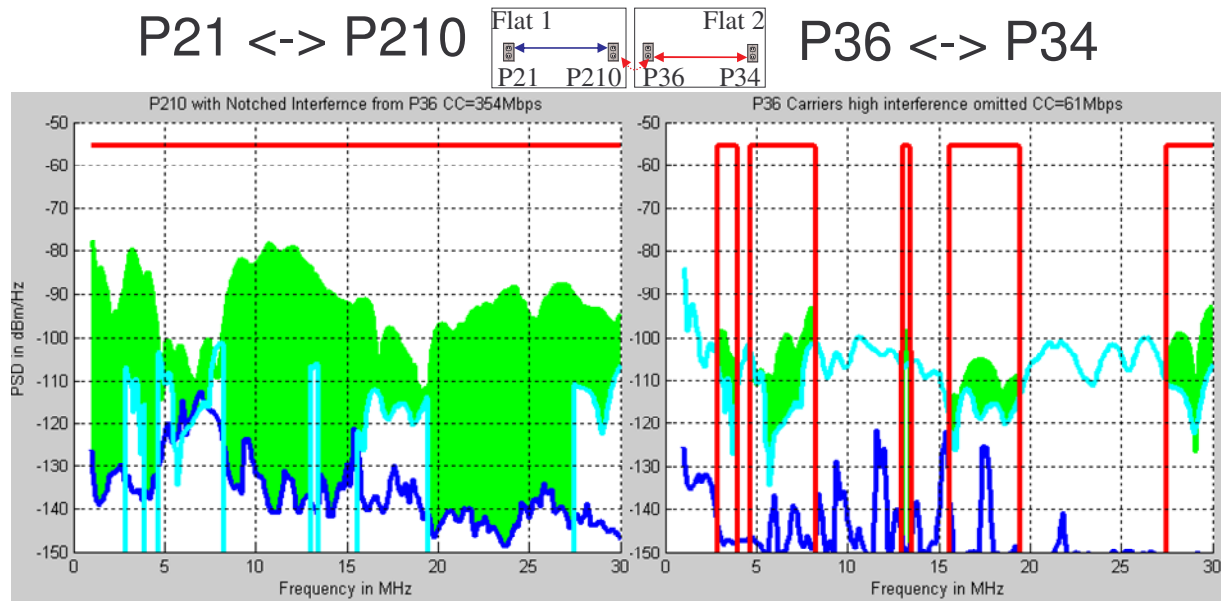


Figure 34: Unusable frequencies are released by one system

The red line on the right hand side of figure 34 represents the feeding PSD of the PLT system in flat 2. It is clear to see which frequencies are allocated. Due to the loss of the poor communication frequencies, the channel capacity has been only slightly reduced from 63 Mbps to 61 Mbps. Some single carriers with positive *SNR* were also removed, in order to minimize fragmentation of communication spectrum in the frequency domain.

The PLT system in flat 1 greatly benefits as a result of removing the unusable frequencies in flat 2. Its capacity rises from 157 Mbps to 354 Mbps. The cyan line on the left side of figure 34 shows the frequencies still interfering with the communication in flat 1 and which frequencies are removed by the PLT system in flat 2. The usable (green) area in flat 1 increases significantly.

By monitoring the shape of the interference in the PLT system in flat 1, it identifies that another PLT system removed carriers from its communication. It would be polite behavior if the PLT system in flat 1 would also remove the interfered carriers from its communication. This is shown in figure 35.

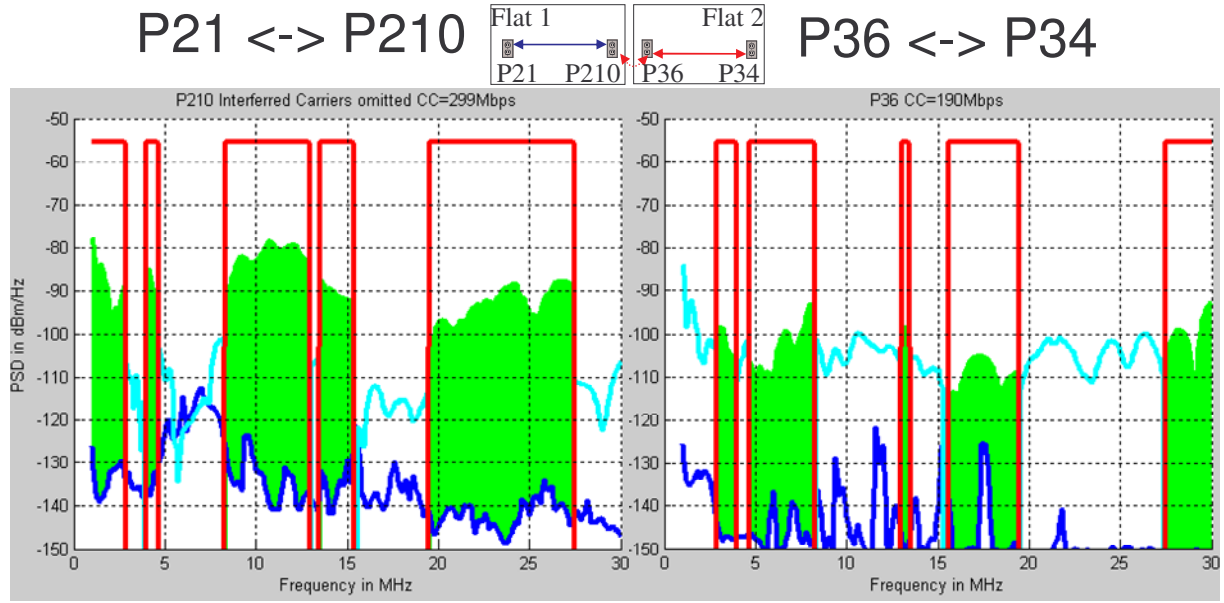


Figure 35: 2nd PLT system frees frequencies with high interference

The PLT system in flat 1 also installed the notches in the carriers with low *SNR*. Here, the modems in flat 2 benefit from the change: Their channel capacity *CC* increased from 61 Mbps to 190 Mbps due to the lower interference. The sum of both capacities in the coexisting case is:

$$CC_{total\ coexisting} = CC_{flat1\ coex.} + CC_{flat2\ coex.} = 299\ \text{Mbps} + 190\ \text{Mbps} = 489\ \text{Mbps} \quad (7)$$

Comparing equation 6 and equation 7, the total capacity of both links increased from $CC_{total\ interfering} = 220\ \text{Mbps}$ in the interfering case to $CC_{total\ coexisting} = 489\ \text{Mbps}$ in the coexisting case. In this example the total channel capacity increases by a factor of more than 2.2.

The idea described above could be optimized to achieve a different fairness policy between the transmissions in each flat. In the example above, the ratio of the capacities between flat 1 and flat 2 is similar before interference occurred and after coexistence is achieved. Here, the individual throughputs are given due to the characteristics of the wires. The concept could be optimized in order to achieve identical channel capacities in both flats, if for example the modem initiating the removal of carriers does not remove all unusable carriers in the first step. In the example above, the system in flat 2 removed more than half of his carriers (figure 34, right side). If fewer carriers are removed in flat 2, the system in flat 1 would remove even more carriers. This results in a better balance of the channel capacities available to both communications.

The main challenge in implementing of such a coexistence concept is the reliable detection of the interfering PLT system, the operation in a highly fragmented communication spectrum and the creation of deep notches or frequency gaps for an OFDM system.

In order to reliably detect the other PLT system, the following parameters can be taken into account:

- All high bit rate PLT systems available today use either OFDM or Wavelet packets as modulation techniques. Both create a rectangular communication spectrum on the mains. Furthermore, the spectrum has some gaps (notches), because the HAM bands are omitted by PLT modems. This gives a PLT spectrum a unique shape which is unlikely to be found on any other noise signal on the mains. In order to detect the shape of the noise spectrum of the pulse-pause transmitted signals, the modem might implement a max-hold function on noise measurements. Strategies of noise measurements are discussed in chapter 5.2.5.
- The specifications of all PLT systems which are sold in large quantities today are documented in [IEEE_09] – this is not published but known within IEEE P1901. The preamble for synchronizing two communication partners is well known. This preamble is an extremely robust signal which can be detected in the receiver by autocorrelation, without passing the demodulation chain. It has detection properties similar to the CDCF described in chapter 4.2. The occurrence of such a preamble is also unique on the mains grid. Only a PLT modem can be expected to create such a preamble.

Operation in a highly fragmented frequency spectrum needs further investigation. It could be promising, because

- Today's PLT modems are immune to the fading characteristic of the PLT channel by design. PLT modems tolerate some signal eliminations in the frequency domain.
- Overlay OFDM systems like [Bran_07] or dynamic spectrum allocation technologies [DySPAN] will face similar problems and the technology will improve.
- When the communication frequencies are released by the coexisting modems, a filter could be used to prevent the creation of a very fragmented spectrum. Some frequency gaps have to be given to avoid inter-carrier interference of the coexisting modems. In the most fragmented case, a single carrier could remain, which does

not add significant throughput. Perhaps it is necessary to specify a minimum spectrum span to be excluded or allocated.

Integration of deep flexible notches could be possible due to:

- Additional band-stop-filters, tunable in frequency and span. Such filters are described in Chapter 5.3.4.1
- Wavelet OFDM technologies as introduced in [Sandb_95] which create very deep frequency gaps.

The concept was proven by simulations in several examples of measured interference cases in buildings. A fair coexisting scenario was achieved in all cases with an optimal usage of the communication resources. Of course, the stronger the level of interference, the more the total capacity figure improves from the interfering case to the coexisting case. If the level of interference is low, a threshold might be implemented when to activate the concept. Weak interference can be accepted by the communication systems.

The coexistence concept presented here works fine when a few pairs of PLT systems interfere. If one PLT access installation interferes with many in-house systems, no frequencies would be left for the access installation. However, access PLT installations are not expected to be deployed in a large quantity in first world countries. If an access PLT system is involved in such a coexistence scheme, perhaps it could never release the lower frequencies (e.g. $f < 10$ MHz). In such a situation the lower frequencies would be removed automatically by all in-house systems. If all systems transport a high payload the frequency split between in-house and access PLT systems is identical to the static approach shown in section 4.2.

The benefits of the concept described above are:

- It does not require any channel of interoperability such as the concepts under specification today in [IEEE_09]. Such an interoperability channel causes a lot of overhead [Spid_06].
- The proposed concept is very flexible. Allocated resources can be adapted according to the throughput demands of the running application. Due to today's PLT modems using hundreds or more than thousand OFDM carriers, communication resources could be allocated in a very granular way. Compared to the traditional concepts (described in chapter 4.2 and 4.3), only a minimum of resources is wasted.
- If there is only a low amount of interference, which might be accepted by the communicating systems, the traditional concepts as described in chapter 4.2 or 4.3 re-

move a lot of resources from each communication. In the proposal given here, the threshold of when the coexistence scheme is activated could be set granular or frequency dependent.

5 Coexistence between PLT and HF Radio broadcast

5.1 Overview

The frequency range of conventional PLT modems (2 MHz to 30 MHz) overlaps with HF radio broadcast frequencies defined by ITU-R [ITUR_04]. Powerline wires in private homes are not shielded and due to branches, distribution boxes, etc. the powerline network is structured with a certain amount of asymmetry. As discussed in chapter 3.2.2, the asymmetries of the powerline network convert the differentially fed signals into common mode signals, which tend to interfere with radio devices (shown later in figure 49). If a Shortwave (SW) radio receiver (AM or DRM) is operated indoors where a powerline communication is active, the radio reception quality might suffer. When the radio device is connected to the mains power supply and the radio has an insufficient decoupling at its mains port, the conducted path is especially dominant in terms of interference.

The EBU (European Broadcasting Union) has conducted some investigations on PLT: [EBU_06] including some videos showing the potential of interference.

Of course, some might argue that HF radio broadcast is becoming less important, FM radio provides a significantly better signal quality, but it is not a world-wide service. Satellite radio or the upcoming web-radio services compete with today's AM transmissions. This might be true for the industrial countries in the 1st world, but the demand for information exists globally. The HF frequencies have the unique property that a transmission could pass halfway around the globe. However, if the transmission goes halfway around the globe, so do the interferences.

HF radio broadcast is also relatively cheap: The costs needed to construct a HF radio transmission station, as well the annual operational costs are unrivaled by the modern technologies. If a single HF transmission station is located in Thailand, the broadcast could reach 60% of the world's population. Anybody who would like to receive this broadcast needs a receiver costing around 10.- €. In the developing countries HF radio broadcast is especially beneficial in rural areas where there is little or no infrastructure. HF radio is often the only option.

Today, HF radio broadcast is used for following reasons:

- In the newly industrializing and third world countries where the transmission distances are very large and the installation of the FM transmission infrastructure is too expensive.
- Tourists who like to receive their home services in a habitual manner. However, satellite or web services are available in most hotels of industrialized countries.

- Amateur radio listeners or hams. The situation of interference from PLT is different to them. Usually they do not use a kitchen radio equipped with a whip antenna. Furthermore, they have the knowledge how to protect their equipment from interference by using e.g. additional filters. However, due to the motivation receiving extreme weak signals and the sensitivity of their equipment interferences from PLT are relevant.
- Military services permanently use the HF frequency range. However, they have also professional antennas. Their operational area is often far abroad where no alternative to HF transmissions exists. Of course, militaries exercise the operation in their home countries. This should be done as closely as possible to real conditions. PLT is an interference source to an airplane flying over Germany. Tanks or marines usually do not operate in the vicinity of PLT modems.
- New upcoming digital services such as DRM (digital radio mondiale) [DRM_06]. Sales of DRM receivers are not as high as initially expected. However, it will be interesting to see how these services develop. If the frequency resources are polluted, once, a future installation is no more possible.
- It is a fundamental freedom in democracies to receive information from everyone and everywhere. Broadcasters such as Deutsche Welle, BBC World Service, Voice of America and others transmit information in multiple languages using the HF bands. Unlike the internet, it is difficult to censor HF radio broadcast. Only jamming is possible. More important is that radio listeners cannot be monitored by government authorities.
- In the case of a crisis, disaster or earthquake e.g. satellite dishes may no longer be aligned. In this case, HF radio broadcast is the most robust and proven technology and expected to be the first source of information to be reconstructed.

Countries without a well developed wired telecommunication infrastructure expect to support people with internet services over PLT. Such countries are also the main target areas of HF radio transmissions. Therefore the coexistence between PLT and HF radio reception is very important.

This thesis proposes a solution which solves the interference problems.

The first idea was to integrate a PLT modem into an SW radio receiver. The frequency information of where the radio is tuned to would be forwarded to all PLT devices. This fre-

quency has to be excluded from PLT transmissions. This would solve the local interfering situation in the flat where both the PLT system and the radio are operated. However, legacy SW radio receivers are already sold and are not equipped with this new idea.

The next idea was to embed a SW radio receiver into the PLT modem, as depicted in figure 36. The PLT modem might measure the interference caused by its own transmission and reduce the feeding PSD in the affected frequencies accordingly. This also solves the local interfering situation. However, an additional whip antenna (monopole antenna) and a radio device would increase the cost of PLT modems. The reception qualities of HF radio services strongly depend upon the location of the radio device inside a room. It is usually best if the radio is located close to a window. However, the PLT modem is not necessarily installed close to a window and a whip antenna would turn a PLT modem with the size of a few cubic-centimeters into an uncomfortably large object.

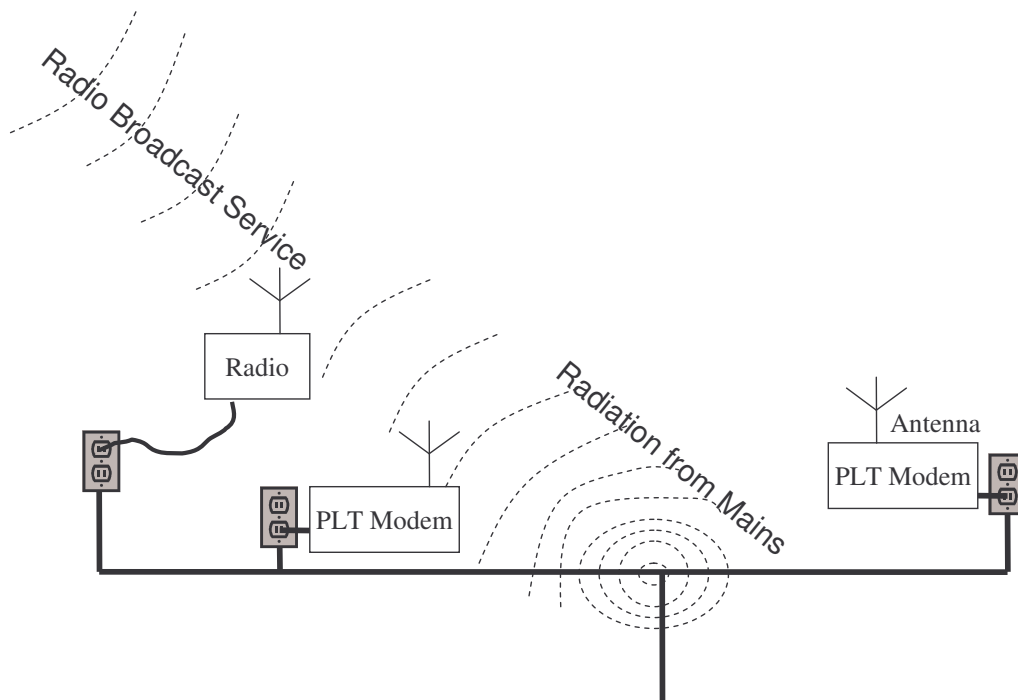


Figure 36: Radiation from PLT (at e.g. an impedance mismatch)

A very straight-forward approach would be to add an interface to PLT modems, where users wishing to receive radio services in the vicinity enter the frequency of their choice and the PLT system has to notch this frequency.

Such solutions only protect radio stations in the local environment. If a neighbor listens to another radio service, it would not be protected. The accumulation of many PLT systems protecting only one individual frequency is still an unsolved problem. Sometimes the propagation

of the HF waves hops with two or three reflections between the surface of the earth and the ionosphere. If the earth bound reflecting area is not protected, the noise would accumulate and reduce the *SNR* of the transmission. To prevent this happening, an autonomous solution is needed for PLT modems notching all receivable frequencies in the target area.

A permanent notching of all HF radio bands would provide such a solution, but this would result in the loss of 21.0% of the communication spectrum of a conventional PLT modem using the frequency range from 2 up to 30 MHz. Additionally, amateur radio (13%) and CB (Citizens' band) radio (7%) allocation overlap with 20% of the PLT spectrum. However, CB radio is not a world-wide operating service. Due to the development of mobile phones, CB transmissions are becoming less relevant. Internet chat rooms offer similar services, today, with significantly more users. Compared to Amateur Radio, CB receivers do not receive very sensitive signals and are not usually operated in a building where a PLT modem is installed. Interferences between PLT and CB transmissions are not expected to occur frequently.

Whether or not the HF frequencies can be used by radio transmissions depends on weather conditions or the reflection quality of the ionosphere. The structure of the ionization layers in the ionosphere vary according to the time of day and seasonal changes. An 11 year sun spot cycle also affects radio reception (Annex A of [Schw_08c]). Radio broadcasters permanently operate monitoring stations in their target area to measure reception qualities and schedule their services accordingly.

A service description channel is included in the specification for the new digital radio service DRM [ETSI_05] for HF bands, which transmits the information to the receiver indicating on which frequency the transmission will continue before a change in the transmission schedule is performed.

Usually, a HF transmission band is either fully allocated with radio services or relatively empty. A permanent default notching of all HF bands would result in a high loss of throughput for PLT modems.

A concept of notching is required to provide optimum reduction of interference between PLT and HF radio broadcast and minimum impact on data throughput and QoS requirements of PLT.

The concept of 'Smart Notching' was therefore developed.

5.2 Concept of ‘Smart Notching’

‘Smart Notching’, sometimes known as ‘Dynamic Notching’, is an adaptive process which automatically notching all frequencies being used by receivable radio services, without any user’s or network operator’s interaction.

The presence of broadcasting signals can be detected by PLT modems by sensing the "noise" (including radio broadcast picked up on the mains cabling) in an electrical socket. Frequencies where HF radio broadcasting signals are identified can then be omitted from the transmitted signal by inserting notches into the transmitting PLT spectrum.

Radio broadcast signals transmitted with a high power from the antenna of a radio station will be received by any wire acting as an antenna, e.g. an electrical power grid. The ingress of a broadcast signal can be detected within the reception range of the radio broadcast signals. The powerline wires are passive and therefore reciprocity is valid. The transfer function or the antenna gain is identical for radiation as well as for signal reception. At frequencies with a high potential of interference, the signal ingress is excellent and there is likely no ingress at non radiating frequencies.

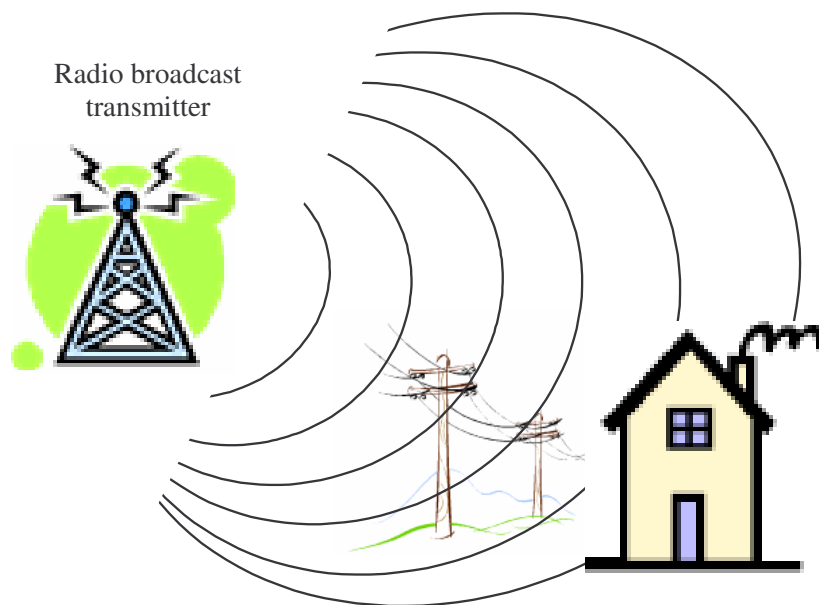


Figure 37: Radio signals ingressing a house’s mains wiring

PLT modems are connected to the mains and are equipped with a very sensitive analog front end. To achieve adaptive modulations (see chapter 5.2.5), PLT modems monitor the noise signal on the mains. This noise information could be reinterpreted by the modems in or-

der to identify a receivable radio station. If done so, the frequencies of all receivable radio stations could be excluded from PLT transmission.

This thesis describes the ‘Smart Notching’ concept in detail. After this overview the influence on the spectrum of the powerlines caused by the ingress from radio broadcast is shown. Thereafter follows an excursion into the sensitivity of SW radio receivers. Knowing the sensitivity of these devices, the threshold of when a radio broadcast signal is receivable can be defined. If it is known which frequencies have to be excluded, requirements for a notch are defined. Before calculating the impact of notching on the throughput of PLT the process of adaptive modulation is described. This allows the realization of the notching concept with a minimal loss of throughput and implementation effort. After the theoretical aspects, the concept has to be verified by a hardware demonstrator system. This development is documented in Chapter 5.3, where the PLT modem itself, detection of ingressing radio broadcast signals and notching is described.

Finally, this concept was proposed to standardization bodies: Chapter 5.4 gives a summary of the discussions.

5.2.1 Radio Signal Spectrum on Powerlines

Of initial interest is a comparison of the signals measured when being connected to the mains and the field measured with an antenna in the air. Comparing the signal strength of a HF radio broadcast station at two locations at once is very difficult. Due to the strong dynamic fading effects of radio transmissions in the time domain, a received HF signal never has the same level it had a moment ago. This time-variant effect was further investigated by monitoring the level of HF radio stations over a period of time.

5.2.1.1 Fading Effects of Radio Stations

Figure 38 shows the levels of three radio stations (5865 kHz, 6025 kHz and 6055 kHz) which were monitored for over a quarter of an hour. The horizontal axis represents the time from 0 to 1000 seconds. The vertical axis is a relative level in dB. All three transmissions showed strong fading effects. The transmission at 6055 kHz (blue curve) is particularly interesting. The recording of the levels was done on the 13th of November 2007, beginning at 14:55h. After 120 seconds, the signal level dropped by 60 dB. Around 3 minutes later, shortly before 300 sec, the signal reappeared, but with a lower level than before. Obviously, there was a change in the transmission schedule of the broadcaster shortly before 15:00h. The new transmission was established just in time for the 3:00pm news. Perhaps the target area of the broadcasting station was changed or the measurement location was supported from another station in

another direction. Changes such as these can be monitored quite frequently in HF broadcasting. An overview of frequency scheduling in HF broadcasting is given in [Schw_08c, Annex A].

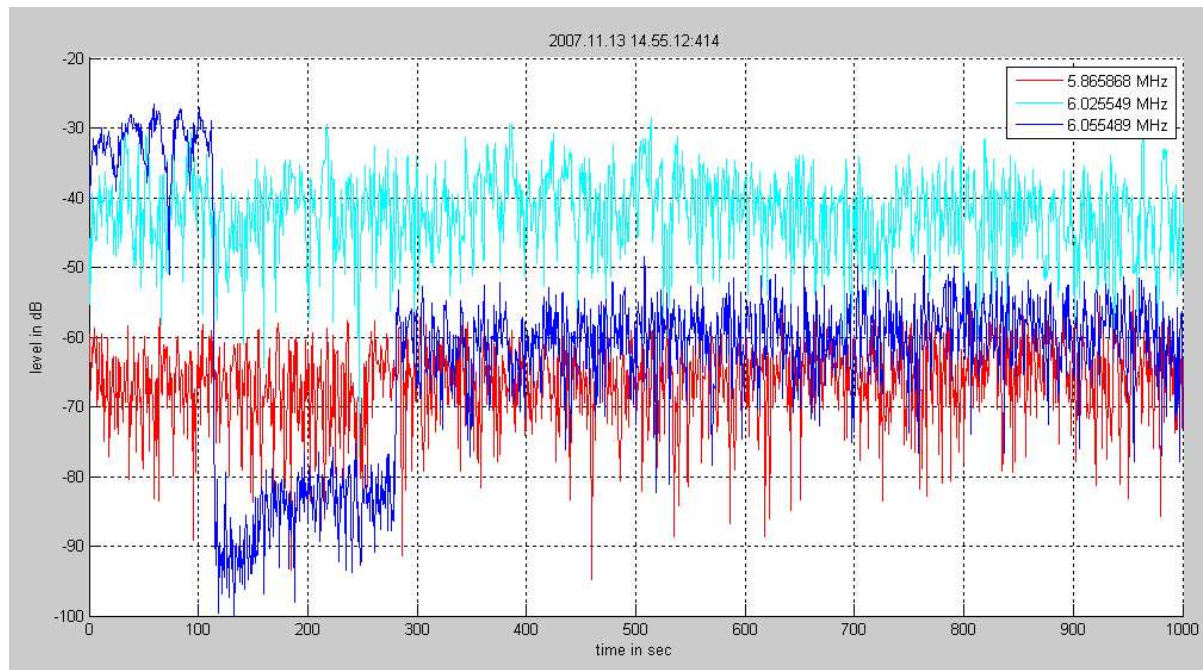


Figure 38: Fading of HF radio broadcast services in time domain

The service at 6055 kHz (blue) shows relatively less fading with the typical characteristics before the signal level drops (time < 110 sec). The fading results in flat hills and deep canyons in the shape of the curve. Fading effects are caused by multi-path propagation between the transmitter and the receiver. The waves from individual paths may overlap constructively or destructively, depending on the phase difference when they arrive at the receiver. The phase of a path may vary with the dynamics in the ionosphere. Depending on weather conditions, an ionization layer can move with more than 100 km/h. This is why Doppler effects impair HF reception and an AFC (automatic frequency control) in SW radio receivers is beneficial, even if the transmitter and receiver don't move. Figure 38 shows the strong fading effects in the service at 6055 kHz after the change in the transmission schedule (time > 300 sec) as well in the other services (red and cyan). The signal level of a station changes more than 30 dB within a few seconds. The AGC of a SW radio receiver must be very dynamic in order to follow such level fluctuations. If HF radio stations are to be detected on the mains, PLT modems have to consider such dynamics of the signal levels.

5.2.1.2 Setup to Record a Signal Spectrum

To compare the levels of the electromagnetic field in the air and the ingress signals on the mains, figure 39 shows the necessary equipment. Such measurements were performed in private flats, hotels and office buildings. The antenna was located in the center of the room with a vertical alignment of the biconal probe. Photographs of these measurements can be found in [Schw_08c]. The Schwarzbeck electric field probe EFS 9218 [Sbck_05] allows calibrated field measurements. It provides a constant antenna factor for the frequencies of interest. A spectrum analyzer is connected using a probe to the mains or alternatively using the antenna. For the measurements in figure 40 and figure 41, the maximum signal level is recorded using the max-hold function of the spectrum analyzer for around one minute.

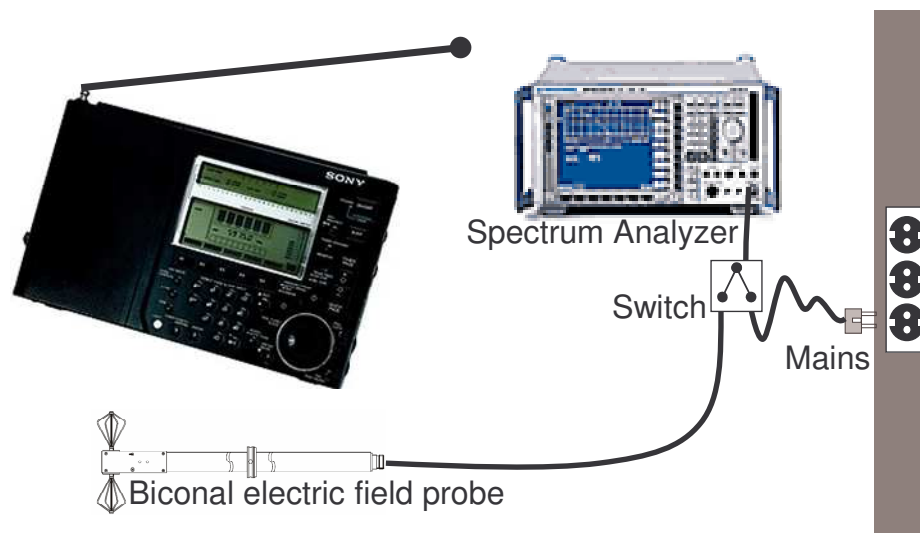


Figure 39: Detection of radio services. Setup for measurements in buildings

5.2.1.3 Recorded Spectrums

Figure 40 shows a one time snapshot of the electrical field in one location of the 49 meter band. The x-axis represents the frequency range from 5.9 MHz to 6.3 MHz. There are 40 kHz per division. The y-axis in figure 40 is interpreted by the spectrum analyzer in dB μ V, but considering the antenna factor of 18 dB/(m) [Sbck_05], the y-axis is converted to the E-field from -2 dB(μ V/m) up to 98 dB(μ V/m) using a scale of 10 dB per division. Some AM services can be easily identified: at 5954 kHz, 6035 kHz, 6155 kHz, 6120 kHz and more. At 5950 kHz, for instance, a DRM transmission is visible.

All sweeps in figure 40 and figure 41 were recorded with max-hold (green line) and min-hold (blue line) to get an impression of the fading of the individual services. In figure 40, the AM service at 5920 kHz was switched off during the recording period. It is neither visible at

the min-hold line, nor in figure 41. The service at 5954 kHz shows an average fading (around 20 dB), the service at 6005 kHz shows almost no fading behavior. The black line represents the latest frequency scan before the snapshot was recorded.

Taking the fading into account, and that some stations might have been switched on or off during the measurements, figure 40 and figure 41 look virtually identical. The Schwarzbeck [Sbck_05] antenna is linearly polarized and shows the typical dipole directivity. The directivity and polarization of the mains grid of a building is not known, but due to the horizontal and vertical wires found in buildings, signals of all directions and polarizations are captured. These differences will also cause variations in the comparison of figure 40 and figure 41.

Figure 41 recorded the conducted signals on the mains. The vertical axis represents the voltage in dB μ V. Using equation 1 and equation 2 the signals might be converted to PSD and compared with the figures presented above.

5.2.1.3.1 Characteristics of a DRM Spectrum

DRM transmissions use OFDM - a modulation scheme with 88 to 228 carriers in a 10 kHz spectrum. The number of carriers used by DRM depends on the transmission mode corresponding to typical propagation conditions. A DRM spectrum appears as a 10 kHz wide rectangle spectrum. The DRM specification [ETSI_05] also allows bandwidth allocations of 5 kHz and 20 kHz. In the HF band, 10 kHz spectra are usually used. Some DRM transmissions may also have a very high single carrier in the center of their spectrum. This is necessary to ensure that legacy transmitting amplifiers keep their linearity. DRM was especially designed in order to use portions of older AM transmitter facilities, such as antennas and amplifiers, avoiding major new investment. Simulcast transmissions use an AM modulated center carrier with the surrounding DRM carriers (e.g. at 5954 kHz in figure 40). DRM has a more variable PAR (Peak to Average Ratio) compared to AM services. This used to cause problems at some old transmitting stations. It explains why the carrier in the center of the spectrum (known from an AM 30% modulation depth) has been kept. In this case, some OFDM carriers in the middle of such a DRM channel are not used and the central carrier has to be filtered away by the receiver.

5.2.1.3.2 DRM and AM

If a PLT modem has to detect these signals, it does not differentiate between AM or DRM. Today's PLT modems have an OFDM carrier spacing f_{CS} of around 20 kHz. The carrier spacing is provided by the system's Nyquist frequency $f_{Nyquist}$ (half of ADC/DAC sampling clock

frequency) divided by the FFT_size implemented by the PLT modem. E.g. the parameters of the system described in chapter 5.3 are:

$$f_{cs} = \frac{f_{Nyquist}}{FFT_size} = \frac{40\text{MHz}}{2048} = 19.53\text{kHz} \quad (8)$$

The carrier spacing f_{cs} of a transmitting OFDM system is identical to the resolution bandwidth of the receiving system using same FFT_size and sample frequency. Equation 8 calculates the resolution bandwidth of the PLT system for noise measurements (in chapter 5.3.3.2 a method to enhance the resolution bandwidth is presented). If the bandwidth of the signal to be detected (AM or DRM) is smaller than the resolution bandwidth of the measurement system, its shape does not matter. Due to the fact that DRM is designed to reuse the transmission facilities (amplifiers, antennas) of the AM equipment, it has the same signal power as an AM carrier, but individual sensitivity thresholds, see chapter 5.2.3.

The stations marked with a green ring were receivable using the automatic frequency scan function of the Sony ICF-SW77 short wave receiver. In total, at a single time instant during the day and at this location, 22 radio stations were receivable with the Sony ICF-SW77 with field strengths between 29 dB($\mu\text{V/m}$) and 68 dB($\mu\text{V/m}$). A detailed presentation of this measurement, including comparisons of the field strength with the conducted signals in all other HF broadcast band is available in [Schw_06b]. The results of another measurement day at another location are presented in [Schw_06c]. Similar tests results were measured during the ETSI plugtest [Schw_07a] in several locations. The report was published in [Schw_08c].

J. Stott's BBC R&D White Paper 114 [Stot_05] published similar measurement results.

All these measurements help to answer the question: Which air-based HF carriers can be detected on the mains network? All radio signals in the air which are stronger than 20 dB($\mu\text{V/m}$) (measured with a RBW of 9 kHz) significantly increase the noise floor on a quiet powerline.

Due to the strong variations in the amplitude of HF radio broadcast signals over time, PLT modems should periodically sense the ingress level of the radio signals. The level of these signals also depends on the modem's location and the structure of the wiring in the electricity grid.

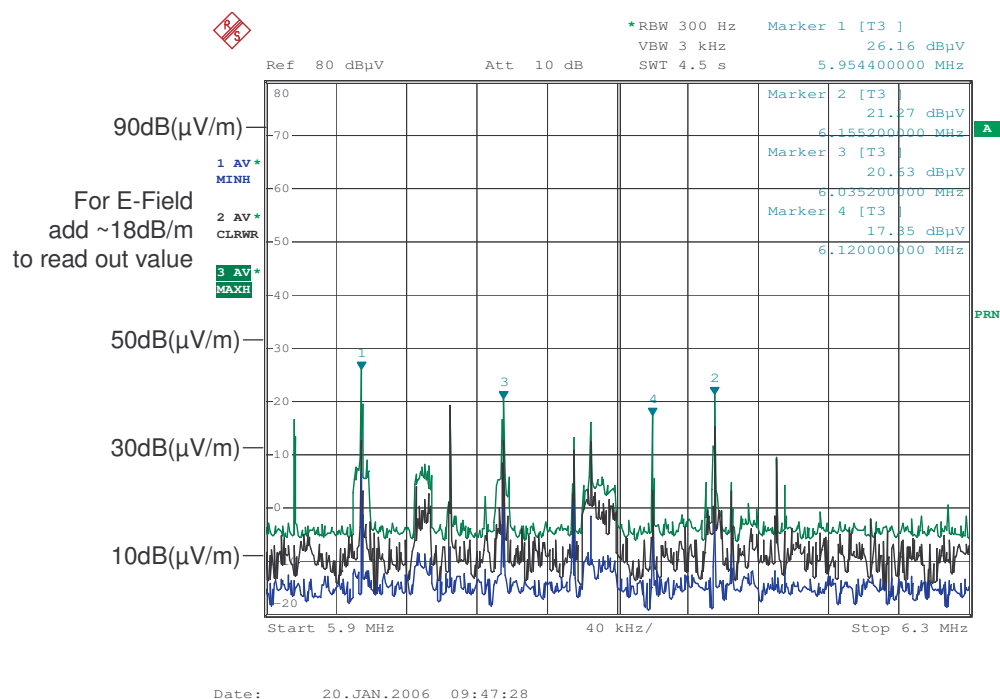


Figure 40: In-door electrical field of the 49m band, any location any time

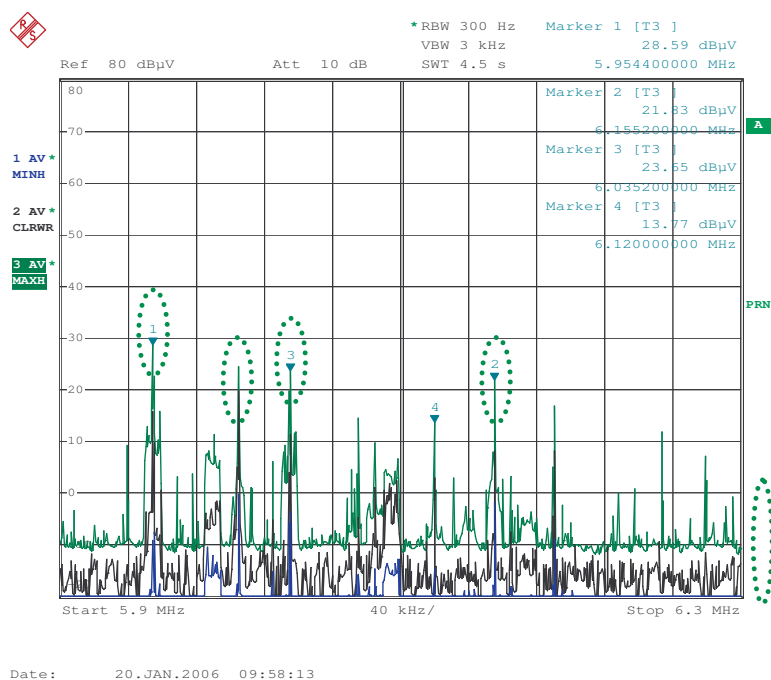


Figure 41: Signal ingress in the 49m band, measured connected at a power outlet

5.2.1.3.3 Noise on Powerlines

As described and measured in chapter 2.1.1, many other noise signals may appear on the mains spectrum. Further noise sources such as switching power supplies frequently enhance the ingress level of radio broadcast services. Later, in chapter 5.2.3 both an absolute as well a relative threshold is defined, when such signal ingress is receivable by a radio device.

5.2.1.3.4 An additional PLT Transmission

For further studies of the interference potential from PLT, the measurement setup from figure 39 was used to check the level of radiation due to PLT in a building. Figure 42 - where a PLT transmission was also set up in parallel - shows an identical spectrum to the one measured in figure 40. The radiated noise level covers most of the radio services.

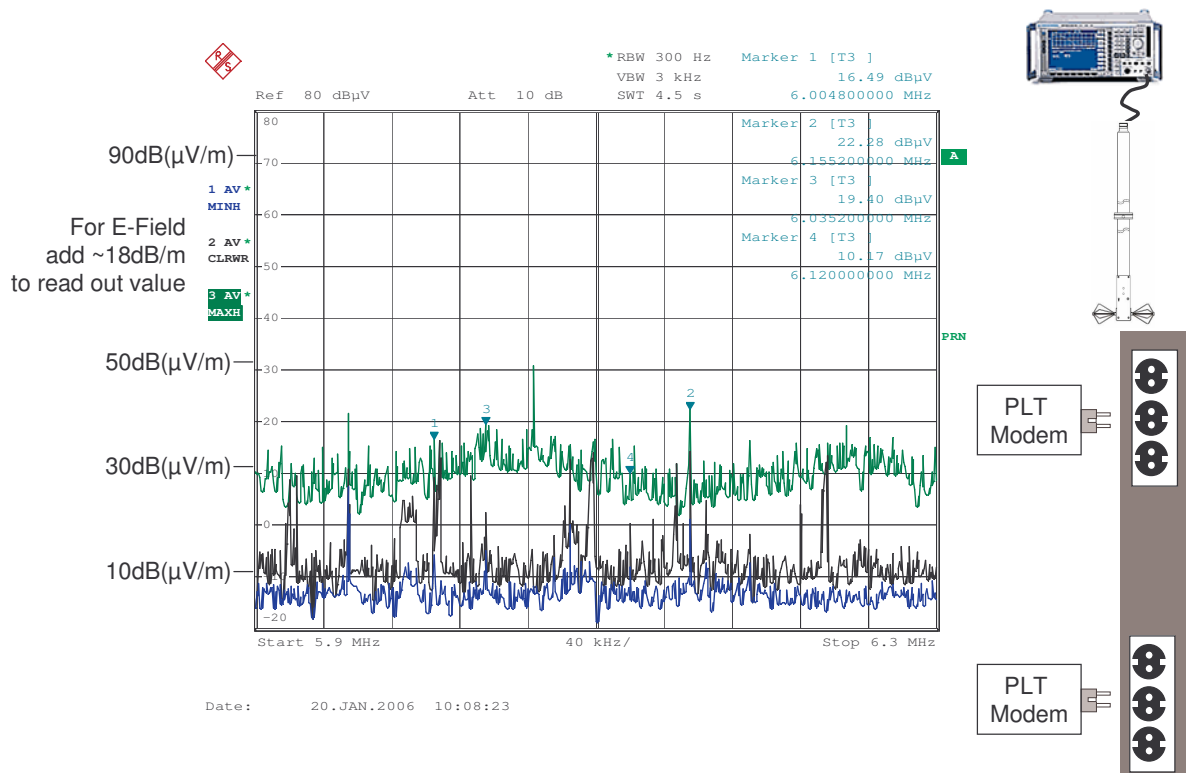


Figure 42: Radiation from PLT

5.2.2 Sensitivity of SW-Radio Receivers

5.2.2.1 AM Receivers

To define a threshold at which a radio station becomes receivable by a CE (consumer electronic) radio receiver, it is essential to know the sensitivity of such devices. Unfortunately, this information is not given in the manuals of the receivers, so it must be measured.

The sensitivity level was verified for the following receivers:

- Sony ICF-7800 (manufactured in 1970 -1980)
- Sony ICF-77 (manufactured in ~1990)
- Sony ICF-SW1000T (manufactured ~1995)
- TECSUN World Receiver 9700 (manufactured ~1998), without power supply
- Sangean ATS 909 (manufactured 2006)
- and a Radio Dummy similar to that used for vehicle testing according to CISPR25 [CISPR_02] (from University of Duisburg-Essen [OPERA_04])

All the receivers were photographed and are shown in figure 43. The construction of the Sony ICF-7800 is interesting because it contains an embedded dipole antenna. All others are equipped with a single monopole whip or rod antenna.

Additionally, the reception behavior is monitored when the receivers were connected to the mains and when they were battery powered.



Figure 43: Selection of AM-Radio receivers and radio dummy

Tests to measure the sensitivity of AM radio receivers are standardized in EN 60315-3 [IEC_00]. Figure 44 helps to explain how the tests are performed.

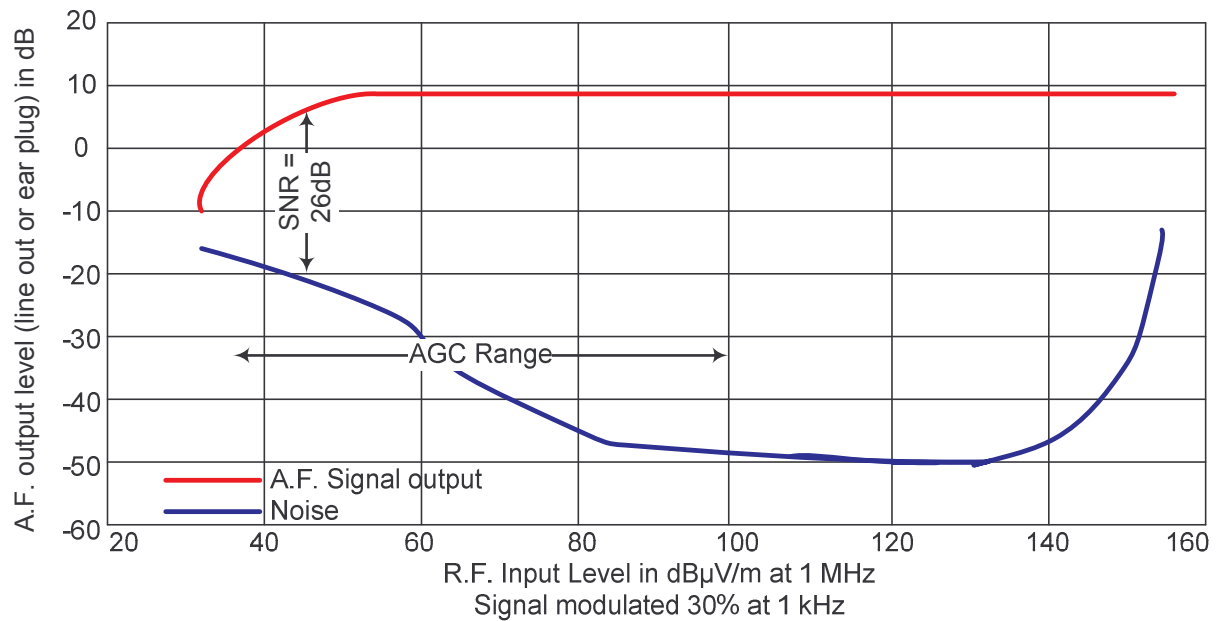


Figure 44: A.F. signal and noise behavior of AM receivers depending on RF input level

As shown in the figure above, both the signal level and the noise at the A.-F. Output (Audio Frequency, measured at the line-out or the headphone plug) of a radio receiver depend on the RF electrical field around its antenna. The RF level has to sweep along the full dynamic range in order to verify the receiver's sensitivity. The horizontal axis of figure 44 spreads from a RF field of 20 dB(μ V/m) to 160 dB(μ V/m). The vertical axis is a relative scale in dB. There are 2 lines in this graph:

- the A.F. output level
- the noise level measured at the same connector as the A.F. signal

At very low RF field levels, the SNR of A.F. is also very low. The noise level is high because the AGC (automatic gain control) is set to the maximum amplification and the A.F. output level is low. The A.F. output increases with the rising RF level. The noise decreases due to the reduced amplification by the AGC. At a certain RF level, the A.F. output becomes stable and at a later point, the noise reaches its minimum. At high RF input levels, nonlinearities in the amplifiers generate distortions and intermodulations causing the noise level to rise. The SNR of 26 dB specified by [ITUR_04] and [ITUR_90] is the distance between the A.F. and the noise level. It is reached for any RF fields higher than 40 dB(μ V/m).

The measurement equipment and setup to perform such tests is shown in figure 45. The setup of the RF equipment (antenna and SW radio receiver) is located in a fully anechoic chamber. The R&S SML generates the AM signal (with 1 kHz, Modulation Depth = 30%), which is received and demodulated by the DUT (device under test). RF frequencies of 6 MHz

and 15.3 MHz were selected for testing. The chamber is designed for immunity tests according to [IEC_06] and produces a sufficiently homogenous field at the receiver location. Only the 6 MHz results are shown in the graphs below, because the other frequency didn't provide different findings. The radio dummy has no embedded AM demodulator, so an R&S FMAS AM demodulator is used. An R&S UPL audio analyzer evaluates the signal level and noise output of the audio signal. The settings of the R&S UPL are RMS detector for the A.F. signal and quasi-peak detector for the noise, with a weighting window specified in [CCIR]. Additionally, a noise generator R&S SUF2 is connected to the power outlet where the DUT was also plugged in. The noise generator is used to test the sensitivity of the DUT when CM or DM noise is present on the mains.

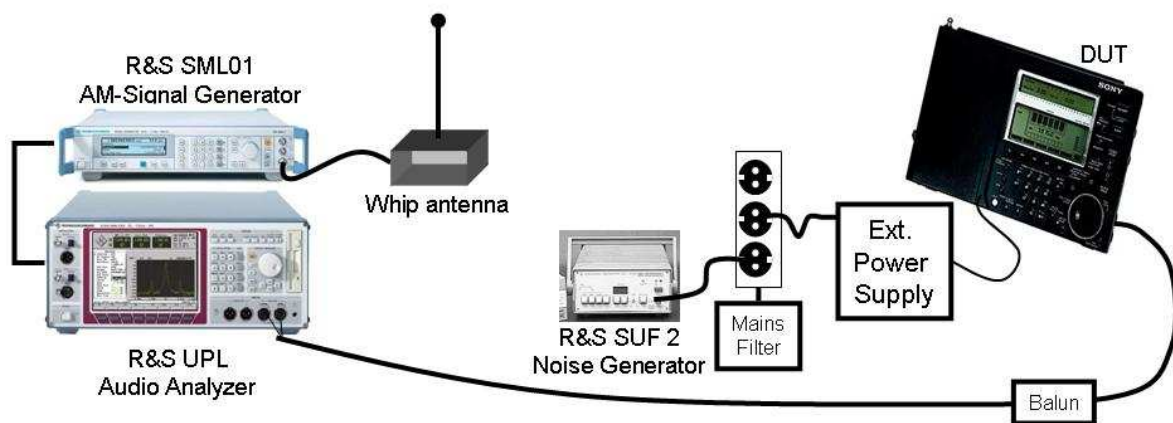


Figure 45: Setup to measure the sensitivity of AM receivers

The level of the radio field is calibrated in the fully anechoic chamber before starting the measurements. There is a homogeneous field, independent of the location above the table. The table is located at a distance of approximately 4.5 m from the transmitting antenna. Figure 46 shows some snapshots of the calibration procedures.

The test is setup with a power sweep in 5 dB steps from 6 dB($\mu\text{V/m}$) to 121 dB($\mu\text{V/m}$). Figure 47 to figure 49 show the results of these measurements. Markers for the 26 dB ([ITUR_04]) sensitivity thresholds are calculated after the interpolation of the lines. At each power level the 1 kHz AM signal was switched to 'off' to measure noise and to 'on', again to measure the A.F. signal with the UPL analyzer. (Of course, the AM carrier was not switched of.)



Figure 46: Snapshots from field measurement in an anechoic chamber

Figure 47 presents the measured sensitivities of 5 AM receivers. For the purposes of the measurements in figure 47, the radio receivers were operated with their power supplies. Two lines are plotted in identical color for each receiver. The top line at the high RF level represents the audio signal and the lower one represents the noise. As specified in [IEC_00] the noise is measured with a quasi-peak detector weighted with the CCIR Filter curve and the audio signal with an RMS detector. (An overview of various detectors is given in chapter 2.2.) This is why the measurements show a negative SNR at low field strengths. (The noise is higher than the A.F. signal.) Functions inside a SW receiver start already at RF fields far below $20 \text{ dB}(\mu\text{V/m})$. At around $18 \text{ dB}(\mu\text{V/m})$ the most sensitive receiver has a positive SNR in the audio signal. The 26 dB sensitivity threshold is reached at $46 \text{ dB}(\mu\text{V/m})$ by the first receiver. For the listener of a radio service it is more important to know at which SNR a human voice can no longer be understood. In [Schw_08c] 17 dB was found to be this threshold.

The sensitivity threshold of the radio dummy is comparable to that of the other receivers.

The ICF 7800 could not make use of its dipole antennas, here. There was a purely vertical polarized field in the fully anechoic chamber. The radio showed the best reception quality

when both rods were oriented vertically. In this situation there is no benefit to having two antennas.

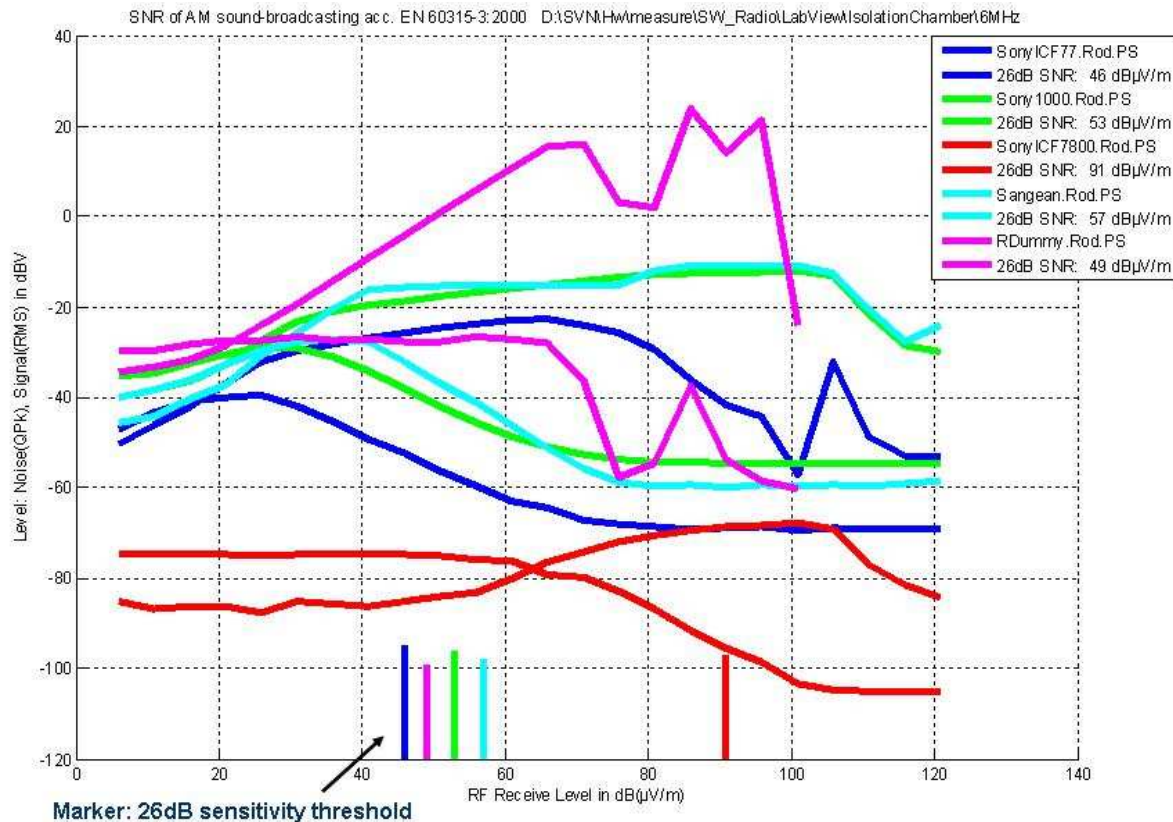


Figure 47: Sensitivities of AM receivers with power supply

The Sony ICF 77 is equipped with a switch to adjust the sensitivity of the antenna. It allows the settings DX, Normal and Local. This is why the dynamic range of the AGC is limited compared to the other devices. The tests were performed with the sensitive DX setting. The R&S FMAS AM demodulator connected to the radio dummy also shows a limited AGC dynamic range. (The RF manual level was set to -70 dBm, which is the most sensitive level.)

Figure 48 shows the same tests with the SW radio receivers being battery powered. Compared to the sensitivity threshold taken with measurements where a power cord was connected, the devices with the monopole antenna show a decreased sensitivity of up to 4 dB. SW radios use the power grid as counterpoise or as a second arm of a dipole structure. This effect was also visible at 15 MHz RF frequency. This phenomenon is more evident inside a building than in the anechoic chamber. In the chamber, the powerlines available for ingress are quite short, so the ingress of the HF signals to the mains is not good. During the measurements in the chamber, the radio was located on the table, the external power supply on the floor. The cable

to the power supply just dropped from the table. The power strip, where the radio and the noise generator were connected, was also located on the floor. A filter was embedded into the power cord of the power strip in order to prevent any influence from the outside. Due to the purely vertical polarized field in the chamber, only the wire dropping from the table was available for signal ingress. SW radios do the same thing with the powerlines as the PLT modems do: they use them for something which the wires were not designed for. This is why SW radio receivers are interfered with by PLT.

A battery driven radio receiver is less affected by interference from the mains. However, it has a decreased sensitivity of receiving radio services (as shown in Figure 48).

It is interesting to compare the noise line of the Sony ICF 77 when it is powered by the mains and when it is supplied by battery. The AGC stays low and does not cause internal noise. This shows how the radio saves battery power.

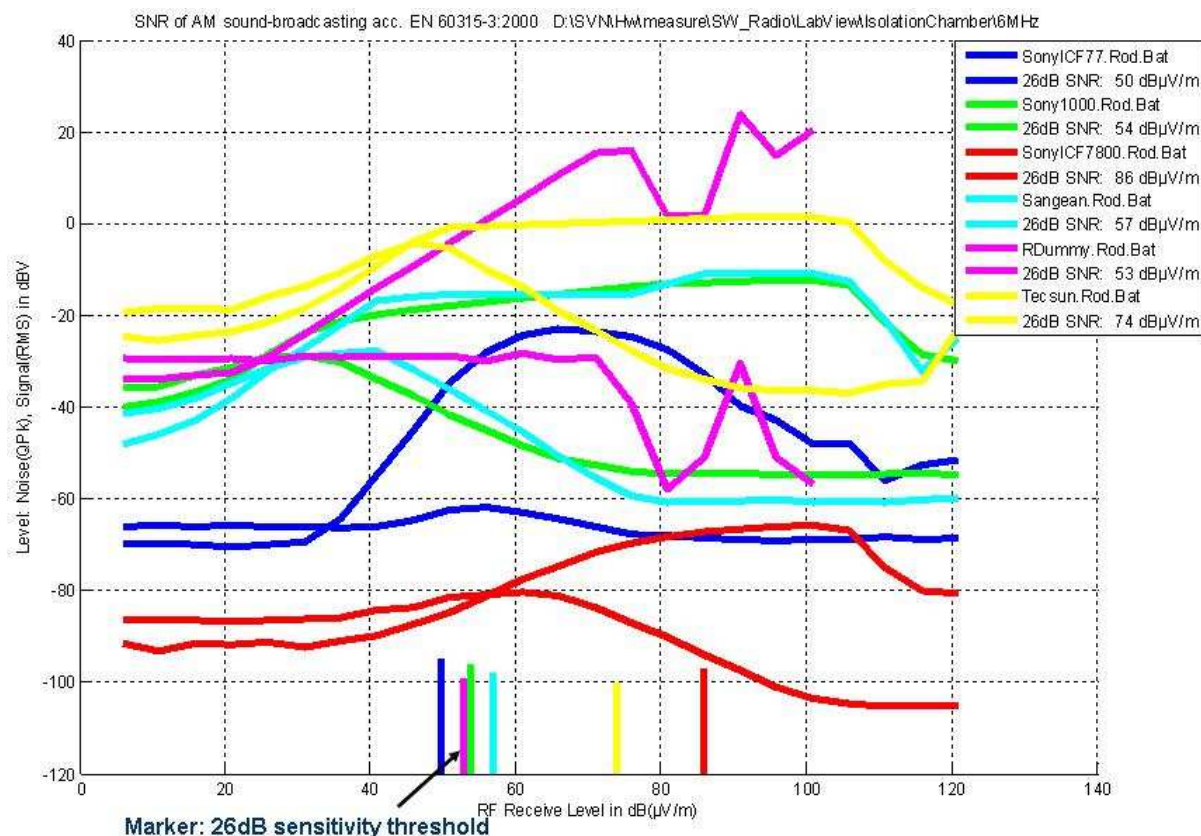


Figure 48: Sensitivities of AM receivers, battery powered

Feeding of differential mode noise signal into the mains has various effects on the individual receivers. The Sony ICF 7800 is quite immune to interference from the mains. Since this radio device is equipped with a dipole antenna, it has implemented a mains filter which blocks

interference better. This radio device does not use the mains as counterpoise. If the antenna input is symmetric then the receiver is less sensitive to interference from the mains.

As expected, if noise is fed into the mains, the noise at A.F. output is increased compared to the setup without interference.

Figure 49 shows results using the Sony ICF SW1000 T. Here, a white noise signal was fed into the mains in common mode as well as in differential mode. 3 levels of interfering signals were tested for CM as well as for DM. The difference between each level was 20 dB. The blue lines represent reference lines without any interference.

- The black, yellow (+20 dB) and pink (+ another 20 dB) lines show the influence of the DM interference.
- The cyan, red (+20 dB) and green (+ another 20 dB) lines show the influence of the CM interference

CM signals cause much stronger interference than DM signals. However, the loudest DM noise of -80dB(m/Hz) significantly decreases reception quality.

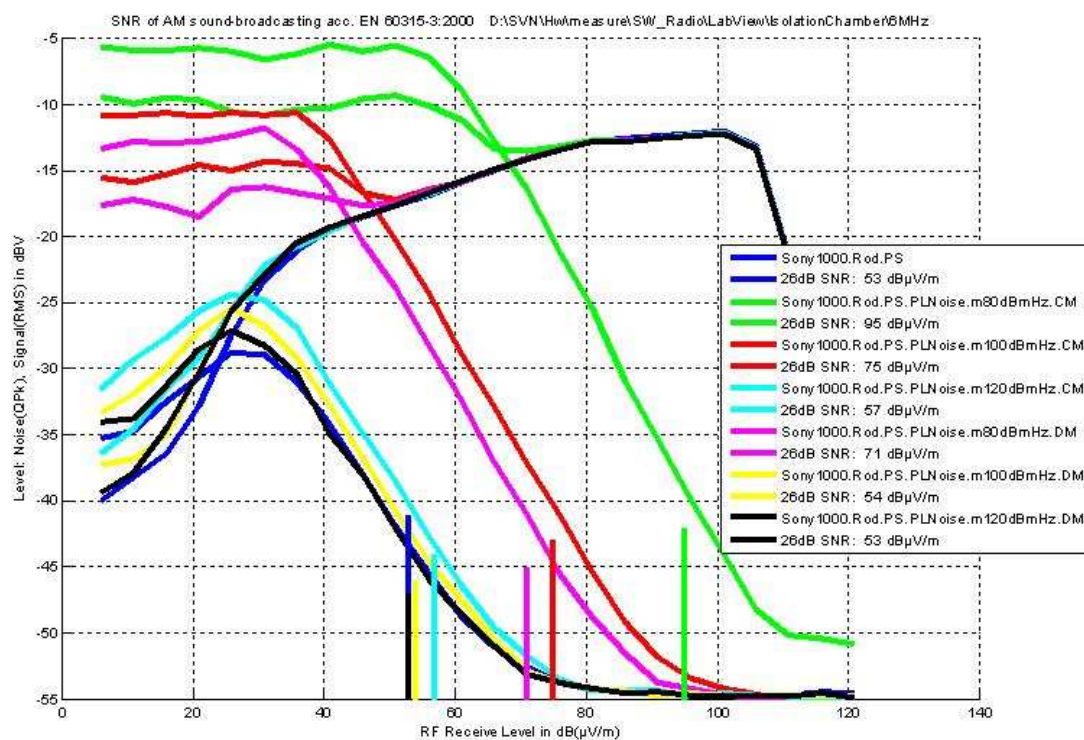


Figure 49: Sensitivities of AM receivers with CM and DM noise on powerlines

Another interesting investigation about the sensitivity of SW radio receivers is to see at which RF level the automatic station scan stops. This shows where the implementation of the radio device assumes the signal to be receivable.

Again, this test is performed in the anechoic chamber. A similar setup to the previous test was used. Figure 50 gives an overview of the setup.

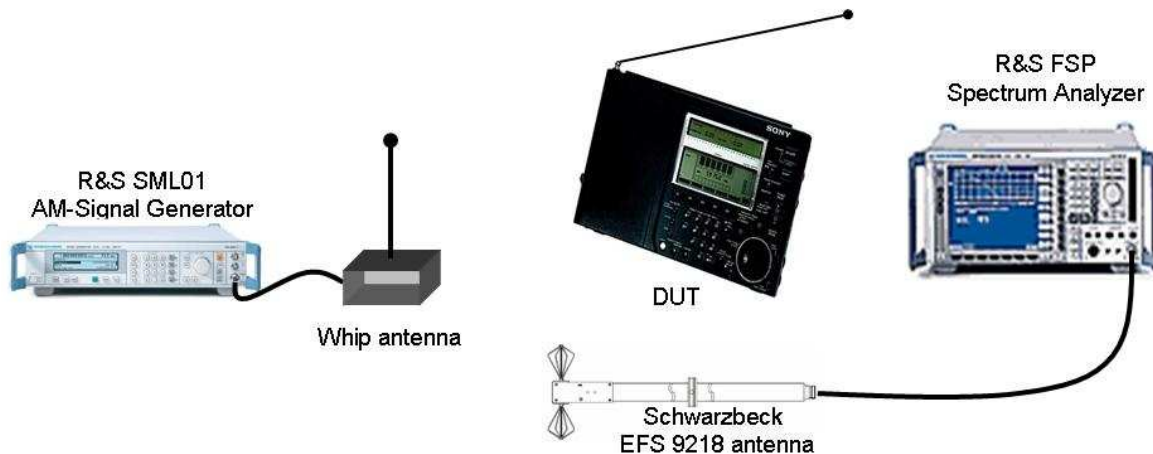


Figure 50: Setup to measure the sensitivity of AM receiver where auto scan stops

The radio devices used for this test are already known from the tests above (the others were not able to perform an automatic station scan):

- Sony ICF-SW77
- Sony ICF-SW1000T
- Sangean ATS 909

The investigated frequencies are 6000 kHz, 9800 kHz and 15500 kHz. The DUT is set to station scan mode (in each of the 49 m, 31 m and 19 m bands). The AM signal generator is connected to the whip antenna located at a distance of 3.5 m from the receiving radio device... Feeding signal power is increased by 1 dB when a band is fully scanned by the DUT. When the station scanning at the DUT stops, the signal field level is recorded. The field strength is measured in dB(μ V/m) using the active biconal antenna [Sbck_05] and a spectrum analyzer.

Table 4 shows the field strength when a SW radio receiver identifies an AM service as being receivable. At the lower frequencies this is far below the minimum sensitivity of 40 dB(μ V/m), which ITU-R specifies for an average receiver in the HF band [ITUR90]. 22 dB(μ V/m) is the most sensitive value found in the AM radio receivers under test.

	Antenna sensitivity	6 MHz	9.8 MHz	15.5 MHz
Sony ICF-SW77	DX	22 dB(μ V/m)	26 dB(μ V/m)	44 dB(μ V/m)
Sony ICF-SW77	Normal	32 dB(μ V/m)	32 dB(μ V/m)	50 dB(μ V/m)
Sony ICF-SW77	Local	60 dB(μ V/m)	55 dB(μ V/m)	67 dB(μ V/m)
Sony ICF-SW1000T	Not available	24 dB(μ V/m)	33 dB(μ V/m)	36 dB(μ V/m)
Sangean ATS909	Not available	33 dB(μ V/m)	36 dB(μ V/m)	37 dB(μ V/m)

Table 4: Sensitivities of AM receiver where automatic stations scan stops

5.2.2.2 Minimum Field Strength for DRM Reception

Unfortunately, there are currently no DRM receivers available which are able to demodulate signals of a similar low field strength to that of AM receivers. Early devices available on the market such as the Roberts MP-40 have a sensitivity of around 20 dB less than the AM receivers. In all locations where field strength measurements are performed [Schw_08c], the number of DRM services that are received by Roberts MP-40 is very low. The number was too low to derive a representative statistic.

If there is not a sufficient number of services to measure, checking the “planning parameters” for digital sound broadcasting at frequencies below 30 MHz [ITUR_03] is another source. [ITUR_03] specifies in Appendix 1 to Annex 1 Chapter 2 $Noi_{intrinsic} = 4.5$ dB(μ V/m) to be the minimum receiver sensitivity. It has to be considered that this is the receiver’s intrinsic noise level. (The field strengths listed in the AM services are the levels of the AM carriers to be demodulated, not the receiver’s intrinsic noise level.)

The external noise from the ITU recommendation for Radio Noise [ITUR_07] shows that man made environmental noises have a similar level to that of a receiver’s intrinsic noise. PLT modems are generally operated in residential areas. Their median frequency is $f = 16$ MHz. Applying equation 11 of [ITUR_07], the median noise figure F_{am} is:

$$F_{am} = 72.5 - 27.7 * \log (f/\text{MHz}) = 39.1 \text{ dB} \quad (9)$$

The constants 72.5 and 27.7 are given [ITUR_07] for the environmental category ‘Residential’. According to figure 51, $F_{am} = 39.1$ dB at 16 MHz is somewhere in between galactic noise and the man made noise of a business area.

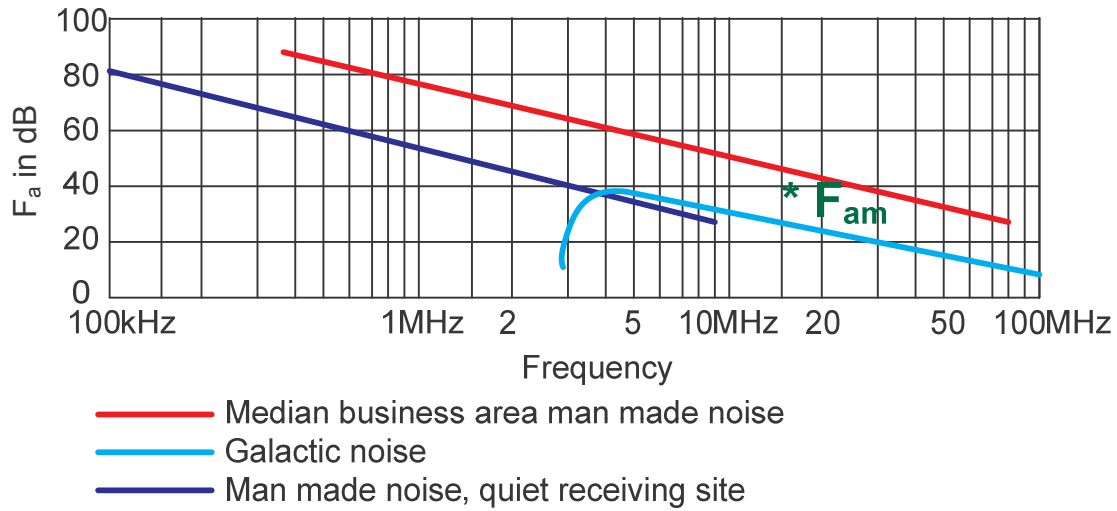


Figure 51: Noise figure F_a according to [ITUR_07]

According to [ITUR_07] the electrical field E_n for a half-wave dipole in free space (whip antenna) is calculated:

$$\begin{aligned}
 E_n &= F_a + 20 \log_{10}(f/\text{MHz}) + B - 99 \quad (\text{dB}\mu\text{V/m}) \\
 &= 39.1 + 20 \log_{10}(16) + 10 \log_{10}(10 \text{ k}) - 99 (\text{dB}\mu\text{V/m}) = 4.2 \text{ dB}\mu\text{V/m}
 \end{aligned} \tag{10}$$

B is the noise power bandwidth (10kHz) of the receiving system in dB(Hz). (The value 99 and F_a are used here as given in [ITUR_07].) If a receiver's intrinsic noise level and the external noise level are similar, the resulting noise of both will be 3 dB higher.

[ITUR_03] specifies the following planning parameters for DRM:

- Several robustness modes (Number of OFDM subcarriers and carrier spacing)
- Spectrum occupancy types (10 kHz in the HF band)
- Protection level number (the lower the protection class, the higher the level of error correction and the lower the average code rate)
- Modulation schemes (16-QAM, 64-QAM)
- Channel models (e.g. the good model has one path and additive white Gaussian noise, bad models have several paths with individual gain, delay, Doppler shift and Doppler spread)

The minimum SNR for a DRM transmission is also specified in [ITUR_03]. In the HF bands, a minimum SNR_{min_DRM} of 14.6 dB is found in ITU's channel model no 5, protection level no. 0 and a modulation scheme of 16-QAM in tables 10, 11, 12 and 13 of [ITUR_03]. Channel model No. 5 is the undesirable ('bad') one for the HF bands. Protection level No. 0 and 16-QAM results in the lowest code rate for DRM. Protection level 0 and 16-QAM is for very heavily protected DRM modes. Here, only low throughput rates could be achieved. This

would result in an audio quality which would sound worse than AM and obviously there is no possibility of including multimedia content within these broadcasts. FM audio quality, which is the main selling point of DRM, could only be achieved by using higher DRM throughput rates. The more 'normal' DRM modes in the tables of [ITUR_03] show SNR values of around 25 dB.

Today's DRM broadcasts usually consist of a multiplex including a 'FAC (fast access channel)', a 'SDC (service description channel)' and the 'MSC (main service channel)' [ETSI_05], [Stot_01]. Each of these channels is protected with an individual error codec. It allows a receiver e.g. to quickly decode the FAC during station scan to derive the service name, then if tuned to a service, the SDC knows the services available in the MSC and how to decode it together with further information such as the frequency schedules. The MSC embeds the data content to be broadcast. The FAC uses a higher level of error codec and requires less SNR. For the MSC, higher bitrates are available due to lower error corrections.

The minimum field strength E_{min_DRM} of the most robust DRM mode can be calculated using $Noi_{intrinsic}$ and SNR_{min_DRM} out of [ITUR_03] and equation 11:

$$\begin{aligned} E_{min_DRM} &= Noi_{intrinsic} + 3 \text{ dB} + SNR_{min_DRM} \\ &= 4.5 \text{ dB}\mu\text{V/m} + 3 \text{ dB} + 14.6 \text{ dB} = 22.1 \text{ dB}\mu\text{V/m} \end{aligned} \quad (11)$$

The minimum field strength of 22 dB($\mu\text{V/m}$) is the theoretical value where a DRM receiver may render a broadcast service transmitted in the most robust mode, assuming the 'bad' channel mode. However, this is only the fast access channel, not the radio service itself.

This is exactly the same field strength as measured with AM receivers in chapter 5.2.2.1.

5.2.3 Threshold to detect Radio Services

Propagation characteristics on HF radio transmissions are not stable. As already seen in figure 38, the fadings in the time domain generate heavy variations in the signal level at the receiver side. ITU-R specifies in [ITUR_92] the probability of a transmission being receivable by the target device. The upper decile deviation of the wanted signal $D_u S_h = 5 \text{ dB}$ ([ITUR_92] Table 3, Step 6). If PLT modems monitor the ingress of HF radio broadcast signals using a max-hold detector, the short term signal variations might be considered. Figure 52 gives an overview of these calculations.

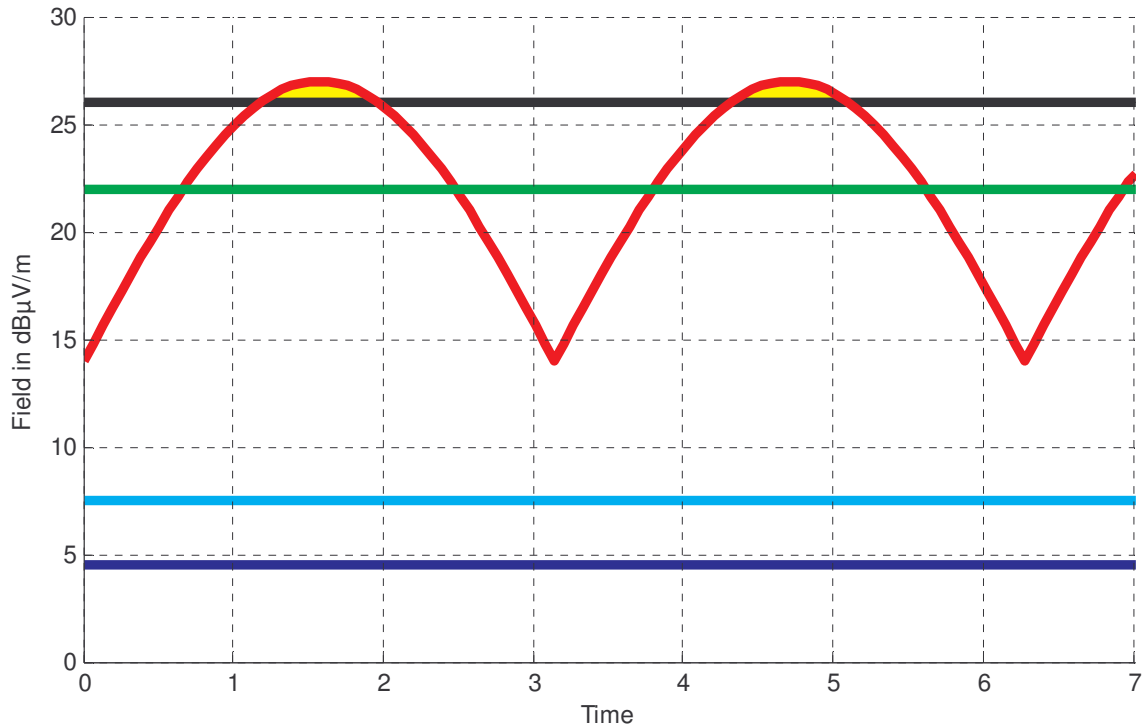


Figure 52: Threshold to detect HF radio broadcast ingress:

Blue: receiver's intrinsic noise level (identical to man made noise)

Cyan: intrinsic noise plus man made noise

Green: minimum receiver's sensitivity

Red: fading of HF broadcast

Black: max-hold with 1 dB headroom (yellow)

The x-axis of figure 52 represents the time in arbitrary units, the y-axis the electrical field in the air. The blue line is the intrinsic noise level that might be expected in a receiver of high quality. The cyan line takes the added man made noise into consideration and the green line includes the theoretical DRM or measured AM receiver's minimum sensitivity. For DRM, this is as calculated in equation 11. The red line shows the expected signal at the receiver's location with the fading statistics from [ITUR_92]. Such signals are inevitably subject to a larger or smaller degree of fading. The top fades are $D_u S_h = 5$ dB higher than the minimum receiver's sensitivity and the lowest fades are 8 dB below. The interleaver of DRM is designed to make receivers immune to such fadings. If PLT modems need a margin $M_{to_detect_threshold}$ of 1 dB for detection, the threshold is exceeded with a probability of 30% in any interval longer than 10 s. The area to detect is marked yellow in figure 52. To detect the top of the fadings, the detection threshold of field strength $E_{field_to_detect}$ in the air results in

$$\begin{aligned}
 E_{field\ to\ detect} &= E_{min} + D_u S_h - M_{to_detect_threshold} \\
 &= 22.1\ dB\mu V/m + 5\ dB - 1\ dB = 26\ dB\mu V/m
 \end{aligned}
 \tag{12}$$

The threshold of 26 dB(μV/m) is given by the black line in figure 52. If PLT modems use an average detector instead of the max-hold one, the threshold has to be lowered by 5 dB. This is implementation dependent for the PLT modem manufacturer.

The reception factor (defined in the plugtest report [Schw_08c]) describes the relationship between the electrical field strength of a radio broadcast station in the air and the received power to be measured at outlets. The setup to measure the reception factor is visualized in figure 53. The radio receiver is used for the SINPO [ITUR] assumption which is described in chapter 5.4.

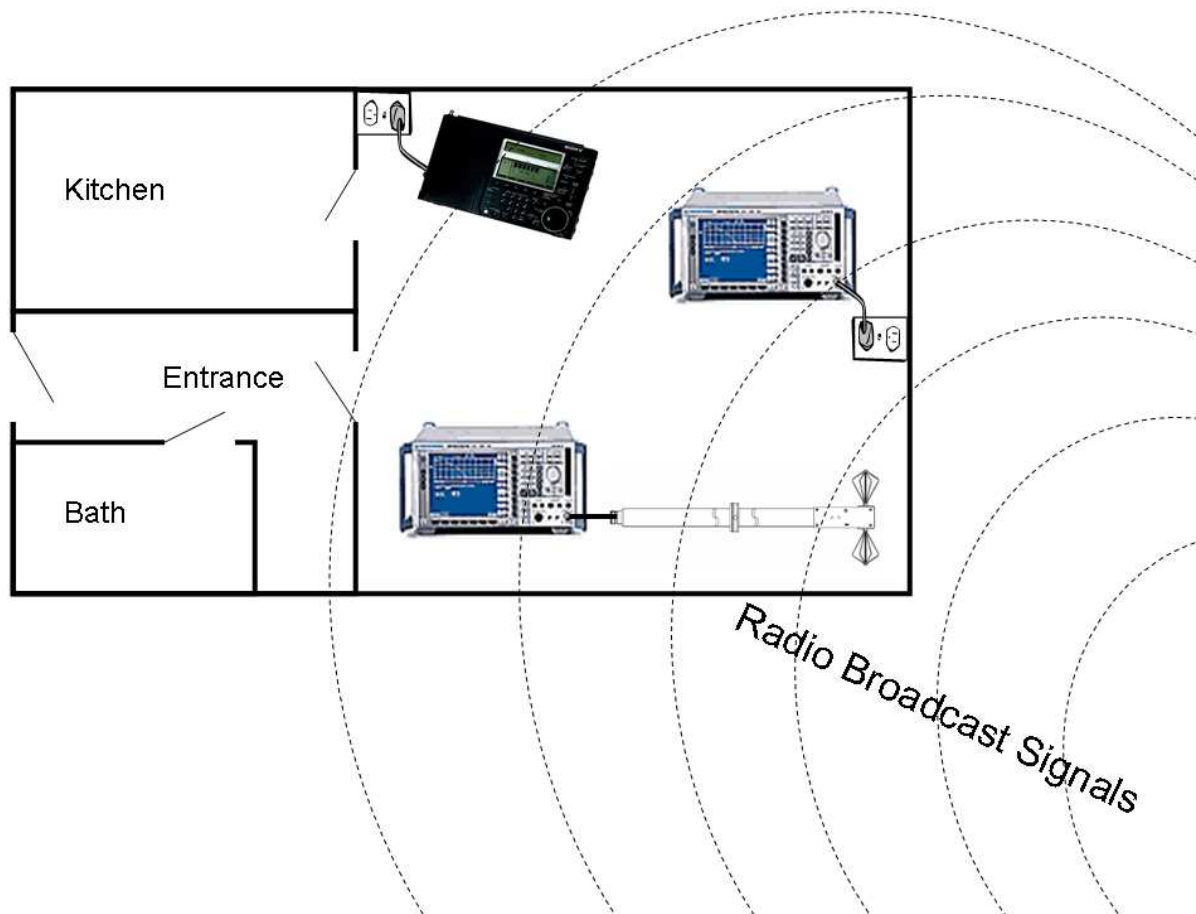


Figure 53: Definition of reception factor, measurement setup in a flat

Measurements deliver a cumulative statistical probability of the reception factor shown in figure 54:

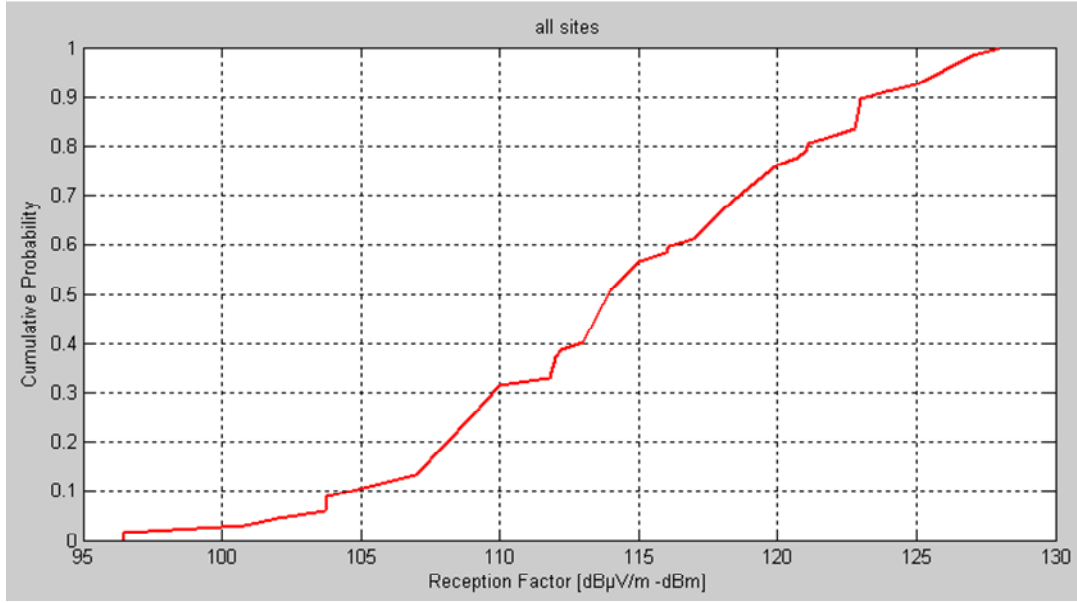


Figure 54: Cumulative probability of reception factor

The lower the value in figure 54, the better the antenna gain of the mains wiring. The median value of the reception factor ($ReFa$) is found to be 114 dB(μ V/m) – dBm. The 80% worst case value is: $ReFa_{80\%} = 121$ dB(μ V/m) – dBm. A reception factor covering 80% of the cases, with an 80% confidence level can be derived from the distribution function shown in figure 54. With this value, the threshold of the signal level connected to the mains $P_{detect_on_mains}$ can be derived with

$$\begin{aligned} P_{detect\ on\ mains} &= E_{field\ to\ detect} - ReFa_{80\%} \\ &= 26\ dB\mu V/m - 121\ dB(\mu V/m) - dBm = -95\ dBm \end{aligned} \quad (13)$$

This level can be verified with a spectrum analyzer using a resolution bandwidth of 9 kHz and an average detector. Resolution bandwidth and detectors used by the PLT modem are implementation dependent.

Besides the threshold level a criterion has to be developed for the separation of SW radio stations from disturbance sources operated at mains. As shown in chapter 5.2.1, the ingress of a broadcast radio station appears as a needle in the noise measurement of a PLT modem. Today's PLT modems are not able to demodulate the AM or DRM signals. However, a needle and even a very stable one in the frequency domain is something unique within all noise sources at powerlines (see figure 3) and can be detected by the modems. Two criteria must be fulfilled for the level of the needle to be identified as a receivable service and worth being protected by PLT modems. The first criterion is a relative threshold because the usable signal

must have a minimum SNR. The second is an absolute threshold when the signal passes the minimum sensitivity level of radio receivers.

The PLT modem is not able to apply weighting windows on the demodulated AM signal and to measure SNR as specified in [IEC_00]. A more simple approach is required. A PLT modem might measure the noise as well as the peak level of signals. As described above, the minimum SNR of an HF service is 14.6 dB for the most robust DRM transmissions. This is the distance between the noise and the peak signal level.

Taking the typical noise sources from figure 3 into consideration, there is not only one noise level. The noise is time and frequency dependent. To check the SNR of a broadcast service, the noise next to the service shall be used. As long as the transmission conditions are good, an HF transmission band is densely allocated with radio stations. Measuring the noise inside the band would result in a value accumulating all radio services, not in the surrounding noise. This is why [Schw_08d] specifies the noise floor to be measured at adjacent frequencies lower and higher than the HF Radio bands. The adjacent frequency blocks must be completely monitored by the PLT modems without any gaps in order to avoid cherry picking of noise values by a PLT modem. Finally, the noise floor is the median value of all measured values. The median value is not affected by individual peaks of e.g. a strong ‘out of band’ radio station.

In [Schw_08d] two criteria or thresholds are given, when a broadcast receiver is defined to be receivable:

- Criterion (1): 14 dB above the noise floor. It is 3 dB lower than the desired SNR of an AM receiver to understand voice (derived from the acoustical measurements above) and around 11 dB lower than that required by a normal DRM transmission (out of [ITUR_03]).
- Criterion (2): the absolute threshold of -95 dBm which is derived from equation 13

For activation, a processing time of 15 seconds is conceded to PLT modems. If the two criteria were passed once, the notch shall be kept for at least 3 minutes. This timing hysteresis is a tradeoff between consumer acceptance listening to a fading broadcast service and the processing capabilities of PLT modems creating a notch. The timings were found by the STF332 [Schw_07a] during the plugtests where the concept was verified [Schw_08c].

To detect such a deep threshold of -95 dBm ($RBW = 9$ kHz) with 14 dB SNR is quite challenging for PLT modems. As previously mentioned in chapter 2.1.1, analog front ends of PLT modems are designed to have their minimum sensitivity somewhat lower than the average

noise level in buildings. E.g. the PLT modem front end silicon AD9867 [Analog_08] has an input voltage noise density of $3.6 \text{ nV}/\sqrt{\text{Hz}}$ at maximum gain settings of the internal amplifier. Assuming PLT modems use the frequency range from 2 MHz to 30 MHz, the resulting bandwidth is 28 MHz. The noise to be detected by AD9867 is

$$Noi_{Sensitivity_AD9867} = 3.6 \frac{\text{nV}}{\sqrt{\text{Hz}}} * \sqrt{28 \text{ MHz}} = 19 \mu\text{V} = 25.6 \text{ dB}\mu\text{V} \quad (14)$$

Conversion $\text{dB}\mu\text{V}$ to dBm , $Z = 100 \Omega$ using equation 2:

$$NP_{Sensitivity_AD9867} = 25.6 \text{ dB}\mu\text{V} - 110 \text{ dB(mW}/\mu\text{V}) = -84.4 \text{ dBm} \quad (15)$$

PSD of the noise sensitivity of AD9867 using equation 1:

$$\begin{aligned} PSD_{Sensitivity_AD9867} &= -84.4 \text{ dBm} - 10 * \log_{10}(28 \text{ MHz}) \\ &= -84.4 \text{ dBm} - 74.5 \text{ dB(Hz)} = -158.9 \text{ dBm/Hz} \end{aligned} \quad (16)$$

PSD of the threshold to detect a receivable broadcast service using equation 1:

$$\begin{aligned} PSD_{threshold} &= -95 \text{ dBm} - 10 * \log_{10}(9 \text{ kHz}) \\ &= -95 \text{ dBm} - 39.5 \text{ dB(Hz)} = -134.5 \text{ dBm/Hz} \end{aligned} \quad (17)$$

The ingress signal of the threshold has to provide an SNR of 14 dB. The ground noise level to measure is:

$$NPSD_{ground \text{ noise}} = -134.5 \text{ dBm/Hz} - 14 \text{ dB} = -148.5 \text{ dBm/Hz} \quad (18)$$

Comparing the noise sensitivity of today's analog frontend integrated silicones (equation 16) and the noise level to be measured by the modems (equation 18) shows there is only a margin of 10 dB identifying such a sensitive threshold.

If the detection of the signal ingress is done with CM signals instead of DM, the threshold could be shifted to a higher value. This would relax the very low signal threshold of equation 13 which helps to avoid false detections by PLT modems.

5.2.4 Requirements of a Notch

When signal ingress is identified as a receivable broadcast service, its frequency should be excluded from the PLT communication. The process of the frequency exclusion in OFDM communication systems is called notching. A notch can be characterized by the bottom level and its width or slopes.

5.2.4.1 Bottom level of the Notch:

Two different approaches can be performed in order to derive the bottom level of the notch: 1st, checking the levels of EMC standards [CISPR_97] and 2nd, feeding signals with this level into power outlets and checking whether it affects radio reception.

Approach Checking:

CISPR 22 [CISPR_97] defines two sets of limits and measurement methods for conducted emissions of telecommunication equipment. One set is defined for the telecommunication port and the other set is defined for the mains port. Of course, the limits and methods are different.. For PLT modems, it is not defined whether the PLT signal port, which at the same time is used for power supply is considered as mains or as telecommunication port. The method for telecommunication ports respects the symmetry properties of the attached cable. As previously mentioned in chapter 3.2.2, the asymmetry of a network is responsible for emissions. PLT modems feed signals symmetrically between phase and neutral wires. However, the method used for devices connected to the mains (specified in CISPR 16 [CISPR_99]) is based on measuring the asymmetric voltage level of either the phase or neutral wire to the ground. From the perspective of a PLT modem, this is the worst case, because this voltage consists of asymmetric and symmetric voltage, i.e. not only the interference relevant part but also the desired signal is measured and compared to limits. There is a lively discussion about this topic in [CISPR_05]. To be on the safe side, the worst case situation is assumed for the bottom level of a notch:

CISPR 22 [CISPR_97] specifies the mains Class B (5 MHz to 30 MHz) level to be $U_{AMN} = 50 \text{ dB}\mu\text{V}$ (RBW: 9 kHz, average detector)

For verification of the mains port limits, an AMN (artificial mains network, specified in CISPR 16 [CISPR_99]) is used. It measures half of the differentially fed voltage at a measurement output. It follows that at the outlet U_{outlet} where the PLT modem is connected, twice the differential voltage is allowed.

$$U_{outlet} = U_{AMN} \cdot 2 = 50 \text{ dB}\mu\text{V} + 6 \text{ dB} = 56 \text{ dB}\mu\text{V} \quad (19)$$

Conversion dB μ V to dBm, $Z = 100 \Omega$ using equation 2:

$$P_{outlet} = 56 \text{ dB}\mu\text{V} - 110 \text{ dB(mW}/\mu\text{V}) = -54 \text{ dBm} \quad (20)$$

PSD_{outlet} of PLT Modem at bottom level of the notch using equation 1:

$$\begin{aligned} PSD_{outlet} &= -54 \text{ dBm} - 10 * \log_{10}(9 \text{ kHz}) \\ &= -54 \text{ dBm} - 39.5 \text{ dB(Hz)} = -93.54 \text{ dBm/Hz} \end{aligned} \quad (21)$$

Subjective Evaluation:

The noise is fed to the mains in the vicinity of the outlet where the radio receiver is connected. The level of the noise is varied to check when interference is noticeable on the SW receiver. Human ears are monitoring the reception to verify if the additional noise influences SW radio reception. The signal level is recorded, when the reception quality was deemed to be impaired (using SINPO [ITUR]). This is performed at many outlets in several buildings with the radio receiver tuned to various frequencies. [Schw_08c] documents some of these assessments. Noise levels up to those in equation 19 ($U_{outlet} = 56 \text{ dB}\mu\text{V}$) weren't noticeable by the receiver. Noise was hardly noticeable once when signals were fed into the mains exactly at this level. If the noise was increased by another 10 dB, human ears were able to audibly detect the interference. However, if the radio was disconnected from the mains - and therefore battery powered - the interference was gone. Often, connecting the radio receiver to another outlet also solved the interference problem.

The value from equation 19 seems to be a good choice for the bottom level of the notch.

The ETSI TS 102 578 [Schw_08d] specified a verification setup to confirm the bottom level of the notch. A resolution bandwidth of 300 Hz was chosen in [Schw_08d] to make the bottom level visible with the spectrum analyzer performing a sweep. Care must be taken when comparing the absolute values of the ingress signal level, the values given in CISPR 22 and the bottom level of the notch. Individual resolution bandwidths are used.

PLT modems having a bottom level of a notch as specified here, no longer cause interference to an SW radio receiver. Power management technologies as described in chapter 4.4 will additionally lower this bottom level.

5.2.4.2 Width or Slopes of the Notch

To avoid interfering with the bandwidth of an identified radio broadcast service, the minimum width of a notch should be at least 10 kHz ($\pm 5 \text{ kHz}$ around the carrier frequency of the radio broadcast). Usually, the channels of radio broadcast services are allocated with a minimum spacing of 5 kHz. The centre frequency is a multiple of 5 kHz. If several neighboring radio broadcast services are identified by the PLT system, the width of one notch may be scaled to integer multiples of 5 kHz.

In the radio broadcasting ICI (inter carrier interference) from other radio stations allocating adjacent channels is a serious problem. Signal amplitudes of adjacent carriers often differ by

more than 30 dB. This is why slopes of potential ICI are very precisely specified. References can be found in [ITUR_90], [ITUR_03], [DRM_06] and [ITUR_06]. The slope of a notch for PLT modems might be derived from the requirements of SW receiver's (AM, DRM) protection ratios.

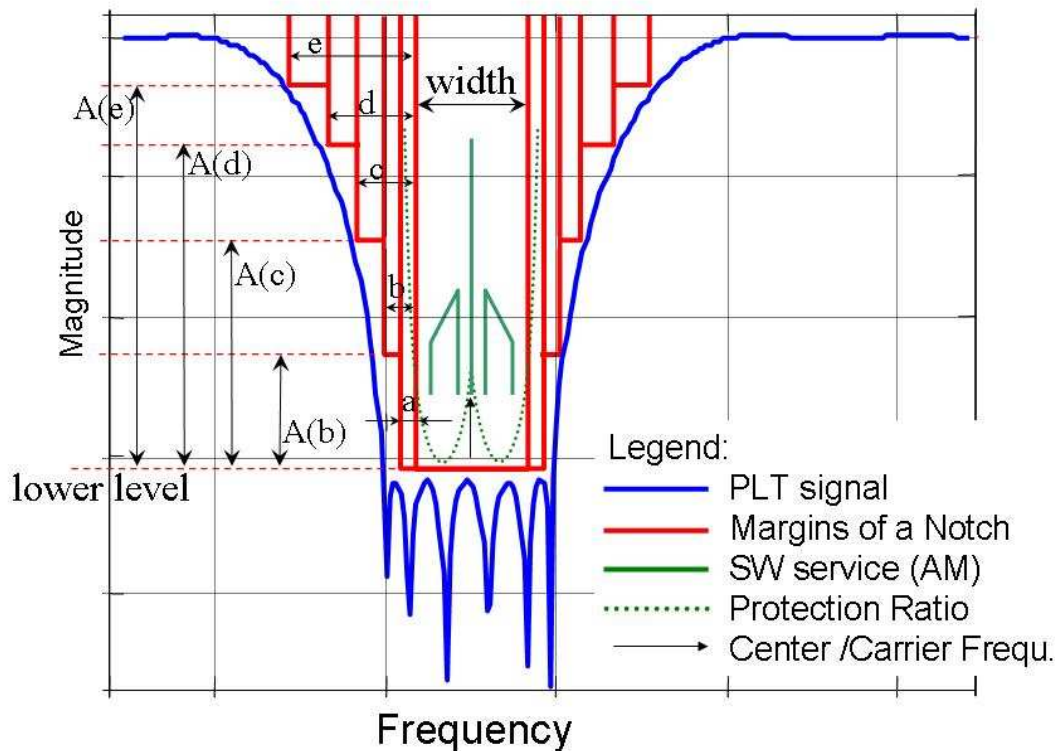


Figure 55: Notch providing protection to an AM service

The definition of a notch for PLT systems should be specified in a way where SW services are not compromised in their reception quality. Figure 55 and figure 56 ([Schw_08d]) visualize how a notch should look. To present an example of 'ideal' and 'non-ideal' scenarios, an AM service to be detected is added with green lines. The spectrum of a HF AM service consists of the carrier (the needle in the middle) and two side bands each 5 kHz wide. The carrier can be detected by PLT modems. The sidebands carry the information to be broadcasted and need to be protected by the notch. Figure 55 shows an example of a good scenario. There is no interference to the AM radio service. Figure 56 shows an example of how interference to the radio service can occur. The margins of the notch and the PLT signal itself (blue line) hit the protection ratio (green dotted line) of the AM service.

The resolution bandwidth of noise measurements is usually identical to the width of an OFDM carrier. To protect one broadcast with a single carrier notch, a PLT modem has to enhance the resolution bandwidth of the receiving FFT (chapter 5.3.3.2), in order to precisely locate the frequency position of the AM carrier. In today's PLT modems, the carrier spacing

(equation 8) is not aligned to the 5 kHz grid of HF radio broadcast. If a HF radio service is located in-between two OFDM carriers of a PLT system and the system is not able to identify the precise frequency of the ingress, at least two carriers should be notched.

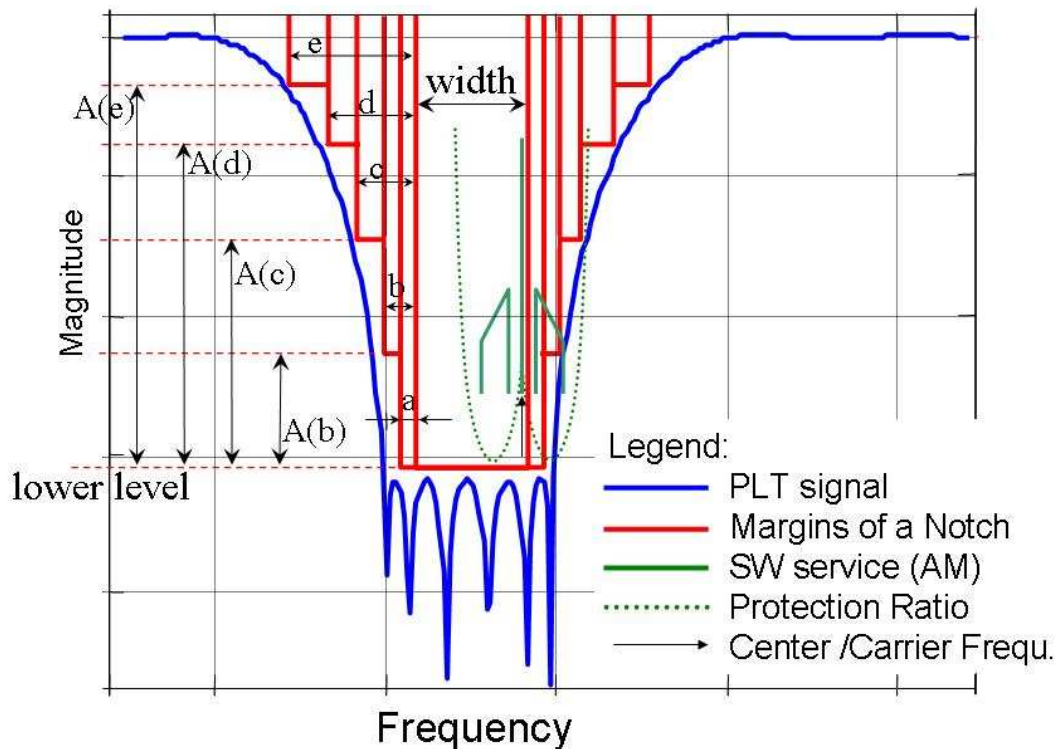


Figure 56: Notch causing interference to an AM service

ICI between HF radio services does not only happen when two carriers allocate the same frequency. It could occur due to the fact that these transmissions travel very long distances and coordination between the broadcasters and individual nations is sometimes difficult. Doppler effects cause frequency modifications. ICI may also occur if adjacent locations (the next or the next after the next, etc) in the frequencies grid are used by broadcasters. As mentioned above, the slopes of protection ratios are defined in

- the minimum receiver requirements for DRM [DRM_06]
- ITU-R Rec. 560-3 1 [ITUR_06]
- ITU-R Rec BS.1615 [ITUR_03] and
- ITU-R Rec BS.703 [ITUR_90].

They all have to be checked in order to derive proper slopes for the notches in PLT modems.

The minimum receiver requirements for DRM [DRM_06] shown in table 5 specify the slopes needed in order to protect the channel from interference by an adjacent service. The

ACS (adjacent channel selectivity) specifies the level of how much the amplitude of the next carrier might surpass the wanted service.

Adjacent channel	Frequency spacing	ACS
1st adjacent channel	10 kHz	25 dB
2nd adjacent channel	20 kHz	35 dB
3rd adjacent channel	30 kHz	45 dB
Further	≥ 40 kHz and < 400 kHz	50 dB

Table 5: Adjacent channel selectivity from minimum receiver requirements for DRM

The values from table 5 are found to be the strictest ones for PLT modems. In the discussion below, these values are compared with the ITU-R recommendations.

ITU recommendation 560-3 1 [ITUR_06] specifies radio frequency protection ratios in HF broadcasting. Figure 57 shows the relative values of the radio frequency protection according to ITU Rec. 560-3 1. Curves A and B refer to different modulation compressions. If any signal spreads in the area below the curves A or B, interference may occur to the AM service. As long as other signals are above the curves, there is no risk of interference. [ITUR_06] also discusses services where the frequency modulating signal is of the order of 4.5 kHz, which is not the case in the HF band. If the bottom level of the notch was verified not to cause any interference to the AM signal (see chapter 5.2.4.1), the maximum point in figure 57 (+17 dB for curve A and +11 dB for curve B) has to be used as a reference. The dashed green line in figure 57 shows the shape of a PLT notch applying the requirements from table 5. The bottom level of the notch is set to the +17 dB point of curve A. The carrier of the AM service is located at 0 Hz, 0 dB. The carrier has a lower protection value than the AM side bands. The 10 kHz point from table 5 – which is ± 5 kHz from the center carrier - specifies that any signal next to the desired channel is not allowed to be more than 25 dB stronger than the desired signal itself. In figure 57, the distance from the maximum level at 5 kHz to curve A is 13 dB. (At curve B this distance is 13 dB, as well). If an additional guard band ‘a’ (identical to frequency span ‘a’ in figure 55) of 2 kHz left and right of the 10 kHz lower area of the notch is given, the value at 7 kHz has to be read out of figure 57 (instead of at 5 kHz). In this case, a protection ratio of 27 dB down to curve A and 25 dB for curve B is read. The green line has a 25 dB step at 7 kHz. Going further in the frequency axis, there is a 10 dB step in table 5 from the 1st to the 2nd adjacent channel. This results in a 10 dB step for the green line at 15 kHz (or after fre-

quency span ‘b’) in figure 57. Comparing the 20 kHz point from table 5 with figure 57, it is apparent that channel suppressions out of the minimum receiver requirements (table 5) are relaxed, compared to the protection ratios specified for AM services. If the 2 kHz guard band ‘a’ is added to a notch, the requirements from [DRM_06] are more relaxed than from [ITU-R_06] in the full side spectrum.

If the DRM adjacent channel suppressions are more relaxed than the protection ratios from [ITU-R_06], this requires a wider notch for PLT modems. The frequency spans ‘a’, ‘b’, ‘c’, ‘d’ and ‘e’ marked in figure 55 and figure 56 are chosen according to the steps defined in table 5.

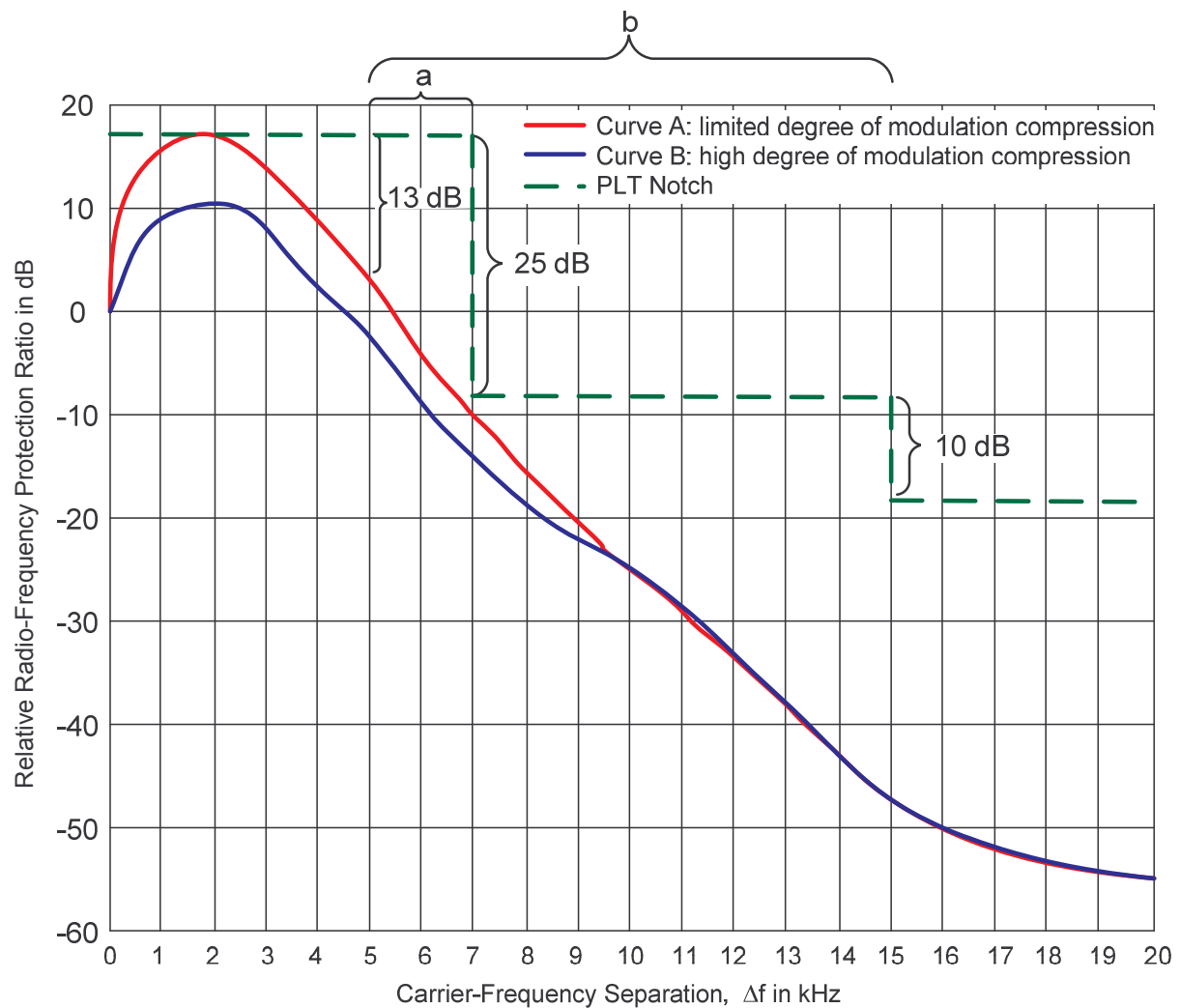


Figure 57: Relative value of the radio frequency protection as a function of the carrier-frequency separation

ITU-R recommendation BS.1615 [ITU-R_03] discusses “planning parameters” for digital sound broadcasting at frequencies below 30 MHz. It specifies relative RF protection ratios between broadcasting systems in dB in the case

- AM is interfered with by digital transmissions (table 6)
- digital transmission is interfered by AM (table 7)
- digital transmission is interfered by the digital transmission (table 8) and
- AM is interfered by AM (table 9).

The abbreviations DRM_B0 to DRM_B3 specify which spectrum occupancy type was selected for DRM. Only spectra with occupancy type 2 or 3 are used in the HF broadcasting range, as they have a nominal bandwidth of 10 kHz. For example, the frequency separation in the “AM interference with AM” case, is the distance between the two carrier frequencies. If it is 0 Hz, the AM carriers of both transmissions overlap. To compare the value from the 1st adjacent carrier of table 5 with table 6 to table 9, the columns of ± 10 kHz are selected. The 2nd adjacent carrier from table 5 has to be compared with the values of the columns of ± 20 kHz. It is again apparent that the channel suppressions from minimum receiver requirements for DRM [DRM_06] are more relaxed than the “planning parameters” of the protection ratios.

Wanted signal (interfered)	Unwanted signal (interfering)	Frequency separation, $f_{unwanted} - f_{wanted}$ in kHz					B_{DRM} in kHz
		-20	-10	0	10	20	
AM	DRM_B2	-48.8	-34.4	6.5	-34.4	-48.8	9
AM	DRM_B3	-47.2	-32	6	-32	-47.2	10

Table 6: Relative RF protection ratios (dB) AM interfered by digital (e.g. DRM)

Wanted signal (interfered)	Unwanted signal (interfering)	Frequency separation, $f_{unwanted} - f_{wanted}$ in kHz					B_{DRM} in kHz
		-20	-10	0	10	20	
DRM_B2	AM	-54.6	-42.8	0	-42.8	-54.6	9
DRM_B3	AM	-53.9	-39.9	0	-39.9	-53.9	10

Table 7: Digital (64-QAM, protection level No. 1) interfered by AM (dB)

Wanted signal (interfered)	Unwanted signal (interfering)	Frequency separation, $f_{unwanted} - f_{wanted}$ in kHz					B_{DRM} in kHz
		-20	-10	0	10	20	
DRM_B0	DRM_B2	-57.4	-46.7	0	-38.4	-53.6	9
DRM_B0	DRM_B3	-55.2	-44.5	0	-36.2	-51.4	10
DRM_B1	DRM_B2	-57.1	-46.4	0	-36.8	-52.7	9
DRM_B1	DRM_B3	-55.5	-44.8	0	-35.2	-51.1	10
DRM_B2	DRM_B2	-55.1	-40.7	0	-40.7	-55.1	9
DRM_B2	DRM_B3	-52.9	-38.6	0	-38.6	-52.9	10
DRM_B3	DRM_B2	-54.3	-39.3	0	-39.3	-54.3	9
DRM_B3	DRM_B3	-52.7	-37.7	0	-37.7	-52.7	10

Table 8: Digital (64-QAM, protection level No. 1) interfered by digital (dB)

Wanted signal (interfered)	Unwanted signal (interfering)	Frequency separation, $f_{unwanted} - f_{wanted}$ in kHz				
		-20	-10	0	10	20
AM	AM	-55.4	-35.5	0.0	-35.5	-55.4

Table 9: Relative RF protection for AM interfered with by AM (dB)

Last, but not least, the recommendation ITU-R BS.703 [ITUR_90] specifies the “characteristics of AM sound broadcasting reference receivers for planning purposes”. Figure 58 shows the relative RF protection ratios for a narrow band system, according to [ITUR_90]. The individual curves A to E differ in the overall bandwidth or the slope of attenuation of the receiver’s selectivity characteristic. It has to be interpreted in the same way as figure 57. If external signals are in the area above the curves, they won’t interfere with the AM service. If they hit the curves or go into the area below, there is a risk of interference. Taking the guard band of 2 kHz into consideration, the channel suppressions according to the minimum receiver requirements for DRM [DRM_06] are more relaxed than all curves in [ITUR_90].

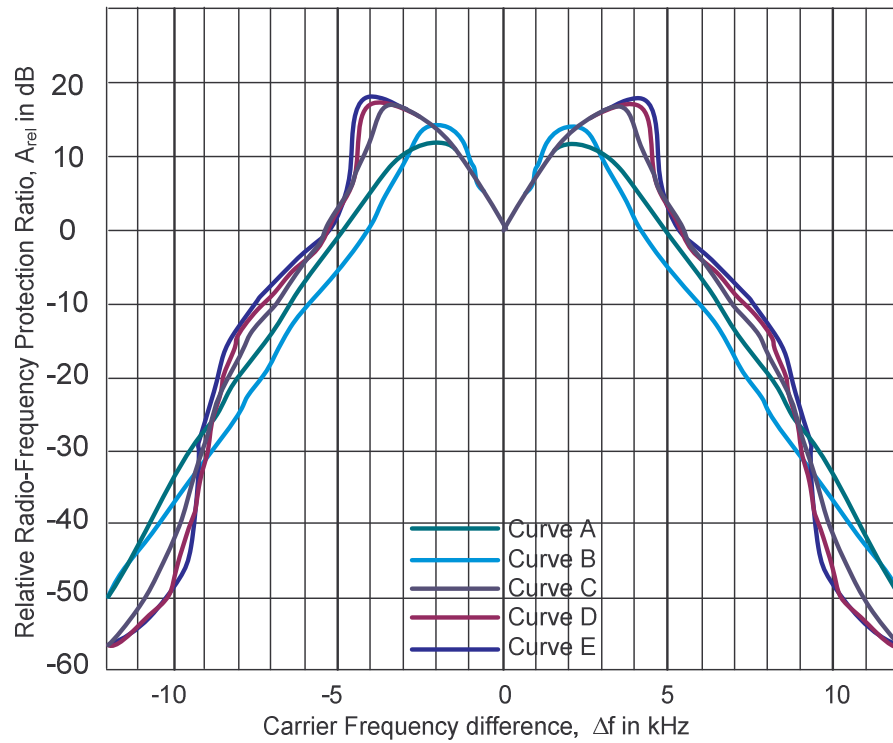


Figure 58: Relative RF protection ratios A_{rel} (dB) for a narrow-band system

Doing these comparisons with all known papers which refer to the issue of protecting radio service from inter carrier interference, the weakest slopes (protecting most communication resources) are defined in minimum receiver requirements for DRM [DRM_06] if a guard band of an additional 2 kHz is added on each side. These values were taken as reference to draft table 2 of ETSI TS 102 578 [Schw_08d] which is repeated here as table 10. The steps, frequency spacings and distances $A(x)$ are visualized in figure 55 and figure 56.

	Frequency spacing	Distance from bottom level of the notch: $A(x)$
1 st step: a	2 kHz	0 dB
2 nd step: b	10 kHz	≤ 25 dB
3 rd step: c	20 kHz	≤ 35 dB
4 th step: d	30 kHz	≤ 45 dB
5 th step: e	400 kHz	≤ 50 dB

Table 10: Definition of a notch: avoid adjacent carrier interference

5.2.5 Adaptive OFDM, Channel and Noise Estimation

Adaptive communications with feedback information was first presented in 1968 in [Haye_68]. To realize notching with minimum implementation efforts, the architecture of today's PLT modems provides good starting conditions. Carrier adaptive OFDM [Lee_05] is used in wired and wireless communications to match the bit load of a carrier (QAM constellation) to the conditions on the channel attenuation and noise. The process of channel adaptation is dynamic. When the channel changes (see chapter 2.1), the adaptation process has to be re-triggered. Some communication systems can do this within milliseconds. Adaptive modulation systems require the knowledge of the channel transfer function at the transmitter. In bidirectional communication systems, this may be acquired by assuming that the channel is identical in each direction (as described in chapter 3.2.4). This is acceptable for the channel, but the noise is usually unique at each receiver. Alternatively, the channel transfer function can also be measured at the receiver, and fed back to the transmitter. Adaptive modulation systems improve the rate of transmission and/or the bit error rates by exploiting the channel information that is present at the transmitter. They exhibit great performance enhancements compared to systems which do not exploit channel knowledge at the transmitter, especially for fading channels. As channel and noise are already estimated to realize an adaptive OFDM, the noise information might be reinterpreted to identify receivable radio broadcast stations. In an adaptive OFDM system, every carrier loads an individual amount of information. It is no additional burden for the system if individual carriers don't carry information because they are notched. The concept is adaptive. The method of using a carrier, notch it later and reuse it again, does not cause any additional work. Carrier individual adaptive modulation is state of the art in today's PLT modems. Notching itself is not new for PLT modems. Thus notching of the amateur radio bands is an already common feature of today's PLT modems.

PLT modems measure the channel transfer function by transmitting known training symbols in the preamble of a communication burst or in a channel estimation procedure. The channel estimator in the receiver compares the received training symbols with the reference symbols to derive the modification by the channel in terms of amplitude and phase of each individual carrier. This information is used by the PLT receiver to equalize data symbols. Figure 59 shows an example of a channel estimation of a PLT link. The horizontal axis represents the frequency of a complex signal in baseband. The vertical axis represents the SNR in dB estimated by the system. The present noise level of around -50 dB is visible in the unused carriers at the far left or right side of the graph. Frequencies with excellent SNR are marked with the red dotted area. These frequencies are allocated with the maximum constellation of this system of 1024-QAM,

carrying 10 bit per carrier. Frequencies with lower SNR are allocated with lower constellations from 256-QAM down to QPSK. Frequencies with less SNR than the most robust implemented constellation requires, can no longer be used for communication and could be notched or suppressed.

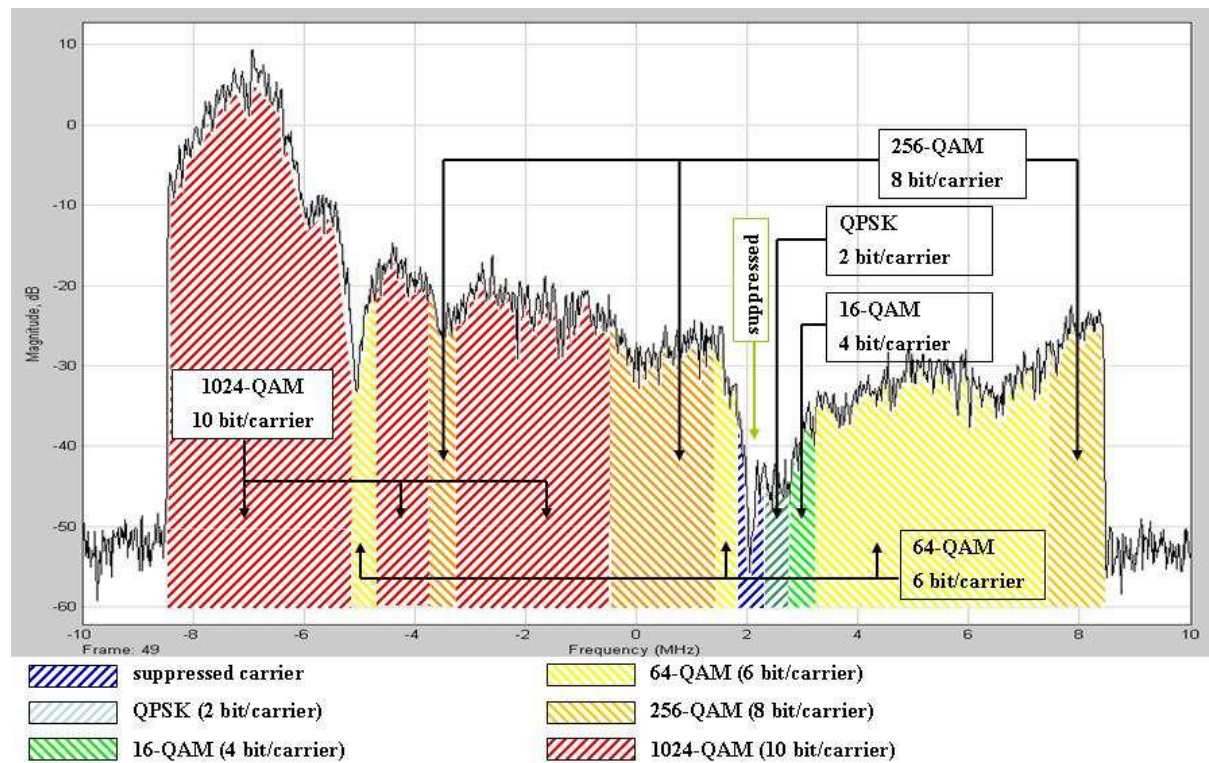


Figure 59: Adaptive channel modulation. Simulation of a frequency scan using the channel data of a measured in-house PLT channel

There are two incentives to omit a carrier from communication: 1st, the desired SNR for the minimum constellation is not available at this frequency or 2nd a radio service has to be protected at this frequency. For wavelet transmission [Sandb_95], an omitted carrier will result in a deep spectral notch. At OFDM, due to the low side lobe suppression (see chapter 5.3.4.1), the shape of the notch might be provided by additional filters. These filters will only be applied if the notch was initiated to protect a radio service.

Both the channel transfer function and the noise have to be measured in order to estimate the signal to noise ratio. The transfer function is measured - as described above - with the transmission of training symbols. If such a training symbol is transmitted several times, the estimation of the channel can be improved by averaging the individual receptions. The noise might be estimated by calculating the variance from the individual receptions. Such a noise measurement has the advantage that it can be done during the PLT transmission without insert-

ing additional ‘quiet times’ for noise measurements. If adaptive power management is implemented as described in chapter 4.4.1, the sensitivity of the receiver should be adjusted by setting the transmit power level. For example, if signals with the threshold to detect a radio service of -95 dBm (chapter 5.2.3) should be detected, the PGA (programmable gain amplifier) of the analog front end almost has to be set to its maximum. (If e.g. an AD9867 [Analog_08] is used as front end device, the AGC is set to -10 dB below the maximum. See equation 16 and equation 18). If the attenuation of the channel is very low, the receiver’s AGC might be at its minimum gain settings and won’t be able to detect weak signals. The transmission power should be reduced to increase receiver AGC settings until the receiver detects low signals at the level of -95dBm.

The noise measurement during communication even works in notched carriers. If the noise is measured by calculating the variance of the received training symbols, it does not matter if the carrier is allocated or notched. Figure 60 shows a result of a channel and noise measurement performed with the use of training symbols. Figure 60 is a snapshot from the PLT modem implementation described in chapter 5.3. The horizontal axis shows the index of the OFDM carriers. It represents the frequency range from 0 Hz up to 40 MHz. The vertical axis shows a relative level in dB. The carrier with the index of 211 is the first carrier used for communication, the one with index 1506 is the last. The topmost curve (blue line) is the channel transfer function derived by averaging 4 training symbols. It shows a relatively flat channel with only one fading of 30 dB. The three other curves are the noise measured by calculating the variance values of the 4 received training symbols. The cyan curve shows the noise signal last measured before the screenshot was taken. It shows a high variation (> 10 dB) of the individual values. The red curve is the median calculated with the latest 20 noise shots and the green one is the max-hold of these 20 shots. The red and green ones are better suited to detect any thresholds. The ‘needles’ of the ingress from HF radio broadcast are clearly visible.

The variance has to be calculated from the absolute values of the received training symbols. The phase of the received signals becomes unstable when the time synchronization at the receiver varies. This could occur with highly attenuated, weak signals or if there is narrow band interference.

Another possibility to derive noise information is to recode the data from the output of the receiver’s FEC to reproduce the transmitted symbols. Comparing these symbols with the received data at the equalizer derives the noise with a high timing resolution.

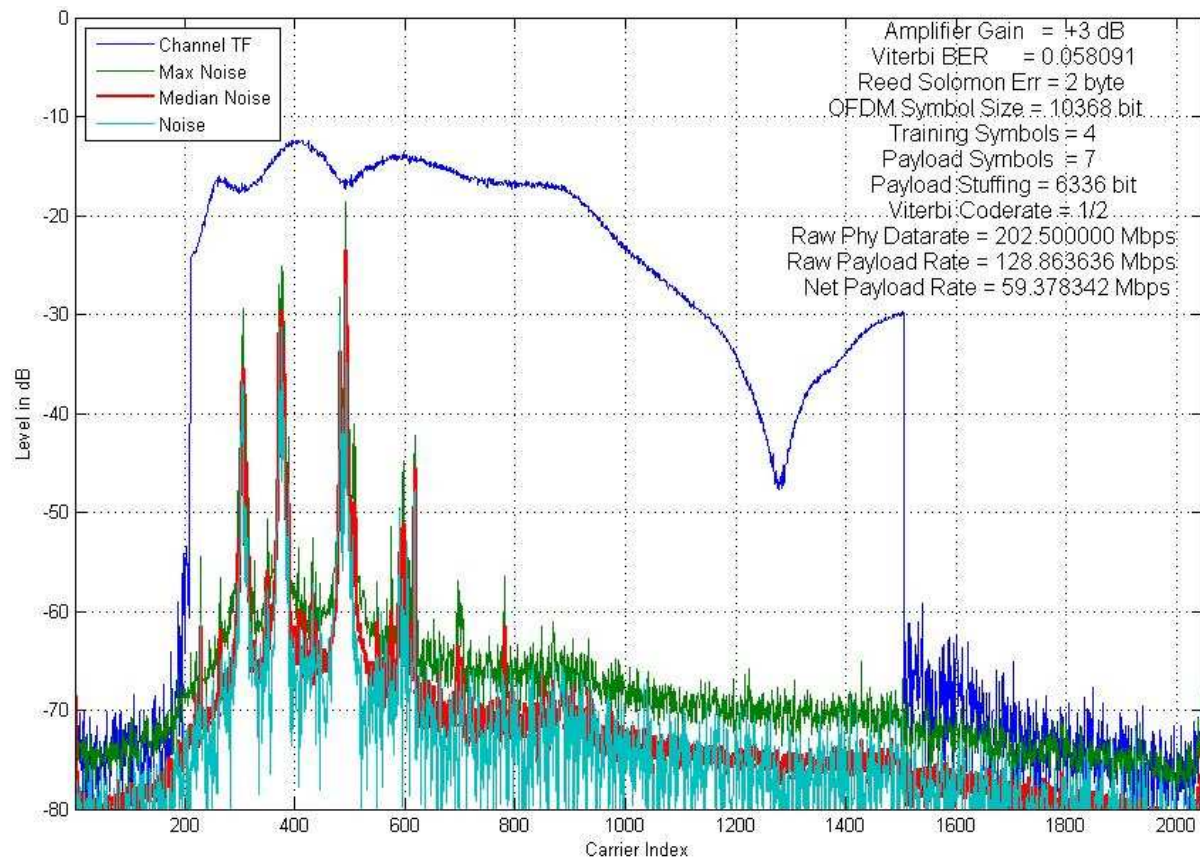


Figure 60: Channel and noise measurement of the PLT demonstrator performed during communication

When multiple training symbols are sequentially chained, there is the disadvantage that noise measurements performed during communication do not detect frequencies at integer multiples exactly matching the training symbol's repetition frequency. Such noise doesn't enhance the variance between the received training symbols. To overcome this, a variable guard interval has to be inserted before the training symbols during the transmission of the preamble for frame start and channel estimation. Figure 61 shows an example of how a new preamble could look if 4 training symbols are used. At the beginning of the burst is the CAZAC sequence which is responsible for the time synchronization of the receiver. Then, 4 training symbols (TrS1, ... TrS4) are transmitted. Each TrS is headed by a Guard Interval (GI) to make the transmission robust against multipath transmissions. In-between the training symbols, a short gap has to be inserted. Inserting a short gap or varying the length of the guard interval has the same effect. Here, gaps are shown to make it more clearly visible. The length of each gap must be unique to avoid that a constant sine wave interferer with a frequency of a multiple of the training sequence repetition frequency influences each training symbol identically. The lengths of these gaps have to be known by the receiver in order to remove them. The insertion of these

gaps costs communication resources during each transmission burst, but simulation shows that one sample gap at one of the 4 training symbols dramatically enhances the quality of the noise measurements. Alternatively, instead of expanding the guard interval, it can also be shortened. It is important to note that the expansion or shortening of the distance between the training symbols does not enable any new signal to influence all training symbols in an identical way.

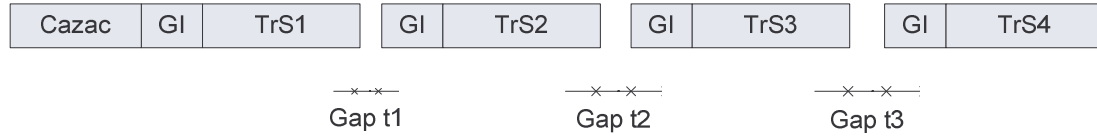


Figure 61: Gaps in between training symbols enhance noise measurement quality

If the noise is measured during communication a further disadvantage is that it is recorded at the receiving modem. The transmitting modem is responsible for the detection of radio broadcast ingress and notching. However, in a bidirectional communication - which is usually the case at PLT - the result of the noise measurement of the return path could be used. In order to capture the communication signal as well as the noise signal within the dynamic range of the receiver ADC, the implementation of adaptive power management as described in chapter 4.4 is a prerequisite for measuring the noise during communication.

Alternatively, the noise could also be measured during any quiet period of the powerlines. The minimum length of such a quiet period is given by the basic OFDM system parameters such as carrier spacing and symbol duration. Equation 8 calculates the carrier spacing of an OFDM system. The OFDM symbol duration is reciprocal to the carrier spacing. For example, a carrier spacing of $f_{CS} = 19.531$ kHz results in a symbol duration T_{Symbol} of

$$T_{Symbol} = \frac{1}{f_{CS}} = \frac{1}{19.531 \text{ kHz}} = 51.2 \mu\text{s} \quad (22)$$

The FFT of the system has to be filled once, in order to capture a noise shot. The time needed here is equal to the system's symbol duration T_{Symbol} . In a multi-node communication system, the MAC layer organizes when the resources are allocated and by whom. E.g. in a CSMA MAC layer, the contention free interframe spacing is often longer than the symbol duration. All such gaps could be used to measure the noise.

To conclude, to activate a notch the noise could be measured during communication or within a transmission break. To reuse the notched frequency by the PLT system the noise has to be measured in a quiet period or within a notch during communication, but the notched frequency must not be used to measure the noise.

5.2.6 Impact on PLT Throughput

To evaluate the impact of ‘Smart Notching’ on the performance of a PLT system, the following assumptions of a PLT modem are made:

‘Smart Notching’ is realized in today’s PLT modems with a carrier spacing of equation 8: $f_{CS} = 19.531$ kHz. The frequency range used is $f_{used} = 2 \text{ MHz} < f < 30 \text{ MHz}$. Due to the guard band of 2 kHz left and right of a protected HF service (introduced in chapter 5.2.4.2), a single notch has to be in minimum 14 kHz wide. The PLT modem is able to detect the exact frequency location of the signal ingress (see chapter 5.3.3.2). The frequency grid of the PLT OFDM carriers aren’t aligned with the frequency grid of radio broadcast channels. Furthermore, it is assumed that ideal notch filters with vertical slopes and no ripples in the pass-band can be realized. The idea presented in chapter 5.3.4.3 enables the implementation of almost perfect notch filters. It doesn’t matter if the side lobes of OFDM carriers are cut by notch filters as the side lobes don’t carry useful information for the PLT system. (The fact that the slopes of a notch specified in table 10 reduce the SNR of adjacent carriers is neglected, here.)

With a statistical probability of 28%, the notch having a 14 kHz bandwidth fits in between two OFDM PLT carriers of $f_{CS} = 19.531$ kHz. In this case, the radio service could be protected with an ideal notch in between two OFDM carries without omitting either of them. With a probability of 72%, the 14 kHz overlaps with one of the two carriers. In this case, the carrier has to be omitted from powerline communication.

The channel characteristics assumed here are based on measurements described in chapter 2.1.1 and in [Schw_08c]. The number of radio services needing to be protected was measured in the tests documented in [Schw_08c], table 19 and table 21. In these two tables, all receivable broadcast stations are listed which were receivable at the test time and location.

An average of around 25 AM radio stations is receivable at any time in any location. Of course this varies during the day and depends strongly on the receiver’s location. When recording table 19 of [Schw_08c], 24 HF radio stations were received. This results statistically in a total of $24 \cdot 0.72 = 17.3$ carriers to be omitted from powerline communication.

Median signal ingress level of all stations in table 19 of [Schw_08c] is -84 dBm. Using equation 1, this results in a $PSD_{signal_ingress} = -124 \text{ dB(m/Hz)}$.

Unfortunately, the attenuation between 2 outlets wasn’t measured at this location, so let’s assume the median attenuation of a PLT channel: $Att = 42 \text{ dB}$ (chapter 2.1.1)

Median noise floor at an outlet is $Noi_{receive} = 11 \text{ dB}\mu\text{V}$ and attenuation is $Att = 42 \text{ dB}$ (chapter 2.1.1). Using equation 1 and equation 2 this results in an $NPSD_{receive} = -139 \text{ dB(m/Hz)}$.

Feeding Level of PLT modem is $PSD_{feed} = -55 \text{ dB(m/Hz)}$.

The Signal to Noise Ratio SNR is

$$\begin{aligned} SNR &= PSD_{feed} - Att - NPSD_{receive} \\ &= -55 \text{ dB(m/Hz)} - 42 \text{ dB} - (-139 \text{ dB(m/Hz)}) = 42 \text{ dB} \end{aligned} \quad (23)$$

The theoretical channel capacity CC_{all} according to equation 4

$$CC_{all} = f_{used} * \text{ld}(1 + SNR) = 28 \text{ MHz} * \text{ld}(1 + 10^{4.2}) = 390.6 \text{ Mbps} \quad (24)$$

For simplification, the capacities which are lost due to the increased noise level at the frequencies, where the radio signal ingress happens, are neglected.

Lost channel capability due to ‘Smart Notching’:

Remaining $SNR_{ingress}$ at the carriers where HF-radio broadcast ingresses:

$$\begin{aligned} SNR_{ingress} &= PSD_{feed} - Att - PSD_{signal_ingress} \\ &= -55 \text{ dB(m/Hz)} - 42 \text{ dB} - (-124 \text{ dB(m/Hz)}) = 27 \text{ dB} \end{aligned} \quad (25)$$

Lost throughput CC_{lost} due to the statistical number of carriers which have to be omitted:

$$CC_{lost} = 19.5 \text{ kHz} \cdot 17.3 \cdot \text{ld}(1 + 10^{2.7}) = 3.0 \text{ Mbps} \quad (26)$$

The theoretical loss of throughput resources due to ‘Smart Notching’ in percent:

$$\frac{CC_{lost}}{CC_{all}} * 100\% = \frac{3.0 \text{ Mbps}}{390.6 \text{ Mbps}} * 100\% = 0.77\% \quad (27)$$

If this calculation is done for the 2nd location analyzed in [Schw_08c], the result is 0.67%. Table 21 in [Schw_08c] lists 28 receivable radio stations. At the 2nd location, the reception quality of radio services was better. More stations were receivable, but the level of ingress was also higher.

A PLT modem does not lose throughput capacities if such ‘bad’ carriers (with a high ingress noise level) are omitted. At the 2nd location, more carriers had to be omitted, but the lost communication resources from these carriers were less, than that of the 1st location.

To minimize the overhead of ‘Smart Notching’ in terms of lost throughput resources, there is a high motivation to implement technologies as described in chapter 5.3.3.2 and 5.3.4.3. This

allows a PLT modem to be able to precisely locate the frequency of the signal ingress and to create ideal notches.

If the full HF radio broadcast bands were omitted, regardless of whether there is radio reception possible or not, 21% of the communication resources of a PLT modem would be lost. The concept of ‘Smart Notching’ allows PLT modems to reuse almost all of the frequencies in the HF bands again.

5.3 Implementation in a Demonstrator System

A feasibility study is implemented in order to prove the concept of ‘smart’ or ‘dynamic’ notching. The PLT system is designed by Sony EuTEC with the main focus on the desired applications and rapid development. The system is Sony EuTEC proprietary, and does not follow any PLT standards such as Homeplug [Homepl], HD-PLC [HDPLC] or UPA [UPA]. As an application, the system transports a high definition video stream from transmitter (Tx) to receiver (Rx) and measures maximum payload data. Its maximum throughput on phy-layer is 212 Mbps. The system doesn’t include a fully interoperable multi-node MAC-layer. It consists of only 2 modems.

5.3.1 PLT Modem System

Each of the Sony EuTEC PLT modems consists of a standard PC running Gentoo Linux [Linux] as the operating system. Each PC has an embedded PCI FPGA board (ADC-PMC2) from ALPHA DATA [Alpha]. This PCI board is equipped with two daughter boards: “ADM-XRC-II” for the PLT codec chains and “ADM-XRC-II Pro” for the tunable notch filters. The notch filter is located in a separate FPGA, because it was added at a later time. Additionally, at the beginning of the notching project, it was unknown how many resources and filter stages would be required.

For prototype implementations, it is always better to have more resources available than finally needed. The synthesis process of the generation of the FPGA bitstream is accelerated dramatically if not all of the capacity of the FPGA is used. The more resources available to the ‘place & route’ algorithm, the faster the synthesis process completes. Toward the end of the project, each generation of the codec bitstream requires more than 8 hours. Timing constraint problems occurred which are not visible in isolated synthesizing and mapping of functional blocks. The ADM-XRC-II hosts a Xilinx Virtex II XC2V8000 FPGA and the ADM-XRC-II Pro a Virtex-II Pro XC2VP100 device. These FPGAs were the largest available at the begin-

ning of the project. As an AFE (Analog Front End), the AD9866 [Analog] evaluation board from ANALOG DEVICES is modified to be connected to the ADM-XRC-II.

In order to control and operate both PLT modems, a 3rd PC (e.g. a Sony VAIO [Sony]) is required to run Matlab [MATW] to monitor the status of the PLT transmission. Figure 62 shows a screenshot of the status monitor application. It consists of 4 subplots visualizing graphically live from top to bottom:

- the SNR and constellations of the OFDM carriers
- BER (bit error rate) of the transmission
- actual data throughput
- AGC settings.

Furthermore, the noise at the power outlet of the transmitting modem can be measured. The top subplot, visualizing the signal to noise ratio, represents the frequency from 4 MHz to 30 MHz on the horizontal axis, and the SNR in dB on the vertical axis. The blue line shows the live SNR measurements. The sharp deep reductions of the SNR e.g. at 6 MHz or at 9 MHz are caused by the ingress of HF radio transmissions. The wide reduction of SNR at 25 MHz is caused by frequency eliminations on the multipath transmission channel. The pink area below the blue line represents the allocated communication resources. The amplitude of the pink area at every individual point (representing a carrier) defines the selected constellation. At around 25 MHz, the SNR is so low that it no longer makes any sense to allocate these frequencies for communication. These carriers are notched. Beginning from the notched carriers at 25 MHz and looking towards the left, 5 steps are visible representing an individual constellation: 4 QAM, 16 QAM, 64 QAM, 256 QAM and 1024 QAM. The matching constellation is chosen, depending on the available SNR at each frequency. The maximum constellation that the system is capable of is 1024 QAM.

The subplots showing the bit error rate, the throughput rate, or AGC setting represent the time on the horizontal axis. The most recent measurement is on the far right. Curves move to the left with the passage of time. The graph history lasts up to one minute. The bit error rate is the value being corrected by the Viterbi decoder. The throughput graph shows 3 curves - representing the data rate on raw phy level (red), on FEC level (green) and the net rate available to the applications (blue). It is interesting to note that at around 15 sec before the screenshot was recorded, the bit error rate increased to its maximum, e.g. a channel change occurred. This was noticed by the system and the constellation was reduced to the most robust settings, which is visible in the throughput graphs. The bit error rate drops to almost zero when using the very

robust constellations. After a readaptation, the throughput and bit error rates returned to their original values.

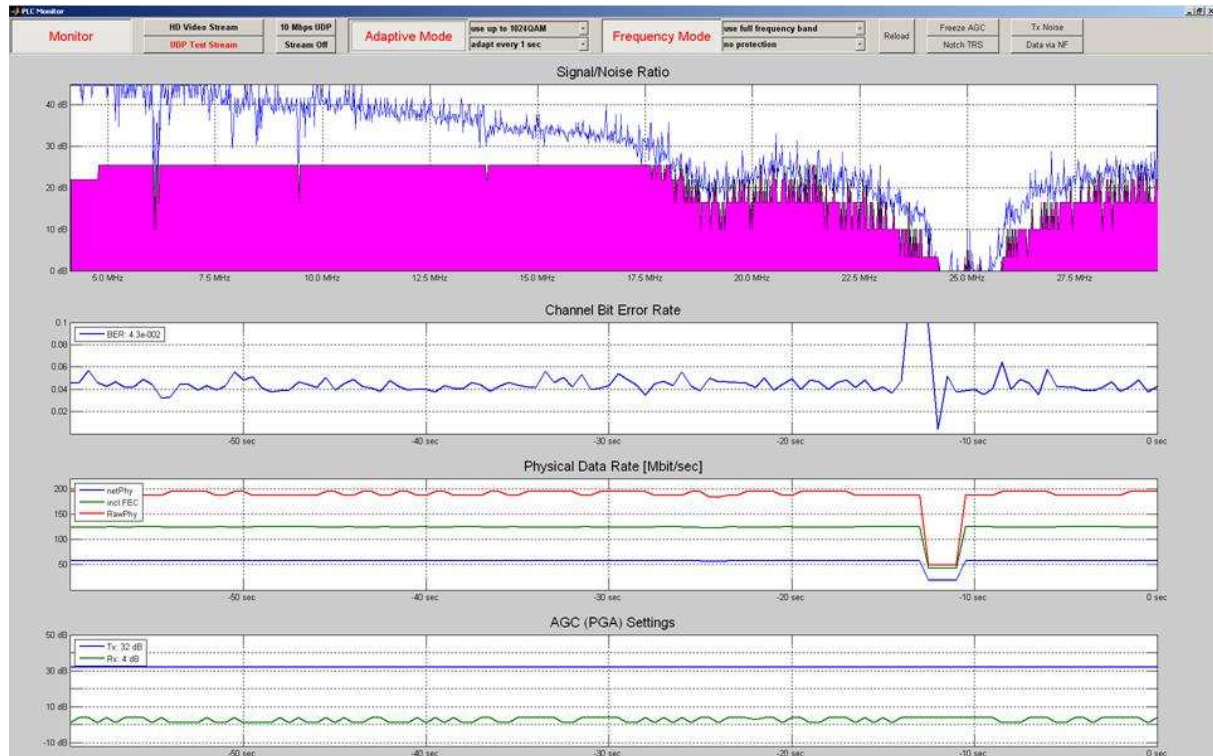


Figure 62: Screenshot of the PLT system monitor application

- Top figure:** measured SNR (blue) and selected constellation (pink).
X-axis: Frequency range from 4 to 30MHz, Y-axis: dB
- 2nd figure:** actual BER. X-axis in time, the past 60 sec,
Y-axis: corrected bits by Viterbi decoder from 0 to 0.1
- 3rd figure:** actual data throughput rate on phy layer.
Red: on raw phy layer, green: on FEC level, blue: net rate.
X-axis in time, the past 60 sec. Y-axis: 0 to 220 Mbps
- lowest figure:** AGC setting. X-axis in time, the past 60 sec, Y-axis in dB.
Green: Rx AGC setting,
blue: Tx AGC setting for measuring the noise signals

The Matlab application communicates with the PLT modems via http protocols. A web-server is running as an application on the Linux system, communicating with the PLT driver on each modem. Further applications are generating UDP payload data to be transmitted and received via powerline. Another pair of applications is forwarding the HD-video stream (MPEG_TS) from the hard-disk of one PLT modem to the 2nd device via powerline. There is a

VLS (VideoLAN server) [VLAN] streaming the data to the 3rd PC where a VideoLAN client [VLAN] renders the MPEG transport stream. This scenario is depicted in figure 63. Several python scripts [Python] are used as applications generating data, forwarding them from source to sink or connecting the web-server with the network driver.

The PLT driver is implemented in C. Here a standard Linux Ethernet driver is used and enhanced with additional APIs and hardware access functions. The powerline network driver is a loadable Linux module, registering a network interface for use with the IP stack. Hence, data is sent and received using the standard Linux networking facilities. Data packets then pass to the PLT modem hardware for transmission, and received packets are injected into the IP stack from the bottom for the usual IP stack routing. If the module is loaded into the kernel, it registers both a network driver and a device driver. While the network driver interfaces with the host's IP stack, the device driver is actually the interface to the FPGA hardware. The APIs are realized as file access functions to monitor and control the system. Driver functions are necessary to calculate the constellation of the carriers from the measured SNR data (variance values of the training symbols, see chapter 5.2.5), for example and program them to the adaptive QAM units of Tx and Rx. An interrupt handshake and the transmission of control packets via PLT guarantee the change of QAM constellations synchronously on both modems. Finally, Ethernet network functions are implemented to encapsulate the control packets into an IP frame and transmit them.

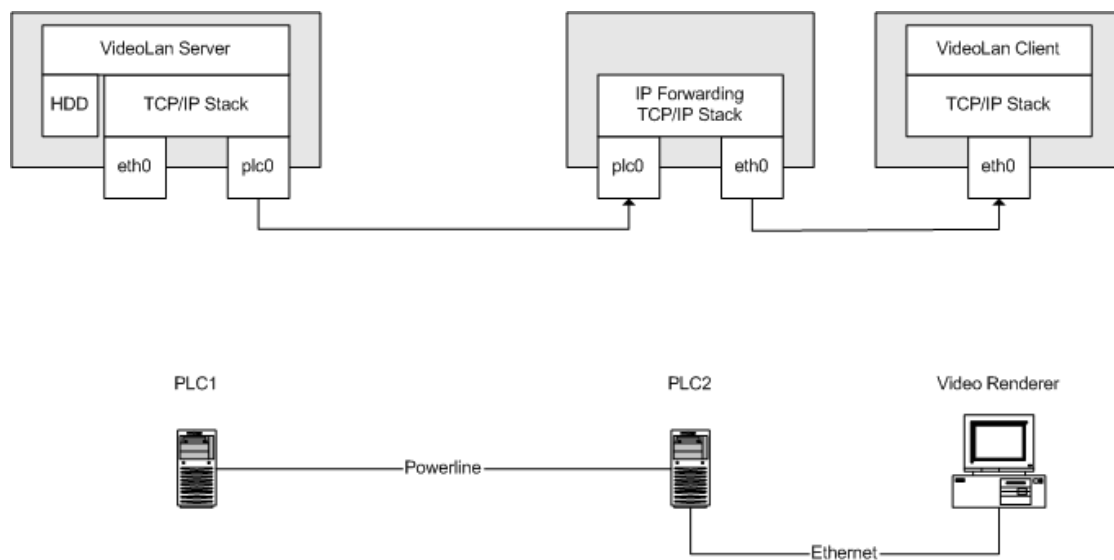


Figure 63: HD video streaming application via PLC demonstrator system

The codec chains are visualized in figure 64. The top row shows the transmitter chain from left to right. The bottom chain represents the receiver units from right to left. The PLT channel

connects the Tx with the Rx path. The PLT drivers and the web interface controlling the hardware are physically running on each of the PCs, they are depicted only once for simplification. After the payload data generation by an application, the driver inserts them into a DMA queue. The handshake of the DMA is implemented in the interrupt service routine.

A RS (Reed Solomon) block encoder [Reed_99] oversamples the data polynomial and converts the data block like an FFT from the frequency into the time domain. Due to the additional data and monitoring the known result of the added portion, the RS codec is able to correct isolated bit errors at any location inside the data block.

The time interleaver rearranges the data in a non-contiguous fashion, in order to support the RS codec. The aim is not to correct a group of closely aligned errors, but to correct some isolated bit errors anywhere in the block. A time interleaver increases the performance of the Reed Solomon codecs. Data on the PLT channel suffers from being corrupted by impulsive noise, for example. The time interleaver separates the broken block into individual bit errors.

The Viterbi codec [Vite_67] is a convolution error codec. It adds a certain amount of redundancy by convoluting the data with a known random data pattern. In the transmitter this is simply implemented with a chain of EXOR gates and shift registers. The receiver uses the trellis trees [Schle_04] to remove the redundancy. Here the added known pattern indicates where bit errors occurred.

The frequency interleaver is responsible for ensuring that adjacent bits in the time domain are not mapped onto the adjacent frequency carriers. In the presence of radio signal ingress, an HF radio band could possibly be no longer useable for PLT. Here, bits on several adjacent carriers are distorted. Multipath propagation on the PLT channel might cause deep fades in the allocated frequencies and adjacent carriers are again corrupted. The frequency interleaver spreads these concentrated erroneous bits to several occasional ones.

The adaptive QAM (quadrature amplitude modulator) is a simple 3-dimensional look up table. If 5 constellations are implemented, the table has 5 fields. E.g. the field for 1024 QAM consists of a 10-bit input array and 1024 complex output entries. The software driver programs the field to be used for each carrier, which in turn decides how many input bits are modulated for each frequency.

The OFDM block consists of a 2k IFFT at the transmitter, converting each complex constellation point out of QAM into a sine wave where the location of the constellation point defines amplitude and phase. This is done for all allocated carriers in parallel. It outputs the complex baseband OFDM symbol in the time domain with a preamble being added to the beginning of

each burst. The TrS (training symbols) are generated by an m-sequence generator [Mart_94] and added to the frequency domain before the IFFT. The TrS are only differentially (2-PSK) modulated. The m-sequence generator outputs only the values 1 and -1. After the IFFT, a guard interval is added to make the transmission immune to multipath transmission. This is achieved by simply copying the tail bits of the OFDM symbol to the beginning of the symbol.

The OFDM block is followed by a line interface filter which suppresses the out-of-band carriers and a quarter period mixer shifting the complex baseband signal by 20 MHz to its ultimate real-valued transmission band. Here, the system's sampling rate is doubled from 40 MHz to 80 MHz. The next part of the preamble is added to the front of the training symbols ahead of this block. The CAZAC [Lüke_92] sequence is responsible for the time synchronization of the receiver. The CAZAC sequence is stored in a memory block and read in the time domain.

The tunable notch filter is added after the mixer stage. This block is described in detail in chapter 5.3.4.

Finally, there is the analog front end in the transmitter consisting of a DAC with an internal oversampling to shift mirror images to higher frequencies, a low pass filter, a line driver amplifier and a coupler to feed the generated data onto the PLT channel.

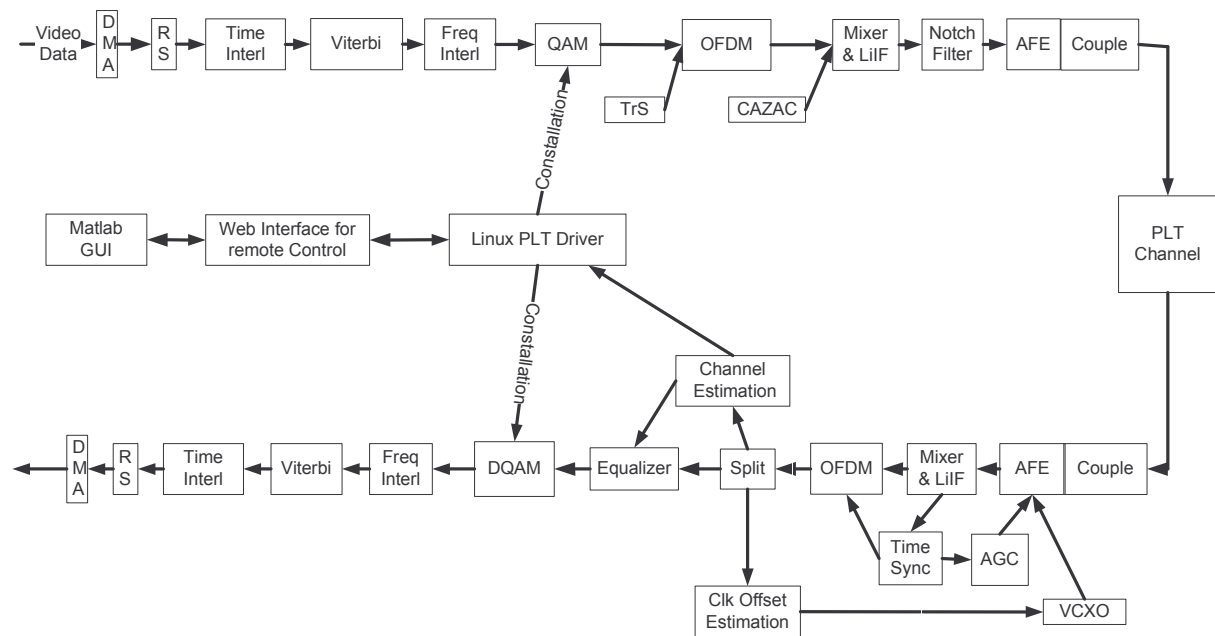


Figure 64: Block schematic of ‘Smart Notching’ demonstrator system

In order to simulate the system, the PLT channel is recorded using a vector network analyzer in various buildings and is reproduced with an FIR (finite impulse response) filter block in Matlab/Simulink.

The identical blocks follow in reverse order for demodulating the data in the receiver.

The AFE includes a band pass filter to isolate the frequencies between 4 MHz and 30 MHz, a PGA is needed for the AGC and the ADC.

After the mixer converts the signals into the complex baseband, the CAZAC sequence is detected by a correlation function. The result of this correlation is used for time synchronization at the receiver with the burst as well as to set the PGA of the AGC.

The OFDM block now performs the FFT operation. It cuts the guard interval and transforms the sample data back into the frequency domain.

A splitter passes the training symbols to the sampling clock offset estimation function, which corrects the clock offset at a VCXO (Voltage-Controlled Crystal Oscillator). Furthermore, the training symbols are passed to the channel estimator - deriving the noise and channel data (see chapter 5.2.5). The channel estimator also delivers the SNR values for the software driver and the channel data to the equalizer, which corrects the subsequent data symbols.

The DQAM retrieves the bit sequence from the complex constellation point of each carrier, depending on the constellation programmed by the driver. The frequency interleaver, Viterbi decoder, time interleaver and the Reed Solomon decoder remove the error protection information added by the transmitter. Finally, a 2nd DMA queue passes the data back to the application.

The combination of Reed-Solomon and Viterbi Codecs with time and frequency interleavers is a classical codec chain which is widely used in communications, e.g. DVB. This codec chain is currently being replaced by Turbo codecs or LDPCs.

Table 11 shows an overview of the basic OFDM system parameters.

Sampling Rate	80 MHz	Number of sub-carriers	2048
Analog Spectrum	40 MHz	Used sub-carriers	1296
Symbol part duration	2048 samples, 51.2 μ s	Sub-carrier spacing	19.53125 kHz
Cyclic prefix duration (GI)	1/16, 128 samples, 3.2 μ s	First used carrier	211
Symbol interval	2178 samples, 54.4 μ s	Last used carrier	1506

Table 11: PLT system basic parameters

5.3.2 Notch Filter Environment

As previously mentioned, the PLT modem was developed first, and the functions of ‘Smart Notching’ were added later. Therefore, a 2nd FPGA (a Virtex II Pro) is added to the system’s hardware. Figure 65 gives an overview of how the new functions are added.

The noise is measured in quiet communication phases at the transmitting modem. The noise measurement control logic in the V2 (Virtex-II) FPGA is responsible for reusing the FFT block in the receiver chain for FFT operation on noise data and to forward the results of the noise measurements to the V2P (Virtex-II Pro) FPGA. This block doesn’t affect original communication logic. A new 2 kByte RAM is added to store the FFT input data.

The noise measurement interface in the V2P receives the noise data and forwards them to the embedded PPC (PowerPC) processor. The PPC then calculates statistics for the noise spectrum, detects frequencies to be notched and programs coefficients of the notch filter in V2P. The data to be transmitted are forwarded from the Tx Line Interface filter to the V2P, where the notch filter is located. After inserting the notches, the data are returned to the V2 where the AFE is connected.

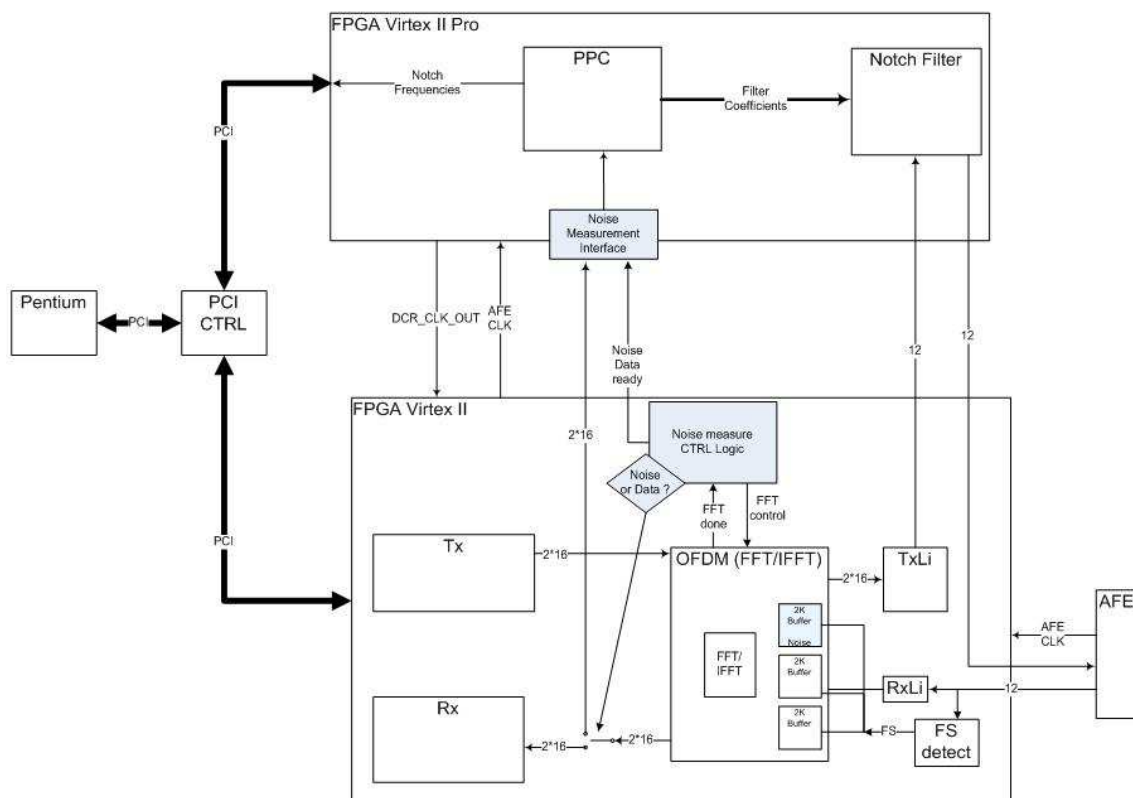


Figure 65: Implementation of ‘Smart Notching’ demonstrator in FPGAs

Figure 66 gives an overview of all blocks required to implement the notch filters. A processor is needed to calculate the notch filter coefficients. This could have also been done by the Linux driver, however, transferring the data via PCI would have caused additional overhead for statistical calculations of the noise data. At the beginning of the implementation, the ETSI TS [Schw_08d] was not yet finalized. Therefore, implementing the important parameters such as thresholds and timings in software allows flexible adaptations of the ongoing drafting process of the ETSI TS [Schw_08d]. Furthermore, Xilinx development tools [Xilinx] enable a simple usage of an embedded PPC. In order to connect the PPC, various bus systems are available from Xilinx as IP-cores. These are the PLB (Processor Local Bus) as the main backbone to connect other IP-cores such as RAM, the PCI interface to the host processor and the OPB (On-Chip Peripheral Bus). An RS232 debug interface is connected to the OPB. The DCR (Device Control Register Bus) is required to connect simple user implemented function blocks which do not include the quite complex PLB interface. The components in figure 66 marked in blue are available in hardware on the V2P FPGA. The grey blocks are IP-cores which could be embedded like LEGO [LEGO] blocks. The yellow components had to be implemented in VHDL.

The DCR noise control block receives signals from V2 FPGA and saves the data to RAM, which is accessible by the PPC for noise spectrum calculations. This block also provides a DCR interface to enable the PPC to control this block. It also sends an interrupt to the PPC when one noise data symbol is completely collected. After the PPC evaluates the noise spectrum, it calculates notch filter coefficients. These processes are described in detail in chapters 5.3.3 and 5.3.4. Finally, the notch filter is programmed.

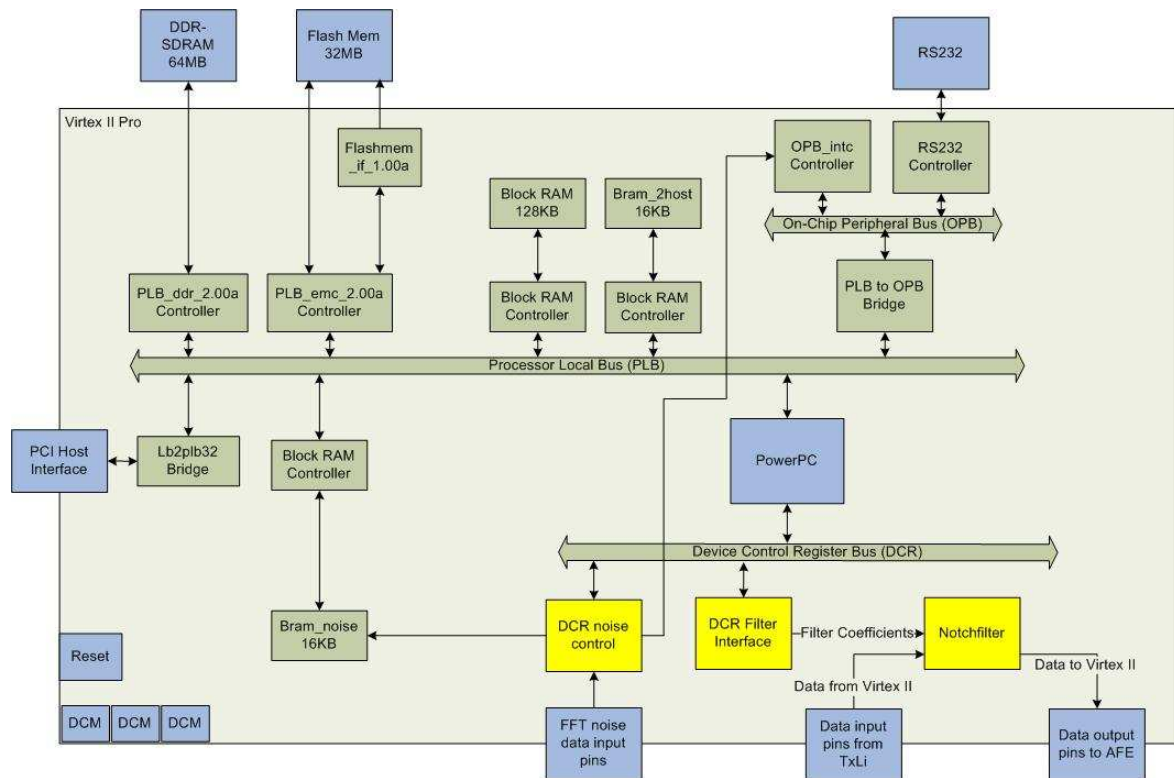


Figure 66: Block schematic of FPGA hosting the notch filters

Figure 67 shows another screenshot of the Matlab application as described above. In addition to figure 62, the ‘Smart Notching’ functions are now activated. The notched carriers are marked with a yellow column in the SNR graph. The debug output from PPC is visualized in the lower left corner. Currently, 16 carriers are notched. Some of them are grouped, giving 9 frequency notches in total. The lower right of the figure shows a max-hold and average noise curve of the recorded noise shots. The data to be transmitted - including CAZAC sequence and training symbols - are affected by the notch filters. Unfortunately, the frequency response of the notch filters shown here has weak side slopes. The steepness of the side slopes depend upon the number of carriers to be notched, their frequency and the number of notches in total. The weak slopes are especially visible in the notches around 10 MHz. In particular, the slope towards the higher frequencies affects the constellation of adjacent carriers. The 31 meter radio broadcast band ranges from 9.4 MHz to 9.9 MHz. It was the most heavily used band at the time the screenshot was recorded. Four individual notches protect the radio services in the 31 meter band. The constellations of the carriers in-between these notches are also affected by the side slopes of the notch filters. Chapter 5.3.4.3 proposes a solution to avoid the effect of side slopes affecting the SNR of adjacent carriers.

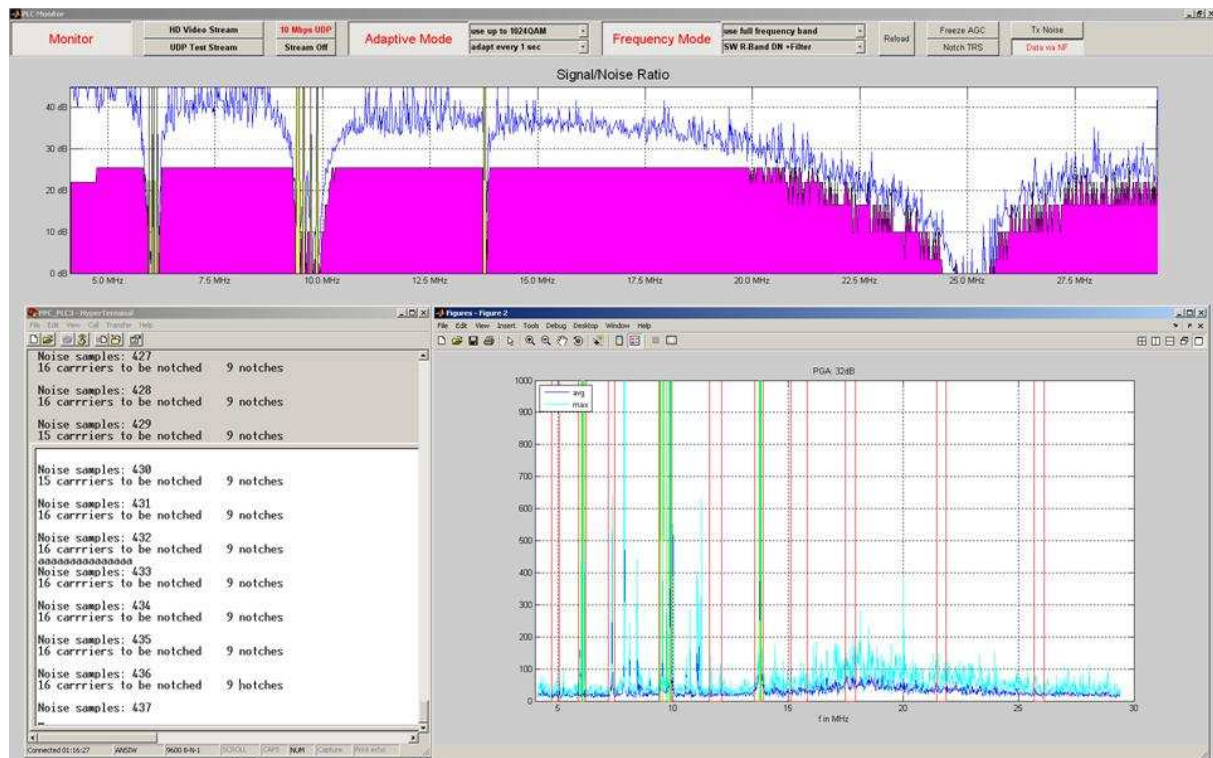


Figure 67: Screenshot of ‘Smart Notching’ demonstrator system

Top figure: measured SNR (blue), selected constellation (pink) and notched carriers (yellow)

X-axis: Frequency range from 4 to 30MHz, **Y-axis:** dB

Lower left: debug output of PPC processing statistics on noise measurements. Actually 16 carriers are omitted in 9 notches

Lower right: measured Noise. **X-axis:** Frequency range from 4 to 30 MHz
Y-axis: a linear value of data captured at the output of the FFT
 Red columns represent the HF radio broadcast bands.
 Green columns show notched carriers
 Blue: average noise values, cyan: max hold noise

5.3.3 Detection of the Presence of Radio Services

5.3.3.1 Detection of Radio Services Using Resolution Bandwidth Given by FFT

In the demonstrator system described here, a noise shot is recorded after every transmission burst. The burst repetition rate is around 500 Hz. The length of each burst depends on the throughput requirements of the application and the channel conditions. A single noise shot is relatively unreliable. The variation in time as well as to adjacent measurement points in fre-

quency domain are around 10 dB. Average, max-hold and min-hold functions of several shots are implemented. The statistical processing of the noise data is implemented in software in the PPC. Due to the high amount of noise data and the processing limitations in the PPC, not every noise shot is written by the DCR noise control unit into RAM (figure 66). For the first noise measurements using the embedded system in buildings, it was very comfortable to have the statistical processing implemented in software. It allows simple toggling between the individual algorithms and to evaluate the parameters such as the number of shots taken for the averaging function. Finally, it is decided to use a sliding window average calculation (equation 28, works like a low pass filter) of $n = 8$ noise shots. Due to the sensitivity of the AFE and the high amount of noise shots recorded, the detection of the threshold using an average calculation is found to be more reliable than using the max-hold value. If $Noi_{meas}(c)$ is the last recorded noise shot of each carrier (c) and n the length of the field, where the average shall be calculated, the formula to derive $Noi_{avg}(c)$ is simple to integrate into hardware:

$$Noi_{avg}(c, t) = \frac{Noi_{meas}(c)}{n} + Noi_{avg}(c, t-1) * \frac{n-1}{n} \quad (28)$$

$Noi_{avg}(c, t)$ is the actual calculated value and $Noi_{avg}(c, t-1)$ is the previous one. Such a sliding average calculation has the benefit of storing only one value per carrier, not the full array for calculating the average.

Figure 68 and figure 69 show the average and the max-hold curves of the noise measurements. The horizontal axis represents the frequency. In figure 69, the frequency axis is enlarged to show the details in the 49 m and the 41 m bands. The vertical axis represents the level in a linear view. The red columns in both figures indicate the HF radio transmission bands. The ETSI TS [Schw_08d] on ‘Smart Notching’ specifies the concept to be only active in the HF bands. The green columns show which frequencies the system identified as being receivable HF radio stations. The AFE and the post processing of the noise data need to be calibrated, in order to define the system’s threshold. It is recommended to do the calibration with the measurement apparatus specified in the ETSI TS [Schw_08d] and feed the test signals with the levels specified there. Of course, the settings of the gain amplifier in the AFE must be considered. Here, the threshold to identify if the service is receivable is set to 500 (black line in figure 69). During the recording of figure 68, 17 carriers were excluded in 8 notches. In the 31 m band and the 22 m band, several adjacent carriers where the noise measurement is higher than the threshold are grouped into one notch.

In figure 68, some out of band radio transmissions are visible at around 8 MHz and 11 MHz. Another noise source is visible, increasing the noise floor by around 20 MHz.

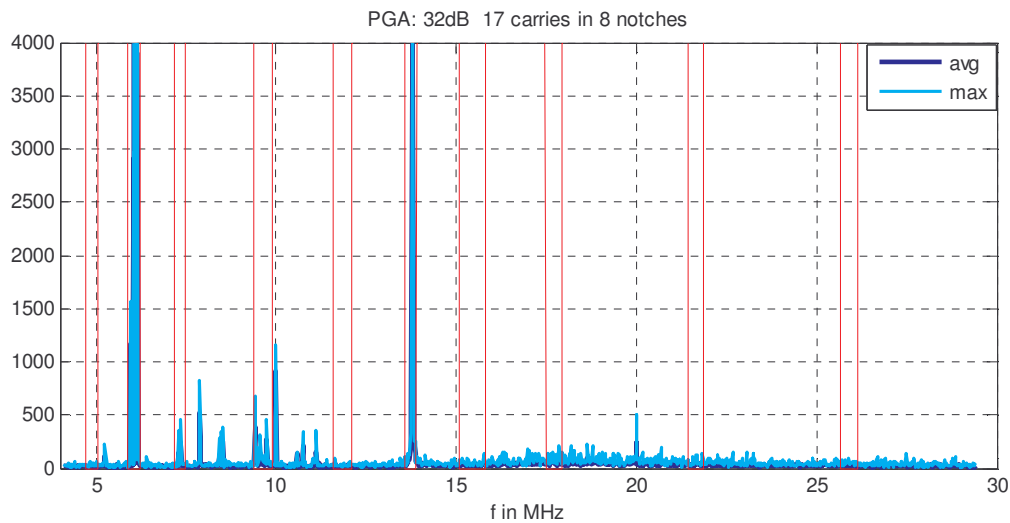


Figure 68: Noise measurement with HF radio bands.

X-axis is the frequency from 4 to 30 MHz

Y-axis is a linear value of data captured at the output of the FFT

Red columns represent the HF radio broadcast bands

Blue: average noise values, cyan: max hold noise

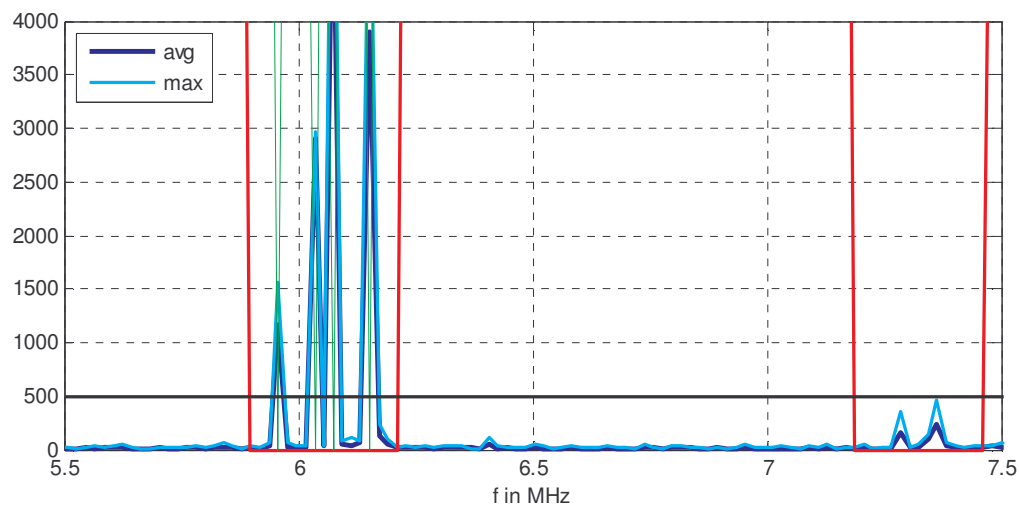


Figure 69: Enlargement of noise measurement in 49 m and 41 m HF radio bands (red) and notched carriers (green). The black line represents the threshold of criterion (2).

Figure 69 shows an enlargement of figure 68. In the 49 meter band, four radio stations ingress on the mains. The following text describes how the two criteria from chapter 5.2.3 are implemented in the notch activation algorithm.

- The threshold of criterion (2) (black line) is found to be the level of 500 during the calibration process of the PLT system. The four radio stations in the 49 meter band exceed the threshold and are protected by a single carrier notch. The signal ingress in the 41 meter band does not exceed the threshold and is therefore not protected.
- To verify criterion (1) the median noise floor is measured around the 49 meter band to be the linear level 20. The relative threshold of 14 dB is converted into a linear factor of 5 ($factor = 10^{14dB/20}$). The linear level 20 multiplied by factor 5 results in a value of 100, which is far below the ingress level of the four services that are visible in figure 69 with more than 1000. These radio stations have an excellent SNR.

5.3.3.2 Enhancement of Resolution Bandwidth by Using Notch filters

As described in chapter 5.2.1 and calculated in equation 8, the resolution bandwidth of an FFT system is given by the system's Nyquist frequency and the FFT size. It is equivalent to the OFDM carrier spacing. This is sufficient for non-notching communication systems, because only signals which are transmitted by the interoperable communication partner have to be received. Here, only the carriers allocated at frequencies with the given carrier spacing are used. There is no need to measure anything outside of the allocated carrier frequencies.

A communication system which has to interpret signals from the outside - i.e. not being transmitted by the communication partner device - has the motivation to detect these signals as accurately as needed for its own function. Figure 55 and figure 56 shows why it is important for a PLT modem to precisely detect the frequency location of the ingress station. If the exact frequency of the radio station is known, the notch should be designed as narrowly as specified in the ETSI TS [Schw_08d] and adjacent carriers might be reused for communication. Figure 70 gives an overview of how to measure the exact frequency location of the radio station in between the OFDM carrier spacing:

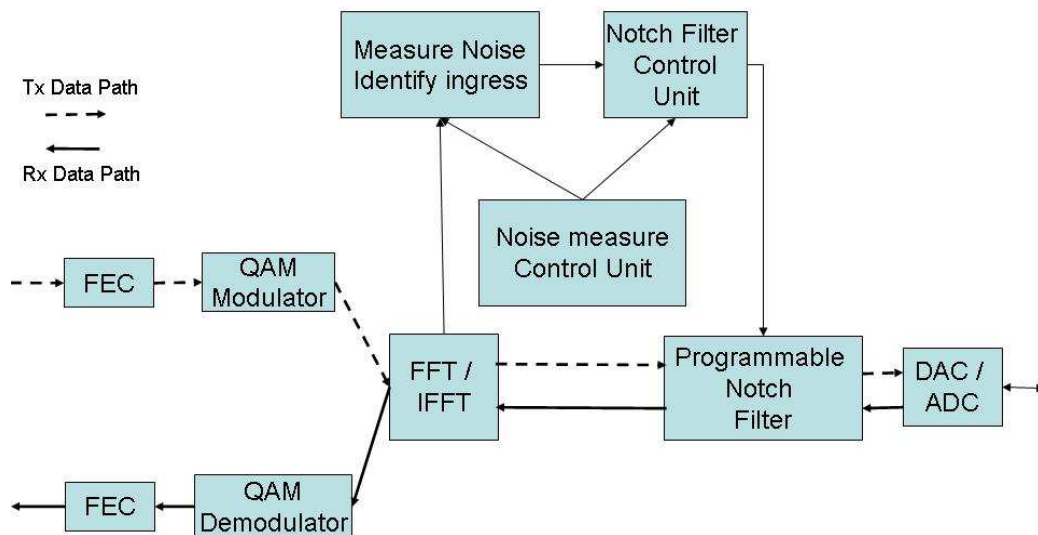


Figure 70: Enhancement of FFT resolution bandwidth

As described above, the programmable or tunable notch filter is only used in the transmitter. If the modem is in receiving mode, the filter can be reused to detect the precise frequency of the radio station. This is an iterative procedure where the programmable notch filter eliminates various sub frequency spans of the resolution span of the FFT.

Normally, HF radio stations allocate a 10 kHz bandwidth and are aligned to a frequency grid (or raster) of integer multiples of 5 kHz. Today's OFDM PLT modems use a larger carrier spacing. It would be an interesting approach to align the allocation of the OFDM carriers to the raster of a radio broadcast service. The PLT modem implementation described here uses a carrier spacing of 19.51 kHz. The programmable notch filter can be reused in the reception path and programmed to provide a 10 kHz notch aligned to the raster frequency of HF broadcasts. The notch should be tuned sequentially to each raster frequency inside the resolution bandwidth of the FFT at frequency points of interest. Comparing the results of the FFT after each tuning step, the ingress can be precisely identified within a 10 kHz span. This could be done in parallel for every frequency span where radio signal ingress is detected. Figure 71 shows how the procedure might work.

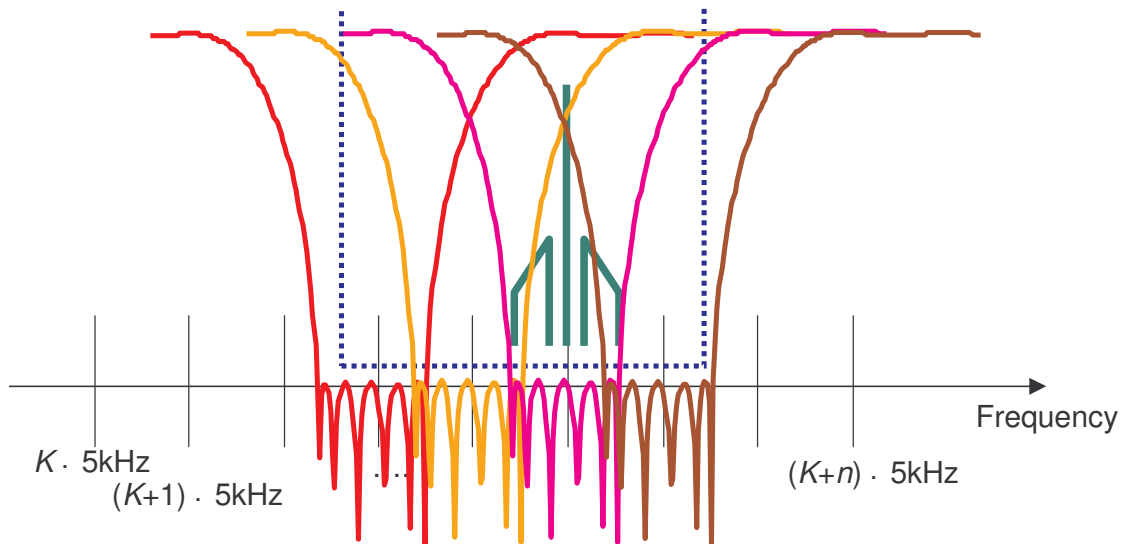


Figure 71: Tune notch to HF radio broadcast raster

Figure 71 shows the frequency on the horizontal axis with the HF frequency grid of 5 kHz marked. The blue curve indicates the FFT resolution bandwidth of 19.5 kHz of the demonstrator system. The green lines represent an AM radio service. Its exact frequency cannot be located within the blue curve using conventional noise measurement techniques. The notch filter is programmed to a width of 10 kHz and tuned to four frequencies within the window marked by the blue curve. This is indicated by the red, yellow, magenta and brown curves of the four notch filters. The notch filter is gradually tuned to the next HF broadcast raster frequency. By comparing the results of all steps the exact frequency location of the radio service can be determined.

Care has to be taken if the frequency of the radio station is shifted by Doppler spread caused by movements of the ionization layers in the ionosphere.

Alternatively, the resolution bandwidth of a modem can be improved by using a larger FFT size for the noise measurements. This has the disadvantage of requiring more chip area and calculation power compared to the solution of reusing the notch filter.

5.3.4 Notching

There are various techniques for creating notches. One simple technique for creating notches is using wavelet transformation [Sandb_95]. Omitting a carrier from the communication is sufficient and the spectrum is notched with a depth depending on the side lobes of the applied wavelet. The waveform of the wavelet is responsible for the shape of the notch. Wavelet transformations were analyzed in [Hess_05]. The demonstrator described here uses an FFT

transformation process. The output of the FFT is very sharp in the time domain, but weak in the frequency domain compared to wavelet transmissions. Windowing could be applied for spectral shaping of FFT systems. Chapter 5.3.4.1 discusses the influence of windowing on the shape of a notch. Another alternative would be to design notches with additional filter stages in the Tx spectrum of the data. This solution is presented in chapter 5.3.4.2.

5.3.4.1 Influence of Windowing on Spectrum and Notch Shape

Compared to wavelet transformation, the FFT process uses a rectangular window. The FFT of a rectangular function in the time domain is a $\sin(x)/x$ function in the frequency domain. The $\sin(x)/x$ becomes 0 at integer multiples of π . Some parts of the signal remain in-between the zeros, which results in the unwanted side lobes of an FFT OFDM system. Figure 72 shows a $\sin(x)/x$ function as green curve. The frequency axis is shown horizontally. The level in a logarithmic view is presented on the vertical axis.

The process of multiplying a window with an OFDM symbol (see figure 73) in the time domain aims to suppress the sharp corners at the beginning and the end of the OFDM symbol in order to get smooth transitions. This affects the shape and distances of the side lobes in the frequency domain. There are numerous types of window functions available for implementation such as Hamming, Barlett (triangular), Kaiser, Blackman, Raised Cosine (Hann), etc. A comparison of various window waveforms with the achieved side lobe attenuation is shown in figure 72 which also serves to illustrate the disadvantage of windowing. The side lobes are suppressed, but the main lobe stays wider. The first time the spectrum reaches zero, the distance for all windows is at least twice the frequency of the rectangular window used by the pure FFT. Windowing is considered to be state of the art in signal processing [Harr_78].

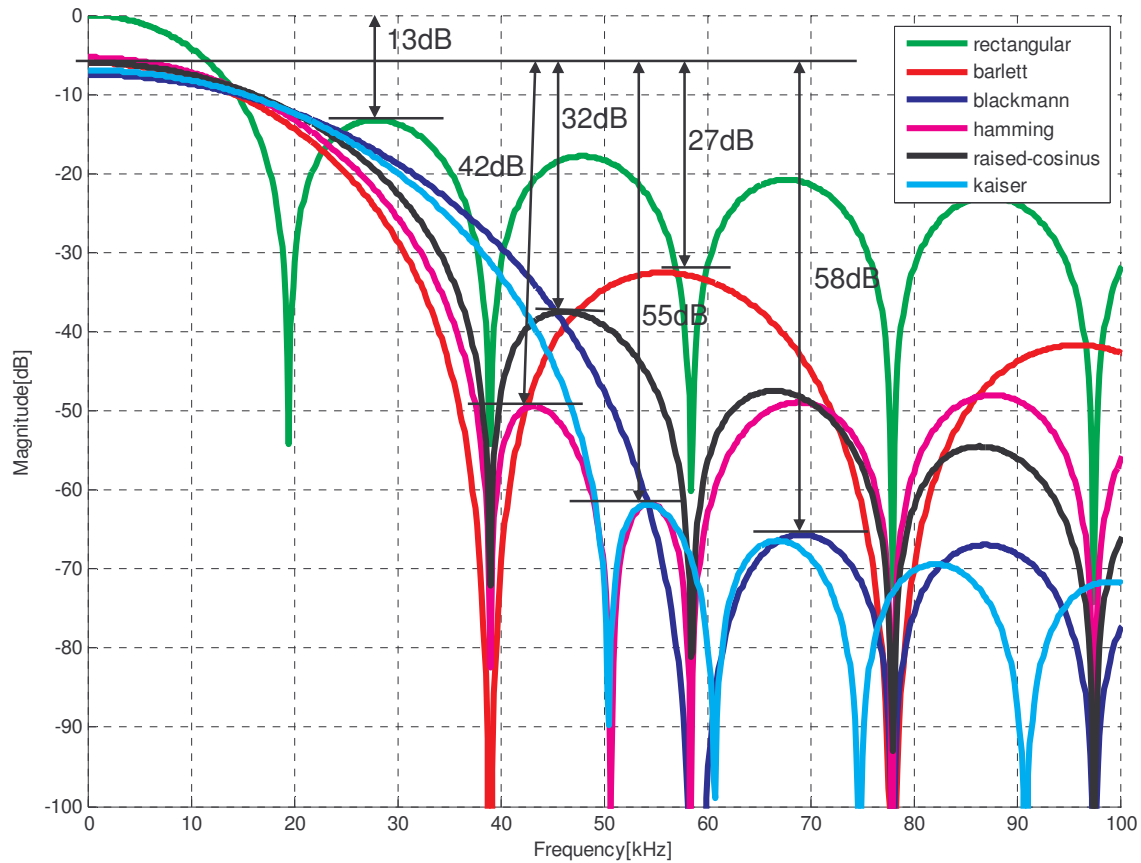


Figure 72: OFDM side lobes. Comparison of various window functions

The process of how a window is applied is shown in figure 73. The original OFDM symbol or the output of the IFFT at the transmitter is marked with 'FFT section'. As described above, the guard interval is copied from the tail samples to the beginning of the symbol. In order to create a window, the symbol has to be expanded further at the beginning and at the end by copying the bits as done for the GI. This expansion is multiplied with the smoothly descending window. The more smoothly the signal approaches zero in the time domain, the lower the side lobes in the frequency domain. Of course, this expansion of a symbol is a waste of communication resources as it doesn't carry useful information and has to be cut by the receiver.

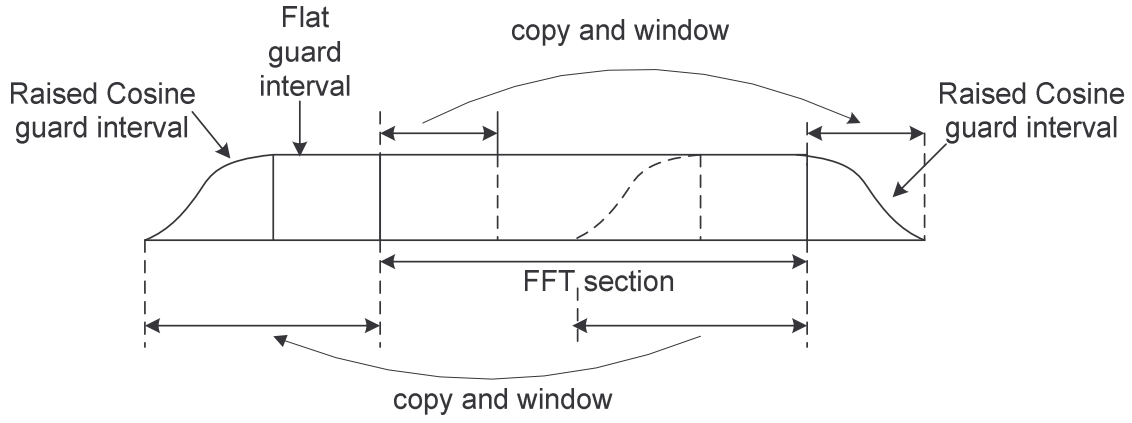


Figure 73: OFDM symbol with GI and window

The two descending slopes in the time domain could overlap, to save communication resources at consecutive OFDM symbols, as shown in figure 74. The guard interval T_{GI} and the descending slopes $T_{roll\ off}$ are added before the FFT section T_{FFT} . The overhead caused by the additional window is called T_{prefix} , when the GI is included and either $T_{postfix}$, or $T_{roll\ off}$ when the GI is excluded. The new symbol time T_s is measured between the middles of the roll-offs before and after the symbol. The overlap region is βT_s , as shown in figure 74:

$$T_{postfix} = T_{roll\ off} = \beta T_s \quad (29)$$

and actual symbol length:

$$T_s = T_{FFT} + T_{GI} + \frac{(\beta T_s)}{2} + \frac{(\beta T_s)}{2} = \frac{T_{FFT} + T_{GI}}{1 - \beta} \quad (30)$$

Total symbol duration:

$$T_{sym} = (1 + \beta) * T_s \quad (31)$$

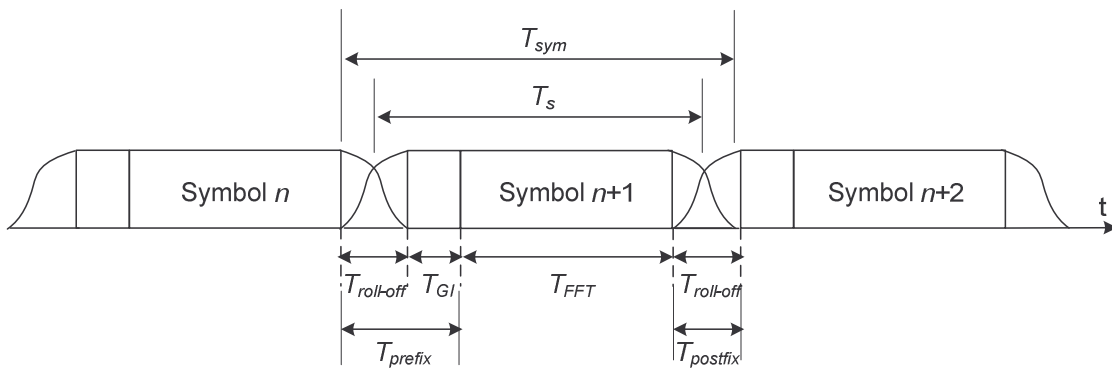


Figure 74: Consecutive OFDM symbols, Guard Interval, windowing, roll-off, ...

The relationship between the actual symbol length and the roll-off factor results in an increase of total samples in an OFDM symbol. There is a balance between this factor and obtaining a better side lobe attenuation.

Figure 75 shows the side lobe attenuation of the demonstrator systems spectrum which could be obtained by varying the roll-off factors (the β values) of the raised cosine window. As visible below 4 MHz and above 30 MHz, increasing the roll-off factor directly increases the amount of attenuation achieved at the side lobes. However, this has the drawback of increased symbol length.

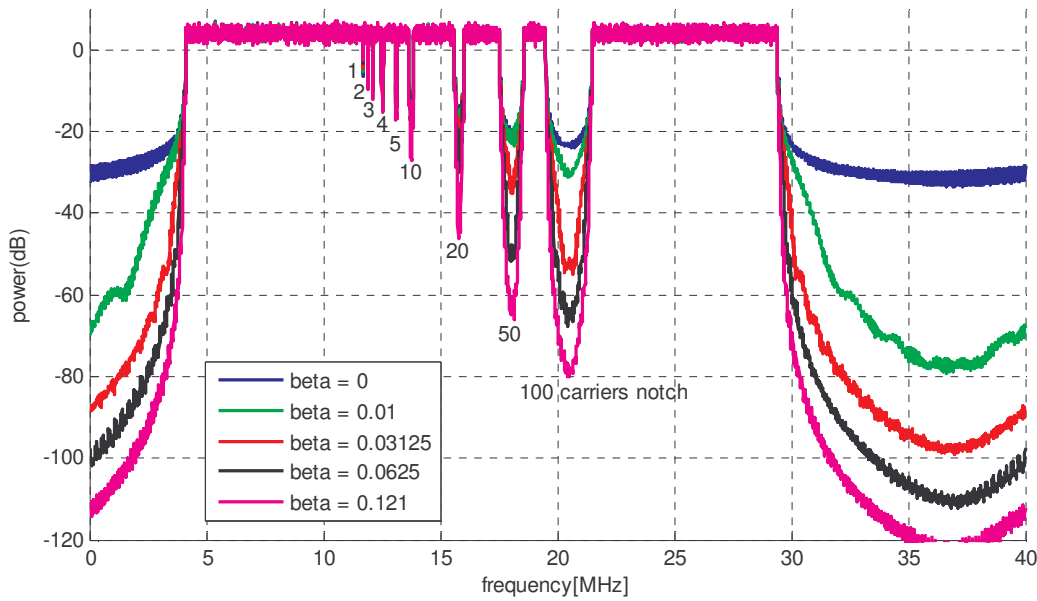


Figure 75: Sideband attenuation comparisons with different roll-off factors

To create notches in the OFDM spectrum, a Matlab / Simulink model is implemented using QAM modulation and notches of omitting a various number of carriers: 1, 2, 3, 4, 5, 10, 20, 50 and 100. Figure 76 shows a magnification of figure 75. A max-hold function is implemented in order to create these figures. The 100 and 50 carrier notches clearly show the spectral benefit of windowing. The influence of windowing is hardly visible up to the point of the 5-carriers' notch. At the 5-carrier notch, the difference between no window and the highest simulated β is around 5 dB. The trade-off for this β is a 27% longer symbol time. At the 10 carrier notch, the center frequency is suppressed by more than 15 dB without windowing, but the adjacent side slopes of the used corner carriers are only improved by 5 dB.

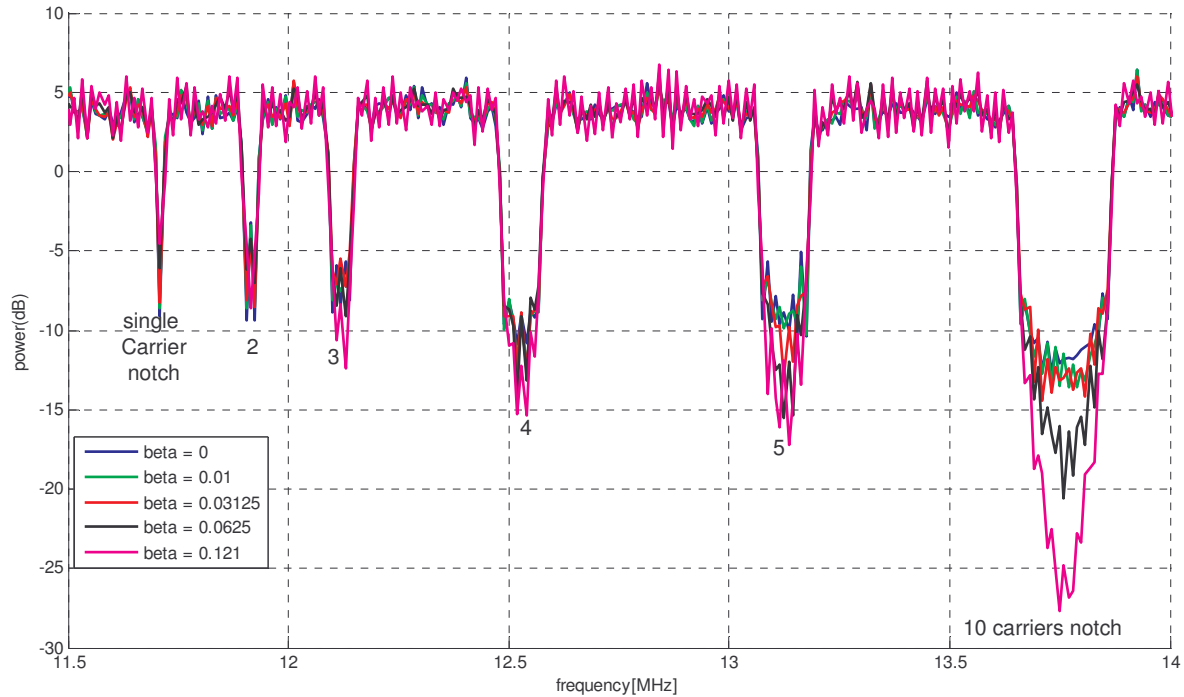


Figure 76: OFDM spectra with different notch widths and depths achieved with different roll-off factors

It is not considered that windowing efficiently improve the shape of small notches. The additional overhead in the time domain is extremely large compared to the improved notch depth. Windowing with a small roll-off factor is sufficient in order to suppress the side lobes outside the used spectrum, but it isn't recommended to increase the depth of a single carrier notch. The implementation of windowing on a PLT communication system is documented in [Husa_08].

5.3.4.2 Adaptive Band Stop Filters

Another alternative method of creating notches is to filter the unintended frequencies using tunable band stop filters.

Various filter types for tunable adaptive band stop filters are evaluated in [Hern_05]. The filter which gives the best possible results is the second order IIR (Infinite Impulse Response). Other literature also recommends IIR filters for tunable band stop filters: [Sando_94], [Wari], [Zahn_04], [Cho_89], [Josh_99], [Soder_92] and more. The main advantage of this filter type is the relatively low hardware costs. The total multiplications required to achieve a given depth of a notch is significantly lower than that of FIR (Finite Impulse Response) filters. The disadvantage of IIR filters is, as the name says, the impulse response lasts infinitely. However, as explained later, the ICI does not matter in this case.

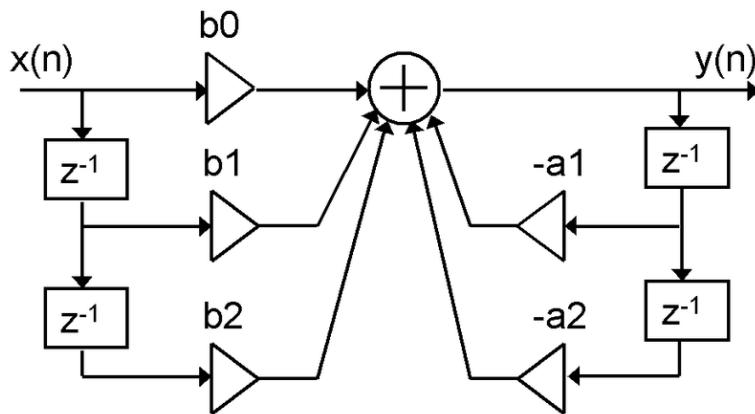


Figure 77: 2nd order IIR filter direct form I

In the case of using PLT to filter all frequencies where radio stations are present, multiple notches must be created. Using the structure shown in figure 77, a single notch might be created. Measurements in buildings [Schw_08c] show that at least 20 notches could be possibly created by PLT modems. The structure of figure 77 must be readily and often available. If less notch filters are implemented, notches have to be grouped around adjacent carriers which results in the loss of communication carriers where no interference can be expected. For multiple notches, the cascaded structure (figure 78) is found to be optimal. Notch filters have to be inserted sequentially. If fewer notches are requested, the straight through path of an IIR filter could be programmed as a passage causing minimum latency. The cascaded arrangement looks like depicted in figure 78.

Each stage of $H_1(t)$, $H_2(t)$, ... $H_n(t)$ consists of three identical sub-stages $H_{n1}(t)$ to $H_{n3}(t)$ of figure 77, each providing a certain attenuation. This is the structure selected for the implementation in the V2P FPGA. Initial design test results of the second order IIR notch filters [Soder_92] to create notches with 30 dB attenuation in a bandwidth of 10 kHz for three different frequencies are shown on the right hand side of figure 78.

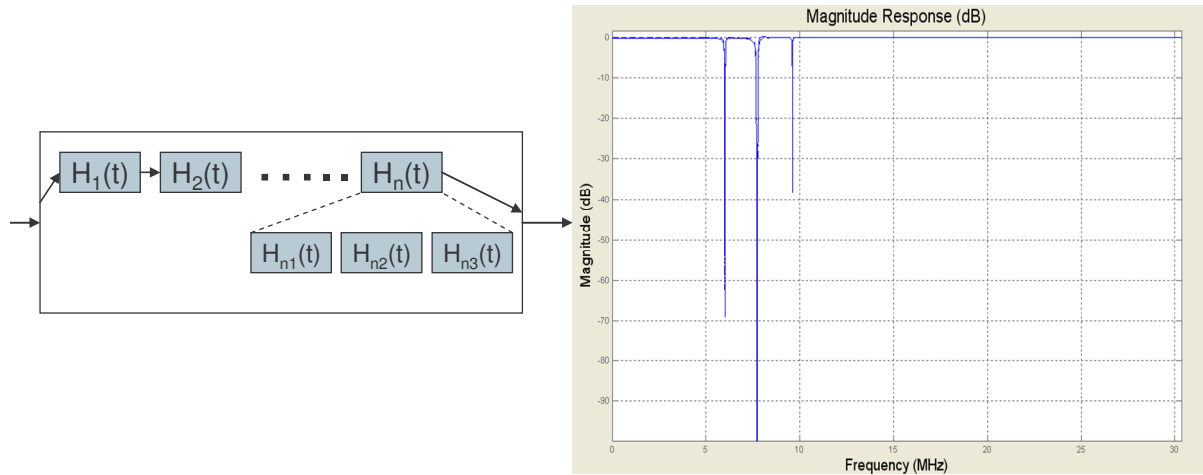


Figure 78: Notch filter stages and frequency response of a filter having 3 notches

[Ferdj_94] presents a method using second order IIR filters with shorter impulse responses. The zeros must be set to the unity circle where the angle is set by the frequency to notch when designing a notch filter. The associated poles have the same angle as the zeros, but are shifted toward the center of the unity circle. The distance between the poles and the zeros is given by the bandwidth of the filter. The closer the zeros are placed to the rim of the unity circle, the higher the attenuation of the filter. The placement of the poles and the zeros is illustrated in figure 79.

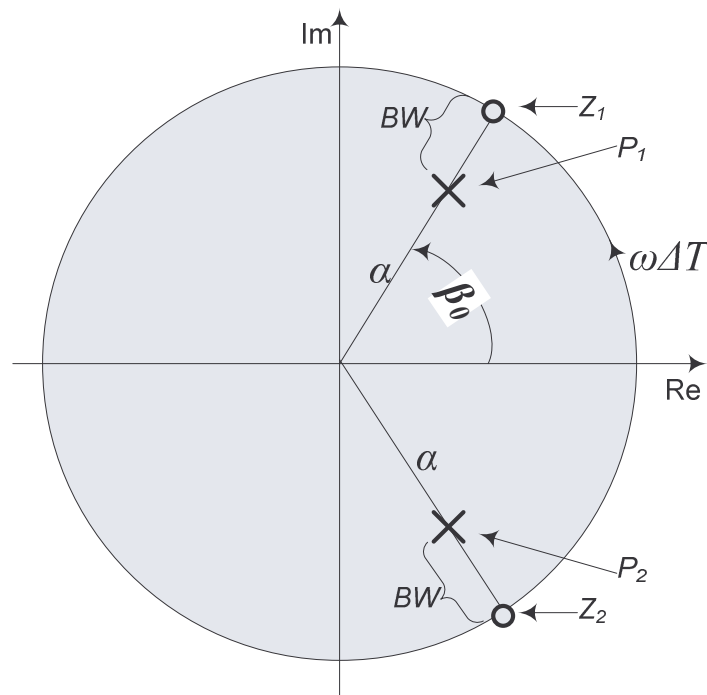


Figure 79: Illustration of pole-zero locations on the unity circle

The transfer function $H(z)$ of a second order IIR filter is

$$H(z) = \frac{(z - z_1)(z - z_2)}{(z - p_1)(z - p_2)} \quad (32)$$

The zeros z_1, z_2 and poles p_1, p_2 are calculated with

$$z_{1,2} = \cos(\beta_0) \pm j\sin(\beta_0) \quad (33)$$

$$p_{1,2} = \alpha(\cos(\beta_0) \pm j\sin(\beta_0)) \quad (34)$$

As shown in figure 79, β_0 sets the frequency of the notch. α must be smaller than 1, otherwise the filter becomes unstable. $1-\alpha$ is the distance between the zero and pole and defines the bandwidth. Equation 33 and equation 34 could be inserted to equation 32 and simplified to

$$H(z) = \frac{1 - 2\cos(\beta_0)z^{-1} + z^{-2}}{1 - 2\alpha\cos(\beta_0)z^{-1} + \alpha^2 z^{-2}} \quad (35)$$

The bandwidth BW_{3dB} where the attenuation equals 3 dB is calculated in [Ferdj_94]. F_s is the sampling frequency.

$$BW_{3dB} = \frac{(1 - \alpha^2)2\sqrt{2}}{\sqrt{16 - 2\alpha(1 + \alpha)^2}} \frac{F_s}{2\pi} \quad (36)$$

The following general characteristics were observed: the wider the notch in the frequency domain, the shorter the impulse response in the time domain, but the higher the amplitude of the impulse response immediately after the impulse. It can be considered to be like a “constant area” or, equivalently, energy being sent out after the impulse.

Equation 35 and equation 36 can be simplified to the algorithm presented in figure 80 for implementation in Matlab. This algorithm is converted to C in order to be cross-compiled and executed on the PPC of V2P FPGA. A look up table is linked to the embedded C code for calculations of the $\cos()$ and $\tan()$ functions. A CORDIC [Volde_59] algorithm might be used for the trigonometric functions if this function is ported to VHDL.

```

fnotch = 7.123; % in MHz
BW      = 0.02; % in MHz
Fs      = 80;   % 80 MHz sampling frequency

BW=2.66*BW;      %notch BW correction to use it with our algorithm
BW=BW*pi/(Fs/2); % align on unit circle
Wo=fnotch*pi/(Fs/2); % align on unit circle

beta = cos(Wo);
k = 1/(1+1.229588*tan(BW/2));

% coefficients for IIR Filter
b = k*[1 -2*beta 1];
a = [1 b(2) (2*b(1)-1)];

% Visualization
zplane(b,a);
h=fvtool(b,a,'Fs',Fs*1e6)
axis([0 40 -50 1])

```

Figure 80: Algorithm to calculate IIR filter coefficients

Entry values for the algorithm in figure 80 are the desired frequency of the notch `fnotch`, the bandwidth of the notch `BW`, and the system's sampling frequency `Fs` in MHz. The results are the variables 'a' and 'b', consisting of a vector with 3 entries each. These coefficients can be directly inserted into the 2nd order IIR filter direct form I shown in figure 77. The resulting visualization when the algorithm is pasted to Matlab [MATW] is shown in figure 81.

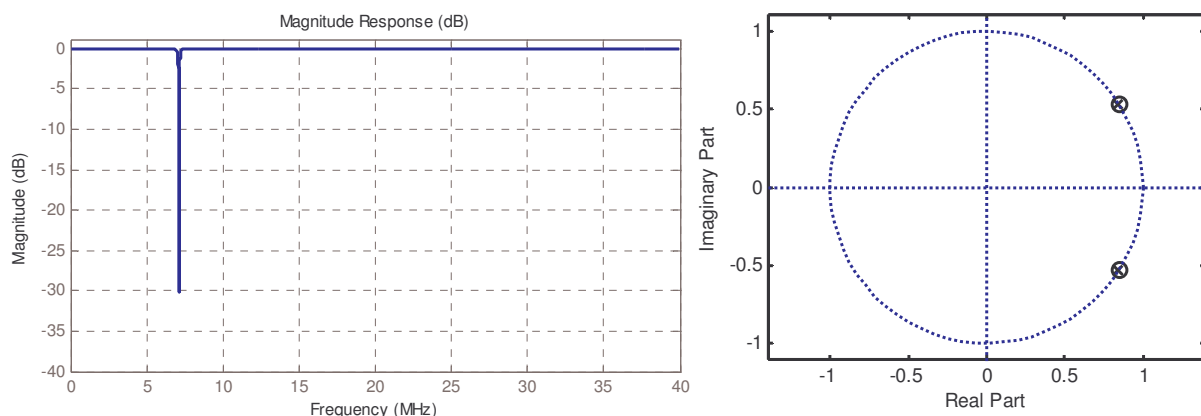


Figure 81: Magnitude and pole-zero plot of a notch

A magnification of the pole-zero plot shows that the filter is stable. The dotted line in figure 82 represents the unity circle and the pole is located inside the circle.

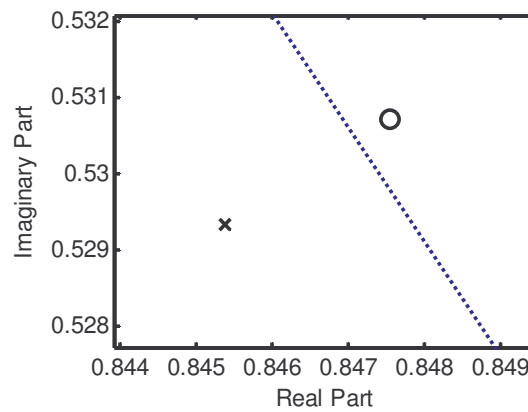


Figure 82: Magnification of the pole-zero plot for proving filter stability

Filter stability can become critical if the coefficients ‘a’ and ‘b’ are converted into fixed-point numbers when programming the hardware. In the V2P FPGA, 18-bit multipliers are available in hardware. No stability problems were identified.

The Matlab filter visualization tool (`fvtool`) allows a quick look at the phase response of the filter. A jump of 360° can be seen at the notch frequency. The steepness of the phase jump correlates to the bandwidth of the filter. Phase jumps in a notch don’t cause any problems, because this frequency is not used by the communication. (The equalizer in the receiving modem requires a stable phase rotation of the channel at the allocated carriers.)

Care has to be taken when reprogramming the filter coefficients in the hardware when a notch has to be shifted from one frequency to another. The desired filter coefficients can only be programmed once the filter has been flushed, otherwise instabilities can occur which don’t pass off in a reasonable amount of time. This can be achieved by resetting the filter to its through path and blocking the return path in the filter.

The attenuation achieved by this filter algorithm is frequency dependent. It achieves huge attenuation at certain frequencies due to the use of trigonometric functions (e.g. there is more than 250 dB attenuation at 10 MHz). The attenuation of one sub-stage shown in figure 78 is not sufficient at all frequencies, which is why three sub-stages are cascaded for every single notch. All notches are performed using the three sub-stages in order to simplify the demonstrator system. Here, the use of hardware resources could be optimized. To demonstrate the necessity of the three sub-stages, a simulation is performed using 45 carriers in 11 notches. Figure 83 presents the result as plotted by the Matlab filter visualization tool.

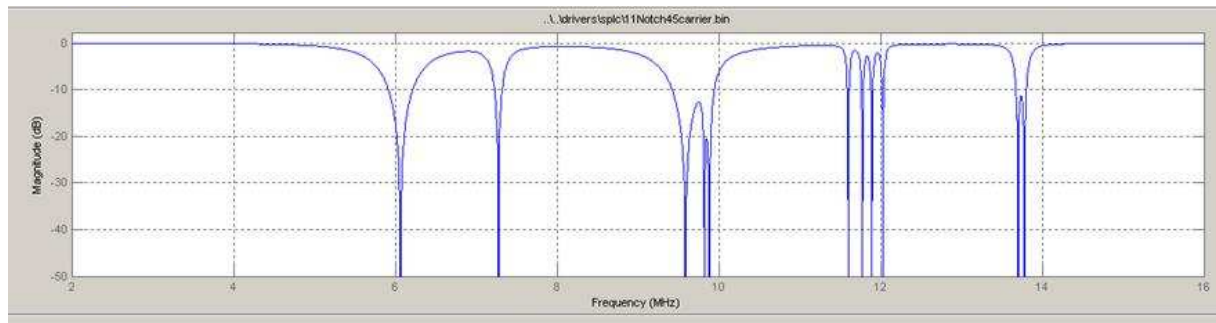


Figure 83: Frequency response of simulated notch filters.

X-axis: Frequency from 2 to 16 MHz, Y-axis: Magnitude in dB

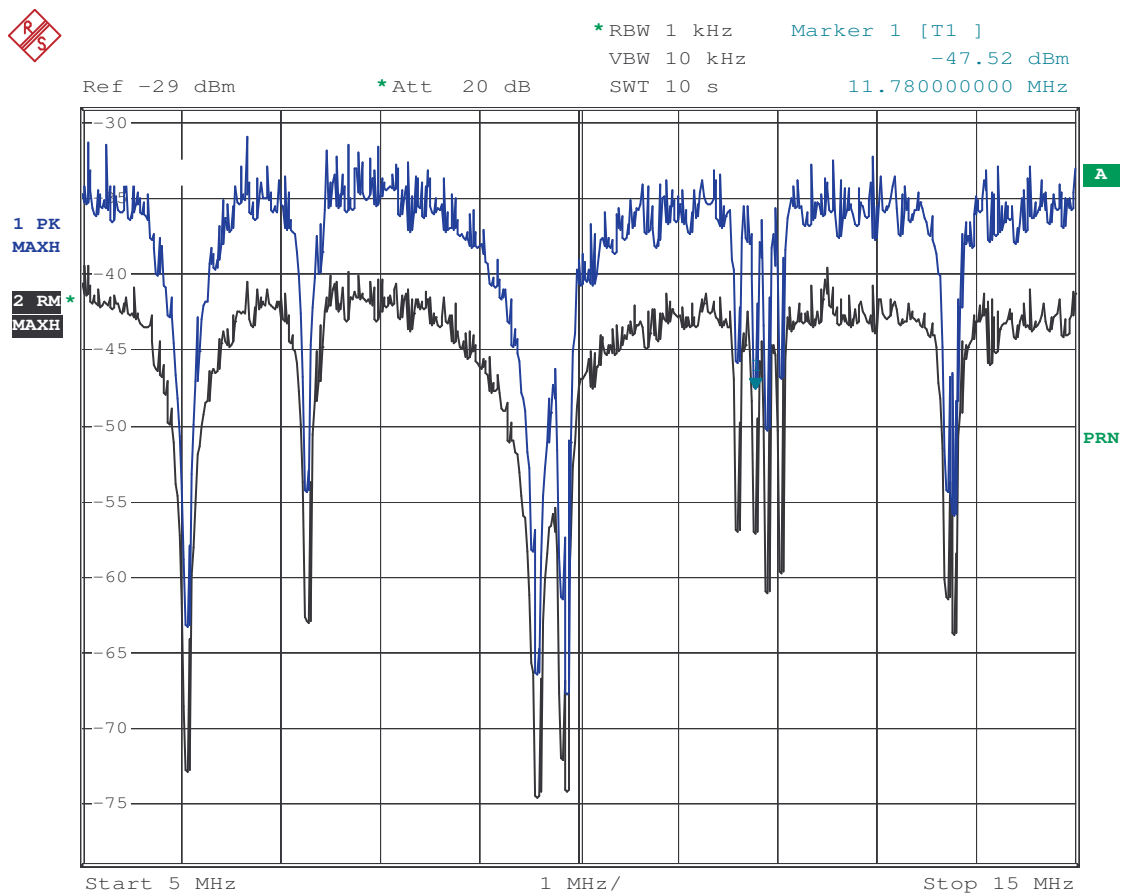


Figure 84: Measured notch filters, 45 carriers in 11 notches: 1 sub-stage

X-axis: Frequency from 5 to 15 MHz, Y-axis: Magnitude in dB

Black: RMS detector (max hold), blue: peak detector (max hold)

The filter coefficients of this simulation are copied to the demonstrator hardware. Initially, using one sub-stage (figure 84) and later using three sub-stages (figure 85) for each notch. The analog spectrum results are measured with a spectrum analyzer. Both graphs show the frequencies from 5 MHz to 15 MHz on the horizontal axis and the level using 5 dB per division

on the vertical axis. The blue curve is measured using a peak detector and the black curve using the RMS detector. Comparing figure 84 and figure 85, it becomes obvious that a single stage for the notches at e.g. 7.3 MHz or around 12 MHz does not achieve the required depth.

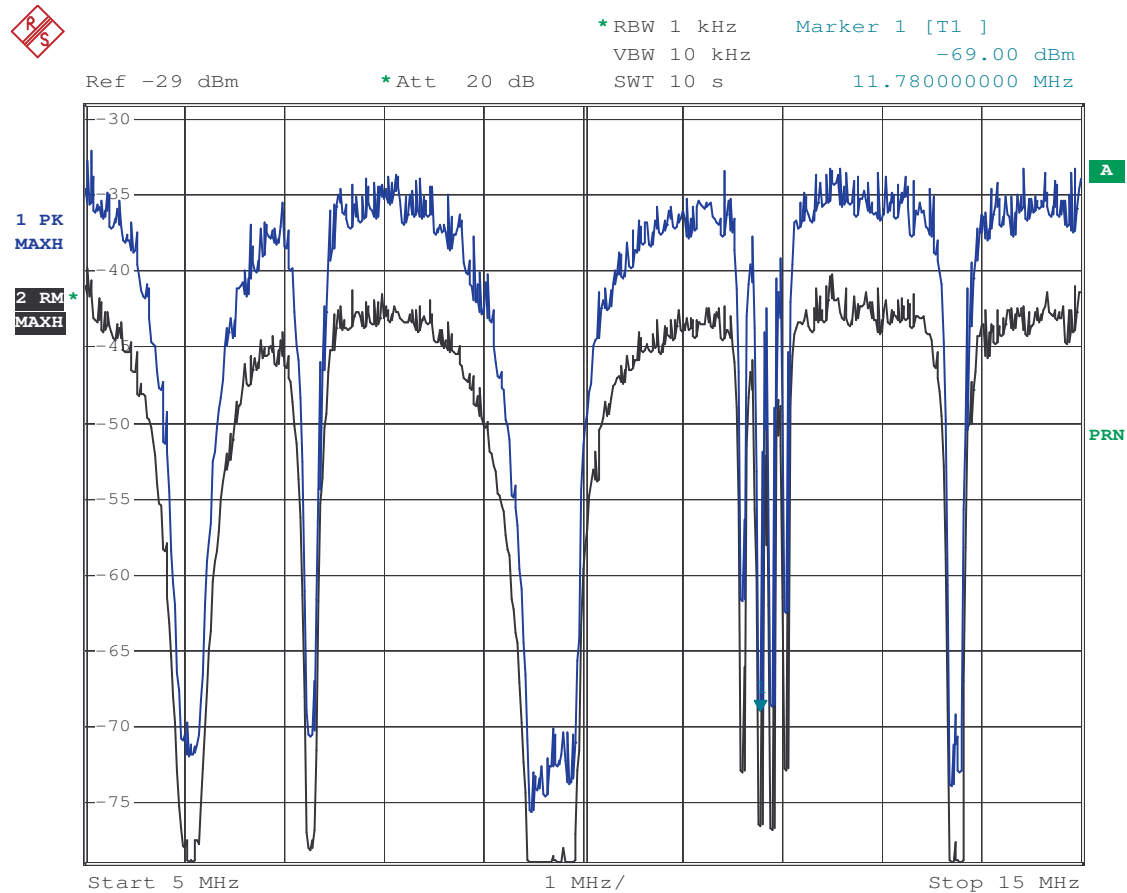


Figure 85: Measured notch filters, 45 carriers in 11 notches: 3 sub-stages

X-axis: Frequency from 5 to 15 MHz, Y-axis: Magnitude in dB

Black: RMS detector (max hold), blue: peak detector (max hold)

An oscilloscope is then used to monitor the impulse response. In this case the end of a transmission burst through a notch filter as simulated in figure 83. The output of one sub-stage (figure 87) is compared to the output of three sub-stages (figure 88). As expected, the impulse response of one sub-stage passes off much faster than in the case of three sub-stages. The apparently infinitely lasting impulse response doesn't cause any problems to the PLT transmissions. The impulse response is generated by the weakly attenuated resonance circuits in the filter stages, which oscillate at exactly the frequencies requiring filtration. As these frequencies are notched and not used by the communication system, they don't cause any inter-symbol interference. Figure 86 shows the group delay of the notch filter from the algorithm presented

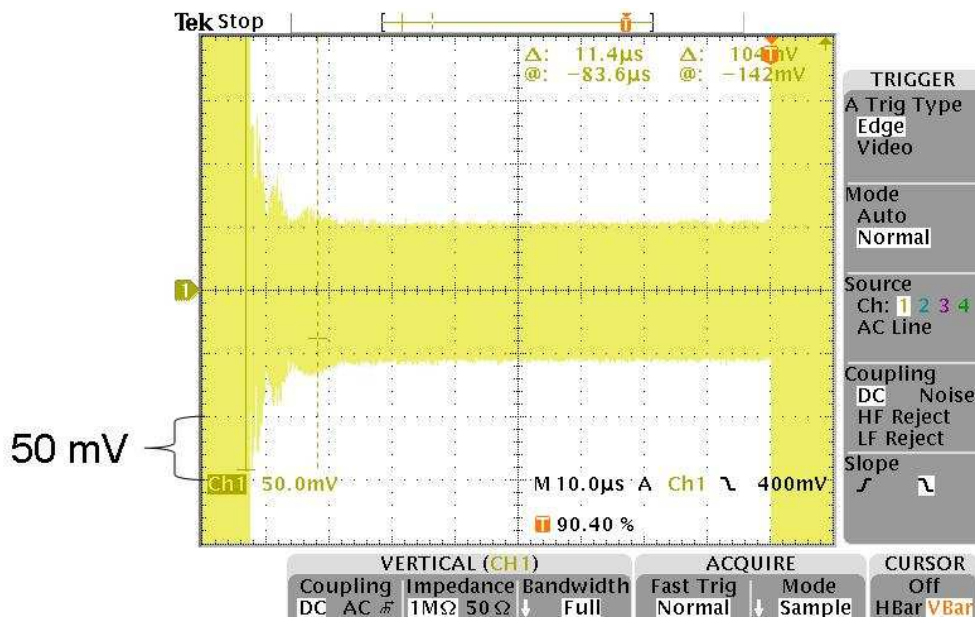


Figure 88: Impulse response of notch filter 3 sub-stages

The filter structure of the 2nd order IIR filter direct form I (shown in figure 77) is implemented in VHDL using VisualElite [Mentor] as a graphical design entry tool. A screenshot from one stage of the notch filter is shown in figure 89. Care has to be taken in the timings of the backward paths where the multiplications with coefficients ‘a’ are performed. They are located on the right hand side of figure 89. Multiplications and subtractions must be completed within one clock cycle. The delay and timing skew of the individual bits caused by the multiplication and subtraction operation must be smaller than a clock cycle. An additional latch would misrepresent the results. The skew of a multiplier is around 6.3 ns for the V2P FPGA used in the demonstrator system. A subtraction causes a further skew of 2 ns. Here, the clock rate is 80 MHz resulting in the sample time of 12.5 ns. Any differences in the signal run times between the components will enlarge the skew. Timing errors will occur if the total skew exceeds the sample time, resulting in less freedom for the ‘place&route’ process to locate the components during the generation of the FPGA’s programming bitstream.


$$P_{Readout} = -95 \text{ dBm} + 20 \text{ dB} - 6 \text{ dB} = -81 \text{ dBm} \quad (37)$$

The read out value of the bottom level of the notch is -89 dBm, as specified in the ETSI TS [Schw_08d]. The notch must fall below this value in the span of 14 kHz as specified above. The stations at 21.83 MHz and 21.84 MHz are grouped into one single notch.

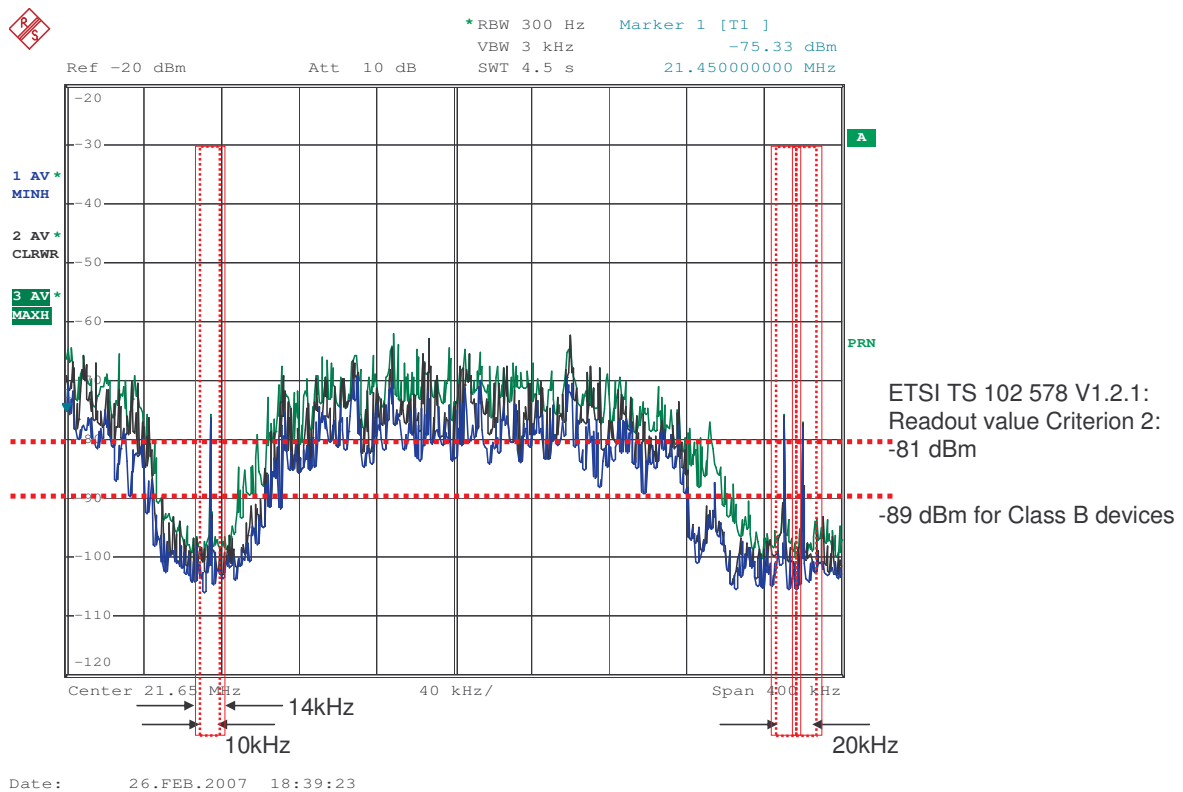


Figure 90: Measured notch with thresholds from ETSI TS 102 578 [Schw_08d]

5.3.4.3 Boost Carriers Influenced by the Slopes of a Notch

The side slopes of the notches are more attenuated than specified in chapter 5.2.4.2, as shown in the spectral plot recorded on the analog side in figure 85, in the SNR measurements of the demonstrator system in figure 67 and even in the simulation of the filter stages in figure 83. This results in an unintentionally lower SNR for the carriers located there which leads them being loaded with a more robust constellation. There is an unnecessary loss of data throughput for PLT systems. Especially for isolated carriers where notches are inserted very closely to the left and right of the carrier an unwanted attenuation may happen. Figure 91 describes a proposal of how to overcome this problem.

The notch control unit of the PLT transmitter programs the tunable or flexible notch filters. This unit knows the transfer function of the notch filters. It should calculate the unintended attenuation on the adjacent non-notched carriers. If this attenuation isn't calculated, the notch control unit could measure the lost SNR of these carriers by comparing the channel response recorded by the receiver, both with and without the notches. The affected carriers should be individually boosted after the QAM in the transmitter depending on their unwanted attenuation. This would cause a flat spectrum on the left and right side of the notch. If the carrier is

boosted, the side lobes (presented in chapter 5.3.4.1) are also amplified. However, when monitoring a notch, it is visible that the side slopes descend gradually from the flat area down to an almost vertical shape close to the center frequency. The cutting of the OFDM carrier side lobes by the filter doesn't cause any problem in communication, as they don't carry any useful information. With limited hardware resources, it is difficult to create notches in a rectangular shape. It is no problem for a notch filter to create high attenuations, but the slopes are not optimal. The side lobes of the boosted OFDM carriers are highly suppressed by the deep attenuation in the center of the notch. The main lobe of the boosted carrier compensates the unintended attenuation of the notch filter at this frequency. Any ripple in the pass-band of the notches can also be compensated with this technology, which reduces the usage of hardware resources in the notch filter or improves the shape of the notch. Of course, when boosting carriers, the specified side attenuations of a notch (in table 10 and figure 55) should not be affected.

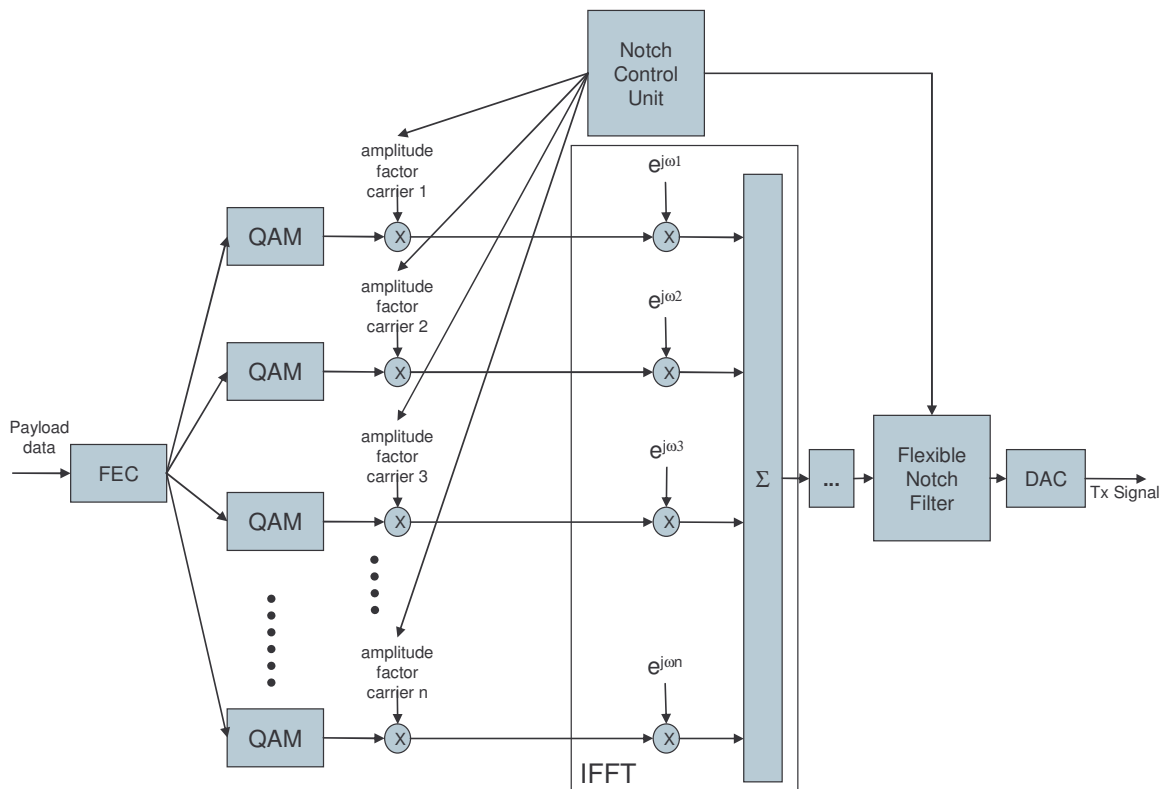


Figure 91: Block schematic to boost carriers influenced by the side slopes of a notch

5.4 Verification of 'Smart Notching' in Buildings

In order to verify the implementing of 'Smart Notching' in the prototype system it should be tested in buildings under real conditions.

As shown in Chapter 5.2.1, HF radio broadcast transmissions change their transmission frequency from time to time. Frequency hopping of a HF radio station requires a ‘Smart Notching’ implementation in order to comply with the ETSI TS [Schw_08d] in all criteria. Such a scenario was very interesting to monitor under live broadcasting conditions in a private building. During the ETSI plugtest, a radio broadcast station in Skelton (UK) was available to schedule the transmission of any radio services according to the plugtest demands. To verify the dynamic behavior of the PLT system, the Skelton transmission toggled from 7225 kHz to 7320 kHz. Two SW radio receivers were used to monitor this event at the test location in Stuttgart (Germany). Each of the radios is tuned to one of the frequencies. There was also a PLT transmission running in parallel inside the building from the ‘Smart Notching’ demonstrator system.

Figure 92 shows a timetable overview of the actions occurring at the test site. The horizontal axis represents the time in seconds. Before the station hop took place, the 1st radio receiver which was tuned to 7225 kHz received a good quality AM signal. This frequency was notched by the PLT system. There was no interference from the PLT system to this radio station. The PLT signal was clearly be noticeable on the 2nd radio receiver, which was tuned to 7320 kHz.

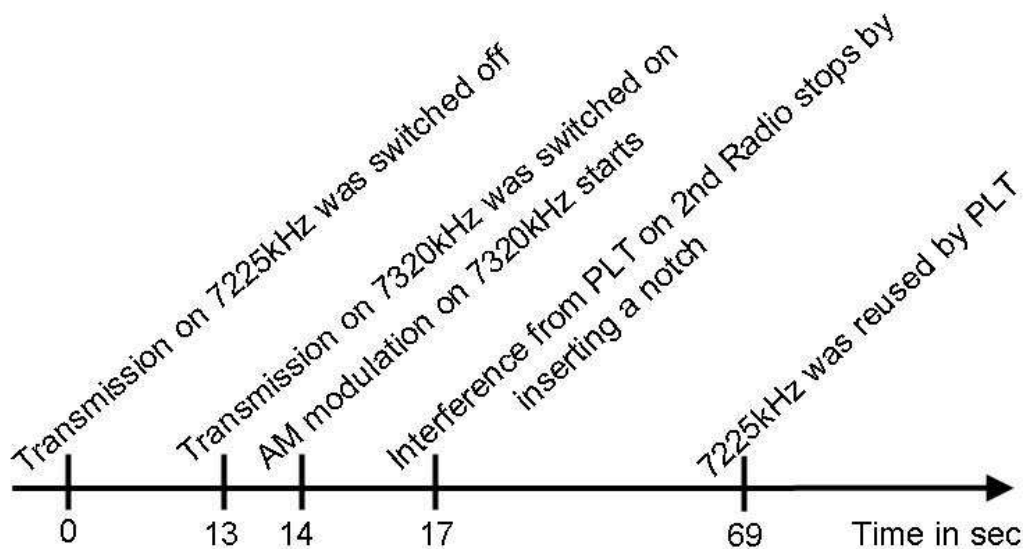


Figure 92: Frequency hopping of a notch recorded at verification of the demonstrator

The trigger for the time axis in figure 92 was set to 0 sec when the radio broadcast signal went silent on the 1st radio receiver. The Skelton transmitter had stopped its broadcast. 13 seconds later, the start of the transmission at 7320 kHz was noticed on the 2nd radio receiver. A further second later, the AM modulation started at 7320 kHz. The service could be heard on

the 2nd radio receiver, but it was still interfered with by the PLT transmission. The PLT device detected the presence of this radio station another 3 seconds later and inserted a notch to protect 7320 kHz. This was noticed when the interference stopped on the 2nd radio device. Around one minute later, the frequency at 7225 kHz was reused by the PLT system. The PLT signal was now noticed on the 1st radio receiver which was still tuned to this frequency.

To assess the quality of an AM radio station, the SINPO assumption was standardized in [ITU-R] with the properties of signal strength, interference, noise and propagation individually estimated. The signal strength and propagation can be measured using a spectrum analyzer. Noise and interference levels are estimated by human ears. In this way, it is difficult to identify the source of the noise. The listener's impression is noted without taking any further action. PLT was often the dominant interferer during the ETSI plugtest, when 'Smart Notching' was not activated. Finally, the overall estimation is given as an average of individual properties. The SINPO assumption was performed for a total of 168 times during the plugtest. Each of them is noted in the plugtest report [Schw_08c] including the signal levels at the mains as well the E-field. Figure 93 shows a histogram of the occurrence of the overall SINPO estimation. The horizontal axis represents the SINPO level:

- Level 1: unusable. No listener will stay tuned to a service with such a bad quality
- Level 2: poor. A human voice might be understood
- Level 3: fair. Music might be enjoyed, with limited quality
- Level 4: good AM audio quality
- Level 5: excellent. Usually, an AM service will never reach level 5. Only DRM supports this level in the HF band

The SINPO assumption was done 3 times for each radio station received at the site of the plugtest. Initially with PLT switched off (brown column) and later with a PLT transmission running having the 'Smart Notching' concept activated (green column). And finally, when PLT transmission was running, but no notches were in place (blue column). To ensure that every station was captured, a station scan was executed in all HF transmission bands using the Sony ICF-SW77. The SINPO assumptions were performed at every station which was found.

The vertical axis of figure 93 represents the number of occurrences.

Figure 93 shows that there was no difference in the reception quality of HF radio services when the PLT system was transmitting data with 'Smart Notching' activated and when the PLT was off. The brown and green columns have an identical height. When the PLT system was transmitting data without inserting notches, many radio stations degraded to an unusable quality.

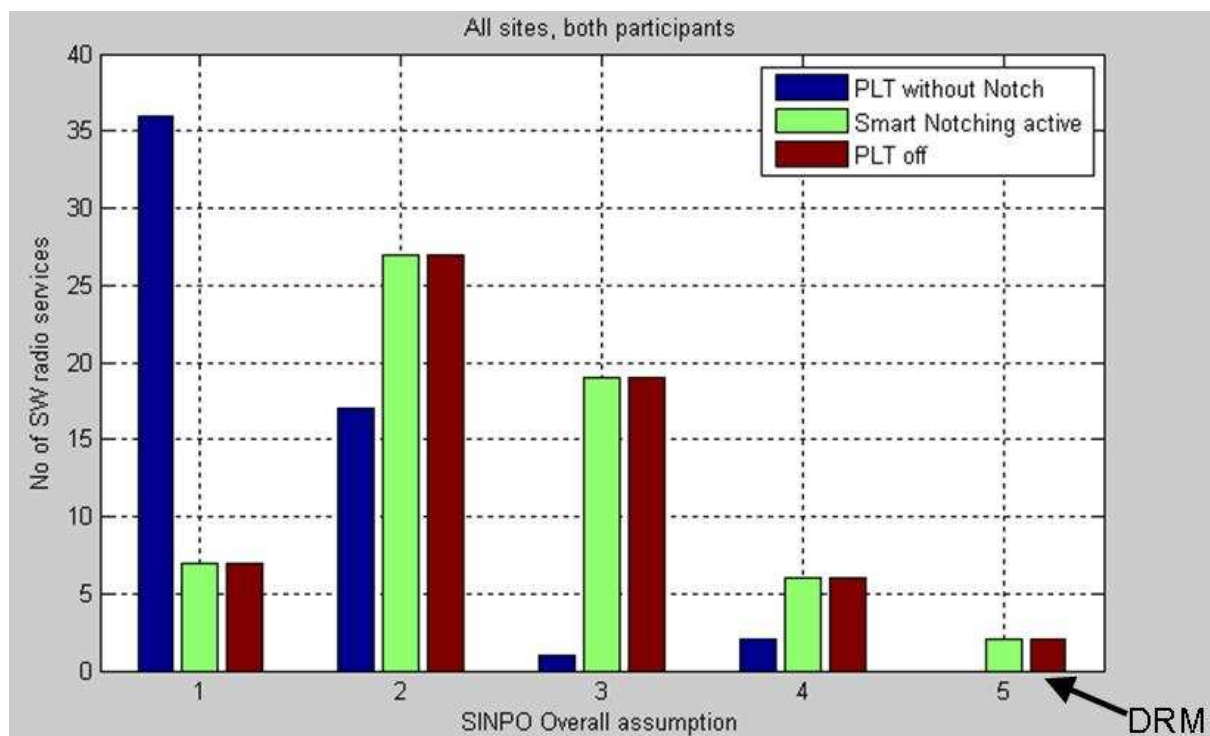


Figure 93: Result of subjective assessment of sound quality:

Not notched (blue), notched (green) and PLT off (brown)

5.5 Standardization of ‘Smart Notching’

Reports about interference from PLT to HF radio broadcast were published quite early [Stot_03]. The new high bit rate PLT modems using multiple communication carriers at various frequencies with adaptive constellations enable the realization of the ‘Smart Notching’ concept. The idea was initially presented to ETSI PLT [ETSI_99] in January 2004 [Schw_04a]. Since November 2004, the radio broadcast community has taken ‘dynamic notching’ into consideration for use in powerline modems: [Stot_04] and [Stot_05]. In order to prove if any new technology works reliably, an implementation has to demonstrate its functions, which is why ETSI PLT created the special task force STF 332 [Schw_07a] to perform a plugtest with PLT modems and SW radio receivers.

During the ETSI plugtest in October and November 2007, various tests and measurements were performed using PLT modems and radio receivers. One of the test participants was the demonstrator system described in Chapter 5.3. A description of some of the plugtest highlights were given in chapter 5.4.

5.5.1 EBU Statement

After performing the plugtest and publishing the results, the European Broadcasting Union (EBU) published a statement with regard to the ETSI specification of the PLT ‘Smart Notching’ system. The statement is available at [EBU_08] and is to be found in appendix A. The EBU is content that any system fully meeting the specification will offer adequate protection to HF (Short Wave) broadcast transmissions.

5.5.2 ETSI PLT, CISPR I PT PLT, ECANB, CENELEC, IEEE, ITU and others

The concept of smart notching has been launched into the relevant standardization organizations:

ETSI [ETSI_99]:

On the 2nd of July 2008 at the meeting No.47, after more than 60 contributions to ETSI PLT WI21 [Schw_06a] and 27 revisions of draft TS 102 578, the technical standard was unanimously approved by the ETSI PLT Technical Committee without any objections. The approved document is available for download from the ETSI website:

[Schw_08d] ETSI TS 102 578 V1.2.1 (2008-08) PowerLine Telecommunications (PLT); Coexistence between PLT Modems and Short Wave Radio broadcasting services.

CISPR [CISPR_05]:

The ‘Smart Notching’ demonstrator system was presented to CISPR I PT PLT in January 2008. The group announced that they will ‘work on adaptive dynamic notching and adaptive power management techniques for potential inclusion in any future CD or CDV related to PLT equipment’ in CISPR/I/257/CD [CISPR_08a]. The concept itself is described in CISPR/I/258/DC [CISPR_08b]. It is considered in CISPR/I/269/DC [CISPR_08c]. Finally (so far), the group adopted the adaptive EMI mitigation techniques of ‘Smart Notching’ and ‘adaptive power management’ (chapter 4.4) as a normative annex to their latest CIS/I/301/CD [CISPR_09a] and CIS/I/302/DC [CISPR_09b]. Accepting adaptivities is almost ‘revolutionary’ in the world of EMI standardization.

European Commission of Associated Notifies Bodies (ECANB):

The ECANB approved their Technical Guideline Notes 17 (TGN17), including ‘Smart Notching’. TGN17 V2.0 [TGN17] guides: When being consulted to provide an opinion on PLT conformity assessment, Notified Bodies are strongly encouraged to base their opinion on additional mitigation measures. They have to be implemented according to adaptive mitigation techniques to protect radio services.

ETSI – CENELEC Joint Working Group (JWG):

The adaptive or dynamic notching concept was taken into prEN 50529-3 [CENE_08].

IEEE:

It is included as ‘stand alone dynamic notching’ to the IEEE P1901 [IEEE_09] baseline document, which was approved in December 2008 in Kyoto.

ITU:

The concept of ‘Smart Notching’ is proposed to ITU-R [ITUR_08] [ITUR_09], ITU-T [Schw_05c], and others.

In each case, lively discussions have been initiated. ‘Smart Notching’ seems to be the trigger for a change of paradigms in EMC coordination...

6 Outlook to Future EMC Coordination

The classical concept of EMC requires constant emission and immunity limits against high frequency signals. The emission limit of all devices and their own immunity threshold defines the operating range. Devices working within this range operate without producing any interference in their environment. This classical concept of guaranteeing EMC as shown on the left side on figure 94 has the drawback that some resources are left unused. Furthermore, devices need costly shielding, even though there are often no signals causing disturbance. All frequencies are shielded by the device, independent of where and when the device is operated. In short, the resources are not used efficiently.

In some cases, the reception of a low power signal is disturbed despite the fact that surrounding devices comply with the relevant EMC standards. Unfortunately, this is the real condition shown on the right side in figure 94. From both an economic and a technical point of view this is not satisfactory. In this case, stricter limits should have been chosen.

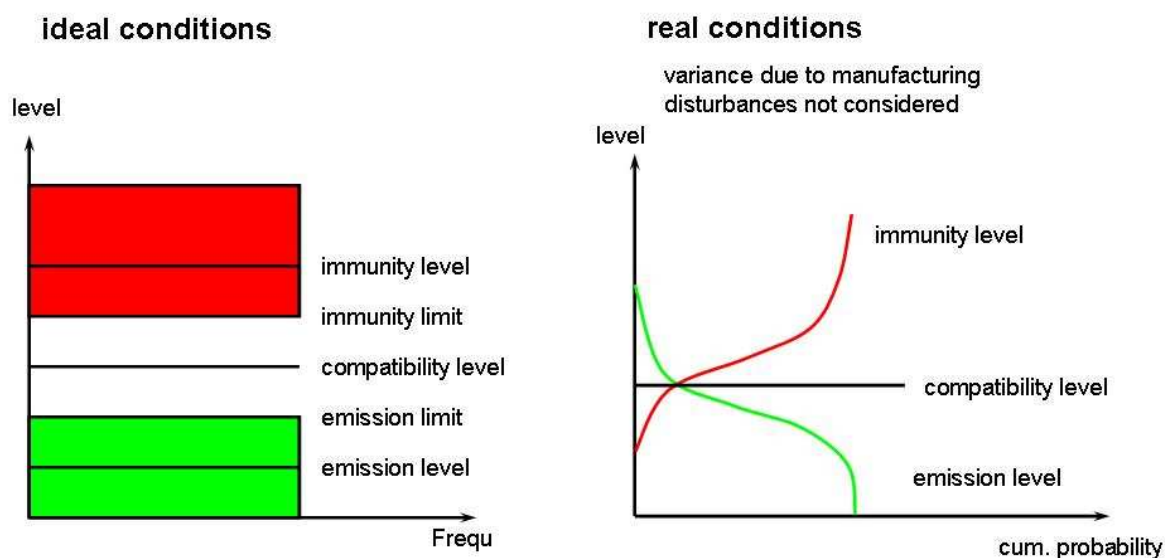


Figure 94: EMC coordination, ideal and real conditions

Since radio systems receive a large range of signal amplitudes, they are typically the most sensitive devices in the home environment. Therefore, radio signal protection dominates the process of EMC coordination in the area of high frequency signals. EMC coordination has been performed for several decades by simply defining limits for electromagnetic emissions produced by equipment. In the past, this simple approach was adequate. Classical disturbance

sources such as commutator machines or switched power supplies occasionally produce emissions in a wide frequency band. A selective and at the same time flexible suppression was not possible. Therefore, suppression was designed by limiting the maximum emission to a value a few dB below the limit. The established limits are increasingly discussed by the radio people, since the limits were designed under certain conditions regarding spatial, time and frequency probability of disturbance sources. Today, a larger number of modern disturbance sources produce continuous emissions in a broad frequency band, so that the original preconditions are not necessarily valid any more. Additionally, new radio systems appear. In former times (when the limits were once defined), an external antenna and a separate grounding of the receiver was common practice. Nowadays, the same reception quality is expected from radio receivers without any earth connection and using only an internal (whip) antenna.

Modern wired communication systems based on OFDM technology (e.g. ADSL, VDSL, PLT) are able to integrate adaptive EMC measures into their design. They can use the spectrum in a very flexible way.

For example, powerline communication modems - as discussed in this thesis - use this approach. Compared to conventional PLT modems, which could interfere with high frequency radio services, the modems using the concept of 'Smart Notching' do not disturb radio receivers.

The frequency range of conventional PLT modems (2 MHz to 30 MHz) overlaps with HF radio broadcast frequencies. Powerline wires in private homes are not shielded and are structured with a certain amount of asymmetry. If a SW radio receiver (AM or DRM) is operated indoors where a powerline communication is active, the radio reception quality might suffer. Having communication systems in the same frequency range and coupling paths in between - conducted as well as radiated - makes disturbance situations inevitable.

Due to the antenna properties of the low voltage distribution grid, the electricity cables in a building receive signals from radio broadcast services. PLT modems equipped with 'Smart Notching' detect the existence of such radio services by measuring the signal's spectrum on the mains network. After an analysis of this spectrum, the PLT modems exclude frequencies receivable by SW radio devices. This process is called 'notching'. Thanks to the adaptive OFDM transmission with a high number of carriers, 'Smart Notching' causes only a minor decrease in the transmission bit-rate as only low SNR carriers are lost. Continuous analysis allows the system to minimize interference and to optimize throughput depending on the current conditions.

Electromagnetic compliance is achieved in a different way in such adaptive systems: instead of rigid constraints, ‘Smart Notching’ devices can comply and improve EMC. According to the definition of the IEV (International Electrotechnical Vocabulary), a product is electromagnetically compatible if it works satisfactorily in its electromagnetic environment without introducing intolerable electromagnetic disturbances to anything else.

It is clear that all aspects can be addressed by a more flexible spectrum usage of the wired communication systems. By design, they can adapt themselves to the electromagnetic environment in order to protect radio services. Discussions in some standardization committees show that the way towards this new paradigm is difficult. Traditionally, there are inflexible limits. Lively discussions to find a consensus between the concerned parties can be expected. Sometimes, industry claims that the people standardizing EMC are too rigid, but if they would not have been resolute in the past, applications such as PLT would not be possible today. Anyhow, to achieve technical and economic progress we need constructive discussions and open thinking. The ‘Smart Notching’ mechanism for PLT modems presented in this thesis is an example for a new way in EMC coordination.

Further examples of adaptive coexistence or EMC with other applications are:

- Frequency Notching is specified for DVB-C2 systems [Hass_09]
- OFDM overlay systems [Bran_07]
- Cognitive Radio [Rajb_07]
- Frequency Management with Mobile Satellite Services [Rick_96]
- Dynamic Spectrum Management for DSL (DSM) [Stanf], [DySPAN]

These technologies demonstrate the feasibility of such concepts.

Some videos illustrate the implementation of the PLT ‘Smart Notching’ system in a flat:

- PLT with Sony ICF SW 77 [Schw_07c]
- PLT with Sangean ATS 909 [Schw_07d]
- PLT with Roberts DRM receiver [Schw_07e]

A wrap up of ‘Smart Notching’ including an animated presentation can be found at [Schw_08e].

7 Conclusions

PLT is very well suited for data transmission in buildings. It provides a huge gain of comfort for the user. There is currently no alternative media for building an in-house backbone network medium, where applications like HD video streaming are enabled by throughput rates of more than 200 Mbps on the physical layer. Throughput rates could be enhanced by using frequency ranges above 30 MHz. The robustness of PLT is enhanced by the usage of the 3rd wire, the protective earth. This enables MIMO technologies to communicate via up to 8 paths between 2 power outlets. The coverage to achieve HD video transmissions over the especially bad, highly attenuated links is improved enormously.

A burden of today's PLT systems is the potential interference to HF radio broadcast. The main part of this thesis describes a concept of adapting the transmission spectrum to the locally receivable HF radio services. The ingress of the radio broadcast signals on the mains grid is detected by PLT modems. The PLT transmission automatically excludes (notches) frequencies allocated by receivable radio services. The process works adaptively in time and frequency domain in an autonomous way. The loss of throughput rate by the frequency notching is expected to be less than 1% of the total throughput rate achieved by today's PLT systems. This thesis describes a detailed implementation of such a dynamic notching system for the first time.

The concept was proven under the critical supervision of a representative from the radio broadcast community (EBU). All HF-radio services receivable by a SW-radio device were protected by the PLT modems during this plugtest.

Today, the concept of 'Smart Notching' which is also known as 'Dynamic Notching' is standardized by ETSI and under discussion to be included into a harmonized norm of EMI for PLT.

Notching is considered to be the key solving the long lasting discussion about EMI of PLT. It has also been shown that MIMO enhances the robustness of PLT over bad communication links. These solutions are necessary for PLT to reach maturity for being integrated into consumer electronic devices and home appliances on a large scale.



European Broadcasting Union

Union Européenne de Radio-Télévision

Technical Department

Département technique

9 January 2008

EBU S/EIC²

Statement with regard to ETSI specification of PLT "Smart Notching" system

The latest version of the Coexistence Specification (ETSI TS 102 578 v1.1.16 – 2007-11; PowerLine Telecommunications (PLT) Coexistence between PLT Modems and Short Wave Radio Broadcasting) services was considered by the EBU S/EIC group at its meeting on the 28th and 29th November 2007.

Within the provisions:

the document concerns itself specifically with a system of dynamic notching (referred to as "Smart Notching") whereby a PLT modem omits, or 'notches' certain frequencies and frequency ranges from the signal which it uses to communicate with other PLT modems. Other aspects of PLT systems and system design outside the scope of the specification are excluded;

- the protection (dynamic notching) system is designed only to protect HF broadcast transmissions services in specified bands between 2 MHz and 30 MHz;
- the EBU S/EIC group is content that any system fully meeting the specification will offer adequate protection to HF (Short Wave) broadcast transmissions. The EBU S/EIC group will therefore recommend to EBU members that are also members of ETSI that they should support the adoption of the specification within ETSI.

Further to this a representative of the EBU, Mike Hate, was present during the tests described in document

ETSI TR 1XX W124 v2.1.x (PLT44_TD_12r1_ETSI_TR_W124_Part2_V2_0_3.doc).

The EBU S/EIC group confirms that this document is a fair and accurate report of the tests carried out and the results obtained.

² S/EIC stands for: **S**pectrum management **C**ommittee / **E**lectromagnetic **I**nterference and **C**ompatibilities. This is one of many EBU project groups dealing with different subjects relevant to Broadcasting.

A	Ampere
dB	decibel (logarithmic unit)
dBm	$10 * \log_{10}(P_1/1 \text{ mW})$
dBV	$20 * \log_{10}(U_1/1 \text{ V})$
dB(m/Hz)	Power Spectral Density
dB(/m)	Antenna factor
dB μ V	$20 * \log_{10}(U_1/1 \mu \text{ V})$
dB(μ V/Hz)	Voltage Spectral Density
dB(μ V/m)	Electrical Field strength
dB(μ V/m)-dBm	Coupling factor k_{sym} or Reception factor ReFa
F	Farad $1 \text{ F} = 1 \text{ A}^2\text{s}^4/(\text{kg m}^2)$
ft	foot $1 \text{ ft} = 0.30480 \text{ m}$ (Shoe Size of 48½ in Europe)
GHz	Giga Hertz $1 \text{ Hz} = 1 \text{ s}^{-1}$
Hz	Hertz $1 \text{ Hz} = 1 \text{ s}^{-1}$
KB	Kilo Byte
kHz	kilo Hertz $1 \text{ Hz} = 1 \text{ s}^{-1}$
kg	kilo gram
km	kilo meters
km/h	kilo meters per hour
kV	kilo Volt
m	meter
Mbps	Mega bit per second
MB	Mega Byte
MHz	Mega Hertz $1 \text{ Hz} = 1 \text{ s}^{-1}$
ms, msec	milli second
mV	milli Volt
mW	milli Watt
ns	nano second
s, sec	second
U	Unit
V	Volt $1 \text{ V} = 1 \text{ kg m}^2/(\text{As}^3)$
W	Watt $1 \text{ W} = 1 \text{ VA} = 1 \text{ kg m}^2/\text{s}^3$
Ω	Electrical impedance $1 \Omega = 1 \text{ V/A} = 1 \text{ kg m}^2/(\text{A}^2 \text{ s}^3)$
μ s	micro second

Curriculum Vitae

Personal Information

Born: 5th of Oct. 1969 in Backnang, Germany

Citizenship: German

Education

1976 – 1980: Walterich Grundschule Murrhardt

1980 – 1989: Heinrich von Zügel Gymnasium Murrhardt

1989 – 1990: Compulsory Conscription of Military Service,
Telecommunications Battalion, Veitshöchheim

1990 – 1993: University of Cooperative Education (Berufsakademie) Stuttgart,
Electronics, Telecommunication. Earning of the degree Dipl. Ing. (BA)

2007 – 2009: University of Duisburg-Essen, additional studies for doctoral process

Employment History

1990 – 1993: ANT Nachrichtentechnik:
Student of University of Cooperative Education, Diploma Thesis:
Microwave pre-distortions for linearization of traveling wave tubes.

1993 – 1995: Bosch Telecom, Development Engineer
in Advanced Development Department

1996 – 1997: Grundig, Development Engineer
in Business Unit Multimedia / Satellite Receivers

Since 1997: Sony, Development Engineer to Principal Engineer
in European Technology Center

Bibliography

- [3GPP] 3rd Generation Partnership Project (3GPP) <http://www.3gpp.org/article/1te>
- [Ahol_03] J. Ahola, Applicability of Power-Line Communications to Data Transfer of On-line Condition, Monitoring of Electrical Drives, Lappeenranta 2003, ISBN 951-764-783-2
- [AHS_07] U.S. Census Bureau, Housing and Household Economic Statistics Division: American Housing Survey, December 19, 2008
<http://www.census.gov/hhes/www/housing/ahs/ahs.html>
- [Alpha] Alpha-Data <http://www.alpha-data.com/>
- [Amem_06] Physical characteristics of the Japanese AC power wiring system, CISPR/I/PLT-PT (Brussels/Amemiya, Osabe, Akiyama) 06-02, January 2006
- [Analog] ANALOG DEVICES: AD9866: 12-Bit Broadband Modem Mixed Signal Front End
<http://www.analog.com/en/rfif-components/rxtx-subsystems/AD9866/products/product.html>
- [Analog_08] ANALOG DEVICES AD9867: Broadband Modem Mixed-Signal Front End
<http://www.analog.com/en/rfif-components/rxtx-subsystems/ad9867/products/product.html>
- [Baig_03] F. Baig, Powerline Communication: Study of Noise Sources, Diploma Thesis, 2003, University of Stuttgart, Institute of Telecommunications
- [Barn_66] Barnouw, Eric. (1966). A tower in Babel: A history of broadcasting in the United States, volume I, to 1933. New York: Oxford University Press.
- [Barn_68] Barnouw, Eric. (1968). The golden web: A history of broadcasting in the United States, volume II, 1922 to 1953. New York: Oxford University Press.

- [BNetzA_01] Reg TP 322 MV 05 Teil 1: Messvorschrift für die Messung von Störfeldern aus Anlagen und Netzen der Telekommunikation im Frequenzbereich 9 kHz bis 3 GHz“, Oktober 2001
- [Bran_07] S. Brandes, M. Schnell “Mitigation of Dynamically Changing NBI in OFDM Based Overlay Systems”; Lecture Notes Electrical Engineering, Multi-Carrier Spread Spectrum 2007, ISBN 978-1-4020-6128-8
- [Broa_84] R. Broadridge 'Power line modems and networks' 4'th International Conference on Metering Applications and Tariffs for Electricity Supply IEE conf. Publ 300 1984 pp 294-296 (London UK: IEE)
- [Brow_99a] P. Brown, Digital Powerline: A Wireline access solution, 1999
- [Brow_99b] P. Brown, “Power Line Communications – Past Present and Future”, 3rd International Symposium on Power-Line Communications and its Applications, Lancaster UK 30.5-1.4.1999, pp. 1-7.
- [Bull_03] S. Bullock, Method and System for Powerline Impedance Detection and Automatic Impedance Matching, US Patent No.: US 6.515.485 B1, Feb 2003
- [CCIR] Weighting window for noise assessment in audio signals: CCIR Rec. 468-4, DIN 45405, CCITT Rec. N21
- [CENE_08] CENELEC, DRAFT EUROPEAN STANDARD, prEN 50529-3 Conducted transmission networks - Part 3: Power line communication (mains network-based) November 2008
- [CEPCA_05] CEPCA Consumer Electronics Powerline Communication Alliance
<http://www.cepca.org/>
- [CISPR_97] CISPR 22:1997, "Information technology equipment - Radio disturbance characteristics - Limits and methods of measurement".
- [CISPR_99] CISPR 16-1-1: "Specification for radio disturbance and immunity measuring apparatus and methods - Part 1-1: Radio disturbance and immunity measuring apparatus - Measuring apparatus".

- [CISPR_02] CISPR 25:2002 Radio disturbance characteristics for the protection of receivers used on board vehicles, boats, and on devices — Limits and methods of measurement
- [CISPR_05] CISPR I PT PLT, Project: CISPR 22 am1 Ed. 6.0; CISPR is the Special International Committee on Radio Interference of the [International Electrotechnical Commission IEC](http://www.iec.ch/cgi-bin/procgi.pl/www/iecwww.p?wwwlang=e&wwwprog=prodet.p&progdb=db1&He=CISPR&Pu=22&Pa=&Se=&Am=1&Fr=&TR=&Ed=6.0).
<http://www.iec.ch/cgi-bin/procgi.pl/www/iecwww.p?wwwlang=e&wwwprog=prodet.p&progdb=db1&He=CISPR&Pu=22&Pa=&Se=&Am=1&Fr=&TR=&Ed=6.0>
- [CISPR_06] CISPR 22:2006 or BS EN 55022:2006, Information technology equipment. Radio disturbance characteristics. Limits and methods of measurement, Nov 2006
- [CISPR_08a] IEC, CISPR/I/257/CD, CISPR22 - Limits and method of measurement of broadband telecommunication equipment over power lines, February 2008
- [CISPR_08b] IEC, CISPR/I/258, Report on Mitigation Factors and Methods for Power Line Telecommunications, February 2008
- [CISPR_08c] IEC, CISPR/I/269/DC, Proposed Approach on EMC emission requirements for PLT, June 2008
- [CISPR_09a] IEC, CIS/I/301/CD, Amendment 1 to CISPR 22 Ed. 6.0: Addition of limits and methods of measurement for conformance testing of power line telecommunication ports intended for the connection to the mains, July 2009
- [CISPR_09b] IEC, CIS/I/302/DC, Comparison of the RF disturbance potential between Type 1 and Type 2 PLT devices compliant with the provisions of CISPR/I/301/CD and EUTs compliant with the limits in CISPR 22 Ed. 6.0. July 2009
- [Cho_89] N. Cho et al, Adaptive Line Enhancement by Using an IIR Lattice Notch Filter. IEEE Transactions on Acoustics, Speech and Signal Processing, Vol. 37, No. 4, Apr.1989
- [Corr_06] Corripio, F.J.C.; Arrabal, J.A.C.; del Rio, L.D.; Munoz, J.T.E. Analysis of the cyclic short-term variation of indoor power line channels IEEE Journal on Se-

- lected Areas in Communications, Volume 24, Issue 7, July 2006 Page(s): 1327 - 1338
- [Dahl_06] Dahlman, et al, The 3G Long-Term Evolution - Radio Interface Concepts and Performance Evaluation: Vehicular Technology Conference, 2006. VTC 2006-Spring. IEEE 63rd, 7-10 May 2006, Volume: 1, On page(s): 137-141
- [Dost_01] K Dostert, Powerline Communications, Prentice-Hall, Upper Saddle, River, USA, 2001, ISBN 0130293423
- [DRM_06] Minimum Receiver requirements for DRM, "Draft version 1.5"
- [DySPAN] DySPAN International Dynamic Spectrum Access Networks (DySPAN) symposium <http://www.ieee-dyspan.org/>
- [EBU_06] EBU: The Digital Haze - Radio Services under threat [zip \(27 Mbyte\)](http://www.ebu.ch/en/technical/publications/userguides/index.php)
<http://www.ebu.ch/en/technical/publications/userguides/index.php>
- [EBU_08] Contribution to ETSI PLT WI21: ETSI PLT45_TD_09, EBU S/EIC, Statement with regard to ETSI specification of PLT "Smart Notching" system, January 2008 from EBU
- [EIAA_04] EIAA – Bob Ivins: European Media Consumption. Increasing the role of the Internet as an advertising medium.
http://www.aol-dmg.de/fileadmin/downloads/studien/eiaa_2004.pdf
- [ETSI_99] ETSI TC PLT <http://www.etsi.org/WebSite/Technologies/Powerline.aspx>
- [ETSI_00] ETSI TS 101 867 V1.1.1 (2000-11); Powerline Telecommunications (PLT); Coexistence of Access and In-House Powerline Systems
- [ETSI_03a] ETSI TR 102 175 V1.1.1 (2003-03); Power Line Telecommunications (PLT); Channel characterization and measurement methods
- [ETSI_03b] ETSI TR 102 258 V1.1.1 (2003-09); PowerLine Telecommunications (PLT); LCL review and statistical analysis

- [ETSI_03c] ETSI TR 102 259 V1.1.1 (2003-09); PowerLine Telecommunications (PLT); EMI review and statistical analysis
- [ETSI_05] ETSI ES 201 980 (V2.2.1): "Digital Radio Mondiale (DRM); System Specification". <http://www.drm.org/>
- [FCC_04] FCC PART 15 - RADIO FREQUENCY DEVICES, July 12, 2004
or more specific: FCC NPRM on BPL, Appendix C: Proposed Measurement Guidelines, Feb 2004
http://hraunfoss.fcc.gov/edocs_public/attachmatch/FCC-04-29A1.pdf
Complete FCC part 15:
http://www.access.gpo.gov/nara/cfr/waisidx_98/47cfr15_98.html
- [Ferdj_94] M. Ferdjallah, R. Barr, Adaptive Digital Notch Filter Design on the Unit Circle for the Removal of Powerline Noise from Biomedical Signals
- [Floo_05] É. Flood, M. Woulfe, N. Zhang Broadband over Power Lines (BPL)
<http://ntrg.cs.tcd.ie/undergrad/4ba2.05/group13/index.html>
- [Gane_03] Ganesan, R.; Das, S.K., Power line transient interference and mitigation techniques, INCEMIC 2003. Volume , Issue , 18-19 Dec. 2003 Page(s): 147 - 154
- [GHn_08] G.hn "next generation" home network technology standard by ITU-T SG15 Q4, <http://www.itu.int/ITU-T/>, <http://q4sg15.itu.int/>, ITU-T Rec. G.9960
- [Gini_00] Ginis, G.; Cioffi, J.M., A multi-user precoding scheme achieving crosstalk cancellation with application to DSL systems, Signals, Systems and Computers, 2000. Conference Record of the Thirty-Fourth Asilomar Conference on Volume 2, Issue , 2000 Page(s):1627 - 1631 vol.2
- [Gold_05] F.Issa, M.Goldberg, E.Marthe, Power Line Communications using low and medium voltage networks, Proceedings of the XXVIIIth General Assembly of International Union of Radio Science, 2005
- [Harr_78] F. Harris, On the use of Windows for Harmonic Analysis with the Discrete Fourier Transform. Proceedings of the IEEE 66 (1): 51–83, January 1978.

- [Hass_09] P. Hasse, J. Robert, D. Jaeger, C. Schaaf: DVB-C2 –die zweite Generation des digitalen Kabelfernsehens, FKT 5|2009, S. 210 - 215
- [Haye_68] J. F. Hayes, Adaptive feedback communications, IEEE Trans. Commun. Technol., vol. COM-16, pp. 29-34, Feb. 1968.
- [HDPLC] HD-PLC Alliance <http://www.hd-plc.org/>
- [Hern_05] J. Hernández, Tuneable digital Filters, Diploma Thesis, Institute of Telecommunications, University of Stuttgart
- [Hess_05] M. Hesse, Wavelet-OFDM für Powerline Communication, Praktikumsbericht, Nov. 2005, Universität Dresden, Sony Deutschland GmbH, Stuttgart
- [Homepl] Homeplug <http://www.homeplug.org/>
- [Husa_08] S. Husaini, Implementation of window function to an OFDM scheme in Powerline Communication System, Diploma Thesis at University of applied sciences Darmstadt
- [IEC_00] EN 60315-3:2000, Methods of measurement on radio receivers for various classes of emission. Receivers for amplitude-modulated sound-broadcasting emissions
- [IEC_06] IEC 61000-4-3, Electromagnetic compatibility (EMC) Part 4-3: Testing and measurement techniques - Radiated, radio-frequency, electromagnetic field immunity test (IEC 61000-4-3:2006)
- [IEEE80211n] 802.11n: <http://en.wikipedia.org/wiki/802.11n>
- [IEEE802.16] IEEE Standard 802.16 "Air Interface for Fixed Broadband Wireless Access Systems"
<http://standards.ieee.org/getieee802/download/802.16-2004.pdf>
- [IEEE_09] IEEE P1901 Draft Standard for Broadband over Power Line Networks: Medium Access Control and Physical Layer Specifications,
<http://grouper.ieee.org/groups/1901/>

- [IEEE_10] IEEE Symposium on new frontiers in dynamic spectrum access networks (DySPAN 2010) 6 - 9 April 2010, Singapore. <http://www.ieee-dyspan.org/>
- [ITUR] ITU-R Rec. BS.1284: "General methods for the subjective assessment of sound quality". See <http://stason.org/TULARC/radio/shortwave/08-What-is-SINPO-SIO-Shortwave-radio.html>.
- [ITUR_90] ITU-R Rec. BS.703 Characteristics of AM sound broadcasting reference receivers for planning purposes.
- [ITUR_92] ITU-R Rec. P.842-2 Computation of Reliability and Compatibility of HF Radio Systems
- [ITUR_03] ITU-R Rec. BS.1615: "Planning parameters" for digital sound broadcasting at frequencies below 30 MHz".
- [ITUR_04] ITU-R Radio Regulations, edition of 2004
- [ITUR_06] ITU-R Rec. 560-3 1, Radio-Frequency protection ratios in LF, MF and HF Broadcasting
- [ITUR_07] ITU-R Rec. P.372-8: "Radio Noise"
- [ITUR_08] ITU-R, Contribution to the Correspondence Group on High Data Rate Power Line Telecommunication, Mitigation Factors and Methods for Power Line Communications, Annex 6 to Document 1A/163, from United States Department of Commerce/NTIA, February 2008
- [ITUR_09] Contribution to ITU-R: Impact of power line telecommunication systems on radio communication systems operating in the LF, MF, HF and VHF bands below 80 MHz Question ITU-R 221-1/1, Annex 2 to Working Party 1A Chairman's Report, Document 1A/TEMP/47 (Edited), March 2009
- [ITUT_96] ITU-T Recommendation G.117: "Transmission aspects of unbalance about earth".

- [Josh_99] Y. Joshi, D. Roy, Design of IIR Multiple Notch Filters Based on All-Pass Filters. IEEE Trans. On Circuits and Systems II, Analog and Digital Signal Proc. Vol 46, No.2, Feb. 1999
- [Khad_03] Y. Khadour, Eignung von Niederspannungsverteilnetzen für Powerline Communication, Dissertation, Universität Duisburg-Essen, 2003
- [LDPC] Gallager, R. G., Low Density Parity Check Codes, Monograph, M.I.T. Press, 1963
- [Lee_05] Lee, et al, Adaptive Modulation Based Power Line Communication System, Lecture Notes in Computer Science, Springer Berlin / Heidelberg, Book Advances in Intelligent Computing, ISBN 978-3-540-28227-3
- [LEGO] LEGO bricks <http://www.lego.com>
- [Lind_08] F.Lindqvist, et al, Crosstalk Channel Estimation via Standardized Two-Port Measurements, EURASIP Journal on Advances in Signal Processing Volume 2008 (2008), Article ID 916865, <http://www.hindawi.com/getarticle.aspx?doi=10.1155/2008/916865&e=html>
- [Linux] Gentoo Linux <http://www.gentoo.org/>
- [LiQi_04] Li Qi, She Jingzhao, Feng Zhenghe, Adaptive Impedance Matching In Power Line Communication, 2004 4' ICMMT, Tsinghua University, Beijing
- [Loub_01] C.R. Loubery, "Einrichtung zur elektrischen Zeichengebung an die Teilnehmer eines Starkstromnetzes", Berlin, Kaiserliches Patentamt Nr. 118717, 15. März 1901
- [Lüke_92] H. D. Lüke, Die Korrelationssignale. Springer Verlag, Berlin, 1992
- [Mart_94] U. Martin Ausbreitung in Mobilfunkkanälen: Beiträge zum Entwurf von Messgeräten und zur Echoschätzung, Erlangen - 1994
- [MATW] Matlab® is a high-level language and interactive environment that enables you to perform computationally intensive tasks. <http://www.mathworks.com/>

- [Mentor] Visual Elite Advanced TLM-RTL Design and Integration Platform,
http://www.mentor.com/products/esl/design_verification/visual_elite/upload/Visual_datasheet_2007.pdf
- [OPERA_04] OPERA deliverable from EC/IST FP6 Project No 507667,
OP_WP5_Deliverable D52_v3.doc, D52: Specification for EMC measurements to be performed
- [OPERA_07] OPERA deliverable from EC/IST FP6 Project No 507667,
OP_WP1_D8.2_IndoorNF_v0.2.doc V 0.2, D8.2: EMC Aspects of PLT Technology, Indoor – Conducted Signals and Near Field Radiated Signals
- [Paul_03] A. Paulraj, R. Nabar and D. Gore. Introduction to Space-Time Wireless Communications, Cambridge Univ. Press, May 2003.
- [Python] Python Programming Language <http://www.python.org/>
- [Rajb_07] R. Rajbanshi “OFDM-Based Cognitive Radio for DSA Networks”, University of Kansas, Sept. 2007
- [Reed_99] I.S. Reed and X. Chen, Error-Control Coding for Data Networks, Boston: Kluwer Academic Publishers, 1999.
- [Rick_96] D. Rickerson, “Symphony or calliope-frequency management with mobile satellite services” MILCOM '96, Conference Proceedings, IEEE Volume 3, 21-24 Oct. 1996 Page(s):943 - 947 vol.3
- [Sandb_95] S. D. Sandberg, M. A. Tzannes, Overlapped Discrete Multitone Modulation for High Speed Copper Wire Communications, Journal on Selected Areas in Communications, Vol. 13(9), December 1995
- [Sando_94] J.P. Sandoz, Large Frequency Range Easily Tunable Digital Notch Filter, GlobalDSP Vol.3, June 1994
- [Sart_01] Sartenaer, T. & Delogne, P., “Powerline Cables Modelling for Broadband Communications”, ISPLC 2001, pp. 331-337

- [Sbck_05] Schwarzbeck EFS 9218 Active Electric Field Probe with Biconical Elements
EFS 9218 and built-in Amplifier
<http://www.schwarzbeck.com/Datenblatt/m9218.pdf>
- [Schle_04] C. Schlegel and L. Perez, Trellis and Turbo Coding, IEEE/Wiley 2004, ISBN 0-471-22755-2
- [Schn_08] Schneider, D.; Stadelmeier, L.; Speidel, J.; Schill, D.: "[Precoded Spatial Multiplexing MIMO for Inhome Power Line Communications](#)", IEEE Global Communications Conference (GLOBECOM), New Orleans, USA, December 2008
- [Schw_02] ETSI STF 222 (Special Task Force of the European Standardization Institute):
http://portal.etsi.org/STFs%5CToR%5CToR222v15_PLT.doc;
Leader: W. Bäschlin, Participants: H. Hirsch, H. Regtop, A. Schwager
- [Schw_03a] ETSI TR 102 269 V1.1.1 (2003-12); PowerLine Telecommunications (PLT);
Hidden Node review and statistical analysis, Rapporteur: A. Schwager
- [Schw_03b] ETSI TR 102 270 V1.1.1 (2003-12); PowerLine Telecommunication (PLT);
Basic Low Voltage Distribution Network (LVDN) measurement data, Rapporteur: A. Schwager
- [Schw_04a] A. Schwager, Contribution to ETSI PLT WI9, RGWI009m01_TD02.pdf
- [Schw_04b] ETSI TR 102 370 V1.1.1 (2004-11); PowerLine Telecommunications (PLT);
Basic data relating to LVDN measurements in the 3 MHz to 100 MHz frequency range, Rapporteur: A. Schwager
- [Schw_05a] Potential of broadband power line home networking, Schwager, A.; Stadelmeier, L.; Zumkeller, M.
Consumer Communications and Networking Conference, 2005. CCNC 2005 Second IEEE, 3-6 Jan. 2005 Page(s): 359 – 363, Digital Object Identifier 10.1109/CCNC.2005.1405197
- [Schw_05b] A. Schwager, Contribution to ETSI PLT: PLT34_TD08_r1.pdf, ETSI PLT:
History of Coexistence and Roadmap of WI20 till PLT#35

- [Schw_05c] A. Schwager, Using a Coexistence Framework to Manage Powerline Networks, ITU Workshop: Opportunities and Challenges in Home Networking, 13 - 14 October 2005, SESSION 6: Electromagnetic Interference in the Home Environment
<http://www.itu.int/ITU-T/worksem/homenetworking/presentations/s6-schwager.zip>
- [Schw_05d] ETSI TR 102 494 V1.1.1 (2005-06) PowerLine Telecommunications (PLT), Technical requirements for In-House PLC modems, Rapporteur: A. Schwager
- [Schw_05e] A. Schwager, Contribution to ETSI PLT: PLT33_TD07.pdf, ETSI PLT: PLC Modem Coexistence
- [Schw_06a] ETSI PLT WI 21 Work Item No. 21:
http://webapp.etsi.org/WorkProgram/Report_WorkItem.asp?WKI_ID=24584
- [Schw_06b] A. Schwager, Contribution to ETSI PLT WI21, PLT36_TD_13_PLT_WI21_Prop_Dynamic_Notching_R1.pdf
- [Schw_06c] A. Schwager, Contribution to ETSI PLT WI21, RGWI020-WI021_02_detect_SW_ingress_onPLC_DombovarStr.pdf
- [Schw_07a] ETSI STF 332 (Special Task Force of the European Standardization Institute):
http://portal.etsi.org/STFs/STF_HomePages/STF332/STF332.asp,
Leader A. Schwager, Participants: M. Hate, H. Hirsch, R. Pfister
- [Schw_07b] A. Schwager, Contribution to ETSI PLT:
PLT44_TD_07_ts_102578v010110.doc, ETSI TS 102 578 (draft version of 12 October 2007): "PowerLine Telecommunications (PLT); Coexistence between PLT Modems and Short Wave Radio broadcasting services"
- [Schw_07c] Video 'Smart Notching' Demonstrator and AM receiver Sony ICF-SW77
http://plc.ets.uni-duisburg-essen.de/sony/SmartNotching_ICF-SW77.wmv
- [Schw_07d] Video 'Smart Notching' Demonstrator and AM receiver Sangean ATS 909
http://plc.ets.uni-duisburg-essen.de/sony/SmartNotching_Sangean.wmv

- [Schw_07e] Video 'Smart Notching' Demonstrator and DRM receiver Roberts MP-40
http://plc.ets.uni-duisburg-essen.de/sony/SmartNotching_DRM.wmv
- [Schw_08a] L. Stadelmeier, D. Schneider, D. Schill, A. Schwager, and J. Speidel, "MIMO for Inhome Power Line Communications," in International Conference on Source and Channel Coding (SCC), Ulm, 2008.
- [Schw_08b] ETSI TR 102 615 V1.1.1 (2008-02) PowerLine Telecommunications (PLT); Plugtests™ 2007 on coexistence between PLT modem systems; Test cases, Rapporteur: A. Schwager
- [Schw_08c] ETSI TR 102 616 V1.1.1 (2008-03) PowerLine Telecommunications (PLT); Report from Plugtests™ 2007 on coexistence between PLT and short wave radio broadcast; Test cases and results, Rapporteur: A. Schwager,
<http://www.etsi.org/plugtests/plt/plt1.htm>
- [Schw_08d] ETSI TS 102 578 V1.2.1 (2008-08) PowerLine Telecommunications (PLT); Coexistence between PLT Modems and Short Wave Radio broadcasting services, Rapporteur: A. Schwager
- [Schw_08e] A. Schwager, H. Hirsch: Smart Notching – New concepts for EMC coordination, Vortrag EMV 2008, Düsseldorf
http://www.ets.uni-duisburg-essen.de/download/public/Abstract_EMV_2008.pdf
http://www.ets.uni-duisburg-essen.de/download/public/EMV_2008_vortrag_hirsch.pdf
http://www.ets.uni-duisburg-essen.de/download/public/EMV_2008_praesentation_hirsch.pdf
- [Schw_09] D. Schneider, J. Speidel, L. Stadelmeier, D. Schill, A. Schwager, 13th ITG Symposium on Electronic Media "Systems, Technologies, Applications", Potential of MIMO for Inhome Power Line Communications, 2009
- [Schz_03] S. Schwarze, Hochratige Datenübertragung über Mittelspannungskabel, Shaker Verlag Aachen, ISBN: 3832210733, 2003

- [Shan_49] C. E. Shannon (1949, reprinted 1998). The Mathematical Theory of Communication. Urbana, IL: University of Illinois Press.
- [Soder_92] M. Soderstrand, K.V. Rangarao, H. Loomis, Improved Real-Time Adaptive Detection, Enhancement or Elimination of Multiple Sinusoids. Proceedings of the 34th Midwest Symposium on Circuits and Systems, 1991. Published in 1992 IEEE, pgs. 1085-1089
- [Sony] Sony VAIO mobile computer <http://vaio.sony.de/>
- [Sony_STC] Sony Deutschland GmbH, Stuttgart Technology Center
<http://www.stuttgart.sony.de/>
- [Spei_05] Speidel, J., “Multiple-Input Multiple-Output – Drahtlose Nachrichtenübertragung hoher Bitrate und Qualität mit Mehrfachantennen”, TeleKommunikation Aktuell, vol. 59, 2005
- [Spid_06] Contribution to ETSI PLT W120, PLT38_TD_11_W20, Coexistence Overhead Analysis from SPiDCOM
- [Stanf] University of Stanford Dynamic Spectrum Management Project,
<http://www-isl.stanford.edu/~cioffi/dsm/>
- [Stot_01] J. Stott, DRM— key technical features,
http://www.ebu.ch/en/technical/trev/trev_286-stott.pdf
- [Stot_03] J. Stott and J. Salter BBC R&D White Paper WHP067, The effects of power-line telecommunications on broadcast reception: Brief trial in Crieff.
<http://downloads.bbc.co.uk/rd/pubs/whp/whp-pdf-files/WHP067.pdf>
- [Stot_04] J.H. Stott, BBC R&D White Paper WHP099 PLT and broadcasting - can they co-exist? <http://downloads.bbc.co.uk/rd/pubs/whp/whp-pdf-files/WHP099.pdf>
- [Stot_05] J.H. Stott, BBC R&D White Paper WHP114, Co-existence of PLT and Radio Services – a possibility? June 2005
<http://downloads.bbc.co.uk/rd/pubs/whp/whp-pdf-files/WHP114.pdf>

- [TGN17] ECANB TGN17 V2.0 Technical Guidance Note TGN on Assessment of Powerline Telecommunications (PLT) Equipment, July 2009
http://circa.europa.eu/Public/irc/enterprise/emccbnb/library?l=/public_tgns/version_2009pdf/EN_2.0_&a=d
- [UPA] UPA <http://www.upapl.org/>
- [Vick_00] R. Vick, K.H. Gonschorek, "Abschlussbericht zur Power-Line Studie", 27 Januar 2000,
<http://www2.ing.unipi.it/~a008328/documenti/powerlines/PowerLineCom/Bibliografia/Rif64.pdf>
- [Vite_67] A. Viterbi , Error Bounds for Convolutional Codes and an Asymptotically Optimum Decoding Algorithm, IEEE Transactions on Information Theory, Volume IT-13, pages 260-269, in April, 1967.
- [VLAN] VideoLAN client and server <http://www.videolan.org/>
- [Volde_59] J. Volder, The CORDIC Trigonometric Computing Technique, IRE Transactions on Electronic Computers, September 1959
- [W_MIMO] MIMO on wikipedia: <http://en.wikipedia.org/wiki/MIMO>
- [Wari] R. Wariar, A tracking digital notch filter – Matras University
- [X10] Specification of X10 code protocol:
<http://software.x10.com/pub/manuals/xtddcode.pdf>
- [Xilinx] XILINX EDK, Embedded Development Kit (EDK)
http://www.xilinx.com/ise/embedded/edk_docs.htm
- [Zahn_04] P. Zahnradnik, M. Vlcek, Fast Analytical Design Algorithms for FIR Notch Filters. IEEE Transactions on Circuits and Systems I, Regular Papers March 2004
- [Zimm_00] M. Zimmermann, Energieverteilnetze als Zugangsmedium für Telekommunikationsdienste, Shaker Verlag Aachen, 2000